ABSTRACT

LEE, DUCK WEON. Temperature and Humidity Control in Multi-layered Garments. (Under the direction of Dr. Trevor J. Little.)

The purpose of this research is to measure a property of a multilayered fabric system by using heat energy and vapor flow in terms of thermodynamics. By observing change in the heat energy and vapor flow passing through the multilayered fabric system, this research is able to provide precise information about a property of individual fabric layer composing the multilayered fabric system.

This new research idea originates from a concept that, when heat energy and vapor flow pass through the layer or membrane, the amount of the heat energy and vapor flow is changed in accordance with a function of the layer or membrane. In particular, the amount of the vapor flow is apparently changed according to the fabric or membranes' structure and material property in a given environmental condition.

The research conducts an experiment by using 'the energy source,' which is newly and innovatively developed, measuring temperature and relative humidity in the multilayered system. Through experimental data, the research calculates the amount of heat energy flow in the microclimates and fabric by using Stefan Boltzmann equation, Newton's law of cooling, Fourier's law, and Clausius- Clapeyron Relation.

The research explains what properties of the fabric layers influence the energy flow attributable to conduction in the multilayered system consisting individual layers. In addition, the research shows that it is possible to build an optimized multilayered system under a variety of environmental conditions.

Temperature and Humidity Control in Multi-Layered Garments

by
Duck Weon Lee

A dissertation submitted to the Graduate Faculty of
North Carolina State University
in partial fulfillment of the
requirements for the degree of
Doctor of Philosophy

Fiber and Polymer Science

Raleigh, North Carolina

2011

APPROVED BY:

_____	_____
Dr. Trevor J. Little Committee Chair	Dr. Abdel-Fattah Mohamed Seyam
_____	_____
Dr. Pam Banks-Lee	Dr. Timothy Clapp
_____	
Dr. Woo Seong Kang	

DEDICATION

Dedicated to my dear parents, Mr. Lee, In Bock and Mrs. Kim, Young Ae, and my family, Lee, Seong Weon, Lee, Mi Young, and Lee, Hae Yoon, who is my spirit in my life, for their boundless faith, unconditional love, and endless supports and blessings

BIOGRAPHY

The author was born in Seoul, the capital of Korea. He completed his school education in Sun Jeong High School in Seoul - Korea. He received his Bachelors degree in Textile Engineering from Kyung Hee University - Korea in Spring 2000. In Summer of 2005, he joined Oregon State University, Corvallis, Oregon to pursue Masters of Science. He graduated in Winter 2006. Following his graduation he joined North Carolina State University in Spring 2003 to pursue Ph. D. in Fiber and Polymer Science under the guidance of Dr. Trevor J. Little.

ACKNOWLEDGMENTS

I would like to express my sincere gratitude to Dr. Trevor J. Little for giving me the opportunity to work on "Temperature and Humidity Control in Multilayered Garments," and for all the support and guidance throughout about four years. I would also like to thank Dr. Abdel-Fattah Mohamed Seyam, Dr. Pam Banks-Lee, and Dr. Timothy Clapp, and Dr. Wooseong Kang for their invaluable inputs through the course of the project. I am also grateful to students, Hun Lee, Hyunil Yoon, and Jessica Won who assist my experiment regarding a human subject. I would also like to thank the staff of College of Textiles, for all the help and suggestions during the course of my Ph.D curriculum. I would finally thank all my friends, who have been very instrumental to go through tough times,

TABLE OF CONTENTS

LIST OF TABLES

LIST OF FIGURES

1. Introduction

The purpose of this research is to analyze a multilayered fabric system by measuring the change in the rate of heat energy flow which originates from metabolic energy of the human body. That is, by observing change in the heat energy flow which is based on the reactions of each fabric's properties, this research is able to provide precise information about a functional capability of the fabric layers composing the multilayered fabric system. Therefore, this research area is related to thermodynamics as a way of investigating the heat energy flow and also the interaction between heat energy flow and the constituent fabric of a multilayered fabric system.

The four types of heat energy flow originate from metabolic energy of the human body; radiation, convection, conduction, and evaporation; each have their own properties and respond differently to multi-layered functional fabrics. Thermodynamics indicates that the amount or rate of each energy flow are changed during it passes through the fabrics and microclimates which provide a specific volume and pressure between two fabric layers. The heat energy changes are directly related to comfort sensation of the human body under various environmental conditions.

Hence, to analyze interactions between heat energy flow and the multilayered fabric system, and to how the interaction ultimately affects comfort of the human body, many existing studies are reviewed in the Literature Review in Chapter 2. Major subject areas discussed include; Comfort and Discomfort, Heat Energy Flow Fundamentals, Energy Types, and Dynamic Moisture Movement Testers. The literature review defines comfort and

discomfort, explains the principles of thermodynamics, reviews energy types, and introduces advantages and disadvantages of various current test methods, such as open cup test method, moisture management tester, Alambeta instrument, dynamic surface moisture movement tester, human-clothing- environment simulator, and gravimetric absorbent testing system.

Current testing concepts and instruments mainly focus on evaporation flow often neglecting the other three types of heat energy flow. This means that other heat energy flows, such as radiation, convection, and conduction are not considered in current fabric evaluation methods. Therefore, the current research develops a system to measure the heat energy flow and the relative humidity in multi-layered garment systems. This is approached from a thermodynamics perspective allowing the determination of the energy flow in terms of conduction, convection, radiation, and enthalpy change of vaporization.

Additionally, this research develops and tests a multilayered system because this setup more accurately reflects a person wearing a multilayered clothing system to protect from various external environments. The laboratory approach to measuring energy flow and humidity changes obviates the need for extensive human trials to evaluating clothing systems. The use of precision temperature and relative sensors record the actual changes through the multilayered fabric systems and the thermodynamics approach calculates the contribution of both the fabric and the individual microclimates. A method of evaluating different fabrics and combination therefore can be used to improve existing clothing systems.

2. Literature Review

2.1. Comfort and Discomfort

2.1.1. Introduction

Comfort has been researched and defined in a number of previous research studies. Jassal (2004) states that comfort is defined as "an optimal state of physiological, psychological, and physical combination between a human being and the environment." Branson (1988) defines comfort as "a state of satisfaction indicating physiological, psychological, and physical balance among the person, his/her clothing, and his/her environment." Milenkovic (1999) states that the meaning of comfort is "the absence of discomfort or a neutral state compared to the more active state of nervous."

Milenkovic explains that many fabrics performing a variety of functionalities, such as moisture management, air permeability, water repellency, thermal insulation, and fit, have been developed to maintain comfort for the human body over a long period of time. These latter functions react with physiological, psychological and physical factors of the human body. The performances attribute a fabric to assist with maintaining the heat balance of the human body to enhance comfort. For instance, if the evaporation function of clothing is not adequate, the human body will feel damp, hot, and clammy. In particular, condensed moisture which is formed in between clothing and skin plays a critical role in the sensation of discomfort. That is, the human body feels discomfort when wet casual wear touches the skin (Wang, 2007).

During the formative stages of the research, a model was developed based on

literature to explain the mechanisms of moisture transfer. Normally, the condensed moisture processes in microclimate can be analyzed in three steps:

1. Sweat ⇨ Liquid (from skin to microclimate)
2. Liquid ⇨ Vapor (from microclimate to clothes)
3. Vapor ⇨ Liquid (condensed water in the clothes)

These condensed moisture processes occur in two scenarios as shown in Figure 1:

Scenario 1: Fabric to skin (no space)

1. Sweat (Liquid)
2. Sweat absorbed (wicked) by fabric
3. Transferred through fabric → evaporation (No condensing)

Scenario 2: Gap between fabric and skin (Space)

1. Sweat (Liquid)
2. Sweat change into a vapor (Moisture rate ↑)
3. a) Vapor transferred through fabric or

   b) Condensed vapor to liquid, then wicking

Figure 1 shows the transformation and movement of vapor in the microclimate in scenarios 1 and 2. In addition, the researcher should take into account additional energy flow types. As can be seen in Scenario 1, radiation, conduction, and evaporation are the main energy flow types, while radiation, convection, and evaporation are active in scenario 2. Since clothing builds a microclimate between skin and clothing, the microclimate's temperature and humidity influence the amount or rate of heat flow. Hence, the properties,

such as fiber material, fabric structure, and fit, should be also considered to create and maintain optimal microclimate.

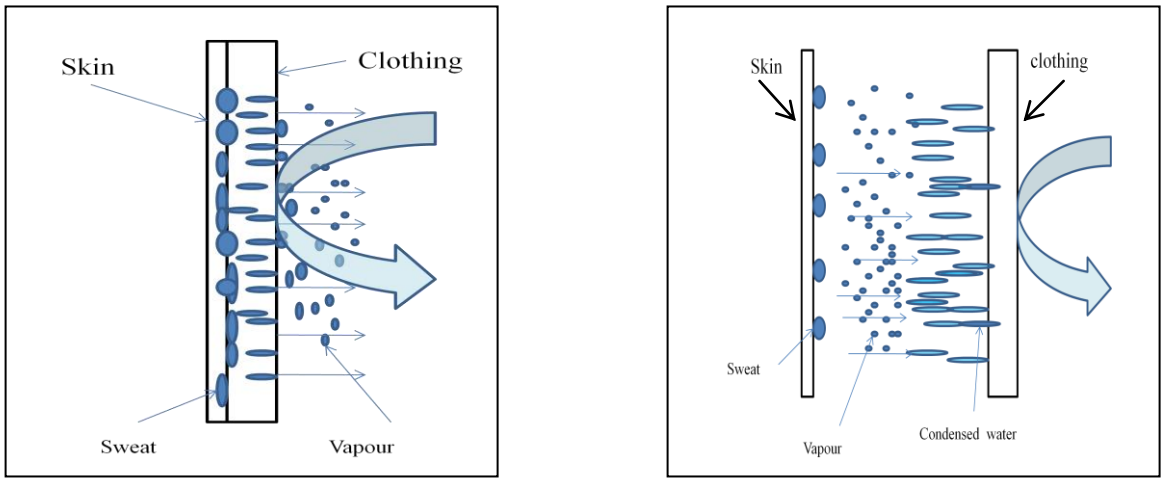

Scenario 1 Scenario 2

Figure 1. Two scenarios of the condensed moisture process (2008)

Rintamaki (2006) explains that consistent accumulation of perspiration impairs a variety of functions, such as air permeability, water permeability, and thermal insulation by heat absorption, on clothing and increases heat strain for the human body. Effects of the accumulation of perspiration in clothing give rise to hot thermal sensation, discomfort, and sweating. Failure to balance between moisture management and the property of the fibers' hygroscopicity causes discomfort in the human body. Therefore, the human body easily feels various discomfort sensations, such as stickiness, clinginess, clamminess, and dampness, if the role of clothing fails to control the internal and external environments, such as temperature and humidity (Sadikoglu, 2005).

Li (2006) indicates that those physiological and psychological discomfort sensations

of the human body can be affected by the garment type, time of day, and body part. For instance, dryness strongly affects psychological tactile comfort. It means that an efficient material function and fabric structure on clothing dealing with dryness influences the psychological comfort sensation for a wearer. Therefore, Chaudhari (2001) mentions that functional activewear should include efficient sweat absorption and vaporization properties simultaneously. Ruckman (1999) has also studied a highly efficient waterproof material to promote thermo-physiological comfort. He suggests that a clothing system is able to control heat energy generated by human movement and perspiration simultaneously because the system plays an important role in efficiently releasing the perspiration through the clothing.

Therefore, the comfort and discomfort sensations are artificially or naturally changed and controlled according to internal and external conditions of the human body (e.g., temperature, quality of the clothing, and psychological situation) (Scheurell, 1985). Kannekens (1994) studies two cases affecting discomfort or comfort sensation:

- A mechanical contact between textile and skin which is significantly related to surface structure and flexibility of the fabric.
- A thermo-physiological aspect, which considers relationships between moisture and heat formed by the microclimate between the human body and garment.

Through those two cases, Kannekens recognizes that comfort levels of clothing are determined by the functional capacities of the clothing (e.g., air permeability, water impermeability, water vapor permeability, thermal conductivity, fabric sound). In particular, Kannekens focuses on microclimate conditions which are determined by the functional capacities because they are related to the amount of heat energy transfer provided by the

metabolic energy of the human body in the second case (Kannekens, 1994).

Ramachandran (2004) explains that a number of pores and pore sizes in the fabric structure are significantly related to wetting and wicking phenomena improving physical comfort of the human body. Dionne (2003) also mentions that physical, psychological and physiological discomfort can be caused by accumulation of perspiration between skin and garment. Wong (2004) concluded that the sensation of humidity and heat tolerance are strongly related to a wearer's comfort, irrespective of the different types of apparel.

In addition, Wong (2003) conducted research on 'neural network predictions of human psychological perceptions of clothing sensory comfort.' The research reported that physical comfort is involved in tactile and thermal sensation contact between the skin and the external environment. Therefore, the physical comfort is mainly affected by three major factors, moisture, tactile sensation, and thermal-fit. Niwa (1999) investigated evaluation methods regarding objective tactile performance by using a variety of materials such as wool, cotton, and acrylics. She tried to convert subjective feelings into objective ones by applying a Kawabata Evaluation System (KES-F) because the tactile property was closely related to the human sense of feeling. In addition, Cho (2005) finds that even fabric sound has significantly influence on athletic performances including physiological and psychological impacts on the wearers.

2.1.2. Heat balance

Heat balance is one of the most important factors affecting comfort for the human body. Therefore, many researchers have conducted studies regarding the maintenance of heat

balance for a long period of time. In the book 'Energy Metabolism,' Miller (1968) mentions that "the heat is appearance of the large part of the energy expenditure originating from the human body." Powers (2007) mentions that "a heat balance is achieved in between the demands placed on the body and the body's response to those demands." However, it is not easy to measure the heat energy flow from the body because it is liberated around the body. The general process generating the heat energy can be explained by Equation 1 for cell work in a human body:

$$\text{Foodstuff} + O_2 \rightarrow \text{Adenosine Triphosphate (ATP)} + \text{Heat} \quad \text{(Eq. 1)}$$

$$\downarrow$$

$$\text{Energy Source}$$

The SI unit of measuring for heat energy is the joule (J). People also use the calorie to measure the heat energy. A calorie is defined as "the amount of heat required to increase the temperature of one gram of water by one degree Celsius (℃)." In addition, this heat energy created by metabolism can be shown as temperature change.

Miller mentions that human body temperature is a balance between the rate of heat gain and heat loss through the management of its energy metabolism and temperature regulation. Miller also states that "energy metabolism is controlled by requirements for temperature regulation of the human body." In addition, temperature regulation is normally governed by a constant rate of heat gain and heat loss from core to environment. Figure 2 shows a schematic of the heat balance without considering external environmental factors around a human body.

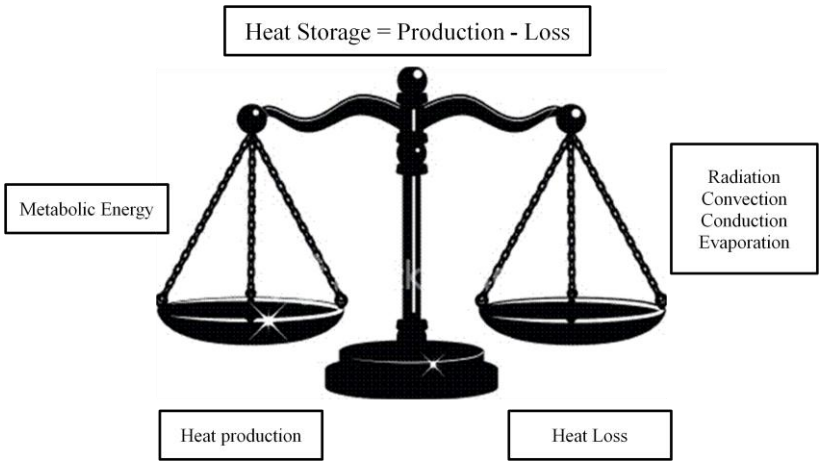

Figure 2. A schematic of the heat balance status

Reproduced from www.sportsscientists.com/2008/10/heat-stroke

Grucza (1983) creates a heat balance equation between the human body and an environmental condition under the first law of thermodynamics;

$$S = M - W - R - C - K - E \quad \text{(Eq. 2)}$$

where, S is heat storage, M is metabolic energy expenditure, W is mechanical work, R is radiation, C is convection, K is conduction, and E is evaporation. In addition, Grucza mentions that heat storage is a result of the difference between the constant rate of metabolic heat production and the exponential course of sweat evaporation in the human body. In particular, evaporation is the most effective factor among four types of heat transfer. The evaporation is divided into three areas, evaporation from the airways, water diffusion evaporation, and evaporation of sweat. However, Grucza explains that it is impossible to control the water diffusion evaporation and the evaporation from the respiratory airways by the thermoregulatory system. In the case of evaporation, perspiration is converted into vapor

by the heat energy of the human body during exercise.

While heat production is provided by a metabolic procedure and is divided into voluntary (exercise) or involuntary (shivering or biochemical heat production), heat loss occurs through four processes including: radiation, convection, conduction, and evaporation.

Rintamaki (2006) refers to three main factors affecting the heat balance:

1. Environmental thermal conditions
2. Metabolic heat production
3. Thermal insulation of clothing and other protective garments

Havenith (2005) states that climatic parameters (e.g., air temperature, radiant temperature, humidity, and wind speed) and personal parameters (e.g., activity rate, clothing insulation, and sweat capacity) have significant influence on the heat balance through inter-reaction among these parameters. Therefore, Havenith explains a heat balance equation for heat production and heat loss with each parameter. Table 1 shows climatic and personal parameters.

Table 1. Climatic and personal parameters

Climatic Parameter	Personal Parameter
Wind speed	Activity Rate
Humidity	Clothing Insulation
Radiation	Sweat Capacity
Air Temperature	

Reproduced from 'Temperature regulation, heat balance and climatic stress (2005)'

In particular, the personal parameters are core factors controlling heat balance. Havenith studies temperature changes by activity rates of the human body to account for the heat balance according to the level of exertion during exercise. For example, when the temperature of the human body is measured in the morning, its mean is about 36.7℃, and when the human does a moderate amount of work, its temperature rises to 38℃~39℃, and when the human works hard e.g., running a marathon, its temperature increases to 40℃. Those parameters ultimately influence on the temperature change, heat balance and comfort of the human body at that time.

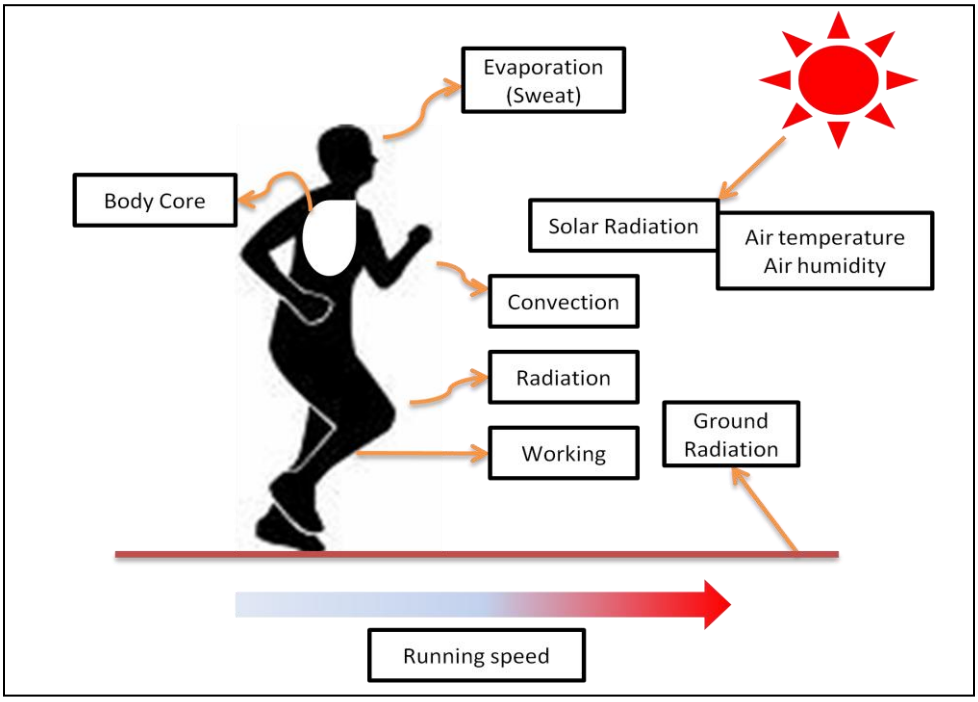

Figure 3. A summary of heat exchange mechanism during exercise

Reproduced from 'Exercise physiology (2007)'

Powers (2007) also illustrates the kinds of environmental factors affecting a running person who is emitting heat energy in Figure 3. It shows a summary of heat exchange mechanisms during exercise. However, it takes into consideration how important the role of clothing is in affecting heat energy flows because the attire's functions, such as air and water permeability, mitigate the properties of both internal and external environments, such as temperature and humidity.

It is not easy to balance all of the factors because they are constantly changing in accordance with internal and external environments. In the case of heat unbalance, Rintamaki explains heat strain causes the heat unbalance between the body and clothing. In particular, sweat emitted from the human body can be accumulated and interrupts thermal transfer, which contributes to the risk of cold strain and increases the wearers' discomfort. Jassal (2004), in another view of heat unbalance, mentions that an active human body provides strong perspiration to regulate its heat balance. However, if the perspiration cannot be efficiently vaporized into the external environment, relative humidity increases, and thermal conductivity of air insulation would also increase in clothing. These processes disrupt the heat balance and cause feelings of discomfort for the human body.

To address the heat unbalance, Ruckman suggests a physical method using ventilation features because it is able to effectively control sweating and thermal sensation in clothing. In particular, he mentions that the ventilation function as a clothing system is specialized in efficiently regulating thermo-physiological balance which is related to heat control and moisture exchange. Sadikoglu (2005) states that heat transfer through a fabric is determined by several factors, such as fabric thickness, the quantity of the air entrapped around the body,

the moisture content, and transportation and motion of external air. This means that the clothing system acts as the second layer of skin in controlling the heat transfer. Ramachchandran identifies two conditions required in the fabric worn next to the skin in order to effectively adjust the heat balance:

- Evaporation of sweat from the skin's surface
- Transference of moisture to external environments while drying the skin

Many researchers, such as Barker (2006), Hearle (2001), and Li (2002), have studied a core factor of vaporization causing discomfort of the human body. They assume that the vapor pressure gradient plays an important role in governing the vaporization which is related to a cooling mechanism. As a result, they found how environmental factors, such as temperature and relative humidity, affect the amount of perspiration vaporized. In the book 'Exercise Physiology (2007),' Powers mentions that Relative Humidity (RH) is the most important factor influencing the rate of evaporative heat because a different level of the RH between skin and air determines the vaporization rate in a given surface area. However, Powers emphasizes that, although the cause of vaporization is the vapor pressure gradient between skin and air, it should be clear that the vapor pressure gradient simply acts as the vapor concentration level. This means that the vapor pressure gradient itself does not cause vaporization; it only decides the amount and speed of the vapor. Table 2 shows a relationship between temperature and RH on vapor pressure.

Table 2. Relationship between temperature and relative humidity (RH)

on vapor pressure

Relationship between Temperature and Relative Humidity (RH) on Vapor Pressure			
Temp	50% RH	75% RH	100% RH
	Vapor pressure (mm Hg)	Vapor pressure (mm Hg)	Vapor pressure (mm Hg)
0°	2.3	3.4	4.6
10°	4.6	6.9	9.2
20°	8.8	13.2	17.6
30°	15.9	23.9	31.9

Reproduced from 'Exercise physiology (2007)'

By placing functional clothing between skin and air, people can optimally adjust the vapor pressure gradient and control the cooling mechanism to improve physiological, psychological, and physical comfort for the human body. For instance, if perspiration is vaporized faster than it is produced on the skin, the skin becomes too dry, which ultimately influences the comfort of the human body. In another example, if the vapor pressure gradient is too steep between RH1 and RH2 (Figure 4), it easily gives rise to the after-chilling phenomenon resulting from strong vaporization. Figure 4 shows a relationship between RH and vapor pressure gradient.

To explain the cooling mechanism, Powers gives an interesting example of how to calculate heat loss through vaporization. If we assume that the vaporization of 1,000 ml of sweat results in 580 kcal of heat loss, and a human body is working on a cycle ergometer at a

VO_2 of 2.0 liters/$\min^{-1}$ (energy expenditure of 10.0 kcal/$\min^{-1}$), and the efficiency of metabolic rate of the human body is 20%, the researcher is able to calculate the sweat and vaporization rate for a human body. The calculation procedure is as follows:

Total energy expenditure = 20 min * 10 kcal/min = 200 kcal

Total heat produced = 200 kcal * 0.8 = 160 kcal

The total natural evaporation necessary to prevent any heat gain = $\frac{160 \text{ kcal}}{580 \text{ kcal/liter}}$

= 0.276 liters

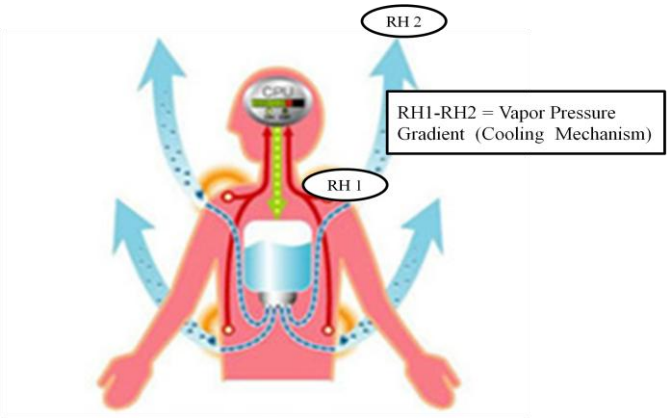

Figure 4. A relationship between RH and vapor pressure gradient

Reproduced from www.xyktf.com/en_aboutacc.asp

Even though this calculation is theoretical, as well as ideal, it provides basic information regarding the actual amount of vaporization during exercise. Through this calculation, the researcher assumes how much the amount of perspiration vaporized affects the body comfort, and how a clothing system is capable of handling the vaporization. In addition, this numerical information yields a method for analyzing change in the amount of enthalpy of vaporization. In addition, Powers indicates three environmental factors affecting

the vaporization of the perspiration:

(1) The temperature and relative humidity

(2) The convective currents around the body

(3) The amount of skin surface exposed to the environment

Miller (1968) studies "A Surface Area Law" that discusses four rules regarding relationships between the rate of heat loss and a given surface area of a body. Following four rules explain the given surface area law:

(1) Heat loss is proportional to a given surface area of the body

(2) If body temperature remains constant, heat production must be equal to heat loss

(3) Heat production is determined by the limited surface area of a body

(4) "If metabolism (heat production) is expressed in terms of the given surface area, it is uniform for animals differing greatly in body size"

These rules illustrate that there are co-relationships between heat loss and heat production and the given surface area of a body. Powers (2007) describes a method to measure mean skin temperature (T_s) of a human body from its total given surface area by using a concept that a fraction of the body is in proportion to individual skin temperature. Hence, Powers calculates the mean skin temperature (T_s) with Equation 3:

$$T_s = (T_{forehead} + T_{chest} + T_{forearm} + T_{thigh} + T_{calf} + T_{abdomen} + T_{back})/7 \qquad \text{(Eq. 3)}$$

where $T_{forehead}, T_{chest}, T_{forearm}, T_{thigh}, T_{calf}, T_{abdomen}$ and T_{back} represent the body's forehead, chest, forearm, thigh, calf, abdomen, and back. From this calculation, the researcher is able to indirectly assume and measure a heat balance of the human body. In addition, Gurcza (1983) suggests another way to measure the mean skin temperature:

$$T_{sk} = 0.50\ T_{chest} + 0.36\ T_{thigh} + 0.14\ T_{arm} \quad \text{(Eq. 4)}$$

where, $T_{sk}$is mean skin temperature, T_{thigh} is thigh temperature and T_{arm} is arm temperature. Through Equation 4, Gurcza measures the mean temperature of the human body to calculate a heat balance equation. However, many researchers have checked different areas of the human body to measure the mean skin temperature in order to achieve their research goals.

2.1.3. Heat Transfer

Das (2007) indicates that heat transfer through a fabric is a critical factor for athletes in governing thermo-physiological comfort. Das finds that convection, evaporation and radiation have great influence on regulating body temperature. As the human body reacts to external and internal environments, heat energy resulting from biological processes, such as blood circulation, tissue conduction, and metabolic energy production, can be transferred into four release mechanisms: radiation, convection, conduction, and evaporation. Therefore, Nilsson (1987) analyzed a correlation between skin blood flow (SBF) and temperature change to investigate relationships among biological processes and the heat energy flows under various environmental conditions and exercise levels.

Rintamaki explains that most of metabolic energy is emitted as heat, and its remainder simply runs a human body's physical movement. It means that, while 0-20% of the metabolic energy is used for mechanical work, 80-100% can be converted into heat energy flow when a human body exercises in the field. Wilmore explains that the amount of calories used is determined by the type of activity or exercise, and it is calculated by the amount of oxygen the human body consumes. The amount of oxygen consumption is absolutely affected by the

level of human physical activity and many other factors such as age, sex, size, weight, and body composition.

For instance, an average adult body needs 0.20 to 0.35 L of oxygen per minute at rest, which means that the human body consumes 1.0 to 1.8 kcal/min, 60 to 108 kcal/h, or 1440 to 2592 kcal/day based on rest status. Wilmore (1999) also gives other examples relevant to energy costs for different types of sports: archery and bowling requires slightly more energy than when at rest, on the other hand, a person who is running around a track needs about 29kcal/min at a 25 km/h (15.5 mph) speed. And jogging consumes 14.5 kcal/min at 11 km/h (7 mph).

Figure 5 provides information regarding heat exchange at rest and during cycle ergometer exercise at a given work rate; heat loss through convection and radiation is not largely related to exercise work rate, while the heat loss by the evaporation consistently increases in proportion to the increase of the exercise work rates. In addition, the researcher is capable of measuring the amount of net or physical efficiency through a difference between energy output and heat production. Physical efficiency is defined as "the mathematical ratio of work output divided by the energy expended above rest," during the exercise. The researcher is also able to estimate heat storage from the difference between heat production and heat loss from Figure 5.

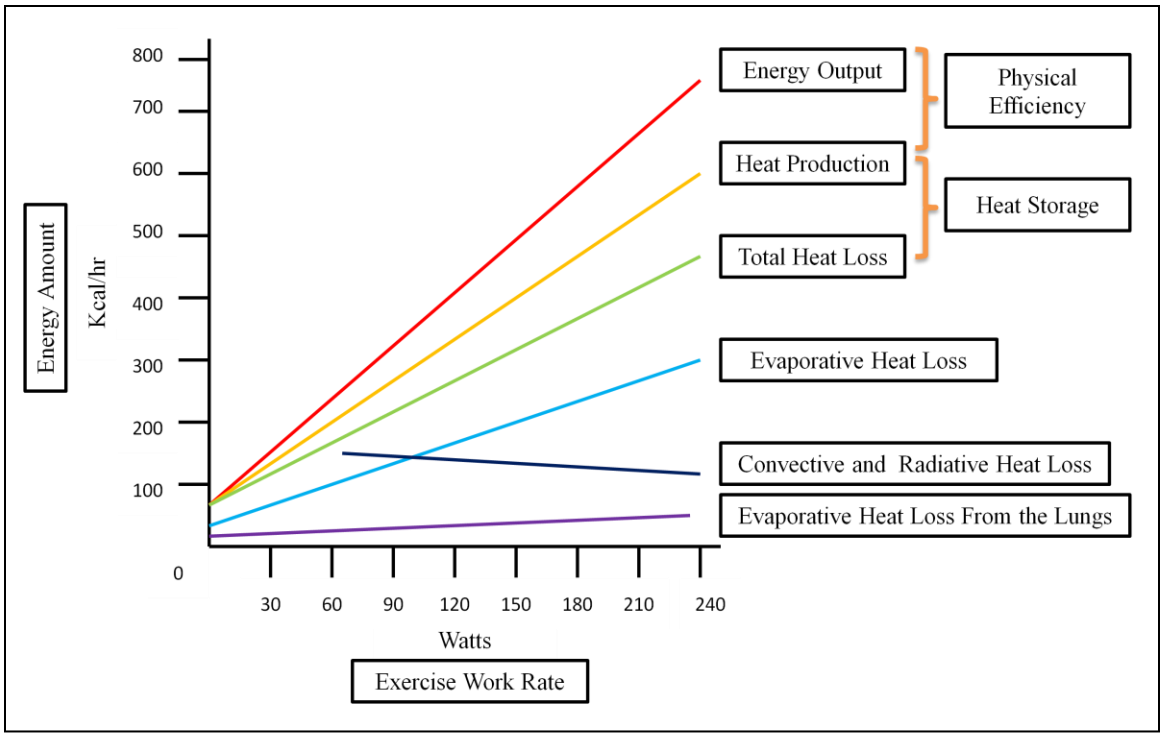

Figure 5. Heat exchange rate at rest and exercise at a variety of work rates during cycle ergometer use reproduced from 'Exercise physiology (2007)'

As the study above mentions, there are four types of heat loss. In the book 'Physiology of Sport and Exercise,' Wilmore (1999) suggests that it is important to recognize their relative contribution regarding heat loss, when comparing two types of body position, at rest and exercise. An experimental result shows that heat production is 10 times higher during prolonged exercise than at rest, consuming about 15 kcal/min at 70% of VO_2 Max. Table 3 shows the estimated calorie amount of heat loss at rest and during prolonged exercise from the experiment. It verifies several researchers' studies, that if human body temperature increases, the amount of evaporation increases in proportion to the increase in its heat production. On the other hands, the percentage of heat loss via conduction, convection, and

radiation are decreased.

Table 3. Estimated caloric heat loss at rest and during prolonged exercise

	Rest		Exercise	
Mechanism of heat loss	% total	Kcal/min	% total	Kcal/min
Conduction and Convection	20	0.3	15	2.2
Radiation	60	0.9	5	0.8
Evaporation	20	0.3	80	12
Total	100	1.5	100	15

Reproduced from 'Physiology of sport and exercise, human kinetics (1999)'

2.2. Heat energy flow fundamentals

2.2.1. Introduction

The purpose of this section is to review fundamentals of energy flow expected to control the energy flow behavior in apparel and ultimately provide a feeling of comfort in the human body (Branson and Abusamra, 1988; Fanger, 1970). In the book 'Fundamentals of Engineering Thermodynamics,' Moran and Shapiro (2008) defines energy as "the amount of work done when force distance is exerted through a distance." A familiar unit of work is Newton-meter (N-m) or foot-pound (ft-lb_f). Energy can exist in different forms (kinetic, potential, thermal, and electromagnetic) and can be transformed from one form to the other. In particular, this section focuses on heat energy, fluid dynamics, and the principles of thermodynamics because the human body creates heat energy flow including water

molecules (Kondepudi, 2008).

Kondepudi (2008) mentions that "thermal energy in a system is transferred into its surrounding by heat which is microscopic and chaotic motion of particles." Isaac Newton and other researchers mention that heat is "an indestructible (caloric) fluid-like substance without mass that is exchanged between material bodies." There are three kinds of heat energy transfer modes: conduction, radiation, and convection. If heat transfer is accompanied with water, an additional mode can be added to the energy transfer mechanisms; evaporation (Wilmore and Costill, 1999). In particular, when the system is at the saturated liquid state, a phase change of the molecules occurs and causes molecules in liquid to move into a vapor phase in accordance with the system's conditions, such as pressure (p), specific volume (v), and temperature (T). This means that the thermal energy flow has a significant relationship with the system's conditions (ASHRAE Handbook, 2009).

A principle of this energy flow is basically explained by the zeroth, first, second and third laws of thermodynamics. However, to accurately understand the thermodynamics laws, it is necessary to first define a system that includes mass and which interacts with the surroundings. Figure 6 shows a schematic of the general system interacting with the surroundings. Therefore, this section studies metabolic energy of the human body because it provides evaporation, radiation, convection, and conduction as an energy resource (Grucza, 1983). In addition, when this heat energy flows through materials, such as metal and fabric, the materials have the ability to conduct heat (Marcus and Blaine, 1998). In general, the conductivity can be measured in watt per Kelvin per meter ($W*K^{-1}*m^{-1}$). Its reciprocal is called thermal resistivity. This section is largely focused on textile thermal conductivity and

resistivity, and interactions between the heat and moisture flow and textile.

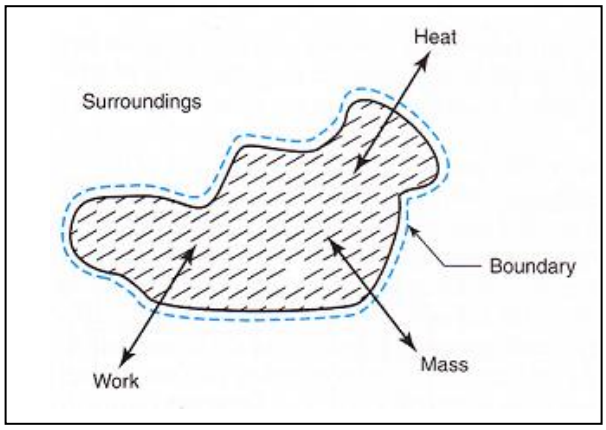

Figure 6. A system interacting with the surroundings

Reproduced from 'Introduction to modern thermodynamics (2008)'

2.2.2. Thermodynamics Laws

Energy can be transferred into the surroundings. Energy movement can be defined by four kinds of thermodynamic laws (Moran and Shapiro, 2008). The zeroth, first, second, and third laws explain the movement of heat in a system. Each law is described as follows: The zeroth law is that "if two thermodynamic systems are each in thermal equilibrium with a third, then they are in thermal equilibrium also with each other (Moran and Shapiro, 2008)." This law is related to thermal equilibrium between systems. For example, if systems A and B are in thermal equilibrium with system C, A is in thermal equilibrium with B. Also, Figure 7 explains the zeroth law, which shows that systems are in thermal equilibrium at the same temperature.

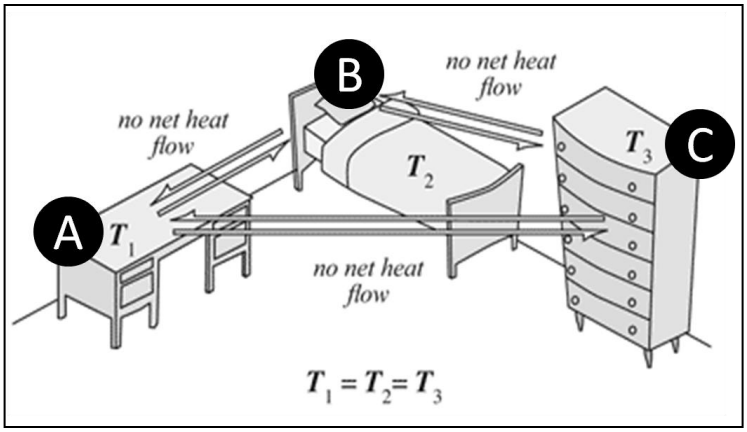

Figure 7. The zeroth law of the thermodynamics

Reproduced from 'Fundamentals of engineering thermodynamics (2008)'

The first law states that energy can neither be created nor destroyed. It can only change in type (Kaminski and Jensen, 2005). A main point of the first law states that it is impossible to destroy or create energy in the universe. This means that energy is always conserved by changing into a variety of energy types, for instance, potential energy can be easily transferred into kinetic energy. When using a speaker for amplifying the volume of a voice, the potential energy of a battery can be changed into kinetic energy to sound the voice in the speaker. At that time, the amount of power which makes the voice heard is the same as the decrease in power of the battery. Accordingly, energy is shown to be as given by Equation 5 in a closed system:

$$\Delta E = Q - W \qquad \text{(Eq. 5)}$$

where, ΔE is the change in all forms of energy stored in the system, Q is the net energy that is added to the system in the form of heat, and W is the net energy that leaves the system in the form of work. In particular, ΔE consists of three factors, kinetic energy, potential energy, and

internal energy. Therefore,

$$\Delta E = \Delta KE + \Delta PE + \Delta U = Q - W \qquad \text{(Eq. 6)}$$

where, ΔKE is the change in kinetic energy ($\Delta\frac{1}{2}mV^2$), ΔPE is the change in potential energy (Δmgz), ΔU is the change in internal energy of the system, m is the total mass, V is the magnitude of the velocity of the system, g is the acceleration due to gravity and z is the elevation. This equation confirms that the total amount of energy remains constant (Moran and Shapiro, 2008).

The second law focuses on a direction of the heat transfer and mechanical efficiency in a system. In 1854, Kelvin explains that "it is impossible for any system to operate in such a way that the sole result would be an energy transfer of heat from a cooler to a hotter body." Kondepudi (2008) also mentions that the second law states that "heat cannot by itself pass from a colder reservoir to a hotter reservoir." Energy is converted into mechanical work when Q_H (high heat energy) is changed into Q_L (low heat energy) through a heat engine. In addition, the energy cannot be fully converted into the mechanical work. The mechanical efficiency of the power cycle in a heat engine is given by Equation 7:

$$\eta_{cycle} = \frac{W_{net}}{Q_H} = \frac{Q_H - Q_L}{Q_H} = 1 - \frac{Q_L}{Q_H} = 1 - \frac{T_L}{T_H} \qquad \text{(Eq. 7)}$$

This equation implies that Q_L should be decreased to increase the cycle's efficiency, which means that the lower the level of Q_L, the closer the efficiency is to unity (Kondepudi, 2008). Figure 8 (B) explains that the heat engine having heat Q_1 converts a part of it into work, W and Q_2.

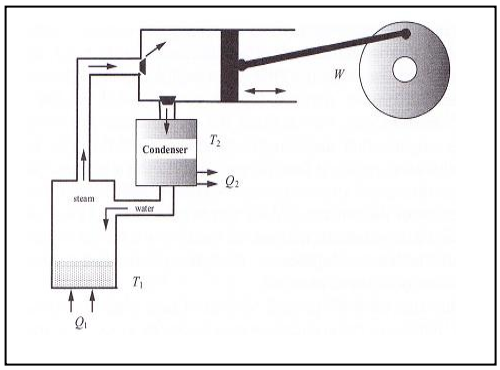

(A)

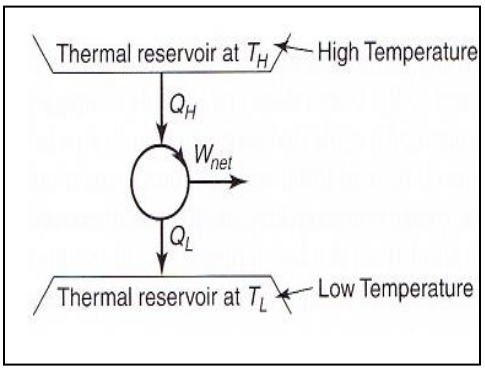

(B)

Figure 8. (A) A diagram of a real steam engine and (B) Power cycle operating two thermal reservoirs reproduced from 'Introduction to thermal and fluid engineering (2008)'

In addition, it is impossible for the system and its surroundings to be returned back to their initial states after the process has occurred in an open system. This means that its reverse flow does not occur in nature. Thus the process is called 'irreversible.' (Logan, 1999; ASHARE Handbook, 2009). Figure 8 shows a schematic of a real steam engine (A) and power cycle operated between two thermal reservoirs (B).

The third law is related to 'absolute zero' temperature, 0° Kelvin. The third law is that, "as the temperature approaches absolute zero, the entropy of a system accesses a constant minimum." This means that, when a system's temperature goes down to 'absolute zero,' its entropy approaches that of a pure perfect crystal whose entropy is zero at '0°' Kelvin. Even though a pure perfect crystal is ideal and theoretical at the absolute zero, the molecular alignment is even, as well as its molecule is identical. The absolute zero corresponds to approximately -459.7 Fahrenheit or -273.15° Celsius. Table 4 summarizes a core content of each thermodynamic law.

Table 4. Core contents of each thermodynamic law

0^{th} Law	Thermal equilibrium among systems
1^{st} Law	Energy can neither be created nor destroyed
2^{nd} Law	A process that occurs will tend to increase the total entropy of the universe
3^{rd} Law	Entropy is a minimum at 'absolute zero' temperature (Kelvin)

2.2.3. Fundamental Factors of Thermodynamics

Moran and Shapiro (2008) define fundamental factors of thermodynamics. Thermodynamics' properties can be measured and characterized through three basic factors, pressure (ρ), specific volume (v), and temperature (T). First, the specific volume (v) simply means the space in cubical units for a given mass. The smallest volume contains enough particles to be significant as a value of statistical average which demonstrates a relationship between entropy and molecular motion under a given p-v-T condition. The specific volume is defined as "the reciprocal of the density, and its SI unit is m^3/kg."

As pressure is given by force acting on a given area of a body in a macroscopic level, it has average molecular force per unit of surface area of a molecular level. The pressure arises during the combined collision motion of many molecules on a molecular level. Therefore, the pressure can be defined by Equation 8:

$$\rho = F/A \qquad \text{(Eq. 8)}$$

where, F is force and A is unit area. Force is measured by manometers and barometers

through the length of a column of liquid, such as water, oil, or mercury. The SI unit of pressure is Pascal; 1Pascal = 1 N/m^2, which is Newton per square meter.

Temperature is referred to as one of the fundamental parameters used to describe thermodynamics using an 'absolute' scale ([°K] = [°C] + 273.15). Temperature implies the degree of hotness. The temperature scale is defined by two methods, the Kelvin scale and the Rankine scale. While the Kelvin scale measures temperature in degrees Celsius (0°: freezing point ~ 100°: boiling point), the Rankine scale uses the Fahrenheit system (32°F: freezing point~212°F: boiling point). These temperature scales mean heat intensity as well as it corresponds to a level of molecular motion.

Many researchers, such as Benedict, Martin, and Hou, have studied the relationships between motion of molecules and associated p-v-T values because they are used to characterize molecular motion or define a phase of molecules in a matter (Benedict, 1937; Martin and Hou, 1955). In particular, kinetic theory explains how molecular motion gives rise to pressure (p) which is occurred by collisions between molecules having different velocities in the ideal gas law (pV= nRT). In the ideal gas law, temperature (T) is proportional to the average kinetic energy of molecules. For instance, p=0 and T=0 (absolute zero) means zero velocity of the molecules' movement in a system; molecules lose their kinetic energy at constant pressure and zero absolute temperature.

In addition, it is important to define and divide the universe into a system and its outside respectively where the zeroth, first, second, and third law of the thermodynamics are applied. Kondepudi (2008) explains the system with three types: isolated, closed and open system based on the method in which they interact with the exterior. A standard which

classifies these types depends on the existence and role of a boundary which allows the exchange of matter and energy between the system and the outside.

Figure 9 shows a schematic of isolated, closed and open systems; the isolated system does not exchange any energy or matter with the outside (A). Such systems can be only found in a laboratory because of the extremely slow exchange that occurs in energy and matter. This isolated system does not exist in nature. The next system is the closed system (B). Even though the closed system does not exchange the matter with the outside, this system exchanges the heat and mechanical energy within the outside. For instance, the Earth, as a closed system, emits radiation after it only absorbs energy from the sun, while it does not exchange matter with the outside. This case can be easily set up in a laboratory. Finally, there is the open system (C). It exchanges both energy and matter with the outside. All ecological systems and living systems including a human body are affiliated with this open system (Kondepudi, 2008).

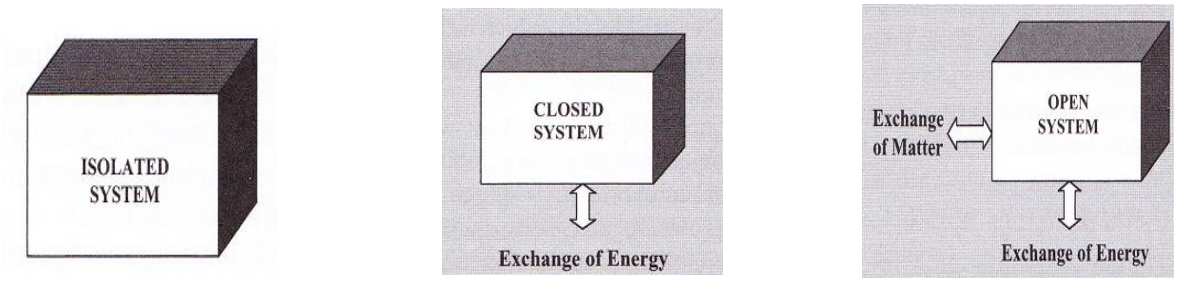

(A) (B) (C)

Figure 9. A diagram of (A) isolated, (B) closed and (C) open system

Reproduced from 'Introduction to modern thermodynamics (2008)'

2.2.4. Phase Change

In thermodynamics, materials or molecules can exist in four phase states, solid, liquid, gas and plasma. However, for our purpose, only three phase states (solid, liquid, and gas) are considered. Moran and Shapiro (2008) mention that the phase can be defined as "a quantity of material that is homogeneous throughout in both physical structure and chemical composition." The definition of homogeneity is that the material is all solid, all liquid, or all vapor in a physical structure. In addition, the phase change of the material is defined as "the transformation of a thermodynamics system from one to another." However, a material normally exists in one or two phases through a process in a system. In particular, fluid dynamics in textiles involves two phases, liquid and vapor (gas). Figure 10 shows a phase change of 1mol of H_2O with the amount of heat at a pressure of 1 atm (A), and a diagram of physical phenomena during a process of the phase change (B).

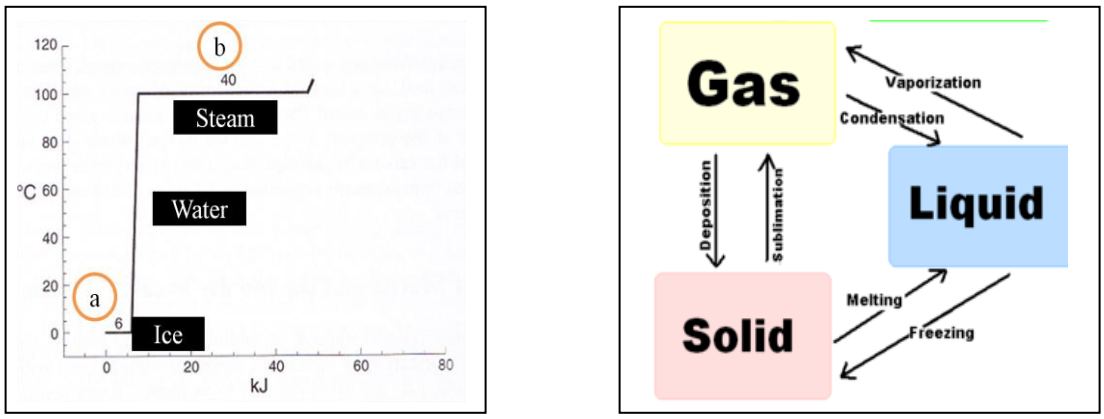

(A) (B)

Figure 10. (A) Phase change of 1mol of H_2O based on consumption of heat energy, and (B) Diagram of physical phase during a process of the phase change

Reproduced from 'Introduction to modern thermodynamics (2008)'

In the ‘a (melting)’ area of Figure 10(A), the absorption of heat does not increase the temperature until the ice melts. To melt 1mol of the ice, about 6 kJ of the heat energy is required. Before reaching the boiling point, temperature increases, then it remains constant until all water is transformed into steam. At that time, approximately 40 kJ is needed to convert 1 mol of water to steam in the ‘b (vaporization)’ area. The heat required does not cause an increase in temperature of the material but only causes a change in phase. In particular, this heat is called latent heat (Kondepudi, 2008). Figure 10(B) illustrates a diagram of the phase change in a closed system.

In the book ‘Introduction to Modern Thermodynamics,’ many researchers, such as Maxwell and Clausius, point out that the phase changes in materials can be explained through molecular motion under an environmental condition. This means that the phase change of the molecules in a system is based on a given condition of thermodynamics’ properties, such as pressure, specific volume, and temperature. The phase change of those molecules is transformed into a variety of phase types, such as liquid, liquid and vapor, solid and vapor, and triple state, in accordance with a given p-v-T condition. Figure 11 shows a graph of phase change of molecules under a given environmental condition (p-v-T) (A) and the relationships among the measurable parameters, pressure, specific volume, and temperature in that condition (B).

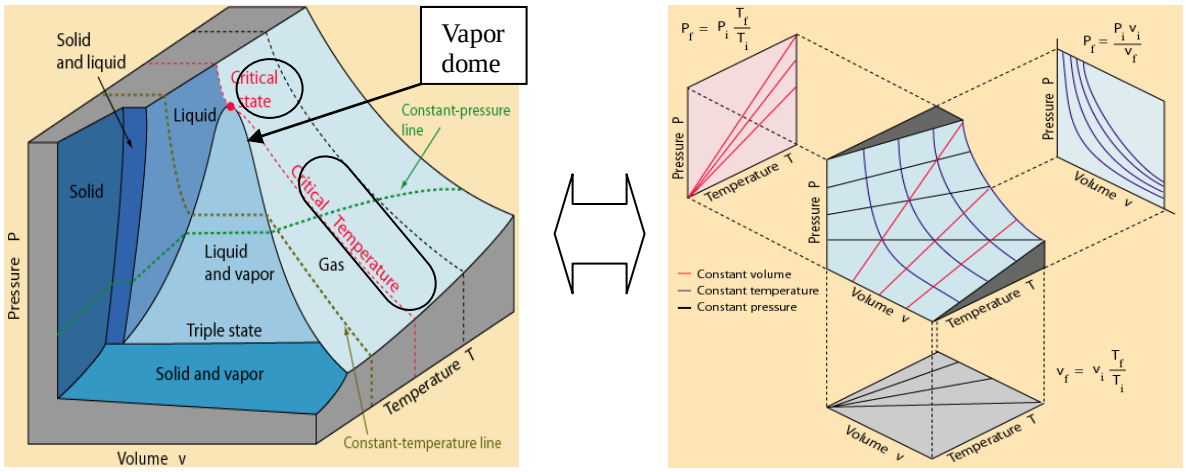

(A) (B)

Figure 11. Thermodynamic surface in p-v-T space (A) and Relationships among p-v-T (B)

Reproduced from http://hyperphysics.phy-astr.gsu.edu/Hbase/thermo/pvtsur.html

Since the shape of the phase change graph is different in accordance with each material, it can be a property of the material. In Figure 11(A), the coordinates of a point signify specific values of a certain pressure, specific volume, and temperature when the ideal gas is at equilibrium on the p-v-T surface. The critical state means the highest pressure on the vapor dome, and the critical temperature means a sloping isotherm line passing over the top of the vapor dome. The position of the critical point in p-v-T relationship is a unique property of gases, such as air, ammonia, and carbon dioxide, as they have different values of p-v and critical temperature (Moran and Shapiro, 2008). The p-v-T relationship is consistent with the ideal gas law (pv = nRT). This means that the pressure is inversely proportional to the specific volume when temperature is constant, while temperature is directly proportional to the specific volume and pressure in Figure 11(B).

Logan (1999) mentions that Van der Waals noticed that the ideal gas law is governed by two main factors: the effect of molecular volume and intermolecular forces between molecules. In addition, McPherson (1993) mentions that these molecules have at least two types of forces; a force of repulsion which increases when molecules come close to each other, and an attractive force which reduces the square of the distance between molecules. If heat energy is absorbed, the molecules undergo increase in vibration which causes the bonds to be broken. This means that the volume and intermolecular forces of the molecules are controlled by the p-v-T relation (Howell and Buckius, 1992; Stoecker and Jones, 1982).

2.2.5. Metabolism

As a human body is representative of a thermodynamic open system, it continuously exchanges energy and matter with its environment. Gordon (2009) mentions that the human body, as the energy source, creates metabolic energy and then remits it in four types of heat energy, convection, conduction, radiation, and evaporation simultaneously. Bass and Henschel (1956) explain that this metabolic energy is basically formed from food, which is transformed into heat production and mechanical power in the body through oxidation. This means that, after a human body consumes food, the digestive system makes amino acids, fatty acids, and glucose from proteins, fats and carbohydrates. These materials, amino acids, fatty acids, and glucose, are ultimately used as energy and water sources through the anabolic and catabolic processes (Powers and Howley, 2007). Finally, production of the energy which is provided by foods is enacted by transfer of electrons from carbon and hydrogen to carbon dioxide and water. Figure 12 and Equation 9 simply describe the oxidation process of glucose

that forms water and 38 kcal/mole of APT energy (Adenosine Triphosphate). As the ATP is a nucleotide that is composited by the adenine (base), ribose (suber), and three phosphate (Pi) groups, whenever one of three phosphate is broken from the ATP, energy is released, and a bond (Pi + ADP: Adenosine diphosphate) is created.

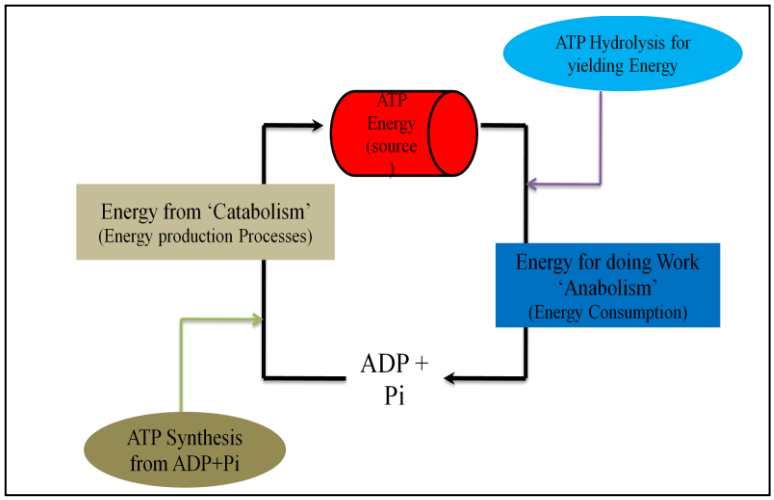

Figure 12. A schematic of Process of Catabolism and Anabolism

Reproduced from http://www.ehow.com/about_4689039_molecule-used-as-fuel-cell.html

$$C_6H_{12}O_6 + 6O_2 \rightarrow 6H_2O + 6CO_2 + 38\ ATP \qquad \text{(Eq. 9)}$$

Parsons (2002) and Hope (1993) mention that heat energy, which is produced by human metabolic processes, can be applied into thermodynamic laws. Therefore, Parsons simply explains Equation 10 illustrating the relationship between heat production and biological change of the human body;

$$H = M - W \qquad \text{(Eq. 10)}$$

where, H is the metabolic heat production; M is the metabolic rate; and W is mechanical

work. This equation explains how the metabolic energy rate can be divided into heat production rate and mechanical work.

Burdett (1983) mentions that rates of H, M, and W can be measured by consumption of oxygen. Normally, a human body has transformed a part of mechanical energy with the amount of the oxygen consumed to make muscle power that runs the mechanical work. This means that metabolic energy consumption is directly related to oxygen consumption. From the activity level and oxygen consumption, the amount of metabolic energy can be measured. Table 5 shows the average metabolic energy rates for different activities which as measured by Burdett (1983).

Table 5. Average metabolic energy rates based on activity levels

Activities	Metabolic Rate M in W
Sleeping	87
Standing	130
Walking (4 km/h)	260
Jogging	600
Rowing (competition)	1800

Reproduced from 'Comparison of mechanical work and metabolic energy consumption during Normal Gait (1983)'

While physical work is run in part by metabolic energy, more than 80% of metabolic energy is transformed into internal heat (H). The 80% of the metabolic energy converted into the

physical work is defined as the mechanical efficiency (η). The relationship is given by Equation 11:

$$H = M * (1- \eta) \quad \text{(Eq. 11)}$$

Snellen (1960) additionally explains that the external work performed is the same as the difference between metabolic heat production and heat loss by evaporation. In addition, this metabolic heat production is significantly related to temperature change in the human body. For example, too much heat production causes perspiration, while too little heat production means a temperature decrease in the human body as adjusting a blood flow rate of the body. This means that the human body controls its temperature by itself. Mitchell (1976) mentions that metabolic energy is transformed into increased temperature and sweating.

Many researchers have measured the metabolic costs of the human body's activities. Civoni (1967) introduced diverse mathematical equations for calculating the metabolic cost based on various human behaviors.

(1) The metabolic cost of walking at a given speed (V) at grade (G) and carrying a given load (L):

$$M = \eta\,(W + L)\,[2.3 + 0.32\,(V - 2.5)^{1.65} + G\,(0.2 + 0.07\,(V - 2.5))] \quad \text{(Eq. 12)}$$

where, M = metabolic rate, kcal/J, η = terrain factor, as defined as 1 for treadmill walking, W = body weight, kg, L = external load, kg, V = walking speed, km/hr, G =slope (grade), %

(2) This case takes into account increase of metabolic cost when the load is located in the hands or on the feet, away from the center of gravity of the body. Therefore,

additional metabolic cost (+M) can be calculated by Equation 13:

$$(1) + M = K L^2 V^2 \quad \text{(Eq. 13)}$$

where, *K*, the proportionality factor, depends on the placement of the load

(3) The metabolic cost of running at a given speed up a certain slope, as a linear function of the expected metabolic cost of walking at the same speed and slope:

$$M_{running} = [M_{walking} + 0.47\ (900 - M_{walking})]\ (1 + G/100) \quad \text{(Eq. 14)}$$

where $M_{walking}$ is the predicted M for walking at the same speed, and G is the slope in percentage.

Belding (1946) explains that "energy exchanges as a function of activities;" which means that metabolic energy can be calculated by the energy balance Equation 15:

$$M + D = (E_l + A) + W + E_s + H_{cl} \quad \text{(Eq. 15)}$$

where, M = Metabolism, D = Heat loss, $(E_l + A)$ = Heat loss as a result of evaporation of water from lungs (E_l) and in warming air (A), W = External work, E_s = Heat loss of vaporization of sweat, H_{cl} = Heat loss through clothing by convection and radiation. From these equations, Belding predicts that sitting consumes about 53 Cals./m^2(body surface)/hr., and climbing a 12 percent grade (slope) at 3.5 miles per hour needs about 424 Cals./m^2(body surface)/hr.

2.2.6. Phase Change in Microclimate

Consolazio and Matoush (1962) explain that metabolic energy creates an energy fluid in a microclimate between the human body and fabric. The microclimate is a place where the

phase change of perspiration occurs under certain environmental conditions. Albert and Palmes (1951) mention that the rate of vaporization of perspiration is determined by a variety of environmental factors, such as skin temperature, humidity, and vapor pressure, in the microclimate.

The heat energy, which originates from metabolic activity, is able to explain how perspiration moves from skin to the fabric using the concept of enthalpy: enthalpy is a thermodynamics' property in a system and it can be used to measure the amount of heat transfer (Moran and Shapiro, 2008). Colin (1966) points out that a human body's heat and perspiration are exchanged in a microclimate in four ways: evaporation, radiation, conduction, and convection. He derived Equation 16 to characterize thermal equilibrium of the human body:

$$Q_E = Q_M - (Q_{CV} + Q_{CD} + Q_R) \quad \text{(Eq. 16)}$$

where, Q_E is heat exchange by evaporation; $Q_M$is metabolic production rate of heat; Q_{CV} is heat exchange rate by convection; $Q_{CD}$is heat exchange rate by conduction; and $Q_R$is heat exchange rate by radiation. This equation explains the relationship between evaporation and ways of heat exchange based on the first law of thermodynamics.

It is important to analyze heat lost through vaporization of sweat to calculate the heat balance of the human body. Woodcock (1962) explains the total heat transfer from the skin to environment through dry clothing with several equations. Equation 17 defines heat transfer from skin at any given temperature and ambient conditions. This equation accounts for how thermal equilibrium can be maintained by an exchange between metabolic heat production and sweating:

$$H = \frac{0.309}{I}[(T_s - T_a) + i_m S(P_s - P_a)] \quad \text{(Eq. 17)}$$

where, T_s is skin temperature; T_a is ambient temperature; I is insulation or thermal resistance of the clothing and the overlaying air layer; P_s is water vapor pressure at the skin boundary; P_a is water vapor pressure of environmental air; i_m is the permeability index, and S is the conversion factor which converts vapor pressure difference to an effective temperature difference.

The heat transfer (Radiation, Convection, Conduction, and Evaporation) through clothing responds to a human body in the microclimate. Hu (2005) explains that sweating and evaporation in the microclimate are main factors that allow cooling of the human body. Ruckman, Hayes and Cho (2002) illustrate that the cooling mechanism in the microclimate influences the perception of clothing comfort, correlates with the absorption and transportation of sweat, and transfers moisture from microclimate between a garment and skin through the fabric. A dynamic sweating hot plate, which operates on the principle of momentary vapor pressure gradient, is capable of assessing microclimate response of the fabric where moisture and heat are added (Yoo and Barker, 2005; Prahsarn, Barker, and Gupta, 2005). Figure 13 explains the process of sweat transport in the microclimate and shows changes of phase from liquid to vapor.

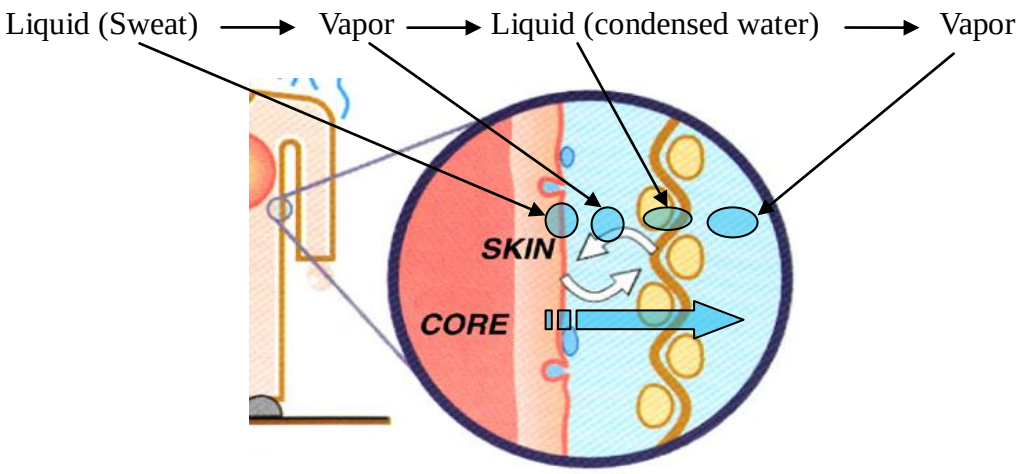

Figure 13. Microclimate and Evaporation Movement by Heat Energy

Reproduced from 'P-smart- a virtual system for clothing thermal functional design Computer-Aided Design (2006)'

Li (2006) notes that water vapor diffusion caused by kinetic and potential energy is an important factor for affecting temperature change in the microclimate. In addition, Kondepudi (2008) explains that the vaporization involved can be explained by the Clausisus-Clapeyron Relation. Rudolf Clausius and Emlie Clapeyron define vaporization as "a way of characterizing a discontinuous phase transition between two phases of matter." Clausius-Clapeyron Relation is Equation 18:

$$\ln\left(\frac{P_1}{P_2}\right) = \frac{\Delta H_{vap}}{R}\left(\frac{1}{T_2} - \frac{1}{T_1}\right) \qquad \text{(Eq. 18)}$$

where, T_1 and P_1 mean temperature and vapor pressure at point 1, T_2 and P_2 mean temperature and vapor pressure at point 2, ΔH_{vap} is the molar enthalpy of vaporization, and R is the gas constant (8.314 J $mol^{-1}K^{-1}$). This equation plays an important role in analyzing

information relating to vaporization and enthalpy. This equation is capable of calculating differences in enthalpy required to vaporize water molecules when it is possible to predict the temperature at a certain pressure in two places.

2.2.7. General Thermal Conductivity and Textile Conductivity

Many researchers, such as Moran (2008), Vignewaran (2009) and Ismail (1985), have studied thermal conductivity in textiles. Moran and Shapiro mention that thermal conductivity is defined as "an ability of the material to conduct heat." Vignewaran and Chandrasekaran (2009) also define the heat conduction as "one method of energy flow from the higher temperature to the lower temperature due to kinetic motion or direct impact of molecules." Janna (2000) explains that "the numerical value of thermal conductivity means how fast heat is conducted by the molecular effects through a material."

Fourier's law defines heat conduction as "the amount of heat flowing per unit surface area per unit time." Fourier states that "heat current or flow is proportional to the gradient of temperature." Equation 19, Fourier's law, explains the rate of energy transfer by conduction (Moran and Shapiro, 2008):

$$Q_x = - kA\frac{dT}{dX} \qquad \text{(Eq. 19)}$$

where Q_x is the amount of energy transferred, A is surface certain area, dT is the temperature difference, dX is a material thickness (distance), and the proportionality constant k is a property called the thermal conductivity, and (-) illustrates that the direction of heat flux is inversely related to temperature gradient. Figure 14 illustrates the Fourier's conduction law.

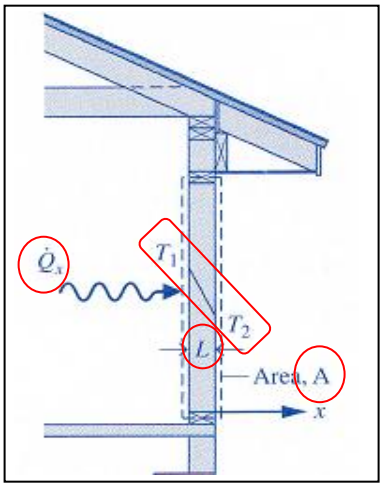

Figure 14. Illustration of Fourier's law

Reproduced from 'Fundamentals of Engineering Thermodynamics

(Moran and Shapiro, 2008)'

After heat energy is emitted from the human body, it tries to pass through textiles. In other words, this heat energy is transferred through the fabric. However, the heat transfer through the fabric might vary according to fabric structure or fiber property (Frydrych, Dziworska, and Bilska, 2002). Therefore, it is important to control the thickness of fabric (dX) to adjust the amount of the energy transferred from human body to an environment through the fabric.

Holcombe and Hoschke (1983) explain that heat transfer is conducted by forced convection of air flow on the fabric structure, by conduction through fibers, and by radiation from the fabric. In particular, the properties, such as the structure and fiber property, of the fabric are important because they are related to change in a p-v-T condition which affects phase change processes, such as vaporization and condensation, of material. In addition,

Baxter (1945) mentions that the thermal conductivity of the fabric consists of two factors: "the heat transmitted through air space and the heat transmitted through a structure formed by the textile fibers." Therefore, the air's thermal conductivity is the first controlling factor, and the fiber's thermal conductivity is the second factor. Mao and Russell (2007) mention that the most important factors affecting the thermal conductivity in the fabric are "the thermal conductivity of the fiber composition and the ratio of fiber to air in the fabric."

Schuhmeister (1877) designs an equation for calculating the thermal conductivity of the fibers considering the thermal conductivity of the fabric and fabric structure which has a certain range of fabric porosities, under a prerequisite that the fibers are uniformly distributed in all directions. As an assumption, one-third of its plane slabs are parallel to the direction of heat flow, while two-third of its slabs are at right angles to the direction of heat flow. Equation 20 demonstrates the thermal conduction power of the fiber-air mixture under this assumption:

$$k_m = \frac{1}{3}(k_1 v_1 + k_2 v_2) + \frac{2}{3}\left(\frac{k_1 k_2}{k_1 v_2 + k_2 v_1}\right) \quad \text{(Eq. 20)}$$

where, k_m is the thermal conduction power of the fiber-air mixture, k_1,k_2 and v_1, v_2 are the conductivity and fractional volume of air and the fibers, respectively, and $v_1 + v_2 = 1$.

Mao and Russell explain that thermal conductivity is inversely related to thermal insulation and present ideas regarding structural properties affecting thermal insulation of materials. This means that, applying the concept of thermal conductivity, one can reduce heat transfer through the fabric. Therefore, to make a thermal insulated fabric, it is necessary to satisfy a balance between forming enough of the fibers to hinder convection and radiation effects, and minimizing the fiber content to decrease the conduction. For example, even

though highly dense fibers in the fabric are able to reduce the convective heat flow, the heat can be transferred by a type of conduction through the dense fibers. Table 6 shows the thermal conductivities of materials used by the textile industry. From this table, air's thermal conductivity is low, while that of PE fiber is high.

Table 6. Thermal conductivities of materials used by the textile industry

Material	Thermal conductivity *k* ($W*K^{-1} * m^{-1}$)	Density ($kg*m^{-3}$)
Nylon 6 fiber	0.25	1140
PET fiber	0.14	1390
PP fiber	0.12	910
PE fiber	0.34	920
Wool Keratin	0.1924	1300
Air (25℃)	0.024	1.29

Reproduced from 'The thermal insulation properties of spacer fabrics with a mechanically integrated wool fiber surface (2007)'

Many researchers have studied thermal insulation. Egan (1975) defines the thermal resistance as "a reciprocal of the heat flow coefficient (1/C)." C means conductance which is "a rate of heat flow through 1 sq ft per 1 ℉ temperature drop." This means that the denominator ($\frac{dX}{kA}$) in 'the Fourier's law' can be considered "the conduction resistance"

(ASHRAE Handbook, 2009). In addition, Janna (2000) points out that vapor condensation serves as a unique thermal insulation factor. For instance, during condensation, a phase change occurs from vapor to liquid at the fabric surface. The liquid covers the fabric surface as if it were a membrane, called the film-wise condensation. Therefore, the membrane establishes a temperature gradient between the fabric surface and environment. This means that the membrane acts as a thermal resistance to heat transfer.

On the other hand, if the condensed vapor forms a droplet on the fabric surface by using special treatments, such as coating and vapor additive, it is able to improve the heat transfer because the liquid does not cover a large portion of the fabric surface. In particular, Janna explains that the heat transfer rates of the drop-wise condensation are 10 times higher than those of the film-wise condensation. Therefore, it is important to know how a fabric surface is treated.

2.2.8. Interaction between Mass and Fabric

This section gives a general discussion of flow of water and gas because it is important to consider their molecular (mass) movement by the energy flow in the textiles. McPherson (1993) defines a fluid as "a substance in which the constituent molecules are free to move relative to each other." The main factor of a driving force for the fluid is the pressure difference working across the fabric length. In particular, this pressure difference can be induced by the surface tension difference between two phases (Verry, Michaud, and Manson, 2006).

The fluid flow can be explained by some theories, such as Fick's law, wicking, wetting,

and capillary power in the textiles; at first, Fick's law describes a diffusion theory of mass flow in a thin membrane, such as fabric. In particular, this theory is capable of explaining the diffusion of water molecular in the fabric. Fick's law consists of two theories; the first law states "the flux of a component of concentration across a membrane of unit area is proportional to the concentration differential across that plane." And the second law is that as "the rate of change of concentration is proportional to the concentration gradient at that point in the membrane." Equation 21 and 22 explain Fick's first and second laws, respectively:

$$J = -DA\frac{\partial \emptyset}{\partial x} \quad \text{(Eq. 21)}$$

$$\frac{\partial \emptyset}{\partial t} = DA\frac{\partial^2 \emptyset}{\partial x^2} \quad \text{(Eq. 22)}$$

where, J is the diffusion flux in dimensions $(\frac{mol}{m^2 * s})$, D is diffusion coefficient or diffusivity in dimension $(\frac{m^2}{s})$, $\emptyset$ is the concentration in dimensions $(\frac{mol}{m^3})$, x is the position, and t is the time. This means that the first law characterizes the diffusion flux from regions of high concentration to regions of low concentration, while the second law describes the rate of accumulation of concentration in the material volume (Ostwald, 1891).

The equation structure of Fourier's law is similar to Fick's law. The difference between both of them is that, while Fourier's law is governed by the temperature gradient of a membrane, Fick's law is governed by the concentration gradient. In the former, the temperature gradient results in the energy flow, whereas the concentration gradient gives rise to the mass flow in the latter. Through these equations, it is possible to describe energy and mass flow passing a thin membrane or fabric. In addition, the phenomena regarding energy and mass flow through fabric are significantly consistent with the definition and role of the

boundary which determines a type of the system. This means that the fabric works as a boundary controlling interaction between human body and its surroundings.

When energy and mass transfer occur within a boundary, they interact with a property of the boundary. This means that heat energy and mass, which are delivered through convection, radiation, and evaporation, go into the fabric by capillary force. In particular, the vapor is condensed and makes a phase change to liquid between the skin and fabric determined by change of pressure (p), specific volume (v), and temperature (T). Condensed water goes through the fabric by a wicking phenomenon. Hernett and Mehta (1996) mentioned that wickability is defined as "an ability to sustain capillary flow." And, wettability is defined as "an ability of the surface to attract fluid when a fabric, yarn, or fiber is brought into contact with liquid."

Kissa (1996) defines wetting as the "displacement of fiber-air interface with a fiber-liquid interface," and defines wicking as "the spontaneous flow of liquid in porous substrate, driven by capillary forces." Kissa mentions that the capillary power is caused by wetting behavior, while spontaneous wetting gives rise to wicking by the capillary power. The wetting process is not different from the wicking one. The wetting process is a prerequisite to wicking. In addition, the wicking processes normally happen in one of two ways; wicking from an infinite liquid reservoir (e.g., immersion, trans-planar, longitudinal wicking), or wicking from a finite liquid reservoir.

Hollies (1957) states that the yarn structure of fabric is more important than chemical nature of the fibers as far as influencing capillary action is concerned. This means that movement of condensed water is controlled by the arrangement of the fibers characterized by

the capillary size and continuity. In addition, wetting of yarn and fiber are significantly affected by the roughness of the yarn surface. Therefore, physical factors, such as fiber cross-sectional shape, the yarn structure, and fabric construction, are important in influencing capillary force. Yoon (1984) mentions that capillary size, contact angle, and the surface tension affect the capillary force. In addition, Verry et al. (2006) defines the capillary pressure drop as "the work needed to replace a gas by a liquid within a unit volume of porous medium in a saturated flow." If its value is negative, the wicking phenomenon occurs. Therefore, an instantaneous absorptive power can be one of the factors having influence on the liquid transport through a fabric. Normally, this capillary power is induced from Laplace equation:

$$P = \frac{2\gamma \cos\theta}{R_c} * 100 \qquad \text{(Eq. 23)}$$

where, P is the capillary power; R_c is the radius of the capillary; γ is the surface tension of the liquid; and θ is the contact angle of the liquid-solid-air interface.

Capillary power shows relationships between capillary size, surface tension and contact angle. Capillary power has a positive relationship with surface tension, while it has a negative relationship with the capillary radius. Whang and Gupta (2000) mention that the surface wetting force includes various characteristics, such as the cosine of the contact angle, the work of adhesion, and the surface energy. In particular, as contact angle (θ) is an important factor is affected by the chemical constitution of fabric material which makes a boundary condition; it builds a contact shape of a liquid. Surface energy is another way of describing the wetting phenomenon. It is defined as "the inherent ability of a surface to interact with another surface." Normally, the higher the surface energy and lower the contact

angle, the surface is more rapidly wetted.

Normally, absorbency phenomena are characterized by the absorbent capacity and absorbency rate. Gupta and Hong (1994) explain that it is difficult to predict accurately by the values of the absorbent capacity and absorbency rate because the capillaries in fibrous structures are tortuous, easily deformed and non-uniform. The total volume of fluid absorbed is determined by the interstitial space between the fibers, the material properties, and the resiliency of the web in the wet state. This means that the structure of fabric and the nature of the fibers have significant influence on controlling the orientation of capillaries and the resiliency of the web. These fluid transport phenomena are important because they lead the gas and liquid to a new condition (p-v-T) of fabric from microclimate. Therefore, a process of their phase change can be largely different in accordance with the fabric structure and the nature of the fibers.

Barker (2006) explains that the distribution and amount of absorbed moisture are affected by the porous character of the moisture barrier component, the type of the thermal line, and the presence of underlying absorbent clothing layers. Li and Holcombe (1998) explain that environmental conditions also affect the sorption behavior of fibers. For instance, hygroscopic fibers release moisture, and heat is taken up by the fibers when humidity falls. On the other hand, they absorb moisture vapor when the humidity rises and latent heat.

Gibson (1997) mentions that water flowing convectively through hygroscopic porous materials has a tendency to be absorbed into fibers and give rise to swelling. This phenomenon, which directly reduces the free air volume within the fabric, tends to close off the pores in the fabric, and accordingly block the convective flow through the material.

Therefore, the swelling fiber causes changes in fabric structure and affects heat and water vapor transmission. This convective flow can be analyzed using Darcy's law given below:

$$Q = \frac{-kA\,(P_b - P_a)}{\mu L} \qquad \text{(Eq. 24)}$$

where Q (units of volume per time) is equal to the product of the permeability, k is permeability of the medium, A is the cross sectional area flow, $(P_b - P_a)$ is the pressure drop, μ is the dynamic viscosity, and across the thickness is L. To have a value of the Q, it is important to accurately measure $(P_b - P_a)$ of L.

2.2.9. Energy Flow Model

This section reviews the published work of many research studying the process of heat energy flow from a human body to an external environment. Gollnick and Hermansen (1973) show that it is important for researchers to accurately recognize and analyze how heat energy transfer affects comfort level between the skin and its external environment through the functional clothing. A goal of their research is to improve comfort for the human body by determining how to deal with heat energy in the microclimate using functional clothing.

For example, Kakitsuba (2004) has observed dynamic changes in local sweat and vaporization rates from microclimates under a hot environmental condition. Therefore, Kakitsuba divides the dynamic changes of heat gain and loss into three stages from skin to clothing in chronological order. In the first stage, the perspiration rate increases, and evaporation phenomenon follows causing water vapor to form in the microclimate. In the second stage, the microclimate is saturated by the water vapor and the vapor slowly condenses in the given space, while perspiration is continuously emitted from the body. The

condensed perspiration is slowly absorbed in the clothing. The third stage occurs when a part of the condensed perspiration passes through the fabric, and evaporation takes place on the clothing surface. Nelbace and Herrington (1942) have already called these three stages, 'reverse evaporation.' They states that the comfort sensation of the human body can be determined by transformation of the perspiration through these stages.

Figure 15 depicts the heat energy flow including evaporation provided by metabolic energy without considering external environmental factors. This figure shows a schematic of transformation of the perspiration and effects of heat energy transfer at each stage. Firstly, the human body creates perspiration and heat energy when it consumes food. Vaporization of the perspiration is governed by heat energy's enthalpy which is determined by a relationship of the internal energy, pressure, and volume in a microclimate condition in the second stage. Next, vapor generated from vaporization of the perspiration is absorbed into a fabric by wetting and wicking phenomena. Lastly, the fabric starts to emit the vapor into external environments by another enthalpy provided by heat energy held by the fabric. In addition, movement of the vapor is affected by conditions in the microclimate and environmental factors, such as temperature and vapor pressure at that time (Fahmy and Slater, 1976).

When heat and perspiration does not get transferred to the external, feeling of discomfort from abrasion on parts of the human body can occurs during exercise as well as after-chilling mainly because of vaporization and condensation. Therefore, researchers need to understand how heat energy flow changes, and what reactions are processed as heat energy passes through functional fabrics.

Based on existing studies, Lee and Little (2009) suggest a new heat transfer model

illustrating a pathway of heat energy flow. This model consists of conduction, convection, radiation, and evaporation from metabolic energy of a human body to an external environment at rest is shown in Figure 16. From this model, it is possible to anticipate how each energy type generated from metabolic energy is changed in a space between the layers or membranes which have different material properties

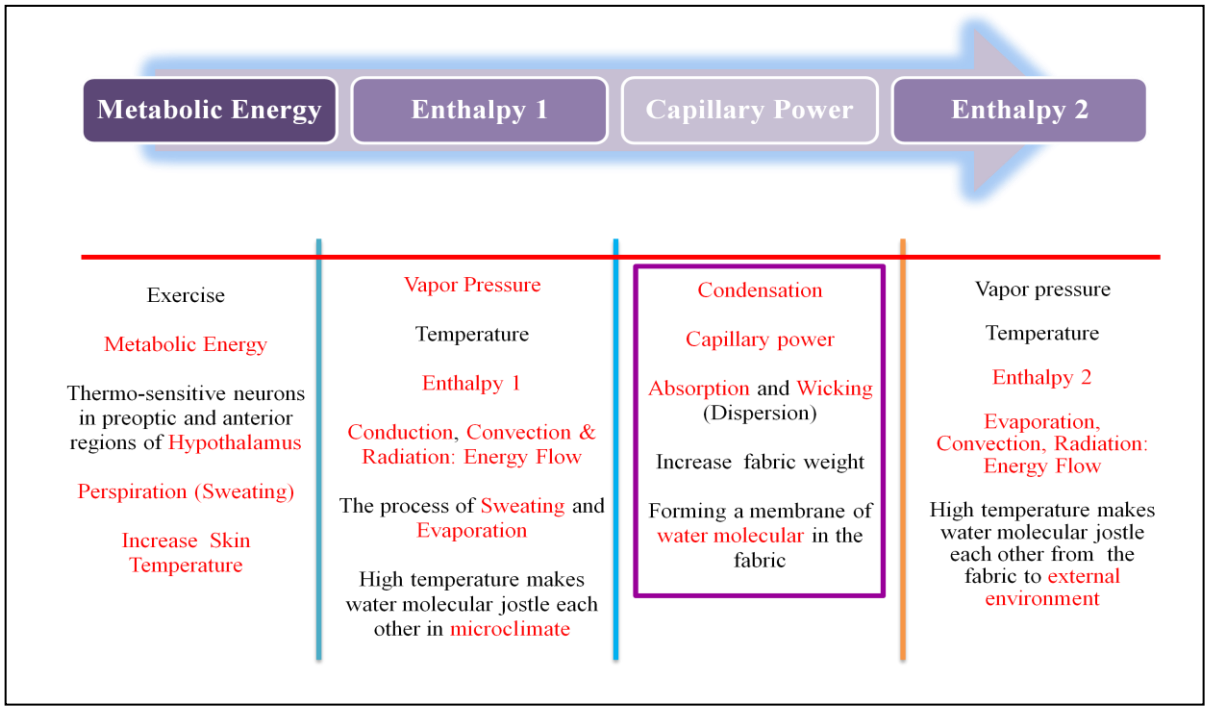

Figure 15. Analysis of Hybrid Energy Flow (Lee and Little, 2009)

.

In addition, Li (2006) observes that the heat and moisture transfer processes occur at the same time between phase changes (e.g., evaporation/condensation, absorption/desorption, freeze/melting) in a given space. He mentions that these types of heat and moisture transferring processes can be governed by the thermal functional performances of clothing,

activity levels of a human body, and external environmental conditions around the human body.

Chen (2008) conducts experiments that measure thermal performance of multilayer thermal insulation system by using radiation energy power. Chen found that heat energy is transferred by thermal radiation, solid conduction which consists of reflectors and spacer conductor and residual gas conduction. To analysis of the performance, he designs a mathematical model describing heat flux through a composite fabric. Through the model and a result of experiment, Chen demonstrates that thermal resistance of a multilayered system can be increased by bonding layers without having air spaces between fabric layers.

For the research discussed in the dissertation, it is shown that the function of each layer can be analyzed in terms of microclimate condition and the amount and rate of heat energy flow. Hence, the researcher is ultimately able to measure how clothing responds to the heat transfer in the human body. Figure 16 shows the heat energy flows (heat loss) and their ratios originating from metabolic energy.

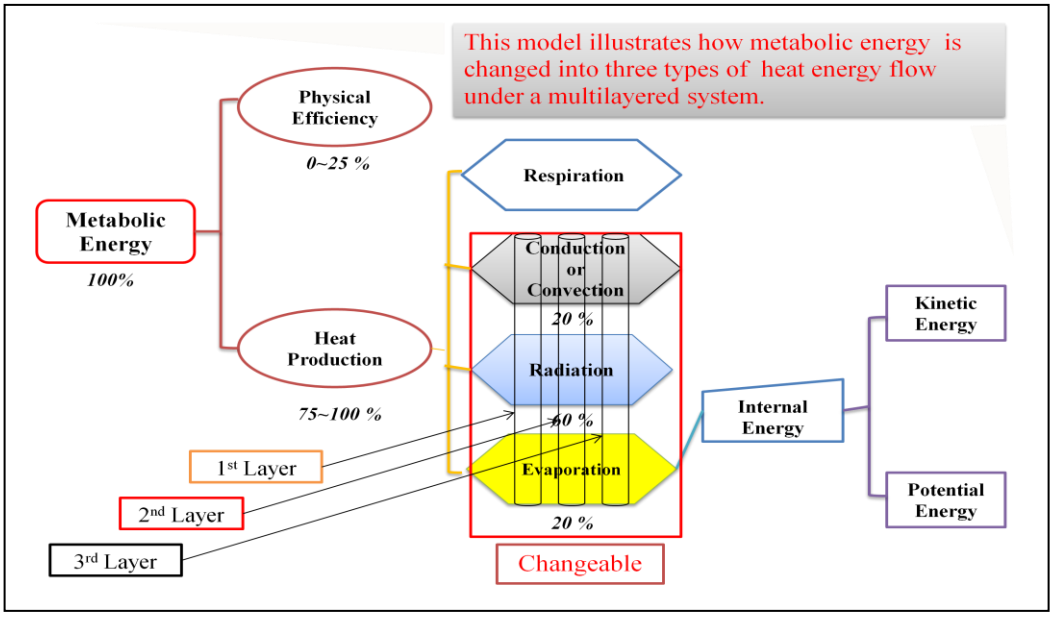

Figure 16. Energy flow model showing all of the energy flows originated from metabolism (2009)

This model is based on the first and second thermodynamic laws which illustrate a principle in the heat balance and heat transfer under a given environmental value (p-v-T) which is formed by the multilayered system. It indicates that these mass and energy transfers are based on the thermodynamics laws in an open system.

It particularly reviews the heat energy flow created from the metabolic process in a human body, and a role of multi-microclimate which is formed by fabric layers. Therefore, it focuses on what energy is and its flow through the fabric. The heat energy flow is transformed into a variety of forms, such as evaporation, radiation, convection, and conduction. It means that the metabolic energy is ultimately governed by the laws of thermodynamics because the human body itself is a small kind of open system in the universe. A theory regarding the phase change of the material provides a theoretical background about

vaporization of perspiration under certain environmental conditions of the microclimate between the human body and clothing.

This heat energy flow, evaporation, conduction, radiation, and convection, interacts with fabric consisting of two phases, fiber materials and air porosities. However, each energy flow mode is governed differently by the fiber material and the process structure of the fabric. This means that the reaction of conduction is different from that of convection and radiation depending on the structure of the fabric.

Therefore, Janna (2000) mentions that thermal conductivity of the fabric can be a property identifying the structure of the fabric by controlling the energy flow. In addition, when the mass goes out into surroundings from a system which is the human body, the fabric works as a boundary controlling the mass transfer with a variety of processes, such as condensation, wetting, and wicking by the capillary power. Therefore, it is important to consider the kinds of processes are involved in the heat energy flow and the role of fabric boundaries in accordance with activity levels of the human body.

2.3. Energy Types

2.3.1. Metabolic Energy

The word ‘metabolism’ originating from the Greek means “change.” The reason this section studies a metabolic process is that it provides heat energy and water in accordance with activity levels of the human body. Schilling (2000) defines metabolism as “the complex physical and chemical processes that are involved in the maintenance of life.” Metabolism is performed through enzymatic reactions and transformations of food molecules in the human

body.

Many researchers, such as Guyton (2000) and Miller (1968), have studied the process of how a human body gets energy to run and maintain an organism's muscles by consuming food through chemical reactions in the metabolic process. According to the "Medical Physiology" of Guyton (2000), nearly all of the energy produced by metabolism is transformed into body heat. This means that, about 20% to 25% of the body's heat energy will be used for muscle, and the remaining will be changed into heat for running intracellular chemical reactions in the body.

The process of metabolism can be largely divided into two kinds of activities that provide energy and water: Anabolism and Catabolism. Guyton (2000) define anabolism as "a process by which living organisms synthesize complex molecules of life from simple one," while Albert-Wallerstrom (1985) defines catabolism as "a process of breaking down large molecules into small molecules." Since anabolism and catabolism are convergent processes, they consistently and repeatedly produce heat energy and water. Another role of anabolism is the formation of larger and more complex molecules, such as peptides, polysaccharides, and lipids needed by the body, while an important role of the catabolism is to break down large molecules to get the required water and to maintain an organism.

In detail, the chemical reactions are also divided into two processes, condensation and hydrolysis, in accordance with anabolism and catabolism; Condensation is related to the formation of large molecules and produces water molecules through the reaction between the alcohol group and glucose. Hydrolysis breaks down large molecules: a digestive system softens up the connections of polymer and produces monomers during insertion of a water

molecule. In addition, several kinds of hormones adjust the speed of metabolic processes. For instance, Thyroxin controls the speeds of those chemical reactions through the thyroid glands during a metabolic process.

Guyton (2000) and Wren (1997) explain that a human body performs aerobic respiration using Oxygen (O_2) to produce the energy called Adenosine Tri-Phosphate (ATP) through the process. If one glucose molecule combines with oxygen, it produces carbon dioxide, water, and energy. According to Rhoads' explanation, the oxygen taken in by the lungs is delivered into the body through flowing blood cells which plays an important role in producing biochemical energy from food. Whenever a cell of the organism needs energy, ATP produces the energy, while bonding the water molecules. Through those processes, one phosphate molecule is released, and it forms adenosine diphosphate (ADP). Equation 25 shows the conversion process from ATP to ADP. Figure 17 illustrates the relationship between ATP and ADP:

$$ATP + H_2O = ADP + Pi + Energy \qquad \text{(Eq. 25)}$$

A main role of ATP generated from the metabolic process is to deliver organic materials, such as sodium, calcium, and potassium, through a cell membrane, to synthesize chemical compounds, such as protein and cholesterol, as well as to supply energy for mechanical work.

Durnin (1974) mentions that these energy calories are used for representing three components; The Basal Metabolic Rate (BMR) uses 50-80% of total calories to maintain the body. While a male's BMR is normally 7,100 kJ per day, a female's BMR is about 5,900 kJ per day. Generally, the BMR is affected by several factors, such as body size, age, gender, and growth, physical activities use about 20% of total calories, which means that the muscles

exerted for physical activities use approximately 3,000 kJ per day and, finally, the thermic effect of food consumption is about 5-10%. Figure 18 shows the components of energy expenditure.

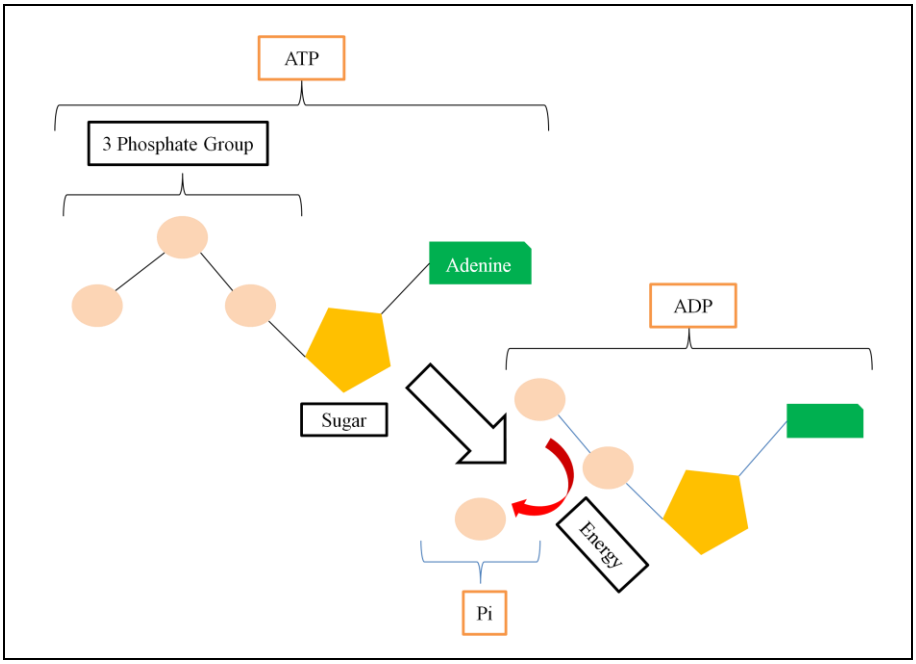

Figure 17. A schematic of production process of the energy from ATP

Reproduced from http://www.revisionworld.co.uk/node/8988

As mentioned above, the human body emits heat energy and water throughout the metabolic process. According to Guyton's book, "the total average amount of water in a man (70 kg) is about 40 liters, averaging 57% of his total body weight (1 liter = 1kg at 4°), and he also loses about 2.37 liters of the water through perspiration." Therefore, about 2,500 kilo-calories (about 11000 kJ) of the heat energy is released from an adult male every day. However, the amount of heat energy emitted from his body is not stable due to internal

factors, such as age and weight; and external factors, such as temperature, humidity, and perspiration.

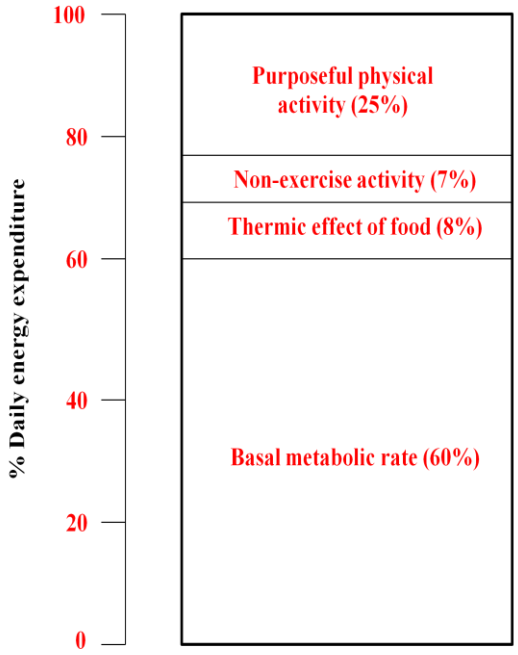

Figure 18. Components of energy expenditure

Reproduced from 'Medical Physiology (2000)'

2.3.2. Radiation

Because radiation is delivered as a type of electromagnetic wave, many researchers have suggested that radiation is a type of heat energy transfer through space. Guyton defines thermal radiation as "electromagnetic radiation emitted from the surface of an object due to its temperature." Therefore, everything which is above 0 K (Absolute Kelvin) is supposed to emit the radiation. For instance, the human body is able to feel heat or warmth from the thermal radiation of the sun without touching the heat source. Figure 19 shows a person's

heat energy which is radiating away in the form of infrared energy.

Hardy (1937) studies a relationship between radiation intensity and wavelength which provides information about the materials' temperature and energy. Normally, the full spectrum of electromagnetic radiation is divided into several ranges of the wavelength, such as gamma rays, x-rays, ultraviolet, infrared, microwave, and radio wave. In addition, to accurately understand the radiation, a concept of a black body should first be clearly defined. Hardy mentions, since the black body is a theoretically idealized object, it absorbs and emits 100 % radiant energy.

Figure 19. Thermographic image of the human body

Reproduced from Reproduced from http://classeshsares.student.usp.ac.fj/PH202/

The release of radiation from a black body depends on temperature change and the thermal radiation which is generated from the black body that characterizes the temperature-dependent spectrum of light. Hence, a blackbody is known as "thermodynamic equilibrium state of light" and shows several colors of visible radiation, such as red, yellow, and blue, based on temperature change. Hence, the researcher should have a basic knowledge of the

black body. Even though the human body is not a black body, researchers are able to compare a ratio at every wavelength emission of the real human body with that of a black body. Figure 20 shows black body radiation in relation to temperature change. It indicates that the higher the temperature, the greater the total amount of radiation.

The Stefan-Boltzmannn equation is applied to explain a radiation process for two viewpoints of the temperature and the object's area. The Stefan-Boltzmannn equation states that "the total energy radiated per unit surface area of a black body in unit time, *j*, is directly proportional to the fourth power of the black body's heat temperature T (absolute temperature)." Equation 26 states the total absolute power of energy radiated for an object's surface area, A (inch per m^2)

$$P = Aj = A\varepsilon\sigma\,(T^4 - T_0{}^4)\ (j/m^2s) \qquad \text{(Eq. 26)}$$

Where, P is total absolute power of energy per area, A is radiating area, *j* is total energy, σ is Stefan's constant, T is the radiator's temperature (Kelvin), ε is emissivity (1 for ideal radiator) Through the Stefan-Boltzmannn equation, the radiation of a human body can be calculated.

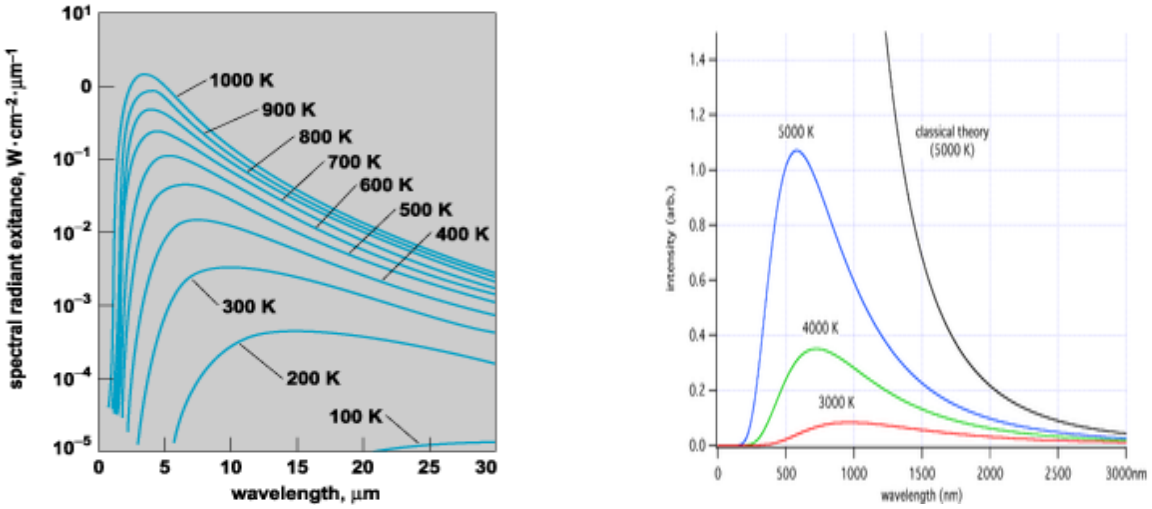

Figure 20. Black body radiation in relation to temperature change

Reproduced from http://en.wikipedia.org/wiki/Black_body

The Stefan-Boltzmannn equation supports Planck's law which indicates the distribution of energy in the spectrum, and is developed to explain the spectral radiant existence in W m^2 μm^{-1}. The concept of Planck's law states that "the spectral distribution of thermal radiation is emitted by an ideal radiator which is a black body." From this spectral distribution, it is possible to predict temperature level of a material. This means that the longer its wavelength, the lower the frequency. Lower frequency is associated with lower temperature in the black body's spectrum. In addition, it assumes that all objects including atoms and molecules make thermal radiation because of their thermal motion or movement. Plancks' law is given in Equation 27:

$$M_\lambda\,(\mathrm{T}) = \frac{2\pi hc^2}{\lambda^5\left(e^{\frac{hc}{\lambda kT}}-1\right)} \qquad \text{(Eq. 27)}$$

where M_λ is the spectral radiant exitance in W m^2 μm^{-1}, T is the black body temperature in

Kelvins, λ is wavelength in μm , h=6.626176* 10^{-34} Js is the Planck constant, c=2.9979246*10^{8}m/s is the speed of the light in the vacuum, k=1.380662*10^{-23}JK^{-1} is the Boltzman's constant.

Body temperature varies at each part of the human body. For example, temperature change in the head and face area of the human body is a little bit higher than that of other parts. In addition, Guyton (2000) explains that a temperature range of nude person starts from around 55℉ (12.8℃) to an extreme of 130℉ (54.4℃) in dry air. However, under these conditions, the temperature range of a human being is generally between 97℉ to 99.5℉. According to research by Hardy (1937), radiation has its maximum value at 22℃ to 23℃, where its amounts are approximately 70% of the total heat loss. The amount of radiation consistently decreases as temperature increases and becomes zero at 35℃. In addition, a temperature zone, where "radiation is the same as vaporization, is called 'neutral zone,' at 31℃." Figure 21 shows temperature differences in relation to measurement of positions and the activity level of the human body.

All objects whose temperatures are over 10℃K emit infrared radiation, and there is a distinct difference regarding the amount of the radiation among the objects. The human body also emits infrared radiation which is below the red and visible light in relation to temperature change. This means that temperature can be an important variable to measure the radiation emitted from the human body.

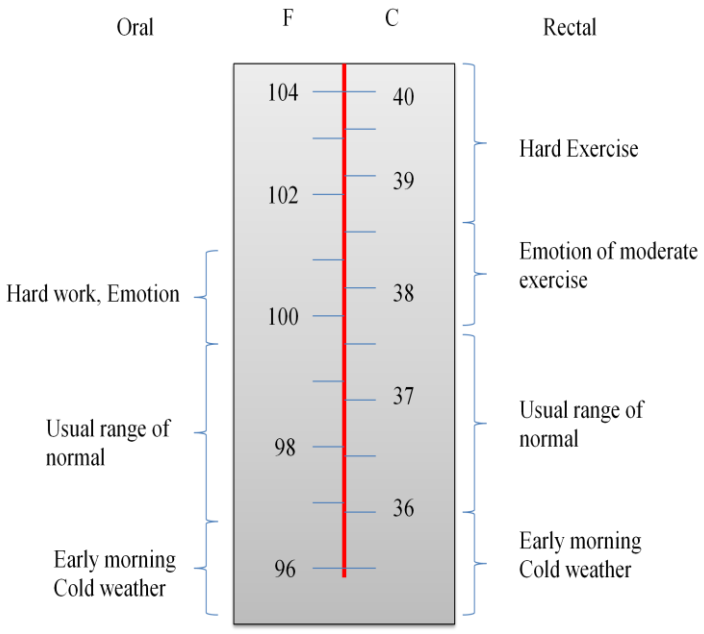

Figure 21. Different temperature according to measurement positions and a level of activities of the human body reproduced from 'Medical physiology (2000)'

2.3.3. Evaporation

Albert-Wallerstrom (1985) states that "the evaporation of sweat is of paramount importance for body temperature regulation, and thereby assuring human wellness in hot environments." Other researchers (Candas et al, 1979; Givoni 1976; Kerslake 1972) point out that the latent heat of vaporization plays an important role in dissipating heat through perspiration at skin temperature. Givoni (1976) mentions that the evaporation ratio of the human body approaches up to 20% of the total heat energy ratio, however, its efficiency decreases after passing 20%. Kerslake (1972) explains that all of the perspiration cannot be evaporated from the skin. About 40% of the perspiration drips off when the skin is fully saturated. Hence, Candas (1979) explains that efficiency of perspiration is determined by the

ratio of evaporated sweat and secreted sweat which drip from the body.

In addition, perspiration alone cannot run a cooling mechanism and is not related to the heat energy flow. This means that the cooling mechanism of perspiration occurs in reaction to external factors, such as temperature, relative humidity and vapor pressure. Figure 22 simply shows the perspiration structure of the human body.

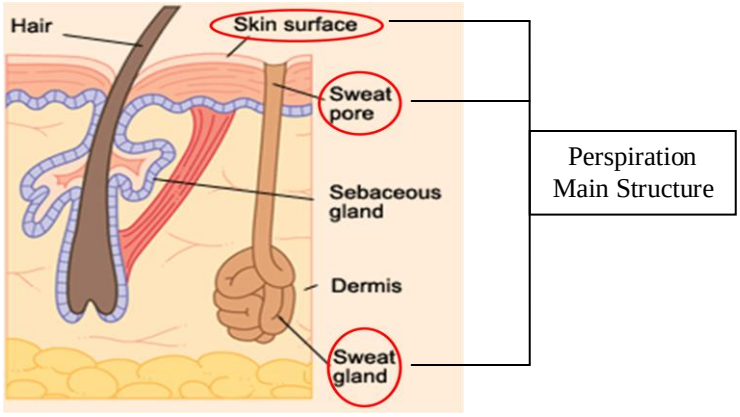

Figure 22. A perspiration structure of the human body

Reproduced from http://www.klimadeodorant.com/blog/hyperhidrosis-faq/72/

Kerslake (1972) showed that air humidity and velocity are core factors affecting the ratios. Ayling (1984) indicated that evaporation rate is controlled by external factors, such as humidity, vapor pressure, air flow, and temperature. For example, Beaumont and Buillard (1963) observe that the reaction of initial perspiration starts within 1.5 seconds in a warm environment (37.5℃) during exercise.

Generally, evaporation of perspiration is another process in which the different temperatures between clothing and skin cause heat energy flow. The temperature difference

causes a divergence of the vapor pressure and induces the evaporation flow in a given volume. This heat energy, which produces kinetic and potential energy, transforms perspiration into condensed water or vapor between skin and external environments. Hence, the heat energy runs and supports the cooling mechanism by causing vaporization of the perspiration. Figure 23 shows a schematic of three energy flows, vaporization, convection, and conduction, from the muscle to external environments.

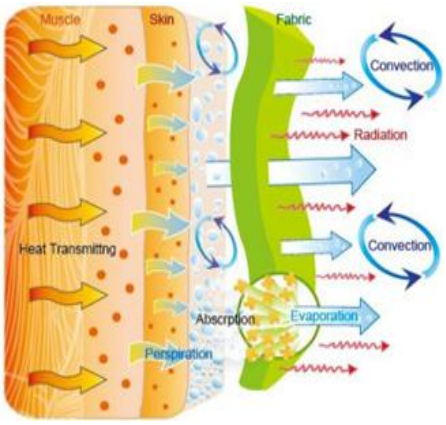

Figure 23. A schematic of heat energy flow from muscle to external environments

Reproduced from http:// www.hyperphysics.phy-astr.gsu.edu/hbase/HFrame.html

In particular, Guyton (2000) states that 0.58 calories of heat energy are consumed in the evaporation of each gram of water from the skin surface. Even though a person is not sweating, he/she is constantly emitting perspiration from the skin and lungs at a rate of about 450 to 600 ml/day. This means that sweating causes heat loss at a rate of 12 to 16 calories per hour. Normally, the human body emits insensible perspiration continuously before it recognizes perspiration as moisture. The human body is able to control the sensible

perspiration, whereas it cannot regulate the insensible sweating because it physiologically occurs in the diffusion of water molecules through the skin and respiratory surface.

In addition, Havenith (2002) and Guyton (2000) explain the heat loss mechanism from the body; if the skin temperature is higher than that of its surroundings, the heat energy flow is emitted by radiation, convection, and evaporation. However, if the surrounding temperature is greater than skin temperature, the body is reversely affected by radiation and convection of the surroundings and emits perspiration to regulate its temperature. This means that the human body continuously reacts with ambient environmental conditions. Figure 24 shows the rate of heat loss through four types of heat energy flow under surrounding environments at rest.

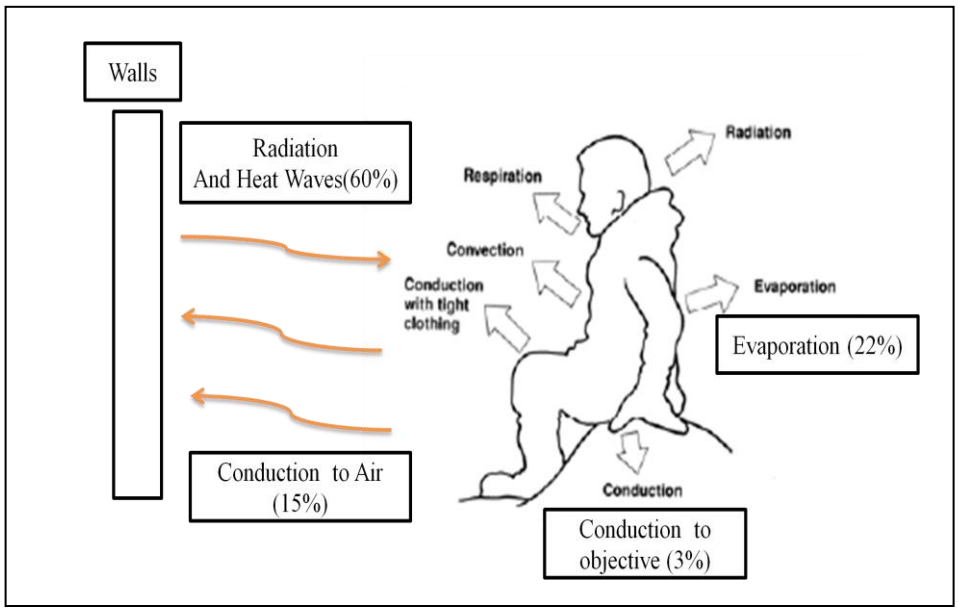

Figure 24. Mechanism of heat loss from the body

Reproduced from Medical physiology (2000)

Havenith (2005) reviewed the work of many researchers who studied the process of heat and mass exchange between a human being and external environments. Based on these existing studies, Havenith posits a heat balance equation for determining and explaining heat generation and heat transfer;

$$DRY\ (R + C + K) = M - W - EVAP - RESP - S \qquad \text{(Eq. 28)}$$

where, M is metabolic rate, W is external work, R is radiation, K is conduction, EVAP is evaporation, RESP is respiratory heat losses, and finally heat storage in the human body. Havenith explains that "the DRY value is used to measure thermal insulation of the clothing, while EVAP is used to calculate the clothing vapor resistance."

2.3.4. Convection and Conduction

Guyton (2000) defined convection and conduction as "a removal process of heat from a body by air current, and as a phenomenon of heat lost from surface of a human body to solid objects, such as chair and bed respectively." Energy flow by convection is transferred into air, and it moves from a high temperature to a low temperature. In a human body, heat transfer by convection is caused by the kinetic energy of molecules in motion by skin vibration generated by an external fistula. Its velocity depends on a temperature difference between skin and an external environment. For instance, if the ambient temperature is the same or higher than skin temperature, no further heat loss occurs from the human body. Figure 25 simply shows how convection and conduction work:

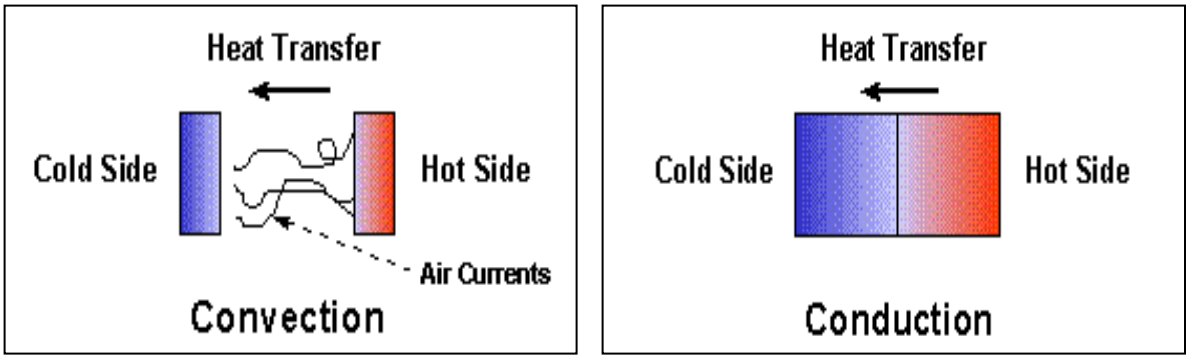

(A) (B)

Figure 25. A physical difference of convection (A) and conduction (B)

Reproduced from http://theory.uwinnipeg.ca/mod_tech/node75.html

Fowler (2005) mentions that convection is a gravitationally induced heat transfer. Therefore, the movement of convection depends on temperature differences occurring at different levels of density. This means that heat energy dispersed by convection moves to a colder place with a higher density. Guyton explains that convection is related to the magnitude of the cooling effect of the wind. This means that "the cooling effect of wind is proportional to the square root of the wind velocity at low wind velocity." For instance, "wind at 4 miles per hour is about twice as effective for cooling as wind at 1 mile per hour."

Kaminski (2005) noted that conduction is another type of heat flow in an isolated solid having a different temperature range. Heat transfer by conduction is transferred between two places where there is a difference in temperature. This means that temperature difference drives the heat transfer. The amount of heat transferred is adjusted by the magnitude of thermal resistance between two places.

While molecular vibration within a material causes heat transfer of the conduction

type, convective heat transfer within a liquid or gas flow occurs at different temperatures from a thermal and fluid engineering viewpoint. de Dear (1996) states convective heat transfer as a result of a vibrating airstream from the body's surface to clothing. de Dear classifies the process of convection from the human body into three modes: the first is natural convection, which is controlled by thermal buoyancy and ambient air speeds lower than 0.2 m/s; the second is forced convection, which has higher speed than 1.5 m/s, and finally mixed mode convection, which has a speed midway between natural and forced convection.

Kurazumi (2004) studied relationships between human postures and convection areas. Kurazumi defines an effective thermal convection area factor as the ratio of the maximum body surface area that is exposed to airflow, compared with the total surface area of the human body. Currently, when researchers calculate the amount of the convective heat transfer coefficient, some researchers have assumed that convective heat transfer naturally occurs through expansion and bouyancy forces.

Galimidi and Stewart (1979) mention that the researcher is capable of measuring the change rate of the convective heat transfer coefficient in relation to a naked human body's movement because the heat exchange rate depends on the velocity of the air free stream between the wet surface on the human body and its ambient environment Therefore, the convective heat transfer coefficient can be different in accordance with the human body's postures or actions. Ishigaki (1993) also illustrates that an accurate convective heat transfer coefficient, through analysis regarding the human body's divergent movements, is required to calculate convective heat loss from the body. Hardy (1937) explains that the amount of convection accounts for about 15% of all of the heat transfer when the human body is in a

static state, and it can be increased according to airflow movement on a human body's surface.

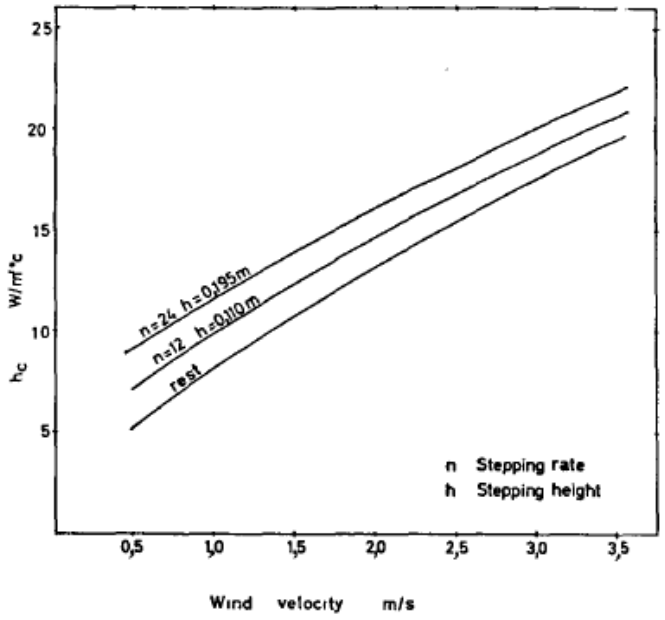

Figure 26. Convective heat transfer coefficient according to a position

Reproduced from 'The effect of body motion on convective heat transfer from a nude man (1979)'

Hence, when a human body makes rapid movement, it causes convective heat transfer as high a value in strength on airflow. However, the convection becomes zero at 35℃ in an external environment based on a result of the experiment. This means that convection has a negative relationship with a warm environment. Figure 26 shows the relationships between the convective heat transfer coefficient (h_c), stepping rate (n), and stepping height (h), as wind speed (m/s) changes. It shows that, if stepping rate and height are high values, convective heat transfer coefficient increases as wind velocity increases. In addition,

convection is significantly related to air flow speed in an external environment.

Many researchers are interested in the thermal state surrounding the human body in order to calculate the convective heat transfer coefficient. Kandjov (1999) says that, as the human body is an open thermodynamic system, it consistently exchanges energy and mass with its surrounding area. Normally, to calculate the amout of heat transferred during neutral convection(Q), the researcher needs information regarding the heat transfer coefficient (h), area (A), and the temperature difference (T_1: Temperature at the surface of the object) and (T_2: Temperature of the surrounding medium such as the temperature of the air). Equaiton 29 is called Newton's Law of Cooling. In this equaiton, it is imperative to consider the value of the convective heat transfer coefficient (h).

$$Q = -hA(T_1 - T_2) \quad \text{(Eq. 29)}$$

In addition, even though the amount of heat flow by conduction is small, it is a part of the heat energy originating from the human body. Fourier's law (Eq. 30) explains the conduction component of heat transfer:

$$Q = \frac{kA}{dx}(T_1 - T_2) \quad \text{(Eq. 30)}$$

2.4. Dynamic moisture movement testers

2.4.1. Introduction

Many researchers have conducted moisture management experiments of using functional fabrics through various and recognized testing instruments in accordance with testing codes, such as those of the American Society for Testing and Materials (ASTM) E 96,

British Standard (BS) 7209, and International Organization for Standard (ISO) 11092 (ASTM E96, 2000; BS7209, 1990; ISO11092, 1993). Milenkovic (1999) states that these testing codes describe detailed testing procedures, conditions of the sample fabrics, and test instruments. These published standard testing codes define the moisture management as water vapor transmission (WVT), water vapor permeability (WVP), or water vapor resistance. Wallace (2002) also defines moisture management as 'movement between moisture vapor and liquid from the surface of the skin to the atmosphere through a fabric.'

Wallace measures moisture vapor transmission rate (MVT) which means the rate of moisture vapor passing through a fabric. The testing instrument measures the amount of moisture vapor in grams that pass through $1m^2$of fabric in 24 hours with a specific driving force. ASTM E 96 describes the open cup testing method to test the MVT. The fabric is set up inside of the beaker containing water. Self-adhesive plastic tape secures the mouth of the beaker ($3000mm^2$). Ambient temperature is about 29-30℃. The weight of each container is accurately checked within 0.1 mg as time passes. Figure 27 shows the moisture vapor tester, open cup testing instrument. During the time of testing the fabric, temperature, pressure, and relative humidity should be appropriately controlled in the testing environment.

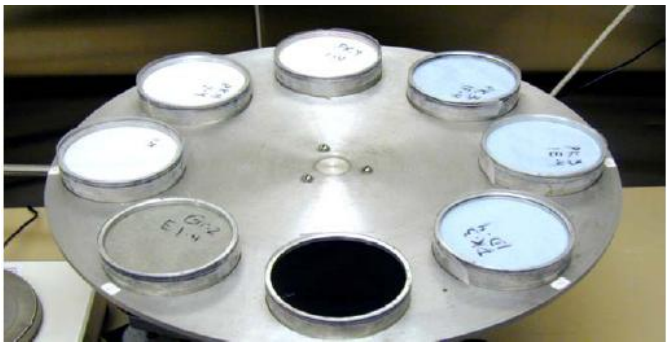

Figure 27. Moisture vapor test – Open cup testing instrument

Kannekens (1994) explains a skin model test developed by the Hohenstein Institute. This method considers a situation of "skin/air/textile" microclimate that is created when a wearer puts on breathable clothing. The skin model test (DIN 54101) can measure thermal resistance ($m^2 * K/W$) or water vapor resistance ($m^2 * mbar/W$). Kannekens explains how to make these measurements using the skin model testing instrument in detail. The test specimen is placed on a porous plate where temperature can be controlled by electric heat. Then water is fed to the test specimen on the plate which is coated by a water permeable membrane. At that time, a steady power is given to measure the amount of water evaporating and water resistance of the test specimen.

However, Havenith (2002) discusses potential errors or mistakes the researcher may cause while conducting the experiment, and that the test may exactly reflected an actual situation which includes external environments. For example, Hes and McCullough (2004) found that these testing instruments and methods need a great deal of time to get an accurate result. Also, many researchers and manufacturers wonder if the results of these measurements accurately reflect a level of moisture management function of the fabrics or not because perspiration which is emitted from human body is not steady but dynamic (Elizabeth, 2006 and Dionne, et al., 2003).

Therefore, other testing instruments, such as dynamic surface moisture tester and moisture management tester (MMT), have been developed to correct those weaknesses of testing instruments and more accurately measure the moisture management function (Scheurell, 1985; Hu, 2005). Even though these new testing instruments are not registered by

international standard testing institutes, currently many researchers and manufacturers take advantage of these testing instruments because they address the weaknesses, such as the excessive time consumption and high cost, of the confirmed testing instruments (Wehner, 1988).

Therefore, a goal of this section explains five dynamic moisture management testers, Moisture Management Tester (MMT), Alambeta instrument (Permetest model), Dynamic surface moisture tester, Human-clothing-environment simulator and Gravimetric absorbency test system (Hes et al., 1996; Eunae, 2006, and Wallace, 2002). Through reviewing procedures and conditions of these testing instruments, the research provides information regarding which testing instrument is more suitable for dealing with moisture management relative to various end users' purposes (Adler, 1984).

2.4.2. Moisture Management Testers

2.4.2.1. Moisture Management Tester (MMT)

2.4.2.1.1. Introduction

This testing instrument is developed by Hu (2005) and measures liquid moisture transport ability affecting the moisture sensation of the human comfort perception. Li (1998) mentions that the human body automatically regulates its biological cooling system by emitting perspiration in order to respond to the external environment, such as temperature and relative humidity. However, the perspiration and vapor may cause discomfort, such as after-chilling and abrasion, between skin and a fabric in the microclimate. Therefore, a functional fabric tries to efficiently manage the perspiration and vapor to improve the tiny

space and ultimately the comfort of the human body.

Therefore, this testing instrument and method explain how to measure the dynamic liquid moisture transport ability through a sample fabric. In particular, it evaluates the moisture management functionality of the fabric through comparison between quantitative information of the overall moisture management and subjective evaluations of the runner's discomfort e.g., damp and clammy. Even though many instruments have tried to measure simple absorbency and wicking based on ISO 9073-8, they don't seem to specialize in measuring the dynamic liquid transport ability of perspiration through fabric materials (Bhat, 1990).

2.4.2.1.2. Apparatus Design

Hu has mentioned that this testing instrument takes advantage of a property of the electric resistance in a fabric. Since the fabric itself normally has a huge electric resistance, the electric current movement is prevented from passing through the fabric. However, Kraning (1978) and Tagaya (1987) mention that fabric saturated by water is changed into a conductor. This means that the water component and water content included in the fabric make the insulation property of the fabric change into a conductor type which allows electric current flow.

Figure 28 simply shows a simple model of the moisture management tester and its sketch. It shows that upper and lower sensors wrap the sample fabric and coppery ring between Vss and GND, and water is provided through a sweat gland. As the water is slowly spread from the top surface of the fabric to the bottom surface of the fabric, the coppery ring,

which is inserted into the fabric, responds to electric voltage. A data logger records change in the electric resistance of the fabric. Temperature and relative humidity of the chamber room are adjusted to 21 +/- 1℃ and 65 +/- 2% respectively. This condition should be equally maintained for 24 hours at least before the test (ASTM D1776, 2004).

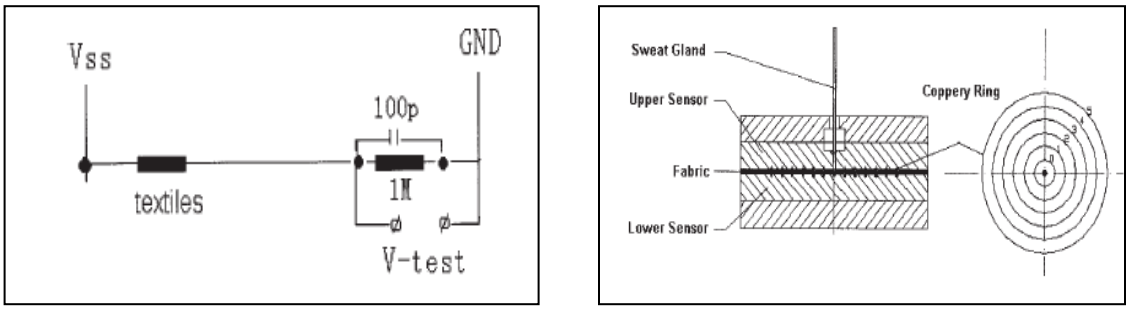

(A) (B)

Figure 28. (A) A simple model of the testing method and (B) a schematic of tester sensor Reproduced from "Moisture Management Tester (MMT): A method to characterize fabric liquid moisture management properties"

As a result of the experiment, the researcher is able to get information about the overall moisture management capacity (OMMC) consisting of 3 factors, such as moisture absorption rate of the bottom side (MAR), one-way liquid transport ability (OMTC), and moisture drying speed of the bottom side (SS). Therefore, the OMMC can be defined as

$$\mathrm{OMMC} = C_1\mathrm{MAR} + C_2\mathrm{OMTC} + C_3\mathrm{SS} \qquad \text{(Eq. 31)}$$

Where C_1, C_2 and C_3 are the weights of the indexes of the MAR, OMTC and SS. These indexes are determined by the end users' purpose. Therefore, the researcher is able to measure and evaluate the dynamic liquid transport ability of the functional fabrics through

numerical information of the OMMC.

2.4.2.1.3. Results and Analysis

As a result of the fabric test using MMT, Hu gets numerical information about OMMC consisting of wetting time, maximum absorption time, maximum wetted radii, and spreading speeds. Also, Hes gets cumulative one-way transport capacity by the fabrics' properties, such as weight, thickness, fabric content, and fabric constructing. In addition, Hu compares subjective data regarding runners' comfort feelings, clamminess and dampness, with the objective data, the OMMC, to identify reliability of the experiment. To conduct a comparison experiment, twenty-eight female participants between ages 18 and 35 run on the treadmill for 20 minutes and then rest for 30 minutes repeatedly. The result of the experiment shows that their comfort sensations have significant co-relationship with the OMMC from 15 to 20 minutes, while they have no relationship with OMMC from 0 to 5 minutes respectively. Figure 29 show a model of Moisture Management Tester (MMT), and Table 7 shows an OMMC result obtained from of eight fabrics for nine factors, such as One Way Transfer Capacity (OWTC), Spreading Rate (SS), and Medium Wetted Radius (MWR). Figure 29 shows a model of Moisture Management Tester (MMT).

Table 7. A result of OMMC of various fabrics

Fabric		WT_t	WT_b	MAR_t	MAR_b	MWR_t	MWR_b	SS_t	SS_b	*OWTC*	*OMMC*
N88P	mean	3.74	3.44	20.07	39.30	15.00	15.00	0.82	0.87	45.31	32.70
	SD	0.56	0.42	3.77	19.01	0.00	0.00	0.09	0.09	17.68	12.98
C98L2	mean	4.98	4.39	23.15	56.25	14.38	12.50	0.75	0.81	38.33	33.43
	SD	1.23	0.48	6.23	22.90	1.77	2.67	0.07	0.16	15.35	10.68
N85L15	mean	3.03	8.32	105.65	135.44	8.13	5.63	1.08	0.49	−10.50	28.73
	SD	0.11	2.66	21.00	43.47	2.59	1.77	0.50	0.16	51.86	27.37
R95C	mean	3.46	119.95	70.54	0.70	10.00	0.00	0.89	0.00	−208.51	−104.08
	SD	0.25	0.00	9.79	0.37	0.00	0.00	0.08	0.00	7.39	3.69
P98L2	mean	3.15	13.52	101.67	194.57	7.50	6.88	1.10	0.30	2.81	50.12
	SD	0.13	3.50	18.72	49.00	2.67	2.59	0.64	0.15	25.43	23.58
E95C	mean	3.17	119.95	93.71	1.18	10.00	0.00	0.93	0.00	−273.96	−136.69
	SD	0.20	0.00	26.41	0.73	0.00	0.00	0.09	0.00	36.97	18.46
A92Np	mean	6.33	4.23	20.46	65.11	8.75	10.63	0.67	0.80	103.74	68.35
	SD	0.98	0.38	8.28	12.82	2.31	1.77	0.09	0.12	9.81	7.26
N95C	mean	7.51	7.16	41.14	22.39	6.88	10.00	0.64	0.58	−18.13	−3.33
	SD	1.98	0.75	32.62	7.24	2.59	0.00	0.30	0.06	17.68	9.47

Figure 29. An actual model of Moisture Management Tester (MMT)

Reproduced from http://www.sdlatlas.com/html/moisture_management_tester_0.html

2.4.2.1.4. Advantages and Limitations

This testing instrument uniquely considers and uses electric properties to measure the dynamic liquid transport ability of the fabrics. As another advantage of the experiment, it delivers numerical result regarding OMMC in a relatively short period of time. However, the

principles of this testing instrument do not follow any international testing standards, and the result of this instrument from 0 to 5 minutes was not matched with subjective results, dampness and clamminess. In addition, the definitions of C_1, C_2 and C_3 are largely unclear, which means that the weight of the indexes is too subjective because they can be determined by means of the end users' purpose. If the end users were different, they might have different results of the OMMC using the same sample fabric

2.4.2.2. Alambeta Instrument

2.4.2.2.1. Introduction

Mikolajczyk et al. (2005) mention that a current major issue in functional fabric market is how to measure and deal with water vapor permeability of sports and protective garments to improve comfort sensation of the human body. However, confirmed testing instruments have some weaknesses, such as too much time consumption and high testing cost, in measuring the water vapor permeability of the fabric. Therefore, an important purpose of the Alambeta testing instrument is to measure the water vapor permeability while eliminating the weaknesses of the confirmed testing instruments. This testing instrument is designed by Lubos Hes (Hes, 1996).

In particular, Hes insists that current testing instruments measuring moisture and dry functions of fabrics are not reliable because of the length of experimental time required, i.e., more than 30 minutes. However, the Alambeta testing instrument he developed is capable of simultaneously measuring water vapor permeability, thermal resistance, and thermal conductivity in a short testing period (Kannekens, 1994; Chaudhari, et al., 2001;

Koronthalyova, 2003).

He points out that experimental time might be a core factor in achieving precise results because external factors, such as the humidity effect and temperature significantly affect water vapor and the drying process of the fabric. Therefore, a main purpose of this instrument reduces the testing time in order to minimize involvement of the external environments affecting heat and energy flow. In addition, Hes states that, this testing instrument is able to analyze and evaluate the effect of structure and composition of the fabric.

2.4.2.2.2. Apparatus Design

Figure 30 shows a schematic of the Alambeta instrument and its photograph. The testing procedures are as follows: At first, prior to mounting the sample fabric, the instrument measures heat value created by a wet porous copper plate with artificial wind. A sample fabric is then placed on the measuring head which has approximately an 80 mm diameter. The heat flow sensor is able to observe and measure the temperature drop of the fabric at that time. Finally, the first and second data sets are compared to analyze thermal comfort properties of the sample fabrics.

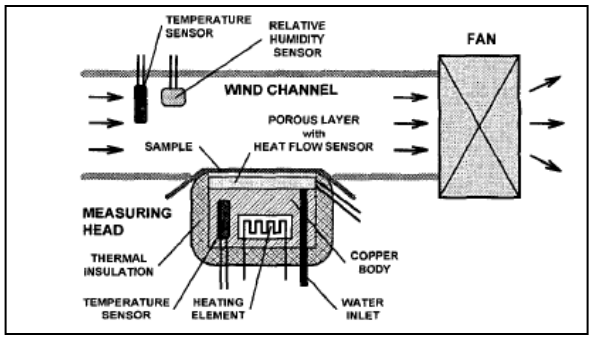

(A) (B)

Figure 30. (A) A schematic of the Alambeta instrument and (B) its photograph

Reproduced from "Thermal comfort properties of textile fabrics in wet state"

Table 8. Sensor and Actuators

No.	Quantity	Electric Range	Sensor
1	Heat Flow Density	(-)0.6…+10mV	Heat Flow Sensor
2	Temperature Difference	(-)0.25…+1.25mV	Differential TC type J
3	Head Temperature	104…120Ω, 52…60mV	RTD pt 100
4	Relative Humidity	1.75…3500KΩ	Polymer Cell
5	Moistening	1…1000KΩ	Electrodes

Reproduced from 'Thermal manikin evaluation of liquid cooling garments intended for use in hazardous waste management (2003)'

As a core system in the Alambeta, a measuring head consists of copper body, water inlet, heading element, thermal insulation, and temperature sensor. It normally regulates the temperature and supports even distribution of water vapor to the sample fabric. Hes states

that temperature of the wind channel is higher than that of a chamber room. In addition, various electric sensors are set up and accurately measure the difference between the first heat value and the second heat value passing through the fabric in the measuring head. Table 8 shows sensors and actuators to measure difference of the heat flow value.

2.4.2.2.3. Results and Analysis

Hes has investigated thermal conductivity, thermal absorption, thermal resistance, and heat flow passing through a fabric by using this new equipment. According to his definition of thermal conductivity, it is the amount of heat transfer which passes from $1m^2$ area of material through the distance 1m within 1s and creates the difference 1K. Fohr (2002) states that thermal properties of the fabrics are affected by various external environmental factors, such as temperature and relative humidity as well as unique fabric properties, such as structure, density, humidity, type of weave, surface treatment and air permeability.

Experimental results show that, as the amount of moisture increases, thermal conductivity of wet 65 % polyester/35 % cotton twill fabrics generally increases. Since thermal conductivity is proportional to the mass, the amount of Koral's thermal conductivity is the highest, while Lina's value is the lowest in Figure 31. Table 9 and Figure 31 show characteristics of five wet 65 % polyester/35 % cotton twill fabrics and their experimental results for thermal conductivity.

Table 9. Characteristics of the Polyester/cotton fabrics

Sample Name	Square Mass (g/m^2)	Warp (Tex)	Weft (Tex)	Warf*Weft (Density)
Jaspis	225	40	40	0.43
Mramor 1	245	40	50	0.45
Koral	275	50	50	0.54
Lina	205	29.5	29.5	0.42
Anton	225	29.5	35.5	0.41

Reproduced from 'Comfort properties of defense protective clothing (1999)'

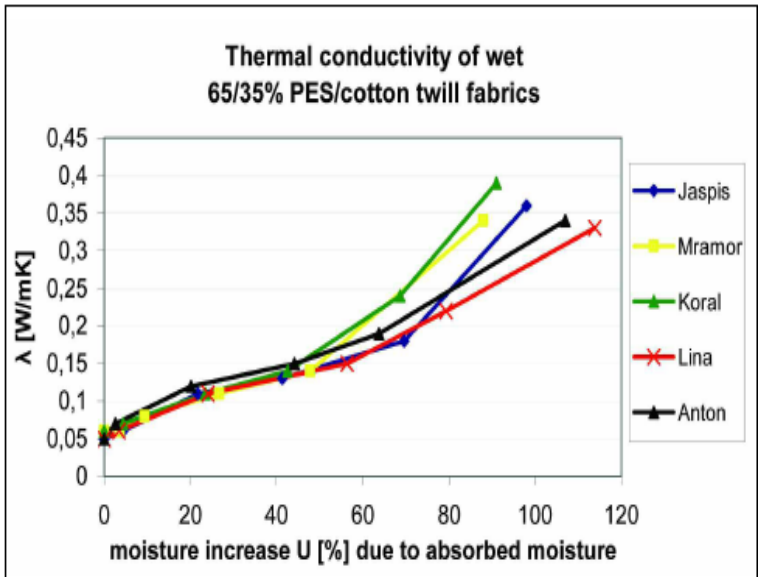

Figure 31. Thermal conductivity of wet 65 % polyester/35 % cotton twill fabric

Reproduced from "Thermal Comfort Properties of Textile Fabrics in Wet State"

2.4.2.2.4. Advantages and Limitations

As Hes stated above, a significant issue of the currently confirmed moisture

management testers, such as ASTM E 96 and BS 7209, is that they require a great deal of time to determine a testing result. However, the Alambeta testing instrument would complete an experiment to get a result within 30 minutes. This means that this testing instrument is able to minimize the influence of the external environments, e.g., temperature and humidity. Another advantage is that the standard methods and their testing instruments need a swatch from an original garment, while the Alambeta instrument is able to test directly a garment without damaging it (Bendkowska, 2005).

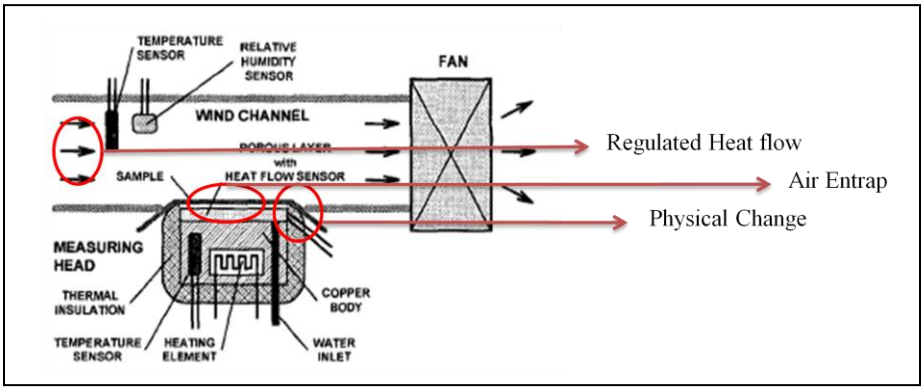

Figure 32. Potential shortcoming the Alambeta instrument

Reproduced from 'Effect of mutual bonding of textile layers on thermal insulation and thermal contact properties of fabric assemblies (1996)'

However, the Alambeta instrument has several measurement limitations, such as moisture and air leakage in the joint between the measuring head and the sample fabric. In addition, it is difficult to maintain a constantly regulated heat flow in a given condition. Also, when the sample fabric is placed on the measuring head, there is a tiny distance gap between the measuring head and the sample fabric about 1-1.5mm. This distance entraps air, which

affects the accuracy of measuring heat flow from the copper body. Another issue is when the measuring head pressures the sample fabric to fix it, a joint part causes a physical change in the sample fabric. Figure 32 shows the error points as noted by Hes.

2.4.2.3. Dynamic Surface Moisture Movement Tester

2.4.2.3.1. Introduction

The purpose of this instrument is to investigate co-relationships between skin comfort and contact with different types of fabric surfaces. Since dynamic moisture movement is related to comfort feeling for the human body in a given environment, this testing instrument focuses on the speed of movement of clothing next to the skin (Lomax, 1990). In addition, Scheurell mentions that heat energy transfer mechanisms causing dynamic moisture movement also influence the co-relationships between the comfort of the skin and the fabrics' surface.

Scheurell found that the amount of water giving rise to a sensation of discomfort in the human body is very small. Approximately 3%-5% added moisture in the fabric was enough to cause the sensation of discomfort. Hence, Huang (2007) mentions that it is possible for this testing instrument to measure the dynamic moisture movement of the fabric by taking advantage of change in cobalt chloride in the experiment. The color change of cobalt chloride paper is evaluated through comparison with Munsell Hue's color index system. Table 10 shows a level of dynamic surface wetness of the fabric based on Munsell Hue's color index system.

Table 10. A level of dynamic surface wetness of the fabric and color index system of Munsell Hue

Color Index	Color Description	Munsell hue	Munsell Hue's Color Index System
1	Royal Blue	5 PB	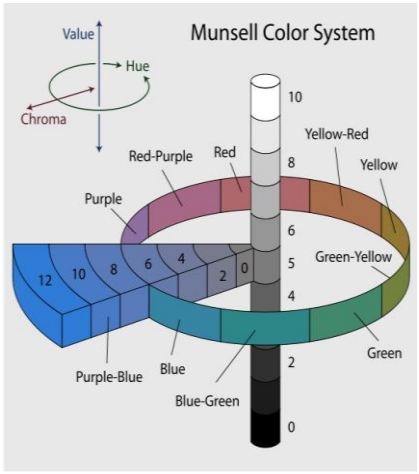
2	Medium Blue	7.5 PB	
3	Dull Light Blue	10 PB	
4	Blue Lav Edge	2.5 P	
5	Lavender Blue	5 P	
6	Lavender	7.5 P	
7	Lavender Pink	10 P	
8	Pink Lavender	2.5 RP	
9	Pink Lav Center	5 RP	
10	Pink	7.5 RP	

Reproduced from http:/en.wikipedia.org/wiki/Munsell color system

2.4.2.3.2. Apparatus Design

This system evaluates the level of dynamic moisture movement on fabrics, which have different ratios of cotton and polyester, by conducting subjective and objective tests together. As an objective method, Scheurell takes advantage of a new testing instrument, the dynamic surface moisture device. Even though this testing system looks simple, it sufficiently considers moisture management testing mechanisms, including skin, microclimate, fabric, temperature and relative humidity (Jasal, 2004).

In this testing system, the testing equipment's devices simply consist of wet chamois replacing a sweating skin, hot plate representing a human temperature, and the cobalt

chloride paper which is a moisture management simulator. As the hot plate steadily increases the temperature of the chamois and water, it gives rise to vaporization, which causes a color response of the cobalt chloride paper on the underside of the sample fabric (Ribeiro, 2002). This means that, using this simple testing method, the researcher is able to compare and confirm condensation levels of the sample fabrics through the color change of the cobalt chloride paper (Braton, 2004). Figure 33 shows a schematic of the dynamic surface moisture device.

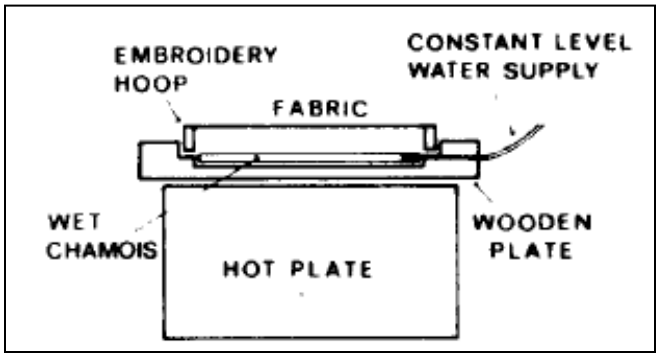

Figure 33. Dynamic surface moisture device

Reproduced from 'Dynamic surface wetness of fabrics in relation to clothing comfort (1985)'

As a subjective method, experimental participants, who wear shirts having different cotton polyester blends, experience discomfort sensations, such as sticky, clammy, damp, and clingy, after running for 30 minute under a given condition of 35 ℃ and 30-90 % R.H. After conducting the subjective and objective experiments, Scheurell studies relationships between subjective rates of clammy and damp sensation, and the color response of the cobalt chloride paper based on the Munsell Hue color index system.

From the results of the comparison, it is possible to verify a relationship between wetness levels of the fabric and comfort feelings of the human body because the result of the color response showing the different wetness levels is related to the sensation of comfort, such as clammy and damp. In addition, the result informs which of tested fabrics having differing ratios of cotton and polyester, is more suitable for comfort in a given environmental condition. This testing process also shows how to convert objective data into subjective data.

2.4.2.3.3. Results and Analysis

This experiment focuses on the moisture movement property of three types of fabrics, such as polyester, cotton/polyester blend, and cotton, which are chemically finished (Roberts et al., 2007). Scheurell mentions that the weight, air permeability, and weave structure of the fabrics have a significant influence on the color change response of the cobalt chloride paper while the fabric is being condensed. Figure 34(A) shows the wetness level of the fabric exposed to moisture in the simulated sweating device over time, while Figure 34(B) illustrates relationships between subjective comfort rating average and the color index of the surface wetness of the fabrics which have different cotton ratios.

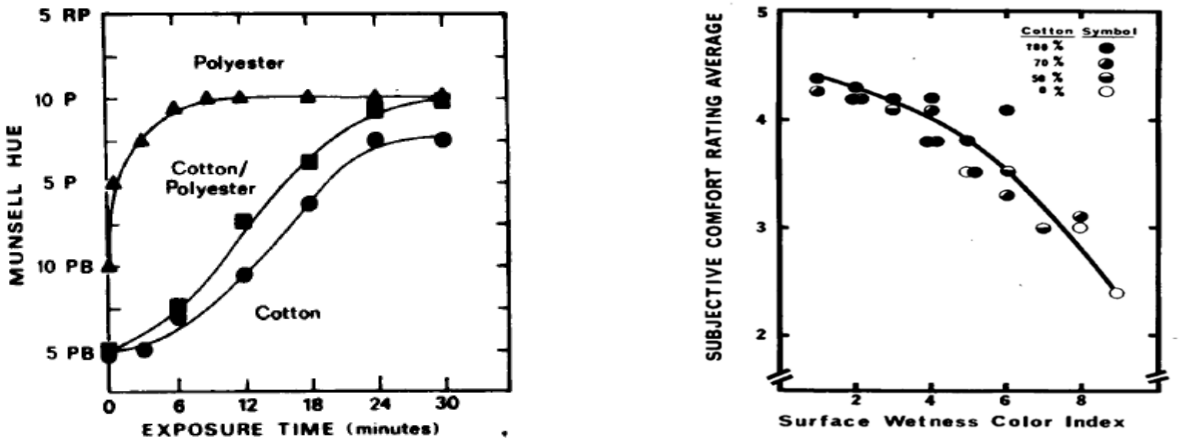

(A) (B)

Figure 34. (A) A wetness level of the fabric exposed to moisture based on Munsell's color system and (B) Relationships between subjective comfort rating average and surface wetness reproduced from 'Dynamic surface wetness of fabrics in relation to clothing comfort (1985)'

From Figure 34(A), the researcher recognizes that moisture movement in the polyester is faster than that of cotton and cotton/polyester blends. However, water mobile films which are inside of the specifically finished cotton fibers produce a certain range of internal micropore sizes, which assists mobility of the moisture movement on the fabric, and finally enhances a comfort level of the human body (Farnworth, 1990). In addition, since this method is a new testing method, Scheurell tries to obtain qualified reliability of this experiment by testing a human object at the same time.

2.4.2.3.4. Advantages and Limitations

The advantage of this testing instrument is an ingenious idea taking advantage of the color change of cobalt chloride paper as a simulator for checking a wetness level. Although

this method is simple and cheap and doesn't require a great deal of time to achieve a data result, it creates a condition similar to a microclimate, which considers skin, small space between fabric and skin, perspiration, and external environments, such as temperature and relative humidity.

However, one limitation of this testing instrument is that color evaluation after conducting an experiment might be different in accordance with researchers' view. It is not easy to accurately assess some colors, such as between purple and blue, and purple and red, based on the Munsell Hue's color index system (Ng, 2005).

2.4.2.4. Human-Clothing-Environmental (HCE) simulator

2.4.2.4.1. Introduction

Clothing consists of various fabric materials and layer systems to protect the human body from dynamic environments. Hence, the purpose of this new testing instrument is to measure the change of heat energy flow in the microclimate of outdoor/protective clothing under two dynamic environments, moderate and subzero conditions. Kim measures temperature, relative humidity, and vapor change in the microclimate, which is formed by three layers of fabric, under the assumption of the winter season using the HCE simulator.

The different types of textile, which form each microclimate, consist of PET knit/fleece, PET knit/micro-porous membrane, and PVC membrane. From the results of the experiment, this research recognizes that the microclimate between skin and clothing is sensitive to temperature change and relative humidity respectively. The microclimate's conditions are also changed by alternation of the fabric materials between the first and second layer

(Gretton, 1998; Modakef, 1986).

In particular, Kim focuses on change in temperature, relative humidity and vapor pressure, and their relationships under the subzero condition because those factors are highly related to thermal comfort performance of the clothing. Based on this experiment, she wishes to find which combinations of the different types of textile are more suitable for dealing with the environmental factors in each microclimate.

2.4.2.4.2. Apparatus Design

This testing system largely consists of two detachable chamber rooms and sweating hot copper plate, which has 20cm diameter, and a data logging system. Two detachable chamber rooms are comprised of “the moderate condition room” and “subzero condition room” respectively. Temperature range of “the moderate condition room” sets up 10-50℃, and that of “the subzero condition room” is -30-+18℃ at 30-98% relative humidity. The accuracy for the temperature and relative humidity is in +/- 0.5℃ and +/- 2% respectively. Figure 35 shows a schematic of the human-clothing-environmental (HCE) simulator, and its diagram of sweating hot copper plate, three fabrics and two sensors in the HCE.

The experimental procedure is that heat energy flow is tested in the moderate condition room (1) at first, and goes to the subzero condition room (2) to compare their change in each room. The sample fabrics, which form two microclimates, have different levels of wetness (2ml and 10ml).

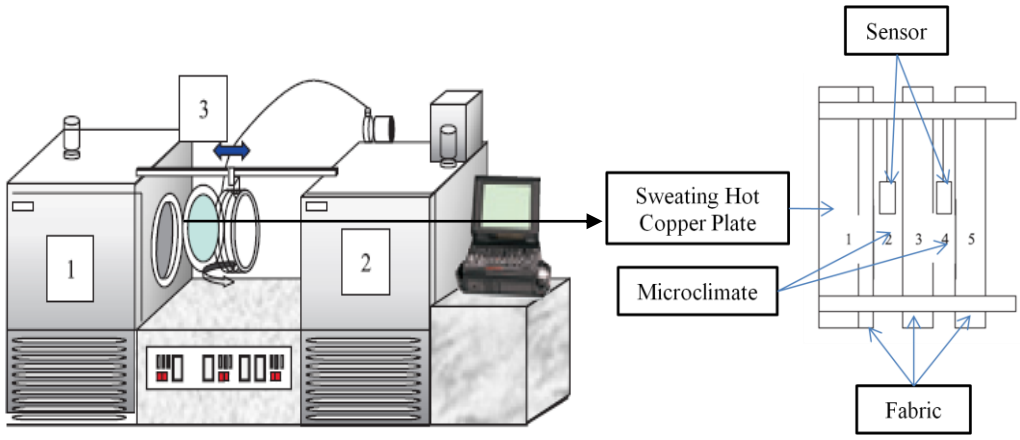

Figure 35. Human-Clothing-Environment (HCE) simulator and its schematic diagram of a sweating hot, copper plate, three fabrics and two sensors

Reproduced from 'Performance of selected clothing system under subzero conditions: determination of performance by Human-Clothing-Environment (2006)'

Temperature and relative humidity sensors are located between the layers. The copper plate, which emits the heat energy flow, is rotated and clings to a rod for transportation into each room. This allows the testing instrument to be capable of measuring changes in microclimate conditions, such as temperature and relative humidity, under sharply changing environments. Table 11 shows characteristics of the sample fabrics:

Table 11. Characteristics of the sample fabrics

	Fiber Type	Description	Weight	Thickness
First Layer	Polyester	Double Knit	(g/m^2)	(mm)
			228	0.96
Second Layer				
1	Polyester	Fleece	261	1.45
2	Polyester	Microporous Membrane	113	0.24
3	PVC	Film	26	0.03

Reproduced from "Performance of selected clothing system under subzero conditions: determination of performance by a Human-Clothing-Environment (2006)

2.4.2.4.3. Results and Analysis

The purpose of this instrument is to observe change in temperature and relative humidity of each microclimate between two layer systems of clothing under moderate and subzero conditions. Figure 36 shows change in temperature in the first and second microclimate in the moderate room and in the subzero room. Kim mentions that the temperature of the first microclimate between the skin and the first layer abruptly drops at 30 minutes and 60 minutes respectively in the first graph, but the shape of the graph is different according to a level of wetness of the fabrics. Kim mentions that a shape of the temperature change in the second graph is more moderate than that in the first graph. These temperature changes show how the heat energy flow changes in a given volume and pressure which are formed by the microclimate.

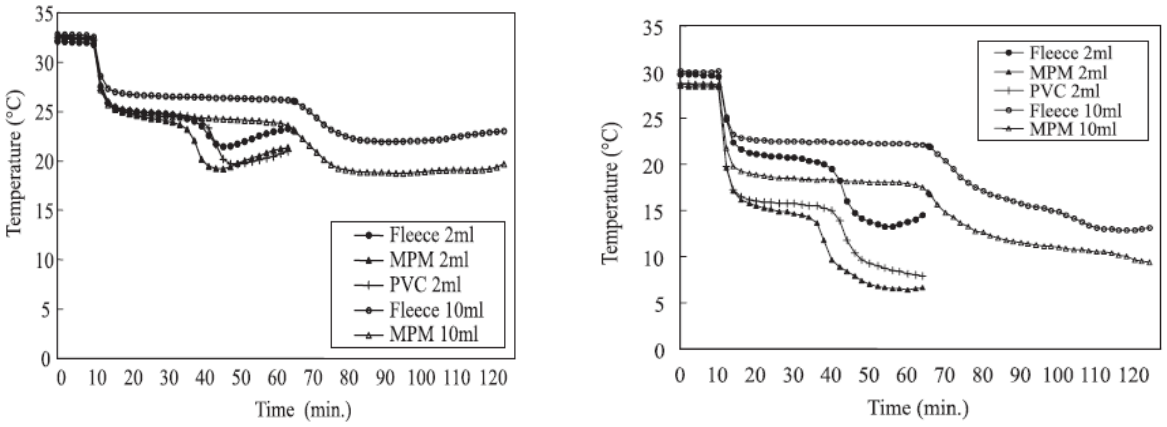

(A) (B)

Figure 36. Change in temperature at the first and second microclimate

in (A) the moderate room and (B) subzero room

Reproduced from 'Performance of selected clothing system under subzero conditions: determination of performance by a Human-Clothing-Environment Simulator (2006)'

In addition, it is possible to show how the movement of water molecules on the fabric can be changed by the heat energy flow which is provided by the copper plate in the same space, determining the amount of water molecules that will be placed in a given air space. Therefore, the amount of water molecules can be measured as checking a relative humidity. Kim mentions that the reason why the relative humidity changes sharply is that the condensation mechanism of the water molecules reacts strongly with the fabrics' surface under subzero condition between 5 and 10min. Figure 37 shows relative humidity of the microclimate between the layers under subzero conditions.

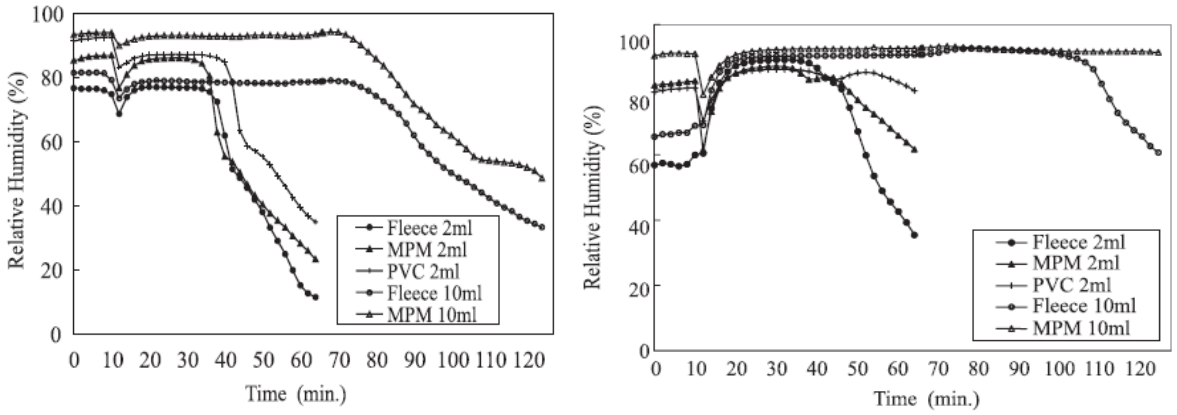

Figure 37. Relative humidity of the microclimate (A) between skin and the first layer, and (B) between the second layer and the first layer

Reproduced by 'Performance of selected clothing system under subzero conditions: determination of performance by a Human-Clothing-Environment Simulator (2006)'

2.4.2.4.4. Advantages and Limitations

The idea of this testing instrument is unique because it is able to observe changes, such as temperature and relative humidity, in microclimate between two layers of clothing under the assumption of a cold winter season. Therefore, this testing instrument is able to observe heat and energy flow under a multilayer system. Through this testing method, the manufacturer is able to get an idea of how to compose a clothing system which is able to suitably respond to external environments. The condition in the microclimate can be easily simulated by this instrument according to the environmental conditions and the clothing system.

However, this system does not consider how far the distance is between the skin layer,

and the first, and second layers of the fabrics forming microclimates. This is important, since the heat energy flow is affected by the distance. Hong (1988) explains that the reason the distance between them is critical is that each microclimate is a closed space, and it can be a core parameter influencing changes in temperature and relative humidity. Thus, the distance is able to influence the experimental results significantly. Another minor weakness is that, when the sample fabrics move to the detachable rooms via the rod, the sample fabrics are exposed to another environment, which may influence the experimental data.

2.4.2.5. Gravimetric Absorbent Testing System

2.4.2.5.1. Introduction

Yoo (2004) mentions that a purpose of this instrument studies is to study moisture vapor transmission rate (MVT), which ultimately measures wet-ability of the fabric through absorbency rate, absorbency capacity, and evaporation rate. Wallace explains that this testing instrument is also able to measure the drying rate of the fabric. Normally, the wetting phenomenon of fabric is conducted by a wicking property which is determined by contact angle as well as surface energy of the fabric between fabric surface and water molecule. Therefore, a hydrophilic finishing process of the fabric to reduce the contact angle can be a critical strategy to improve the wicking phenomenon of the fabric. This means that the wicking property is closely related to the wet-ability of the fabric (Zhuang, 2002; Wallace, 2002; Ansari, 2000)

Laing (2007) states that a drying rate of the fabric is correlated with the relative humidity of microclimate. Therefore, each fabric's various properties, such as porosity,

thickness, and hygroscopicity, can be a function which governs the drying time of the fabric (Li, 2002). In particular, Laing explains that this experimental instrument is helpful in recognizing relationships between fabric structure and vapor/water permeability.

2.4.2.5.2. Apparatus Design

The gravimetric absorbency testing system consists of several devices, including capillary pressure head controller, cover with pins, frictionless bearing, and porous plate. Water is fed to a porous plate which has the ability to appropriately distribute it into the fabric. In Figure 38(B), the cover with pin is also helpful to distribute capillary power generated from a pressure head controller evenly (Das et al., 2007). The role of the pin reduces the space between porous plate and fabric. Under this setting, the sample fabric is placed on the porous plate and is pressed by the pressure head controller in order to test the wetting of the fabric. Figure 38 shows a schematic diagram of the gravimetric absorbency testing system and a part of porous plate.

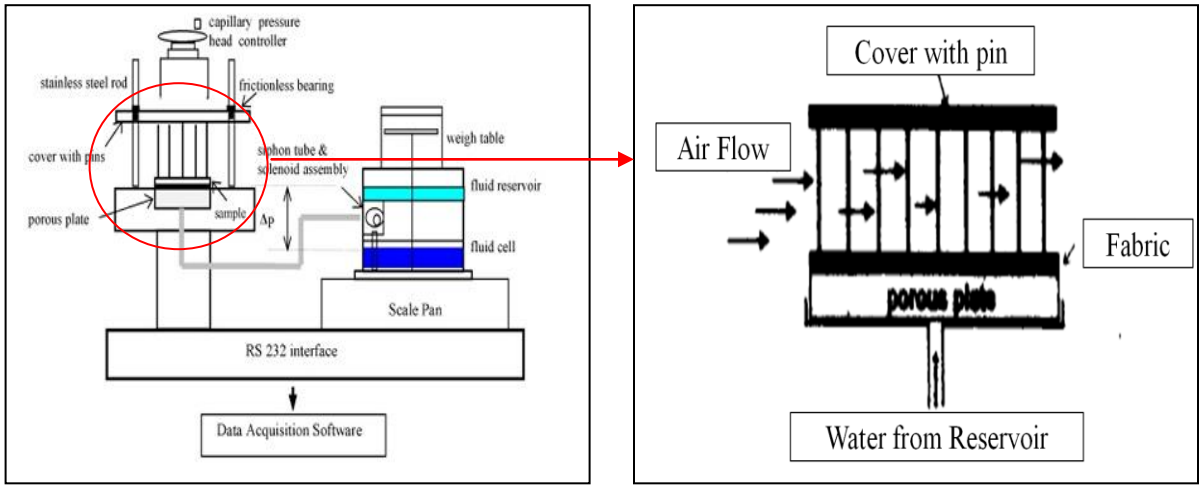

(A) (B)

Figure 38. A schematic diagram of the gravimetric absorbency testing system (A) and a part of porous plate (B) Reproduced from '100% cotton moisture management (2002)' Reproduced from http://www.tx.ncsu.edu/tpacc/comfort/horizontal_wicking_gats.html

While the absorption test for this instrument is terminated when the sample fabric absorbs 0.01g water, the absorption capacity is also evaluated by the weight difference between a fully wet fabric and dried fabric at that time. To conduct the drying test, the sample weight is measured by the change in the amount of the water moisture on the sample fabric before and after the test. In addition, Yoo explains that all of the sample fabrics tested in his experiment were washed at least three times, and the chamber room conditions, such as temperature and relative humidity, are controlled for 24 hours before the test. Table 12 shows information of the sample fabrics Laing tested.

Table 12. Fabric Description

Fabric Code	Structure	Fiber Content	Mass (g/m^2)	Thickness(mm)
KIA	Interlock	Wool	230.88	1.15
KRA	Rib 3118	Wool	219.28	1.12
KSA	Single Jersey 3118	Wool	356.2	1.24
KSC	Single Jersey 3009	Wool	150.92	0.68
KSD	Single Jersey 3029	Wool	197.46	0.8

Reproduced from '100% cotton moisture management (2002)'

2.4.2.5.3. Results and Analysis

Laing finds that the absorption capacity of the sample fabrics is positively related to fabric weight and thickness. In addition, Laing mentions that correlations between fabrics' structure and exposure to water are significantly affected by the fabrics' density and the total water absorbed. However, Yoo explains that he cannot find a positive relationship between absorption capacity and thickness through his experiment. Table 13 shows the results for the absorption capacity of the fabrics tested.

Normally, a fabric, which is treated by a hydrophilic wicking agent, has lower contact angle and is also quickly wetted (Nyoni, 2006). The effect of the wicking agent dealing with contact angle between fabric surface and water molecule has an influence on the absorption capacity in the 100% aramid fabrics. However, even though the wicking finish treatment affects hydrophilicity of the fabric, it cannot change the total amount of water absorbed in a fabric. In addition, Yoo recognizes that the water remaining on the fabric causes a damp and

clammy feeling when conducting the drying test by using air flow.

Table 13. Gravimetric Absorption Capacity

Fabric Codes						
Sample Name		KIA	KRA	KSA	KSC	KSD
Total Water Absorbed (g)	Mean	5.246	5.105	4.791	2.735	3.222
Evaporation (%)	Mean	16.68	17.25	17.72	26.11	22.72

Reproduced from 'Thermal conductivity of fiber reinforced porous calcium silicate hydrate-based composites (2003)'

2.4.2.5.4. Advantages and Limitations

The advantage of this testing instrument is that it prevents overestimation in absorption capacity of the sample by regulating capillary power using the sintered glass pillars of the pressure head controller (Gibson, 1997). It is useful for analyzing wicking phenomenon by experimental results which are related to an absorption rate and capacity of the fabric (Gibson, 2008; McCullough, 2003). However, a limitation of this instrument is that it is not easy to evenly distribute capillary power into the sample fabrics and to maintain constant air flow when the researcher conducts absorption and drying experiments.

3. Experimental Methods

3.1. Research plan

The objective of this research is to measure heat energy flow consisting of conduction, convection and radiation emitted by the human body while wearing a multilayer system of clothing. This concept of the research is based on measuring the role of functional fabric as heat energy flow changes from skin to an external environment. Therefore, the research studies change in the heat energy flow passing through the multilayer system by using a state of the art temperature and humidity sensors and an energy source designed to simulate conditions at the surface of a human body in terms of temperature and relative humidity or vapor pressure.

This approach originates from the concept that a property of layer can be characterized by changes in the amount of the heat energy and vapor flow when they pass through the fabric layer. In particular, the vapor flow of perspiration may cause physical phenomena, such as wicking, wetting, and a phase change, in reaction to the fabric's structure and therefore its material property under given environmental conditions. These physical phenomena have been correlated with the comfort of the human body but it is important to point out that this research is about energy flow rather than a comfort study. Each layer of the multilayer fabric system responds to a different environment, and changes of environments allow the researcher to identify the applicable thermodynamic theory.

For instance, Figure 39 shows the decrease of water vapor permeability of each fabric as time passes. Four types of fabric tested, cotton, coated PU, PTFE, and wool fleece, have

considerably different levels of the water vapor permeability at an initial section of the test time. However, their functional difference slowly diminishes and ultimately reaches the same level of the water vapor permeability as time passes. Hence, the amount of the water vapor passing through the fabrics also changes in accordance with the reduction rate of each fabric property.

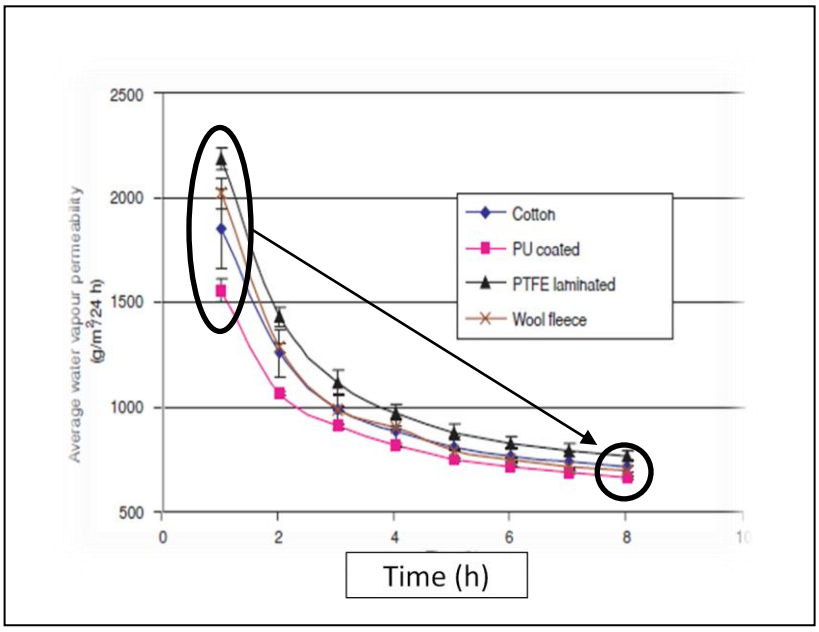

Fig 39. Water vapor permeability of four types of fabrics-one layer

Reproduced from ‘a new calculation method of water vapor permeability at unsteady states (2006)’

The results of this example were formative of a new idea for this research: the amount of heat energy flow. Specifically, the amount of heat energy flow governing a phase change and the movement of perspiration and vapor, are affected by the fabric property and

microclimate's condition which are formed by the fabric layers. The research is able to analyze the fabric property from the perspective of change in the amount of the heat energy flow passing through one fabric layer.

Therefore, this research is important because the amount of heat energy flow is significantly related to the material properties when energy flow passes through a multilayer system. Therefore, it is a key-point to measure changes in the amount of the heat energy flow by using this new measurement approach. Through experimental results, the research will be able to provide precise information regarding what types of fabric forming the multilayer system of clothing is suitable for consumers' needs based on uses and activities.

To explain the heat energy flow from skin to an external environment, various existing theories support this research. Heat energy flow is basically governed by the first and second laws of thermodynamics. In addition, the following theories are used to measure change in the amount and rate of each energy flow; Clausius-Clapeyron Relation (CCR), Newton's Law of Cooling, Fourier's law, and Stefan-Boltzmannn relationship. The following equations are explained in Chapter 2:

1. Clausius-Clapeyron Relation (Evaporation): $\ln\left(\frac{P_1}{P_2}\right) = \frac{\Delta H_{vap}}{R}\left(\frac{1}{T_2} - \frac{1}{T_1}\right)$: (Eq. 18)
2. Stefan-Boltzmann (Radiation): $P = A\,\varepsilon\,\sigma\,(T_1^4 - T_2^4)$: (Eq. 26)
3. Newton's Law of Cooling (Convection): $Q = -h\,A\,(T_1 - T_2)$: (Eq. 30)
4. Fourier's Law (Conduction): $Q = \frac{kA}{\Delta x}(T_1 - T_2)$: (Eq. 31)
5. Energy Flow in the 'Space': Microclimate Distance

In particular, the Clausius-Clapeyron Relation is a core theory because it describes a phase

change and movement of the water molecule simultaneously. The Clausius-Clapeyron Relation is capable of explaining change in enthalpy governing the kinetic and potential energy of perspiration.

It can be seen that each of the above theories requires that the temperature difference in the microclimate be measured as well as the temperature difference across each fabric of the multilayered system. Therefore, it is important to decide two points where the heat energy flow occurs between two fabric layers in order to apply these theories as well as to measure the change in the amount of heat energy flow. The microclimate distance is also important and should be considered as a variable to change heat energy and vapor flow.

In addition, many existing studies support this research theory which illustrates a relationship between the heat energy flow and the role of fabric. Hence, through a literature review; the first chapter explains what comfort and discomfort are, how the human body achieves comfort, and when it feels comfort and discomfort. The second chapter describes heat energy and vapor flow fundamentals, which include the laws of thermodynamics, energy properties, and factors affecting energy flow, the different types of energy flow consisting of metabolic energy, evaporation, radiation, convection, and conduction. In addition, a variety of moisture management testing instruments, such as moisture management tester, Alambeta instrument, and dynamic surface moisture movement tester, which measure moisture management, are fully introduced in the literature review.

To measure changes in the amount of heat energy and vapor flow, this research sets up an experiment simulating actual conditions of the human body and variable external environment based on theoretical backgrounds given in the literature review. Normally, the

human body puts on two or three layers, such as a t-shirt, top shirt, and jacket, to protect itself from the external environment. Therefore, this experiment will set up a multilayer system which builds two or three microclimates among the fabric layers. Since the multilayered system obviously affects the amount and rate of heat energy flow, temperature and relative humidity will be changed in accordance with the number of fabric layers or the fabric material properties or by physical activity levels of the human body. Figure 40 shows a schematic of the microclimate between multilayer and the environmental condition.

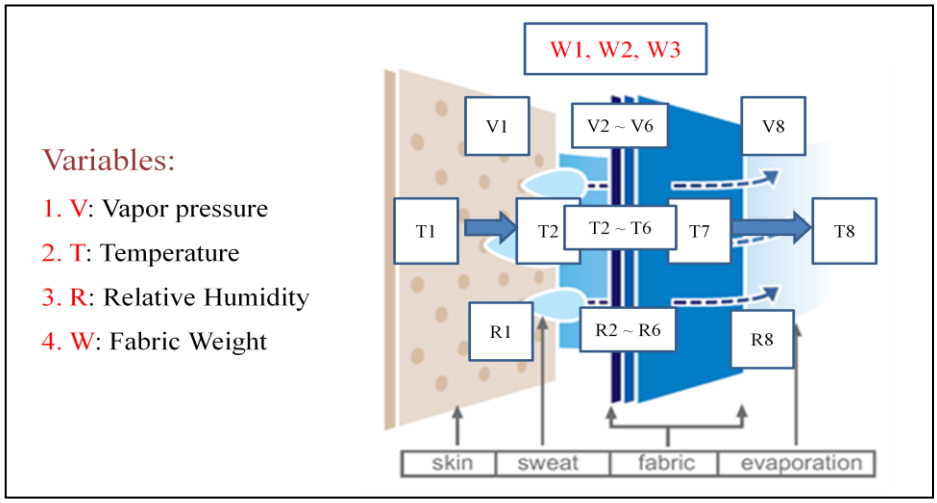

Figure 40. A schematic of the research experiment

Before conducting experiments, fabrics' properties, such as weight, thickness and air permeability are measured allowing a correlation between energy flow and fabric structure. A choice of each fabric forming the multilayer system is systematically performed by analyzing standard fabrics and current activewear based on a survey of the preliminary research. The preliminary research is described in Appendix 2. Hence, activewear companies' material

from adidas, Nike, Asics, and Mizuno were documented as a guide to material selection for the experimental trials.

3.2. Experimental

3.2.1. Introduction

The purpose of experiment is to measure the amount of heat energy flow passing through a multilayered system in order to analyze each layer. Since heat energy flows from area of higher temperature to area of lower temperature, a core requirement of the experiment is measure the points where the heat energy and vapor flow occurs between two layers. Figure 41 shows a schematic of the experiment and positions of sensors reading temperature and relative humidity. By placing the sensor in the front and in the back on the layer, it is also possible to measure the amount of energy conduction in the layers. This means that it is possible to measure change of the amount of radiation, convection, conduction, and enthalpy change of vaporization.

In addition, to accurately measure the amounts of heat energy and vapor flow, the experiment is conducted under a given environmental condition by using specific apparatus and layered materials and an environmental chamber. These ambient experimental condition, apparatus, materials, and measurement procedures are explained through sub-chapters in detail.

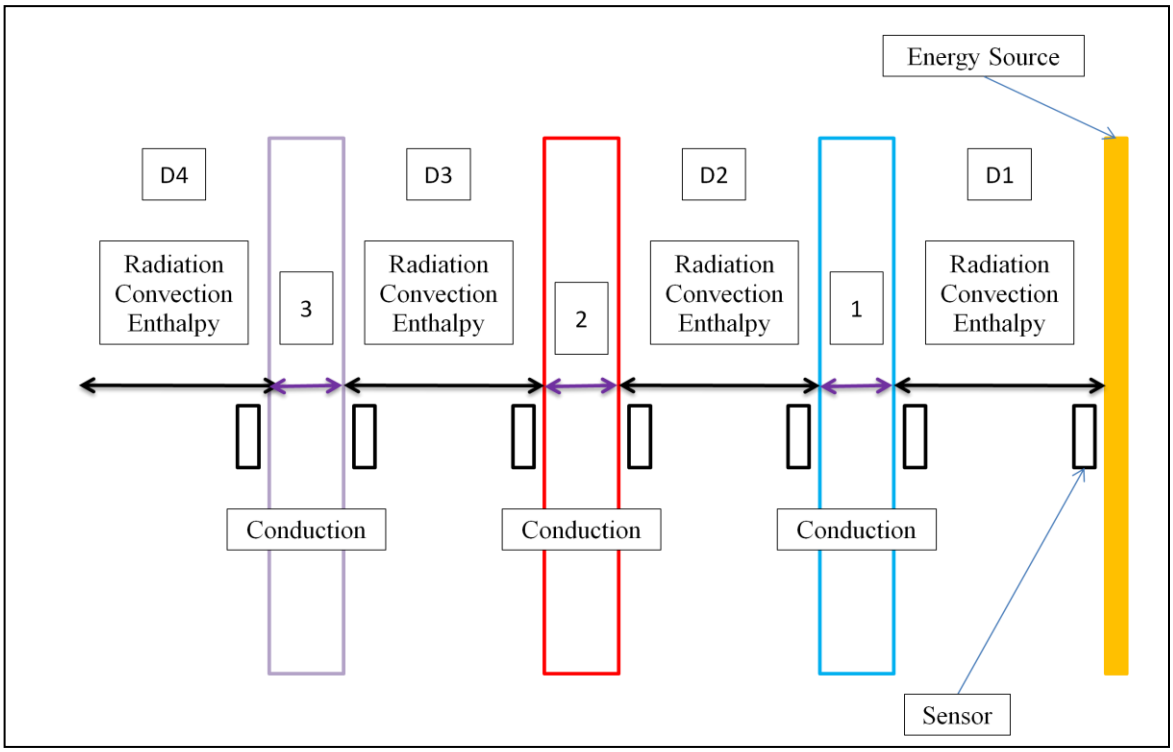

Figure 41. A schematic of experiment and position of sensors

3.2.2. Experimental condition

The experiment was conducted in an environmental chamber room to be able to build a specific experimental environment. The environmental chamber conditions were set up and controlled at three levels of temperature and humidity (Temperature: 12 ℃, 21 ℃, 30 ℃ and Humidity: 75 %, 65 %, 90 %). In particular, the standard condition, following American Society for Testing and Materials (ASTM) D 1776, is a Temperature of 21 +/- 2 ℃ and Relative Humidity (R.H.) of 65 % +/- 2 %. The ASTM's condition is used for testing standard fabrics. In addition, the environmental chamber room's conditions were set as shown in Table 14:

Table 14. Chamber room's specification

Air Temperature	Max R.H.	Min R.H.
10 ℃	88 %	77 %
25 ℃	93 %	32 %
40 ℃	95 %	17 %

Fabrics selected for the energy flow measurement system were mounted in a holder that fitted to the front of the Energy Source. Sensors were inserted into the holder during the assembly of the multilayered test rig. The size of the sample available to permit energy flow was total 4.3 mm from the first sensor to seventh sensor. Figure 41 shows an image of the test rig including the inserted sensors.

3.2.3. Apparatus

A main apparatus is called 'Energy Source,' which has been developed and built by the researcher, to conduct this research project. This Energy Source is equipped with the Energy Source and humidifier to simulate a human body. Hence, the Energy Source is capable of controlling heat energy and humidity. In addition, heat strength from the Energy Source and a level of humidity from the humidifier are controllable. The multilayered test rig is attached to the Energy Source, and the seven sensors are able to read temperature and relative humidity under a variety of environments.

The Energy Source can be largely divided into three parts: The first part is a fabric holder, the second part is the Energy Source frame, and the third part is the humidifier which

includes a water reservoir. Figure 42 shows a schematic of the Energy Source.

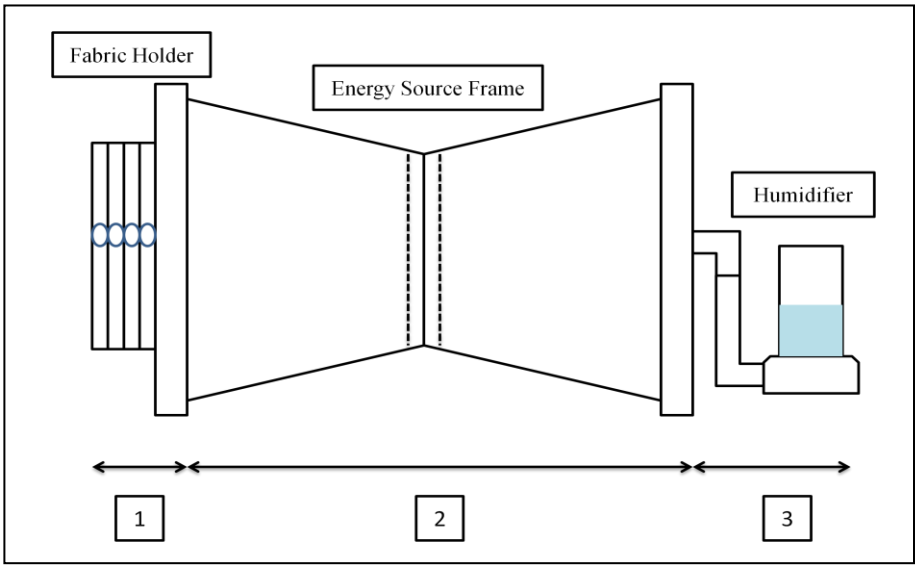

Figure 42. A schematic diagram of the Energy Source

In the first part, the fabric holder (19.6 cm * 27.2 cm) is capable of holding three layer, two layer or one layer of fabrics. Its side also has seven small holes allowing for the sensor cables to pass. The holder, which is made of rubber, minimizes physical change of fabric layers, when it presses the multilayered fabrics. Through fabrication of the rubber holders, it is possible to adjust microclimate distance among the layers.

In particular, it is important not to cause exchange of heat and humidity between the holder and chamber room because three microclimates, which are built among multilayered layers, should not be directly affected by temperature and humidity of the environmental chamber. Hence, that structure minimizes loss of heat energy and Figure 43 show a schematic diagram of the fabric holder. Since these holders are located near the front of the Energy

Source, heat energy flows directly into the multilayered fabric.

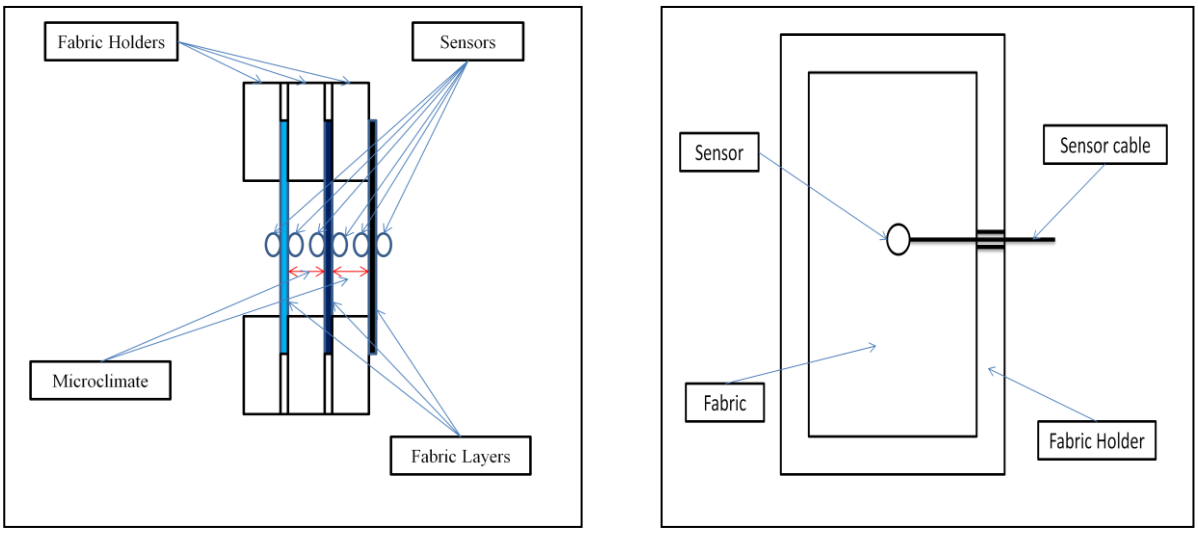

(A) (B)

Figure 43. A schematic diagram of side view (A) and front view (B) of fabric holder part of the Energy Source

The distance of the microclimate plays an important role in transferring heat energy and humidity because thermal conductivity of air is low (0.025W/(m*K)). This means that the rate of the heat energy flow is considerably weak in each microclimate. Since the microclimates distance assumes a space between the skin and clothing during wear, the fabric test rig was fabricated to take this variable into account.

To read temperature and relative humidity through the fabric test rig, six digital sensors (SHT-71) are sequentially placed in front of and in back of each fabric layers as in the above Figure 43. These sensors record temperature and relative humidity information,

and send data regarding temperature and relative humidity to two data loggers (EK-H4) in real-time. As this SHT-71 is produced by SENSIRON Co., its features are as follow in Table 15:

Table 15. Features of SHT-71

Energy consumption	80uW (at 12bit, 3V, 1measurement/s)
R.H. Operation Range	0-100% RH
Temperature Operation Range	-40 – +125℃
R.H. response time	8 sec
Output	Digital

Reproduced by www.sensirion.com/en/01_humidity_sensors/05_humidity_sensor_sht71.htm

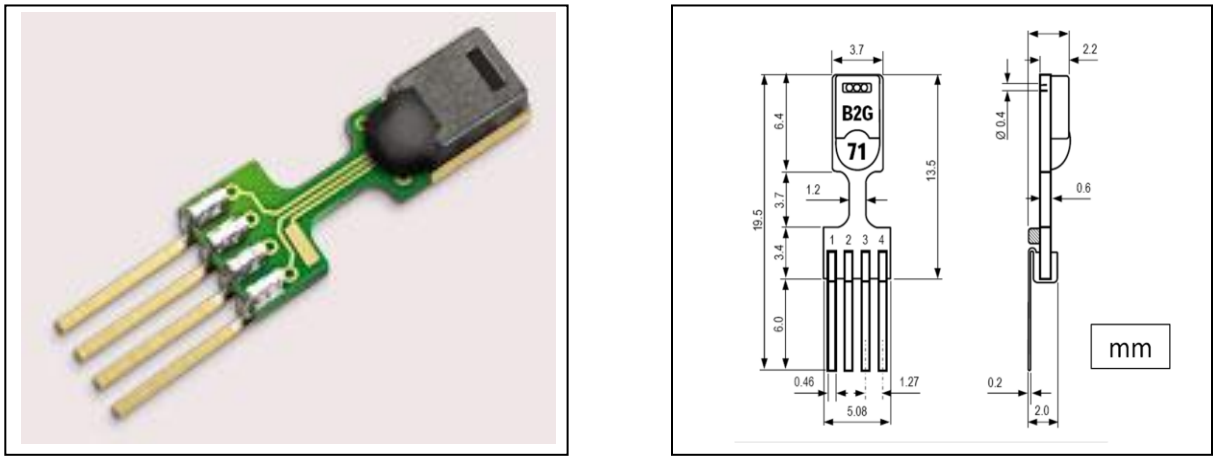

(A) (B)

Figure 44. Actual model (A) and a schematic diagram of SHT-71(B) reproduced from www.sensirion.com/en/01_humidity_sensors/05_humidity_sensor_sht71.htm

Figure 44 shows its actual model and schematic diagram which are provided by SENSIRION Co. As the SHT-71 is a pin type of temperature and relative humidity sensor, it is capable of accurately measuring temperature and relative humidity in real-time simultaneously. Although these sensors are located in either side of each fabric layer, they are too small to disturb heat energy flow.

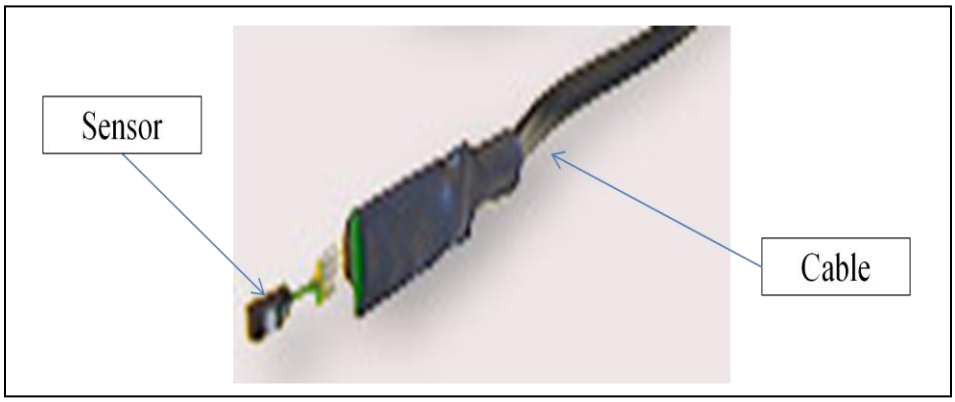

Figure 45. A connection between sensor and sensor cable

Reproduced from www.sensirion.com

This SHT-71 is connected with a specific cable which is specifically provided by SENSIRION Co. Figure 45 shows a shape of the connection between SHT-71 sensor and the sensor cable. This cable is also connected to a data logger, evaluation kit (EK-H4). This data logger displays measured numerical information regarding temperature and relative humidity which are recorded by SHT-71. SENSIRION Co. mentions that 'a role of the data logger directly transfers temperature and relative humidity into numerical data without any additional design work.' In this research, two data loggers are used to be connected with total

7 sensors of the fabric test rig. See Appendix C for Sensirion's data sheet.

In addition, data is continuously stored in an EK-H4 Read-Out Software Installation in a computer. This display shows real time temperature, relative humidity, and dew point data in the form of graphs of temperature and relative humidity. Figure 46 shows actual data logger (EK-H4) connected with sensors and EK-H4 Read-Out Software Installation including COM ports where the data logger is connected.

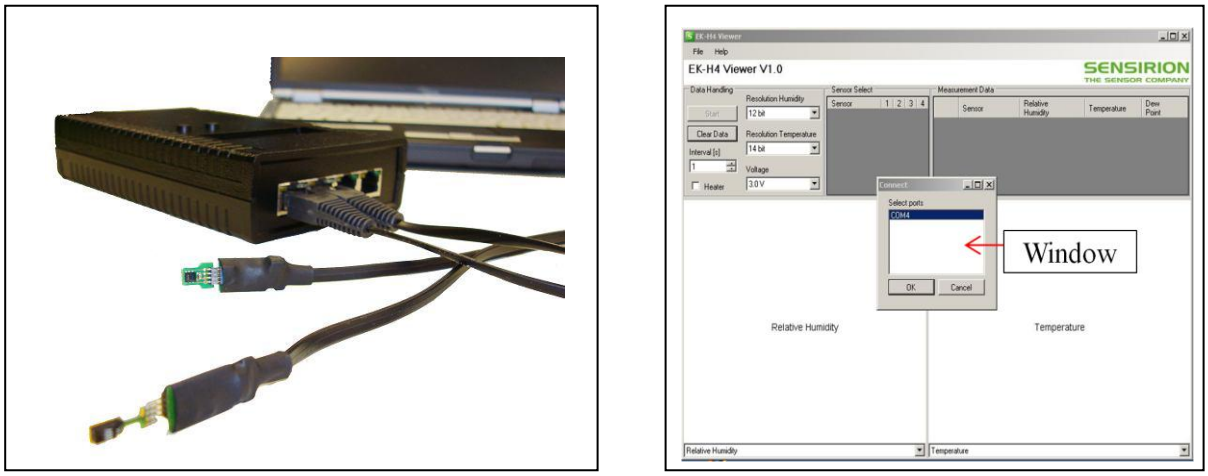

(A) (B)

Figure 46. Actual data logger (EK-H4) connected with sensors (A) and EK-H4 Read-Out Software Installation using USB cable (B) reproduced from www.sensirion.com

Figure 47 shows a schematic diagram of connection among sensor (SHT-71), USB cable, data logger (EK-H4), and computer. Therefore, a device set including a fabric holder, seven sensors, USB cable, data logger, and computer in the fabric holder part, plays an important role in recording and displaying temperature and relative humidity emanating from the Energy Source.

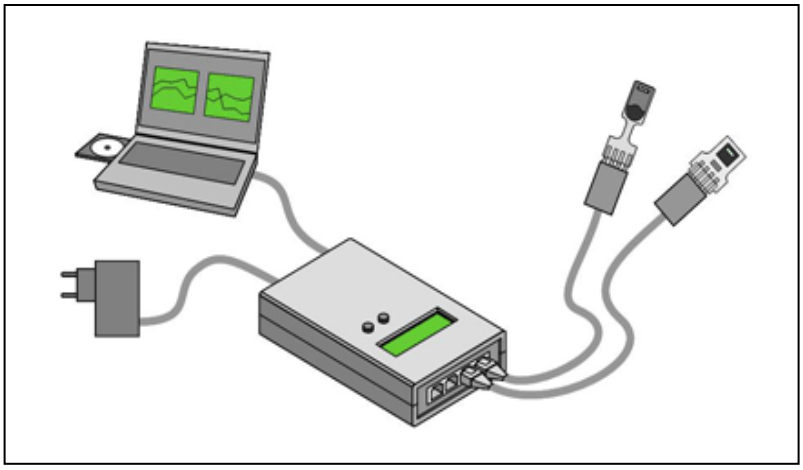

Figure 47. A schematic diagram of connection among sensor (SHT-71), USB cable, data logger (EK-H4), and computer reproduced from www.sensirion.com

The second part is the frame of Energy Source which is made from Styrofoam in order to resist moisture and provide thermal insulation effect. As mentioned above, since the role of the frame of the Energy Source is to replace a human body, it is able to create heat and direct humidity flow from the Energy Source and humidifier. It is important not to exchange heat and humidity in inside of the Energy Source with those of the chamber room except via the test fabrics.

To create heat energy flow in the front of the Energy Source, it uses a Flew Watt heat tape (11.4cm * 18.8cm). This tape is attached to the front of the Energy Source frame. The thickness of this heat tape is minimal (0.03cm) and permanently sealed in a tough, durable, and flexible plastic coating. One advantage of this tape is that, it can be cut to any length to evenly warm up large and small spaces. Also, the temperature of this tape is connected with a rheostat and can be easily controlled. Therefore, the temperature of the Flew Watt heat tape

was adjusted to equal skin temperature of the human body. In addition, perspiration holes were drilled in the heat tape, and through these holes, water vapor created by a humidifier can pass through the front of the energy source to simulate a humane body emitting perspiration.

Figure 48 shows a device set, including Flex Watt heat tape, cable, and dimmer, in a front part of its frame. In the front of this device set, a part of the fabric holder is attached. The attached fabric holder should be completely sealed to prohibit heat transfer between the Energy Source and the chamber room. This means that heat flow and water molecules, which are created by the heat tape and humidifier, are delivered into multilayered fabrics without influence from the external environment. In a middle of the frame, there is a Styrofoam wall with a series of holes to manage movement of vapor, created by a humidifier. Finally, the end of the frame of the Energy Source has a hole connected with a humidifier.

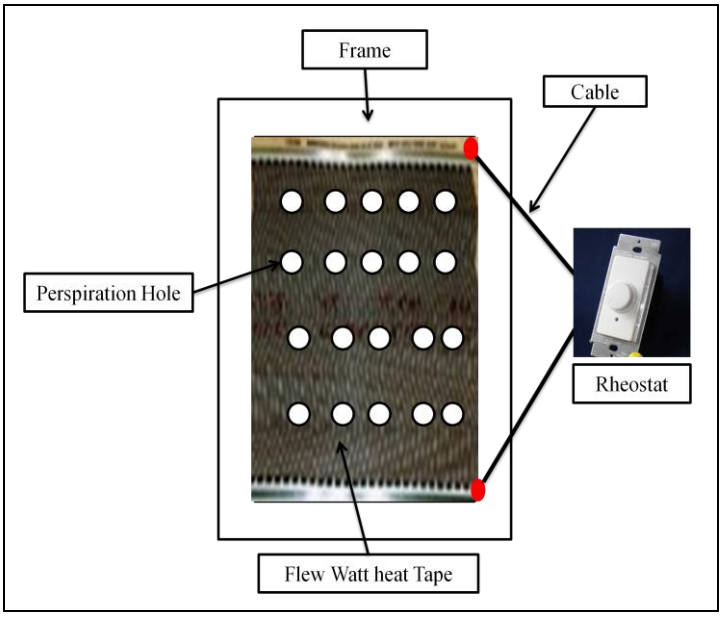

Figure 48. A device set including frame, Flew Watt heat taper, perspiration hole, and rheostat

In Figure 49, the third part is related to a humidifier which has a water reservoir (1-liter bottle). It generates vapor which mimics the perspiration of the human body in an experiment. The vapor flows along inside of the Energy Source frame. The humidity level is set and the amount of water vapor is automatically adjusted by a controller. When the humidifier makes water vapor flow, it is important not to control vapor flow because perspiration and its vapor of the human body slowly moved from skin.

In conclusion, the Energy Source consists of three parts, fabric holder, Energy Source frame, and humidifier. The experimental set up was developed to simulate actual wearing of a multilayered clothing assembly.

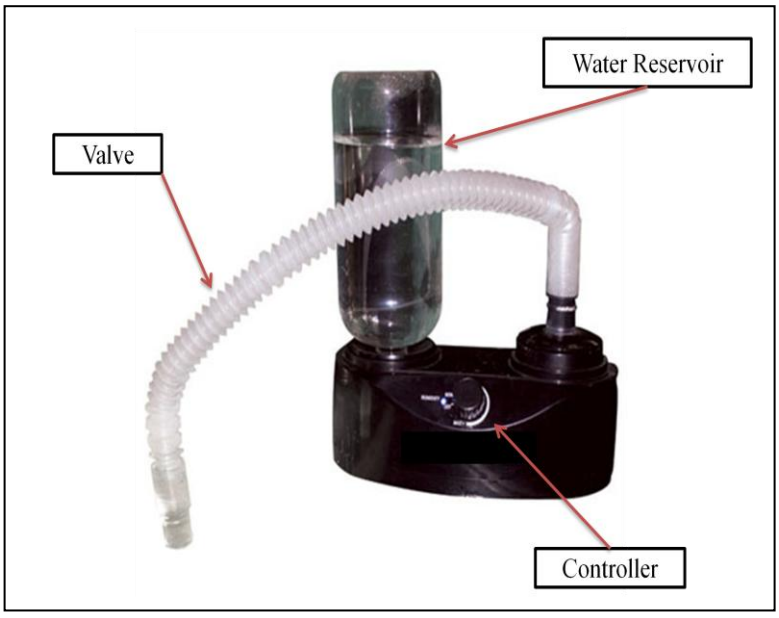

Figure 49. Controllable humidifier including valve and water reservoir

Reproduced from http://www.bestpetsuppliesguide.com/zoo-med-repti-fogger-terrarium-humidifier-for-your-reptile-cage/

3.2.4. Materials

Four types of standard fabrics were obtained from Testfabrics, Inc, and an additional series of fabrics were obtained from activewear products in the market. Table 16 shows information about the four types of the standard layers which are provided by Testfabrics, Inc. These standard layers are used to validate the test apparatus and test the thermodynamic theories as they apply to multilayered fabric clothing systems. The standard fabrics consist of two 100 % cotton fabric and two 100 % polyester fabrics as described in Table 16. They consist of a fabrication of woven and knit.

Table 16. Four standard fabrics from Testfabrics, Inc

No.	Description	Weight ($\frac{gm}{m^2}$)	Width Inches
1	Bleached Mercerized Cotton Poplin	180	64"
2	Cotton Knit	200	30"
3	Texturized Double Knit Jersey (Filament Polyester)	206	60"
4	100 % heat set (Spun polyester)	175	45"

Reproduced from http://www.testfabrics.com/products/fabrics.htm

The activewear fabric types selected included inner wear, T-shirt, and outer jacket which have different material contents. In the fabric test rig, normally, the first layer is an inner wear type, the second layer is a T-shirt type, and the third layer is a jacket type. When the same types of activewear were purchased per layer, one product is cut (11.4 cm * 18.8 cm) to be held by a fabric holder in the energy source, and a second and newly assembled fabric

test rig is placed on the human subject during exercise.

To conduct an experiment, four separation combinations of multilayered compositions consisting of three fabrics layers were assembled. These layers sampled from the activewear are commercially produced for a purpose of absorbing perspiration and controlling temperature of the human. Table 17 shows material contents of four types of actual multilayered compositions. The selection was based on a current market survey of activewear materials and the survey results are included in Appendix B.

Table 17. Material contents of four types of activewear multilayered compositions (%)

	1st Layer	2nd Layer	3rd Layer
A. Multi (1)	Polyester (100)	Polyester (77) / Spandex (23)	Cotton (80) / Polyester (20)
A. Multi (2)	Cotton (50) / Polyester (50)	Nylon (76) / Spandex (24)	Cotton (80) / Polyester (20)
A. Multi (3)	Polyester (92) / Spandex (8)	Nylon (95) / Spandex (5)	Cotton (70)/ Polyester (30)
A. Multi (4)	Cotton (100)	Polyester (100)	Polyester (100)

A.Multi(1): Activewear multilayered system (1), A.Multi(2): Activewear multilayered system (2), A.Multi(3): Activewear multilayered system (3), A.Multi(4): Activewear multilayered system (4)

In addition, the distance between skin and layer (D1) or layer and layer (D2 and D3), material thickness (Δx), material emissivity (ε), convective heat transfer coefficient (h), material thermal conductivity (k), and temperature gradient (T) are known to influence energy flow. The fabric properties are conjunction with various constants in Stefan-

Boltzmannn, Fourier's Law, and Newton's Law of Cooling equations to calculate the amount of radiation, convection, conduction, and enthalpy.

The distance between layers significantly influences the flow and fluctuation of temperature and relative humidity. Therefore, it should be accurately measured, and the same distance was applied to each fabric composition.

3.2.5. Measurements

The measurements provide numerical information about temperature and relative humidity between three layers where heat energy and vapor flow. Hence, change of temperature and relative humidity between three layers of multilayered systems is measured by SHT-71 sensors of the energy source.

Before the test began, the environmental chamber room was controlled at 21℃ and 65% to test the four types of standard multilayered systems. After testing the standard fabrics, temperature and relative humidity conditions of the chamber room are adjusted at 21℃ and 65%, 30℃ and 90%, and 12℃ and 75% and the activewear multilayered systems were tested under the three different conditions of temperature and relative humidity again. Of these conditions, 21℃ and 65% is standard conditions based on ASTM D 1776.

The energy source together with a fabric holder is arranged in the conditioned environmental chamber room. The multilayered fabric system held by the fabric holder is conditioned for at least 24 hours to have the same condition before proceeding to the experiment in the chamber room. The fabric holder, which sets up sensors (SHT-71), is attached to a frame of the energy source. Data loggers (EK-H4) which are connected with the

sensors (SHT-71) log onto a computer, and a Read-out software checks installation of the sensors through a window of the software. Therefore, setting up of the data logger, EK-H4, was as follows:

1. Prepare EK-H4, power supply cable, sensors with sensor cable
2. Connect sensors via sensor cables to the EK-H4
3. Connect EK-H4 via power supply cable to power
4. When green light is shining, the EK-H4 starts automatically

Normally, seven sensors are set up in a fabric holder for the three layers, and then the sensors are eliminated according to a number of layers under test. Tests were conducted on two and one layer systems for the activewear multilayered systems. This means that the experimental setup was able to conduct an experiment by using three layers, two layers, and one layer under the same environmental chamber conditions.

After completing an experimental set-up (about 20 minutes), the temperature of a Flew Watt heat tape tends to rise to 40℃. Temperature climbs slowly, and its change is continuously recorded and stored by the sensors and data loggers. The humidifier is then activated to create artificial perspiration at 37℃ +/- 0.5 ℃, mimicking temperature regulation of the human body under similar situations. The humidifier was not run if the temperature of the Flew Watt heat tape, replacing skin of the human body, was not greater than 37 ℃.

Each test required a time of approximately one and a half to two hours. Enough time was allowed to enable the gathering of appropriate data regarding temperature and relative humidity until a stable set of temperature and relative humidity conditions were attained. The numerical data through the Read-out software program in a computer as well as through the

displays on two data loggers was checked before going on to the next test. Through the displays on the data loggers, it was possible to check if the energy source was working throughout the experiment being conducted under a given environment in the chamber room

As the time interval of 60 seconds is established for the Read-out software, data are stored in the EK-H4 every 60 seconds for about two hours. Therefore, about 120 data regarding temperature and relative humidity is collected from each multilayered system. The extracted data were transferred into an excel file after each test since the collected data would get deleted automatically making the total experimental time approximately three hours. Figure 50 is a schematic diagram of experimental procedures.

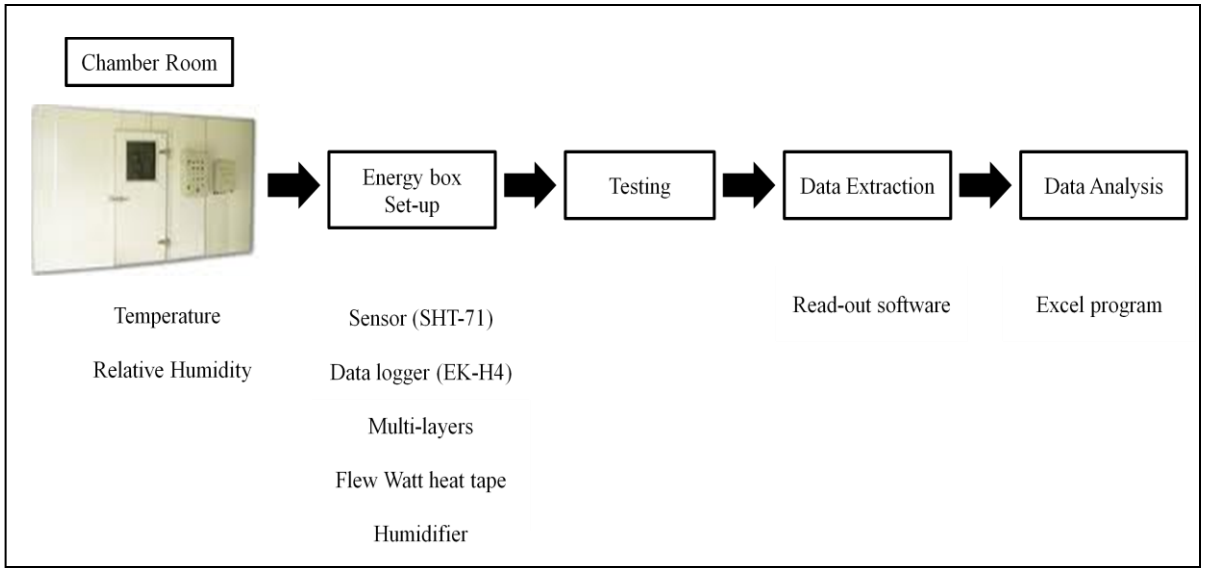

Figure 50. A schematic diagram of experimental procedure

4. Results and Analysis

4.1. Cotton poplin fabric multilayered system

Standard test fabrics were used during the first series of experiments using three layers under standard conditions of temperature and humidity. Table 18 presents physical information of each layer and spacing of the microclimate in the test rig. Physical properties were measured in the lab (such as material thickness, weight, permeability), and thermal properties such as material emissivity, and material thermal conductivity were obtained from references (http://www.engineeringtoolbox.com). It also includes results regarding temperature as measured by the seven sensors and shows the change in temperature across the microclimate and temperature change across the fabric. As the thermodynamic equations require the temperature gradient ($T_1 - T_2$), it is possible to use the recorded temperatures to calculate energy flow. Similarly, the relative humidity is shown for the seven sensors.

As the first standard layer is bleached mercerized cotton poplin, its rigid structure is suitable for using coarse filing yarns in a plain weave and mainly manufacturing a high quality a blouse or shirt. Its thermal conductivity is 0.03 (W/m*k); somewhat lower than polyester (0.05 W/m*k), but similar to the thermal conductivity of air (0.024 W/m*k) which are available from http://www.engineeringtoolbox.com/thermal-conductivity-d_429.html. As cotton fiber is basically hydrophilic and inelastic, it effectively absorbs water molecules and can increase in weight by up to approximately 10 % more (Dasgupta, S. and Hammond, W. B., 1996)

Table 18. Information for the Cotton Poplin multilayered system

	D1(Air)	1st Layer	D2 (Air)	2nd Layer	D3 (Air)	3rd Layer	Standard condition
Material thickness(Δx) ($2gf/cm^2$)	21 mm	0.39 mm	10 mm	0.37 mm	12 mm	0.39 mm	N/A
Material thickness (Δx) ($100gf/cm^2$)		0.34 mm		0.34 mm		0.34 mm	N/A
Material emissivity (ε, 20℃)	N/A	0.77	N/A	0.77	N/A	0.77	N/A
	http://www.endmemo.com/physics/radenergy.php						
Convective heat transfer coefficient (h)	3.122 (W/m^2K): Natural convection, (ASHARE, 2006)						
Material thermal Conductivity (W/m*k)	0.024	0.03	0.024	0.03	0.024	0.03	0.024
	http://www.engineeringtoolbox.com/thermal-conductivity-d_429.html						
Temperature for sensors 1 to 7 (T_1 and T_2) (℃)	37.04 ~ 32.76	32.76 ~ 31.91	31.91 ~ 28.88	28.88 ~ 27.34	27.34 ~ 24.93	24.93 ~ 23.61	23.61 ~ 21.00
Relative Humidity (R.H.) (%)	53.25	59.82	61.62	64.26	65.78	64.80	65.00
Weight(g/cm^2) (5.25 inch*5.25 inch) 5.31 oz/sq yd	N/A	3.2	N/A	3.1	N/A	3.1	N/A
Air permeability (kPa*s/m)	N/A	1.57	N/A	1.59	N/A	1.45	N/A

Figure 51 illustrates the recorded temperature changes for three layers of the bleached mercerized cotton poplin at each sensor under standard conditions for the environmental chamber. The range of temperature over the test time of approximately two hour is from 23.6

℃ to 37 ℃; the first layer is approximately 33 ℃, the second layer is 28 ℃, and the third layer is 23.6 ℃. In addition, as temperature of the last sensor is about 24 ℃ which interfaces with the external environment, it is higher than 21 ℃. This means that heat energy flow, created by a Flew Watt heat tape, plays a role in keeping the temperature range from the first to third layer, even though the last layer is affected by the temperature of the external environment.

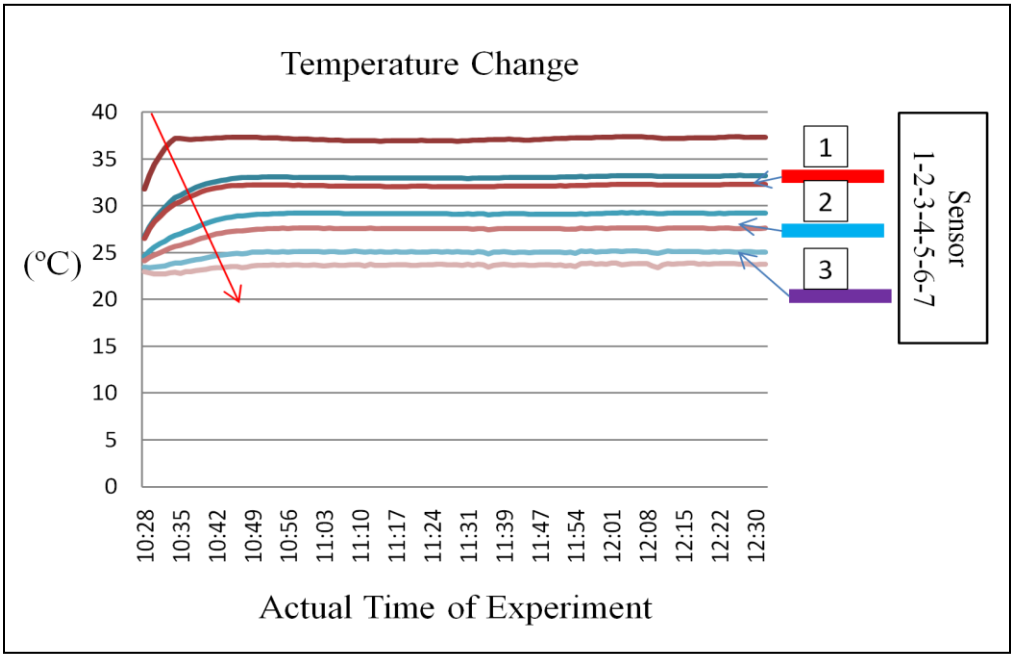

1 First Layer, 2 Second Layer, 3 Third Layer

Figure 51. Temperature change of woven cotton at each sensor and response time difference (red arrow) for sensors under standard conditions in the environmental chamber

When the humidifier generates vapor flow at 37 ℃, the increase of temperature is stopped at about 37 ℃ because water molecules consume heat energy in the vapor flow.

Therefore, temperature profile for sensor one is bent at 37 ℃. However, there is a time difference when each temperature profile is bent in Figure 51. The red arrow indicates the time difference for heat energy at each sensor. Hence, this time difference or reaction time is different depending on the material contents of the layers and this aspect will be discussed further later in this Chapter.

In addition, the data confirms that heat energy flows from high temperature zone to the low temperature zone, as depicted in Figure 51. The temperatures, recorded by each sensor and displayed in graphical from stabilize once the humidity has reached the desired setting and the graphs maintain the temperature difference between sensors. Hence, the data and experimental setup shows that fabrics and microclimates can be clearly divided through distances of the temperature lines. Among three microclimates, the first microclimate (D1) between the first and second sensor has a temperature difference of approximately 4.5 ℃ (37 ℃ – 32.5 ℃). In addition, the second microclimate has a temperature difference of approximately 3 ℃ (31.91 ℃ – 28.88 ℃), and about 2.4 ℃ is noted at the third microclimate. The temperature decline in a microclimate is normally higher than that of a layer. The research assumes that this phenomenon occur due to low thermal conductivity of air in each microclimate.

The temperature difference at the second layer (1.54 ℃ = 28.88 ℃ – 27.34 ℃) is larger than that of the first and third layer. The temperature difference across the first layer is relatively small (0.85 ℃ = 32.76 ℃ – 31.91 ℃) compared with the second layer, even though the layers is made of the the same material. The heat energy flow is higher in the first section (microclimate and first layer) due to the higher temperature and heat flows, easily through the

first layer regardless of its thermo-resistance.

According to Fourier's law, the thermal resistance of the layer is an inverse relationship with the amount of heat energy flow. Equation 32 shows the relationship:

$$R = \frac{\Delta T}{Q} \qquad \text{(Eq. 32)}$$

Where ΔT is temperature gradient between two faces of a textile material, Q is heat flow, and R is thermal resistance. Equation 32 explains why thermal resistance (R) is small when heat flow (Q) is large. Therefore, the data allows calculation of the heat flow or conduction which is related to heat resistance ($T_1 - T_2$).

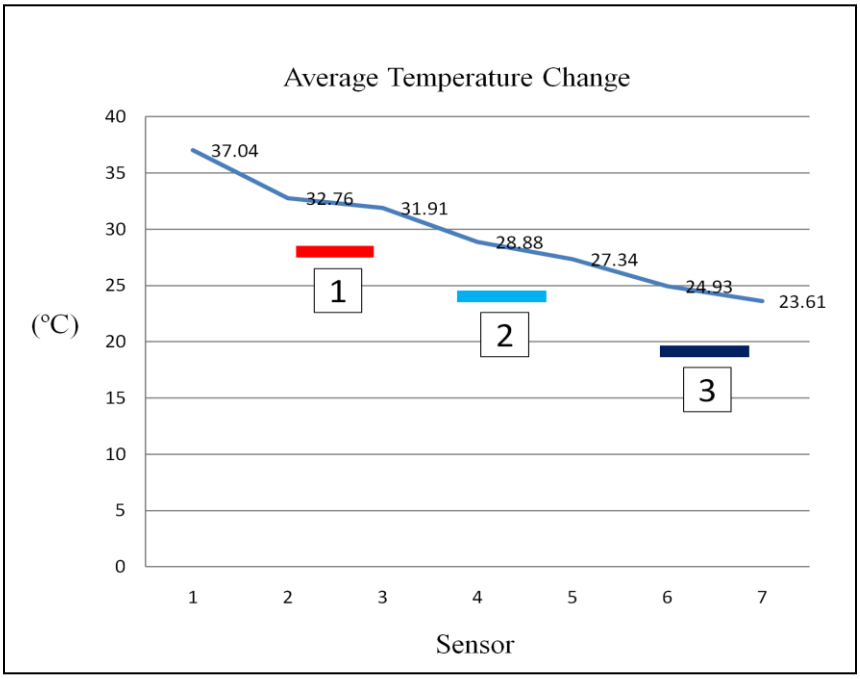

1 First Layer, 2 Second Layer, 3 Third Layer

Figure 52. Change in average temperature for woven cotton poplin at each sensor under standard conditions in the environmental chamber

Figure 52 shows average temperature change at each sensor by using three layers formed by the bleached mercerized cotton poplin under standard conditions in the environmental chamber. The data shows that, even though a multilayered system uses the same material in each layer, there is variation in their thermo-resistance from layer to layer. In addition, the data shows that temperature slowly declines from the third to the seventh sensor, and the rate of temperature decline is governed by the temperature changes in the microclimate with smaller temperature changes though the fabrics. In addition, the decreasing rate of average temperature is sequentially reduced at each microclimate.

Normally, heat energy flow is also related to change in relative humidity. Figure 53 shows the change of relative humidity at seven sensors under standard conditions. Before running the humidifier, the relative humidity ranges are from 30 % to 62 % at the red line in Figure 53. After emitting vapor from the humidifier, the range narrows to between 58 % and 69 % over a time of approximately one hour and entire relative humidity is also slowly increasing. In addition, the relative humidity at each sensor inversely responds to temperature change, i.e. the relative humidity decreases as the temperature increases, before the humidifier turned on. As the relative humidity increases after switching on the humidifier, the temperature is slowed and its level is then consistently maintained at 37 ℃. This phenomenon can be explained by the endothermic reaction (+H: enthalpy) of water molecules which take heat energy from an external environment. Finally, 6 of the 7 sensors indicate about a narrow range of 64 % to 69 % relative humidity except for the first sensor which stabilizes around 58 % to 59 % RH.

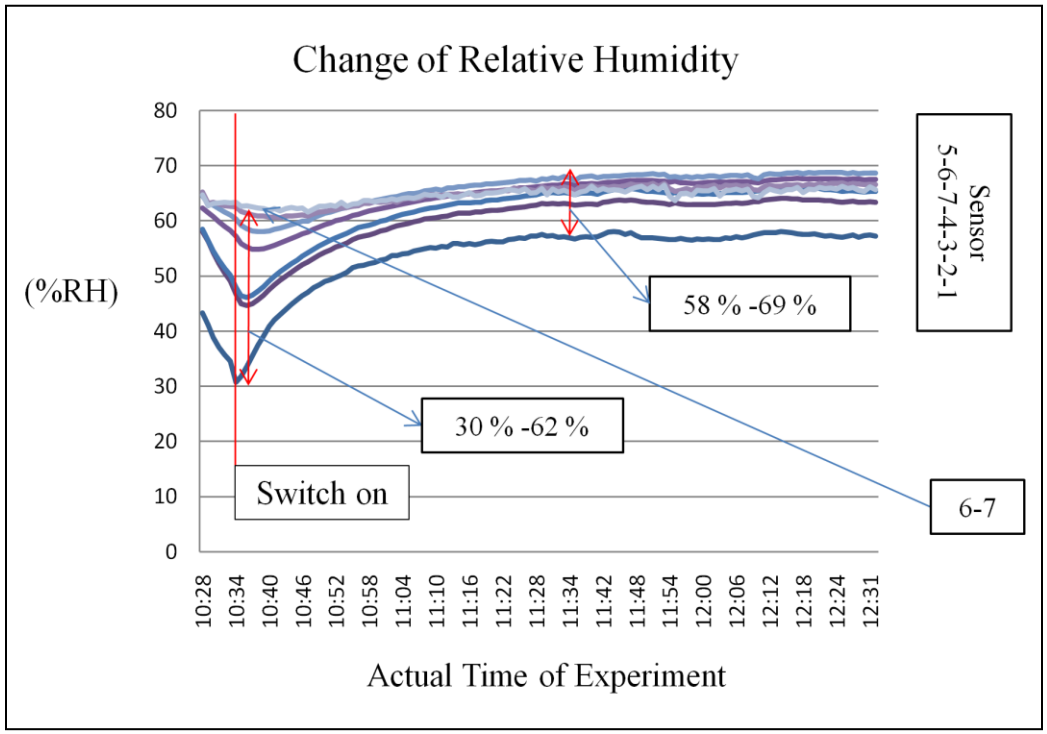

Figure 53. Change of relative humidity of woven cotton poplin at each sensor under standard conditions in the environmental chamber

Although temperature increases, the sixth and seventh sensors show essentially the same % RH in Figure 53. This indicates that the area around the third layer is significantly affected not only by its internal environment but also by the external environment. Hence, the level of the relative humidity at sixth and seventh sensors is consistently maintained at 65 % relative humidity much like the external environment.

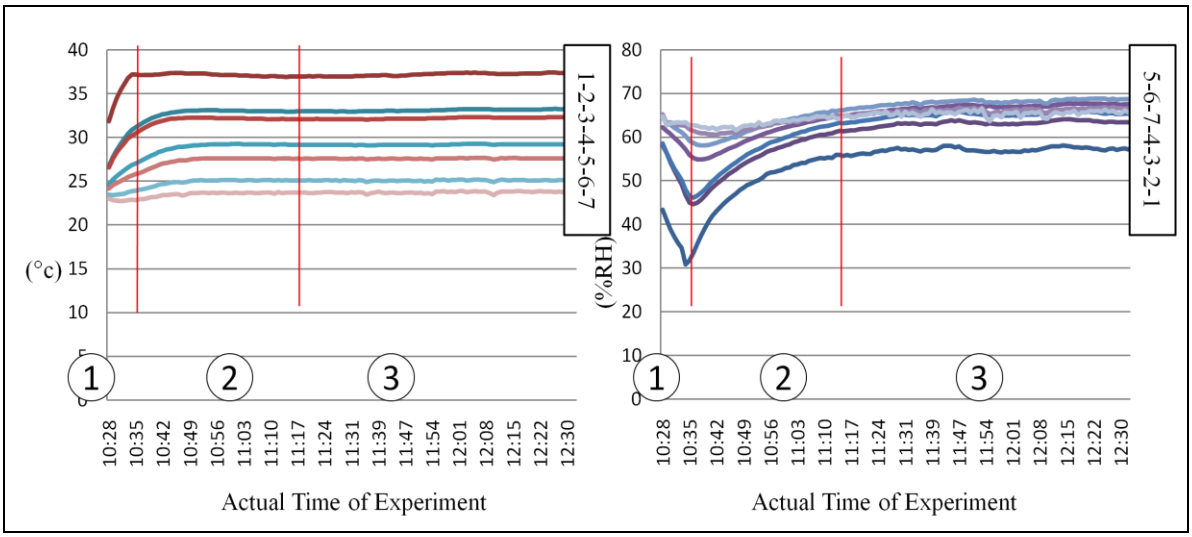

1: Before switching on humidifier, 2: Adjustment of Vapor flow and temperature,

3: Stabilization section

(A) (B)

Figure 54. Response time of temperature (A) and relative humidity (B) of multilayered system consisting of cotton woven poplin against internal and external environments

Figure 54 shows response time of temperature and % relative humidity of the multilayered system consisting of cotton poplin layers. The research divides the graphs of temperature change and relative humidity change into three areas (1, 2 and 3) respectively. In both the graphs, the number one is a time when temperature of a Flew Watt heat tape increases. On the other hand, the relative humidity in the multilayered system is inversely decreased in accordance with temperature increase on the heat tape. It takes about 7 minutes to increase up to 37 ℃. The number two is the time when relative humidity is increased rapidly due to vapor flow generated by a humidifier, and an increasing temperature in the multilayered system is slowed because water molecules in the vapor consume heat energy. It

then takes about 40 minutes to reach stabilization (Number 3 in Figure 54) of conditions. Hence, these response times of the layers composing the cotton poplin multilayered system can be described as a property of a multilayered fabric system

Figure 55 shows average relative humidity at each sensor under standard conditions. Since the highest level of relative humidity is 65.78 % at the fifth sensor, the difference between the highest and lowest is approximately 12 %. Therefore, the research data shows that the area between the third layer and microclimate has a high % RH and in a temperature range from 24 ℃ to 27 ℃ in comparison with other microclimates or layers. However, it should also be noted that for these cotton poplin fabrics, the difference in % relative humidity between the second and seventh sensor is only 5 % RH making it a considerably stable multilayered fabric system.

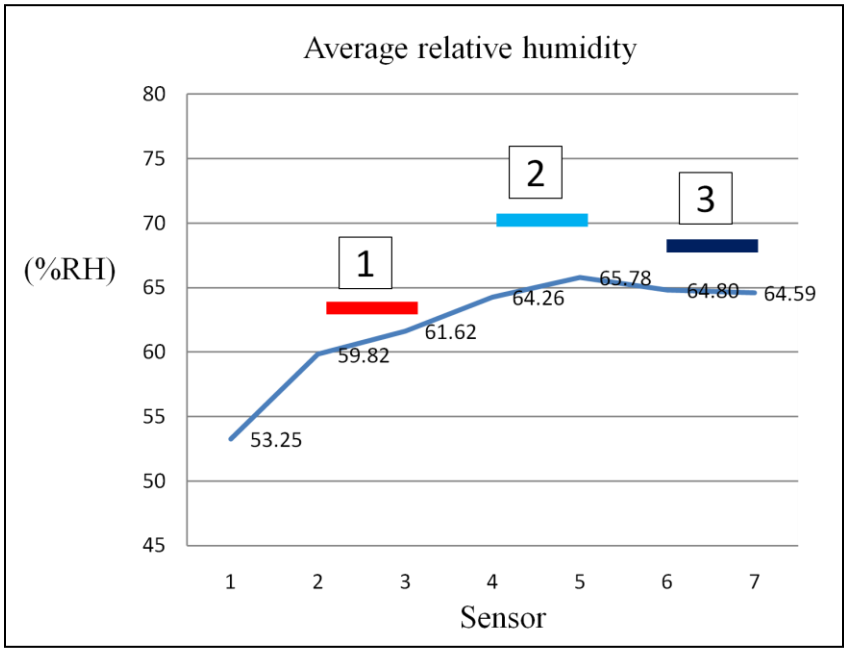

Figure 55. Change in average relative humidity for woven cotton poplin at each sensor under standard conditions in the environmental chamber

As mentioned above, there is almost no change of relative humidity at the sixth and seventh sensors (64.80 % and 64.59 %) in Figure 55, and this level is similar to external relative humidity. In addition, the level of relative humidity at the fifth sensor is close to that of the sixth and seventh sensors. Hence, the data suggests that although water vapor, generated by a humidifier, is freely moved and condensed among the layers, the last layer is influenced by the external environment. From Figure 55, it can be seen that the change in % relative humidity in each layer is less than that of any of corresponding microclimates. Therefore, the cotton poplin fabric layers play a role of reducing sharp change of the relative humidity between energy source and external environment. This indicates that each layer alleviates the effects of the vapor pressure and may help prevent the well known after-chill effect by using a multilayered system.

Based on numerical information of average temperature and relative humidity in Figure 52 and 55, and using the four thermodynamics equations, the amount of radiation, convection, conduction, and enthalpy of vaporization between layers and microclimate is calculated and shown in Table 19. To calculate heat energy flow, the Clausius-Clapeyron Relation (CCR), Newton's Law of Cooling, Fourier's law, and Stefan-Boltzmannn equation were used. An example of the calculation is shown in Appendix A. Table 19 shows the results regarding the amount of radiation, convection, conduction, and enthalpy of vaporization, passing through the standard multilayered system consisting of cotton woven poplin layers.

The resultant data in Table 19 shows that the influence of conduction is greater than that of the radiation or convection. The enthalpy change of vaporization is the rate of energy

flow and is the highest in the microclimate closest to the energy source and it then remains at an almost constant level through the remainder of the microclimates. The energy flow due to conduction is the lowest for the fabric layer closest to the energy source and increases for fabric layers two and three. The increasing conduction rate is matched with a decreasing temperature in each layer as shown in Figure 52. Particularly, heat transfer occurs largely due to water molecules, which have high heat conductivity, in the second layer; On the other hand, the enthalpy change of vaporization is high in the first microclimate because water molecules in the vapor flow are affected by heat energy of the energy source. The amount of energy flow due to radiation is small in terms of watts for this woven cotton poplin multilayered system but, like convection, contributes to the energy flow through the multilayered system.

The data and analysis suggest that it is necessary to use all four thermodynamics equations to characterize the energy flow through a multilayered textile assembly. Further, methodology shows that it is necessary to measure the temperature difference across both the microclimates and the fabrics, i.e. use 7 sensors to record temperature and relative humidity in the three layer fabric assembly.

Table 19. The amount of radiation, convection, conduction, and enthalpy change for the woven cotton poplin multilayered system

	D1(Air)	1st Layer	D2 (Air)	2nd Layer	D3 (Air)	3rd Layer	Standard condition
Radiation (Watt)	0.60	N/A	0.32	N/A	0.25	N/A	0.26
Convection (Watt)	2.91	N/A	2.06	N/A	1.64	N/A	1.78
Conduction (Watt)	N/A	14.25	N/A	27.22	N/A	22.14	N/A
Enthalpy Change (ΔH) (W/hour)	26.54	N/A	11.93	N/A	12.42	N/A	12.31

4.2. Cotton knit fabric multilayered system

The second series of experiment were conducted by using three layers under standard conditions in the environmental chamber, i.e. the environment was the same as the cotton woven poplin multilayered system. These knit cotton fabrics were obtained from Testfabric, Inc. Table 20 shows physical information, such as material thickness, material emissivity, convective heat transfer coefficient, and material thermal conductivity, composing the second multilayered system. Those are 100 % cotton knit fabrics. As thermal conductivity of cotton is 0.03 W/m*k, it is relatively low compared to polyester (0.05 W/m*k). On the other hand, it is similar to air (0.024 W/m*k).

As cotton is a hydrophilic material, it absorbs water molecules. In addition, since this fabric is knitted, its structure is elastic and can be easily stretched. Cotton knit fabric in the second multilayered system is more bulky and has less drape in comparison with cotton

woven fabric of the first multilayered system. Therefore, the air permeability and the weight of the layers are different from those of the first multilayered system. Also, the cotton knit fabric is heavier and thicker than that of the first multilayered system.

Table 20. Information of the cotton knit fabric used in the second multilayered system

	D1(Air)	1st Layer	D2 (Air)	2nd Layer	D3 (Air)	3rd Layer	Standard condition
Material thickness (Δx) ($2gf/cm^2$)	21 mm	0.88 mm	10 mm	0.87 mm	12 mm	0.86 mm	N/A
Material thickness (Δx) ($100gf/cm^2$)		0.74 mm		0.74 mm		0.73 mm	
Material emissivity (ε, 20 ℃)	N/A	0.77	N/A	0.77	N/A	0.77	N/A
	http://www.endmemo.com/physics/radenergy.php						
Convective heat transfer coefficient (h)	3.122 (W/m^2K): Natural convection, (ASHARE, 2006)						
Material thermal Conductivity (W/m*k)	0.024	0.03	0.024	0.03	0.024	0.03	0.24
	http://www.engineeringtoolbox.com/thermal-conductivity-d_429.html						
Temperature gradient ($T_1 - T_2$) (℃)	37.08 ~ 33.68	33.68 ~ 32.72	32.72 ~ 29.60	29.60 ~ 27.88	27.88 ~ 25.31	25.31 ~ 24.13	24.13 ~ 21.00
Relative Humidity (R.H.) (%)	48.88	57.90	59.37	64.22	67.42	64.65	65.52
Weight (g/cm^2) (5.25 inch*5.25 inch) 6.8 oz/sq yd	N/A	4.1	N/A	4.2	N/A	4.2	N/A
Air permeability (kPa*s/m)	N/A	0.35	N/A	0.32	N/A	0.27	N/A

Figure 56 illustrates temperature change of the cotton knit multilayered system at

each sensor under standard conditions. As a range of temperature is from 25 ℃ to 37.5, temperature is slightly higher than that of the first multilayered system. In particular, the temperature at each layer is different from the first multilayered system. For example, while temperatures of the first and second layers are each 34 ℃ and 29 ℃ in the stabilization section of the cotton knit multilayered system, they are 32.5 ℃ and 28 ℃ in the cotton poplin multilayered system. Therefore, it is presumed that heat transfer in the cotton poplin multilayered system is more active than that of the second multilayered system. This indicates that thermal resistance of the first multilayered system is higher than that of the cotton knit multilayered system. This means that, as the layers disturb heat transfer through their high thermal resistance, it is possible to decrease temperature of the multilayered system.

From the sequence of temperature and humidity sensors, the research has confirmed that heat energy flows from an area of higher temperature to an area of lower temperature. In addition, it is possible to identify places where the layers are located because of the differences between the temperatures recorded by the sensors as shown in Figure 56. Although temperature difference across the layers is not as large as that of microclimates, the difference has a significant influence on vapor pressure as well as the speed of movement of water molecules in a given space. Therefore, it is important how the structure of the microclimate in the multilayered system is built due to the impact of vapor flow affecting temperature change.

In the cotton knit multilayered system, the temperature difference (1.7 ℃) in the second layer is higher than those of the other two layers (0.97 ℃ and 1.18 ℃). This area of the multilayered system is measured by the fourth and fifth sensors, and is impacted by both

internal and external conditions. The fourth sensor is affected by the internal heat energy created by the Flew Watt heat tape, on the other hand, the fifth sensor is governed by the external environment of a chamber room. As mentioned in the first multilayered system, this area is also significantly affected by water molecules, which have high heat conductivity, in vapor flow. Hence, temperature difference of the second layer is larger than that of the first layer or third layers.

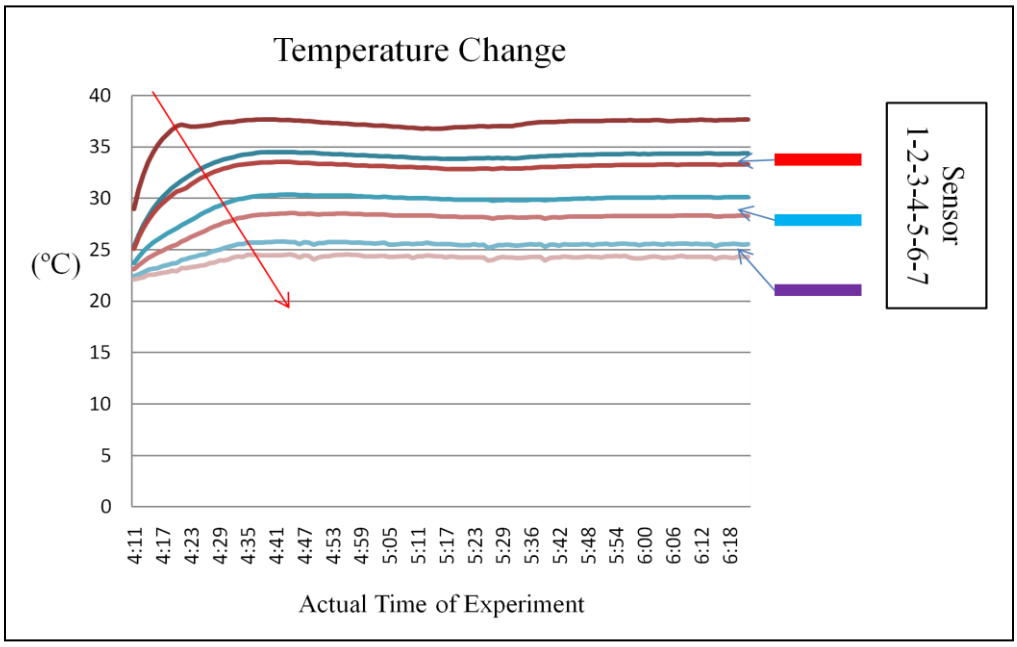

Figure 56. Temperature change of cotton knit at each sensor and response time difference (red arrow) for each sensor under standard conditions in the environmental chamber

Figure 57 shows average temperature change at each sensor under standard conditions. There are three boxes, red, blue, and purple, showing the location of the first, second and third fabric layers, respectively. The data shows that, even though transfer of heat energy and vapor pressure dominate in microclimates, heat flow diminishes as it passes through the

layers. In addition, the change of the heat flow across the second fabric in the multilayered system is obviously different from that of the first fabric, even though material contents are identical (100 % cotton knit). This indicates that the conditions in the multilayered system affect the rate of heat transfer. Hence, the vapor pressure between two layers can differ according to structure and thickness of the fabric layer and the microclimate. For instance, while decreasing rates of temperature are respectively approximately 9 %, 10 %, and 9 % in the first, second, and third microclimate of the cotton knit multilayered system, the data earlier showed 12 %, 10 %, and 9 % in the first, second, and third microclimate of the cotton poplin multilayered system. Therefore, the data and experimental setup distinguish between fabrics and recognizes that the heat flow rate of the cotton knit multilayered system is compared to the cotton poplin multilayered system.

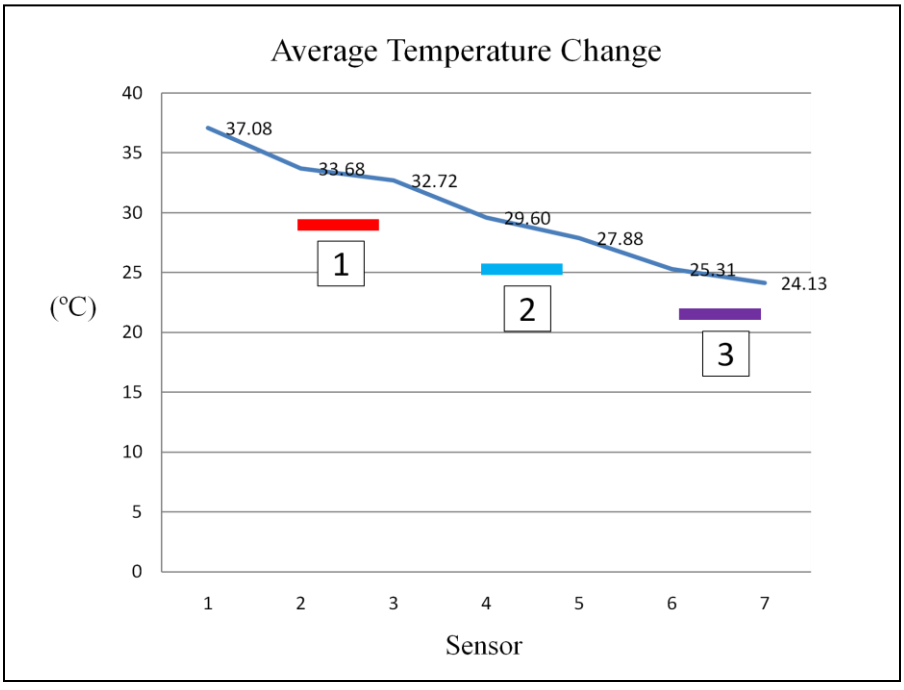

Figure 57. Average temperature change of cotton knit at each sensor under standard conditions in the environmental chamber

Figure 58 shows change of relative humidity at each sensor in the second multilayered system under standard conditions in the environmental chamber. The range of relative humidity in the cotton knit multilayered system ranges from 28 % to 62 %. Also, the level of the relative humidity of the cotton knit multilayered system is higher than that of the cotton poplin multilayered system. However, the range of relative humidity of the cotton poplin multilayered system is lower than that of the cotton knit multilayered system, i.e. the relative humidity in the cotton poplin multilayered system ranges from 63 % to 69 %, while that of the cotton knit multilayered system ranges from 61 % and 71 %.

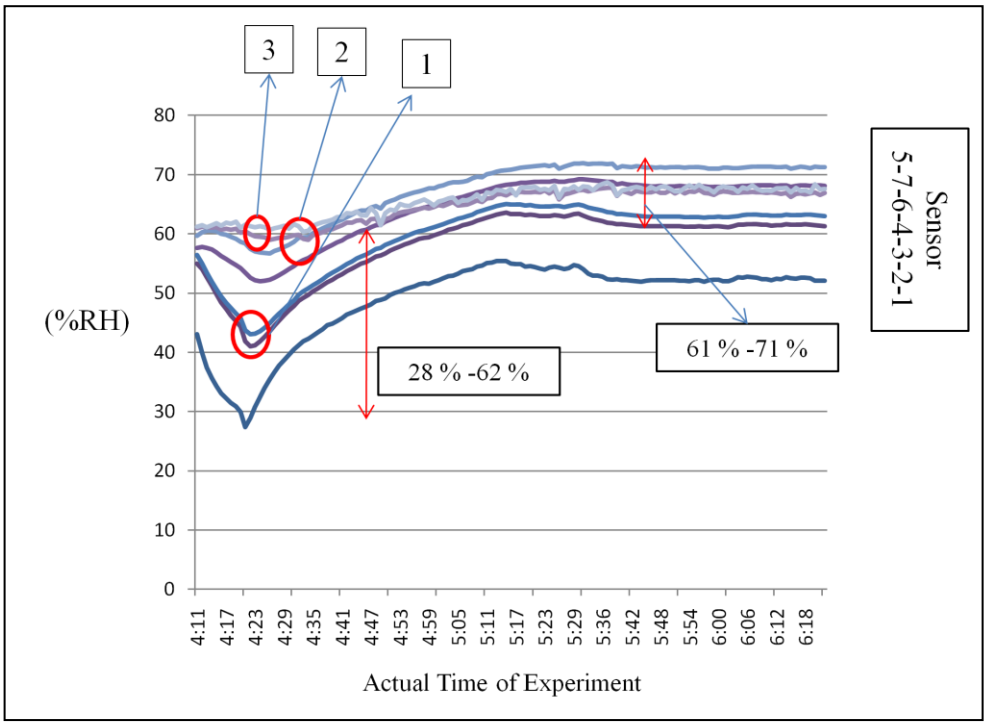

Figure 58. Change of relative humidity of cotton knit at each sensor under standard conditions in the environmental chamber

In Figure 58, the second and third layers (2 and 3) maintain a similar level of relative humidity, while the level of relative humidity of the first layer is lower. Relative humidity at first sensor in the second multilayered system is relatively lower than that in the first multilayered system. However, the relative humidity of the first layer slowly rises to 62 % for about fifty minutes. Therefore, the data suggests that it take a time to build humidity in the first microclimate when water molecules are moved easily from the surface on a Flew Watt heat tape to the first cotton knit layer whose material property absorbs and holds water molecules. In addition, the relative humidity of the first and second layer increases, while the temperature decreases, and the % RH of the third layer is relatively stable because the outside third layer is governed by the external environment.

The change of relative humidity can be divided into three areas as the experimental time increases and is closely related to temperature change. Figure 59 shows response time of temperature and relative humidity in the cotton knit multilayered system. Stage one in Figure 59 indicates that relative humidity is decreased according to increase of temperature. It takes eight minutes to climb up to 37 ℃. Stage two is where the vapor flow generated by the humidifier balances the relative humidity with temperature. This suggests a process of balancing internal and external condition under the multilayered system for about fifty minutes. The response time of this section is longer for the cotton knit than that of the cotton poplin multilayered system.

Stage three signifies the stabilization section where vapor density is consistently balanced with saturated vapor density within a given space at mainly 60 % to 70 % of the

relative humidity. This relationship between actual vapor density and saturated vapor density for relative humidity can be precisely explained by Equation 33:

$$\text{Relative Humidity} = \frac{\text{Actual vapor density}}{\text{Saturated vapor density}} * 100\% \qquad \text{(Eq. 33)}$$

In Equation 33, a capacity of the saturated vapor density has a positive relationship with temperature. Therefore, the research recognizes an inverse relationship between temperature and relative humidity through analysis in the three sections.

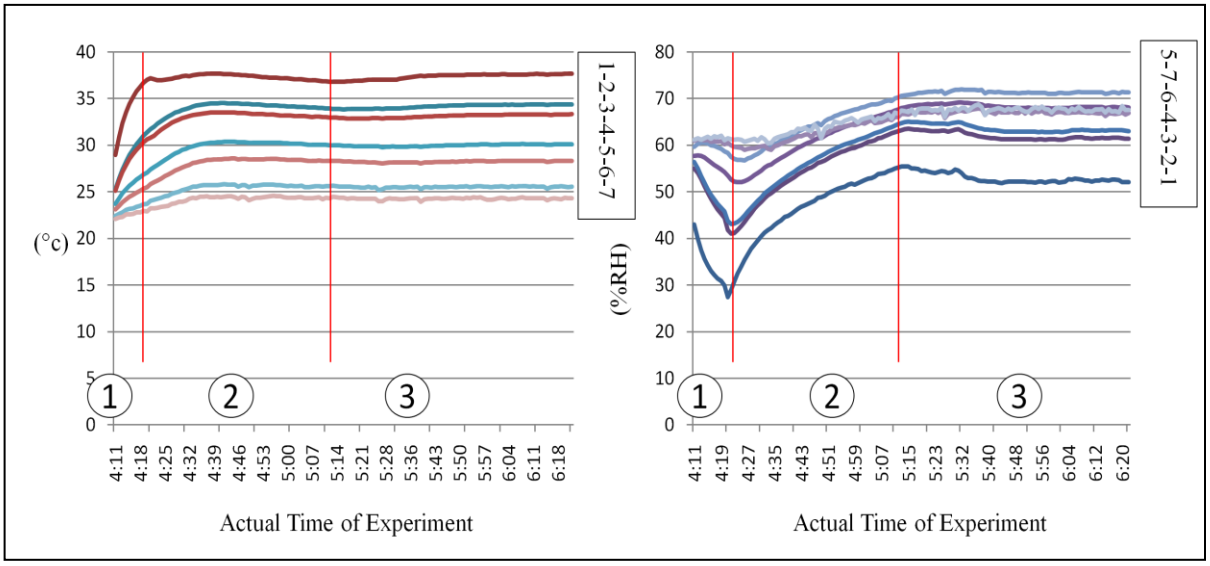

(A) (B)

Figure 59. Response time of temperature (A) and relative humidity (B) of multilayered system consisting of cotton knit under standard conditions in the environmental chamber

Figure 60 shows the average relative humidity at each sensor under standard conditions. Since the range of average relative humidity is from 48.88 % to 67.42 %, this range is considerably wider than the range of the first multilayered system (54.25 % to

64.59 %). Since the difference in relative humidity across the second layer is about 3 %, it is larger than those of the other two layers. In addition, increasing rates of average relative humidity are 18 %, 8 %, and 4 % in the first, second, and third microclimates respectively. These increasing rates are higher than those of the cotton poplin multilayered system.

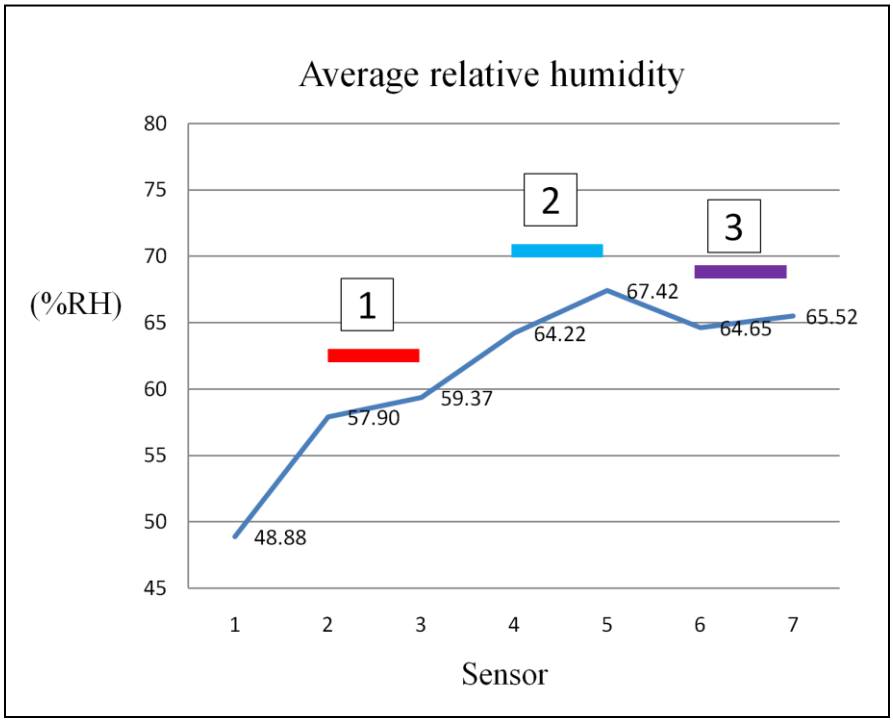

Figure 60. Average relative humidity of cotton knit at each sensor under standard conditions in the environmental chamber

The research presumes that the difference of the increasing rates from one fabric to the other is related to the layers' air permeability because permeability controls movement of water molecules in air flow. In Table 18 and Table 20, the research confirms that the air permeability of the second multilayered system is lower than that of the cotton poplin

multilayered system. This demonstrates that water molecules can be moved freely by air flow between layers and microclimates. Also, convective heat transfer is activated by the air flow. Therefore, it is important to know how to fabricate fabric from a thermodynamics point of view.

Based on numerical information of average temperature and relative humidity in Figure 57 and 60, the research measures the amount of radiation, convection, conduction, and enthalpy of vaporization between layers and microclimates. To calculate the variation of the heat energy flow, the research uses Clausius-Clapeyron Relation (CCR), Newton's Law of Cooling, Fourier's law, and Stefan-Boltzmannn equation.

Table 21. The amount of radiation, convection, conduction, and enthalpy change for the cotton knit multilayered system

	D1(Air)	1st Layer	D2 (Air)	2nd Layer	D3 (Air)	3rd Layer	Standard condition
Radiation (W)	0.48	N/A	0.33	N/A	0.26	N/A	0.31
Convection (W)	2.31	N/A	2.12	N/A	1.75	N/A	2.13
Conduction (W)	N/A	7.13	N/A	12.93	N/A	8.97	N/A
Enthalpy Change (ΔH) (W/hour)	16.61	N/A	11.54	N/A	11.54	N/A	12.53

Table 21 shows the resultant data regarding the calculated amount of radiation, convection, conduction, and enthalpy of vaporization, passing through the multilayered system consisting of cotton knit layers. In particular, the amount of the conduction and

enthalpy change of vaporization in the cotton poplin multilayered system is higher than those of the cotton knit multilayered system. However, heat energy flows, radiation, convection, conduction, and enthalpy change of vaporization, of the cotton knit multilayered system shows similar trends when compared to the cotton poplin multilayered system.

4.3. Textured Polyester Knit multilayered system

The third experiment was conducted by using three layers of a textured polyester knit fabric under the same standard conditions in the environmental chamber. Testfabric, Inc provided this double knit fabric which was made from textured filament polyester and a double knit. Table 22 shows physical information, such as material thickness, material emissivity, convective heat transfer coefficient, and material thermal conductivity for the textured polyester double knit fabric.

Table 22. Information for the textured polyester double knit fabric used in the third multilayered system

	D1(Air)	1st Layer	D2 (Air)	2nd Layer	D3 (Air)	3rd Layer	Ex (Air)
Material thickness (Δx) ($2gf/cm^2$)	21 mm	0.79 mm	10 mm	0.79 mm	12 mm	0.78 mm	N/A
Material thickness (Δx) ($100gf/cm^2$)		0.72 mm		0.72 mm		0.71 mm	
Material emissivity (ε)	N/A	0.80	N/A	0.80	N/A	0.80	N/A
	http://www.optotherm.com/emiss-table.htm						
Convective heat transfer coefficient (h)	3.122 (W/m^2K): Natural convection (ASHARE, 2006)						
Material thermal Conductivity (W/m*k)	0.024	0.05	0.024	0.05	0.024	0.05	0.024
	http://physics.info/conduction/						
Temperature gradient ($T_1 - T_2$) (℃)	36.89 ~ 33.87	33.87 ~ 33.10	33.10 ~ 30.44	30.44 ~ 28.83	28.83 ~ 26.15	26.15 ~ 24.83	24.83 ~ 21.00
Relative Humidity (R.H.) (%)	53.68	63.84	66.07	72.74	77.72	73.18	75.62
Weight (g/cm^2) (5.25 inch* 5.25 inch) 5.6 oz/sq yd	N/A	3.4	N/A	3.2	N/A	3.4	N/A
Air permeability (kPa*s/m)	N/A	0.05	N/A	0.05	N/A	0.04	N/A

Figure 61 shows temperature change of multilayered system consisting of filament polyester at each sensor under standard conditions in the environmental chamber. The range of temperature is approximately 26 ℃ to 37 ℃, and the heat flow in the fabrics and in the microclimates is obviously distinct and is shown in Figure 61. The temperature at the first

fabric layer is approximately 35 ℃, the second fabric layer is about 30 ℃, and the third fabric layer is at 26 ℃. Although average temperature of the textured polyester double knit multilayered system is slightly higher than the average temperature of the cotton poplin and cotton knit multilayered system, the overall shape of the temperature graphs can be seen to follow a similar pattern.

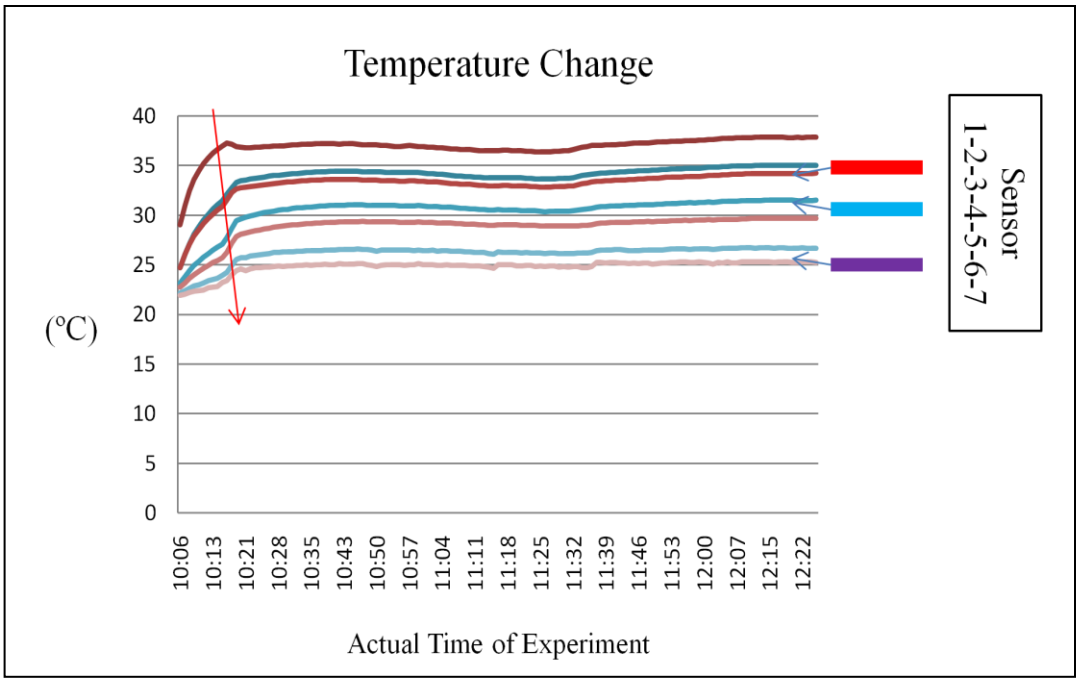

Figure 61. Temperature change of textured polyester double knit at each sensor and response time difference (red arrow) under standard conditions in the environmental chamber

The average temperature difference across the second textured polyester knit fabric layer is higher than across either of the other two layers. This phenomenon is similar to that found with the cotton poplin and knit fabrics. It is clear that the second textured polyester knit fabric layer plays a critical role in energy flow but to fully explain the mechanism, it is

important to first discuss the % RH data.

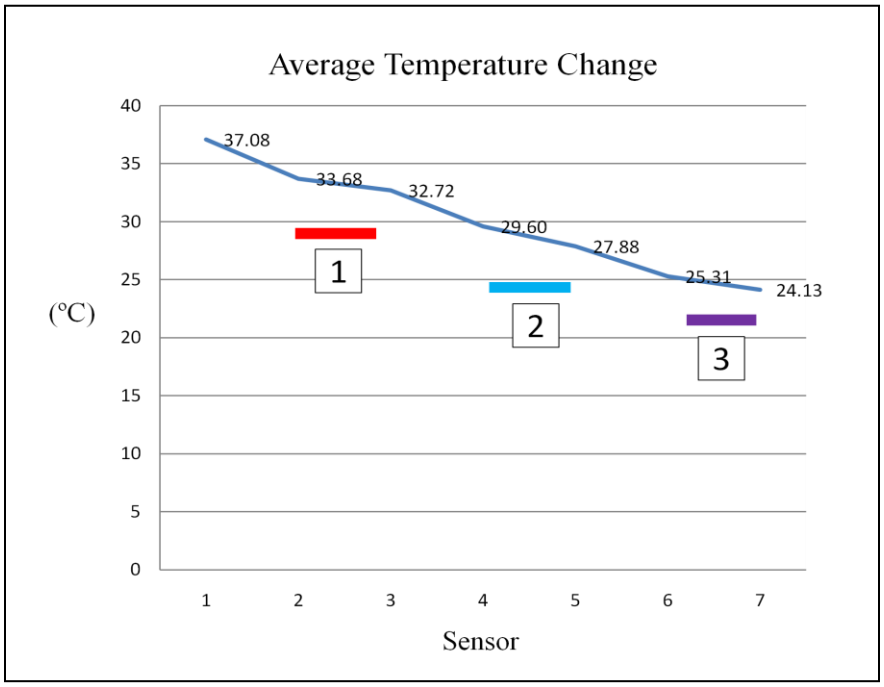

Figure 62. Average temperature change of polyester layers at each sensor under standard conditions in the environmental chamber

Figure 62 shows average temperature change of the textured polyester knit multilayered system. Since the range of temperature change is from 24.83 ℃ to 36.89 ℃, its range is less than that of the cotton poplin and cotton knit multilayered systems. As temperature of the last layer is 24.83 ℃, it is slightly higher than the other two cotton multilayered systems. In particular, temperature declines rapidly until the second layer and microclimate. On the other hand, there is almost no temperature difference (0.77 ℃) across the first layer because the energy flow rate for heat transfer, generated from the Flew Watt heat tape, passes across the first layer without resistance. These temperature gradients,

$(T_1 - T_2)$, in layers are proportional to the amount of energy flow in Stefan Boltzmann equation, Newton's law of cooling, and Fourier's law.

It will be noted that the air permeability of the textured polyester double knit fabric is higher than that of the other two cotton fabrics layers. As polyester is a hydrophobic material, water molecules are not absorbed but are freely transferred between layers. Therefore, the heat and vapor transfer can be increased through the porous structure of the double knit. Hence, a slightly higher temperature suggests that the rate of heat flow is higher for the polyester double knit fabric.

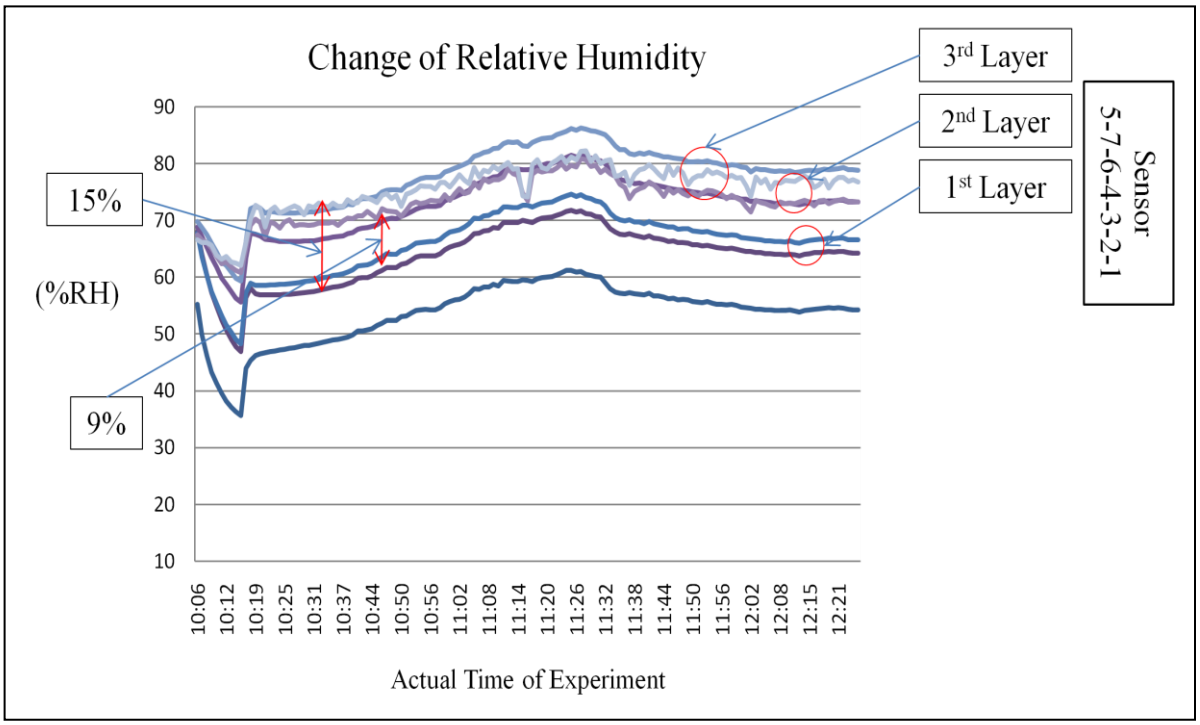

Figure 63. Change of relative humidity of textured polyester double knit fabrics at each sensor under standard conditions in the environmental chamber

Figure 63 illustrates change of % relative humidity at each sensor under standard conditions in the environmental chamber. The range of relative humidity is from 38 % to 72 % at first, thus it is wider than the other cotton poplin and knit fabric multilayered systems. The level of relative humidity of the second and third double knit layers nearly overlaps even under the wide range of the relative humidity. Consequently, the difference in relative humidity between the first and second double knit layers is approximately 9 %. The % relative humidity increases 15 % from the second sensor to the fifth sensor as shown in Figure 63. The fifth sensor records % RH up to 88 %, and then decreases to 80 % at the sensor.

Figure 63 shows different % RH profiles for the textured polyester double knit compared to cotton poplin and cotton knit multilayered fabric systems. It is postulated that this is due to movement of water molecules creating the difference in % RH relative humidity between layers. Therefore, the data suggests that these differences between cotton and polyester fabrics evaluated are, in part, related to their hygroscopic difference. This suggests that the hygroscopicity of the materials determines the number of water molecules in a given space and more water molecules in a given space between polyester layers are not absorbed. Whereas, there are fewer water molecules between cotton layers, i.e. lower % RH, and the hydrophilic property of cotton absorbs water molecules as regain.

Figure 64 shows change of temperature and relative humidity as the experimental time proceeds. The first stage is where temperature is increased by a Flew Watt heat tape, and the second stage illustrates a process of adjusting a balance between actual and saturated vapor density after activating the humidifier. Because the last section is a stabilization area,

the relative humidity ranges between 53 % and 80 %. For the textured polyester double knit fabric, relative humidity of the fabric layers reacts quickly to vapor flow generated by a humidifier in this multilayered system presumably due to the air permeability of the fabric. Therefore, the response time takes about one hour and twenty minutes in the second section. This means that response time when actual vapor density is balanced with saturated vapor density is considerably longer than those found for the cotton poplin and cotton knit multilayered system.

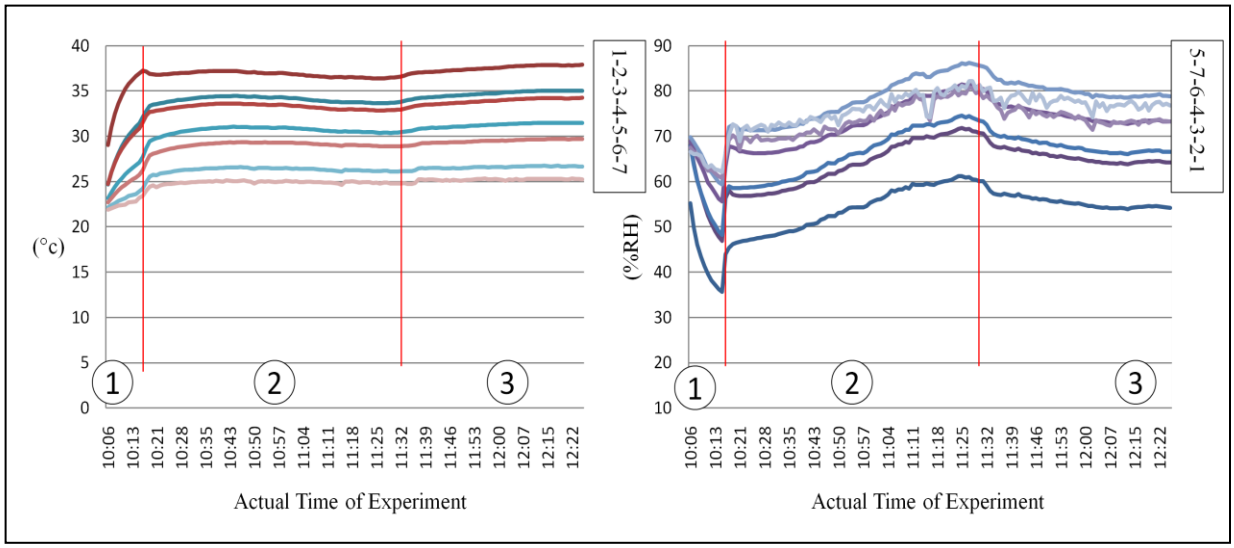

(A) (B)

Figure 64. Response time of temperature (A) and relative humidity (B) of multilayered system consisting of textured polyester double knit

Figure 65 shows average relative humidity at each sensor under standard conditions in the environmental chamber. It shows that the highest level of % relative humidity is formed in the second layer and in the third microclimate. This illustrates that the second layer

makes the greatest difference in the relative humidity among three layers. In addition, the rate of % relative humidity is the highest in the first microclimate between the first and second sensor. On the other hand, % relative humidity (2.23 % = 66.07 % – 63.84 %) of the first layer is lower than the other two layers, which means that capability of saturated vapor density inversely increases due to high temperature around this area. This phenomenon is also explained by Equation 33.

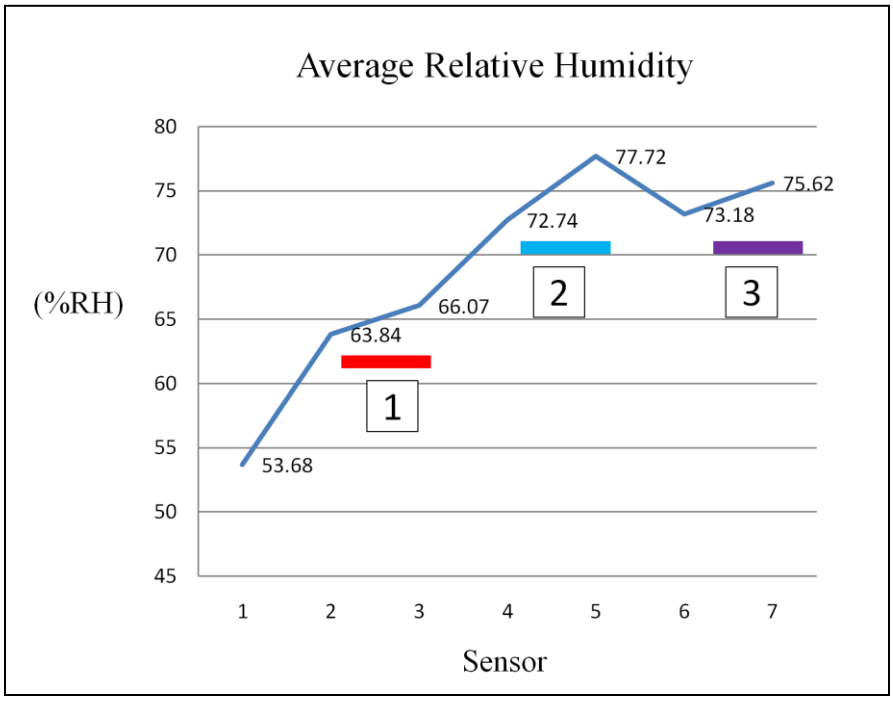

Figure 65. Average relative humidity of textured polyester double knit at each sensor under standard conditions in the environmental chamber

Table 23 shows variation of radiation, convection, conduction, and enthalpy change of vaporization, passing through each microclimate and textured polyester double knit fabric layer building the multilayered system. Through the numerical amount information regarding

heat energy and vapor flow, the research verifies that the Energy Source is able to demonstrate Clausius-Clapeyron Relation (CCR), Newton's Law of Cooling, Fourier's law, and the Stefan-Boltzmann equation with Figure 63 and 65. A type of heat energy flows, radiation, convection, conduction, and enthalpy change of vaporization, of the textured polyester double knit fabric multilayered system is similar to the first cotton poplin multilayered system

Table 23. The amount of radiation, convection, conduction, and enthalpy change for the textured polyester double knit multilayered system

	D1(Air)	1st Layer	D2 (Air)	2nd Layer	D3 (Air)	3rd Layer	Standard condition
Radiation (W)	0.43	N/A	0.30	N/A	0.29	N/A	0.39
Convection (W)	2.06	N/A	1.81	N/A	1.82	N/A	2.61
Conduction (W)	N/A	10.62	N/A	22.21	N/A	18.45	N/A
Enthalpy Change (ΔH) (W/Hour)	11.54	N/A	11.17	N/A	12.31	N/A	12.34

4.4. Spun polyester woven fabric multilayered system

The fourth experiment to validate this approach to measuring energy flow used spun polyester woven fabrics from TestFarbics, Inc. and under the same environmental condition as the three previous trials. The layers' weight and thickness of the spun polyester woven

fabric is similar to those of the cotton poplin multilayered system. Table 24 shows material information for the spun polyester woven fabric multilayered system.

Figure 66 illustrates the average temperature changes of a multilayered system consisting of spun polyester layers measured by each sensor under standard conditions in the environmental chamber. The range of temperature of the spun polyester woven fabric system is from 25 ℃ to 37.5 ℃ and it remained the same over two hour experimental time. The overall range of the temperature is similar to that of the multilayered system that consisted of cotton knit layers. Temperature of each layer is as follows: the first layer is located at 34 ℃, the second layer is placed at 30 ℃, and the last layer is at approximately 25 ℃. These temperature positions of each layer are similar to those of the cotton knit multilayered system, even though this multilayered system is made of spun polyester woven layers.

Table 24. Information for the spun polyester woven fabric multilayered system

	D1(Air)	1st Layer	D2 (Air)	2nd Layer	D3 (Air)	3rd Layer	Ex (Air)
Material thickness (Δx) (2gf/cm^2)	21 mm	0.49 mm	10 mm	0.50 mm	12 mm	0.48 mm	N/A
Material thickness (Δx)(100gf/cm^2)		0.41 mm		0.41 mm		0.41 mm	
Material emissivity (ε)	N/A	0.80	N/A	0.80	N/A	0.80	N/A
	http://www.optotherm.com/emiss-table.htm						
Convective heat transfer coefficient (h)	3.122 (W/m^{2}K): Natural convection						
Material thermal Conductivity (W/m*k)	0.024	0.05	0.024	0.05	0.024	0.05	0.024
	http://physics.info/conduction/						
Temperature gradient ($T_1 - T_2$) (℃)	37.22 ~ 33.66	33.66 ~ 32.79	32.79 ~ 30.13	30.13 ~ 28.41	28.41 ~ 26.11	26.11 ~ 24.17	24.17 ~ 21.00
Relative Humidity (R.H.) (%)	53.68	63.84	66.07	72.74	77.72	73.18	75.62
Weight (g/cm^2) (5.25inch*5.25inch) 5.0 oz/sq yd	N/A	3.0	N/A	3.1	N/A	3.0	N/A
Air permeability (kPa*s/m)	N/A	0.09	N/A	0.07	N/A	0.07	N/A

However, response time of spun polyester woven multilayered system against vapor flow is different from that of the cotton knit multilayered system. The main difference is that the multilayered system consisting of spun polyester woven fabric reacts to vapor flow quickly and the slope of the red arrow shows the shortest response time of the fabrics decreased earlier. Conversely, the cotton knit multilayered system responds to vapor flow slowly. This difference may be attributed to the material properties of cotton versus polyester

which are used for the second and fourth multilayered systems.

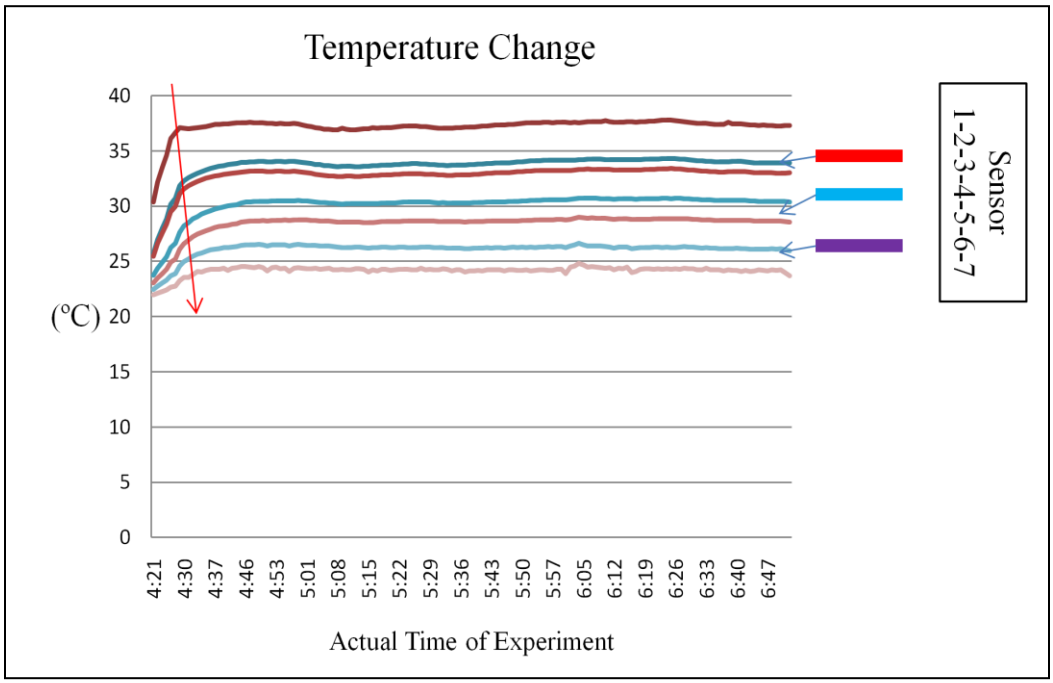

Figure 66. Temperature change of spun polyester fabric at each sensor under standard conditions in the environmental chamber

Heat energy, generated by a Flew Watt heat tape, flows from higher temperature to lower temperature, i.e. from sensor 1 to sensor 7 as shown in Figure 66, and follows the second law of thermodynamics. In addition, areas of fabrics and microclimates are clearly separated, which means that temperature difference of the fabrics is small, while that of microclimates is large because their heat conductivities are different. This means that temperature is considerably decreased in the microclimates for the spun polyester and is similar to the other three multilayered systems. Temperature difference is the smallest at the

first layer as with the other three multilayered systems. This shows that strong heat energy flow almost disregards the thermal resistance of the first layer when the temperature is 37 ℃ and the difference in temperature between sensor 2 and sensor 3 is 0.87 ℃. However, the overall temperature of the fourth multilayered system is slightly lower than that of the third multilayered system, even though both multilayered systems consist of polyester layers fabrics. It is suggested that fabric construction also plays a role in managing energy flow in multilayered fabric systems.

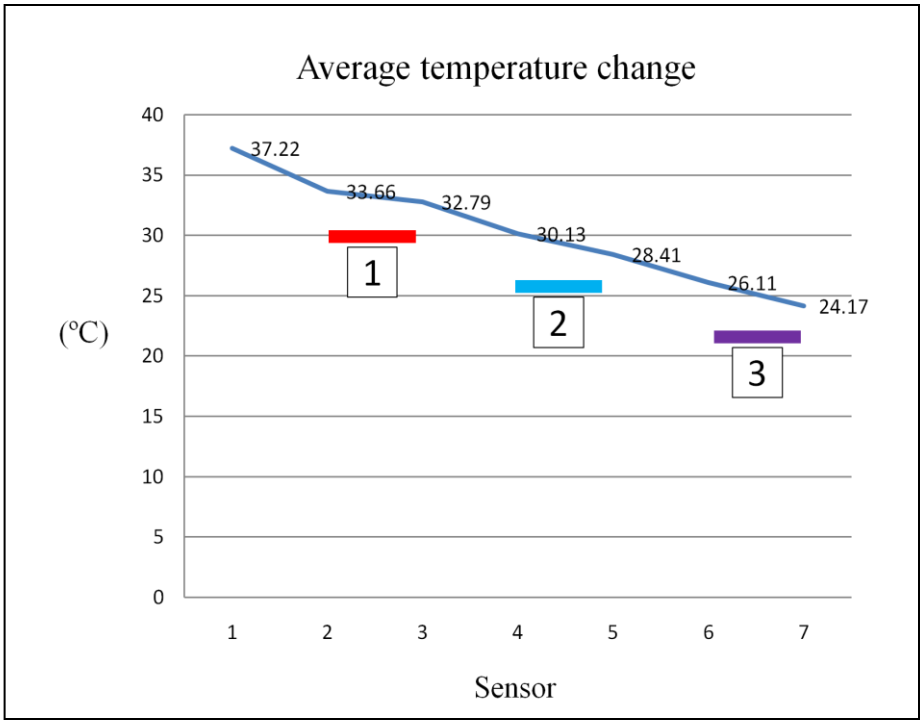

Figure 67. Average temperature change of spun polyester layers at each sensor under a standard condition in the environmental chamber

Figure 67 shows the average temperature change at each sensor under standard

conditions in the environmental chamber. According to the average temperature change in Figure 67, a range of average temperature change is from 24.17 ℃ to 37.22 ℃. Temperature differences in three layers are 0.68 ℃, 1.76 ℃, and 1.94 ℃ respectively. Except for a decreasing rate of temperature in the first layer and microclimate, temperature loss shows a linear trend from the third to seventh sensors, i.e. energy flow is linear for this fabric type, thickness, microclimates, and conditions for an external environment.

As the total temperature difference of the spun polyester multilayered fabric system is approximately 13.05 ℃, it is similar to the temperature loss of the textured polyester multilayered fabric system which was 12.95 ℃. In addition, the rate of temperature decrease in the first microclimate is always high, which indicates that its role is important in reducing heat energy flow. Therefore, the research recognizes that heat energy flow can be controlled according to the position and distance of the microclimate in the multilayered fabric system.

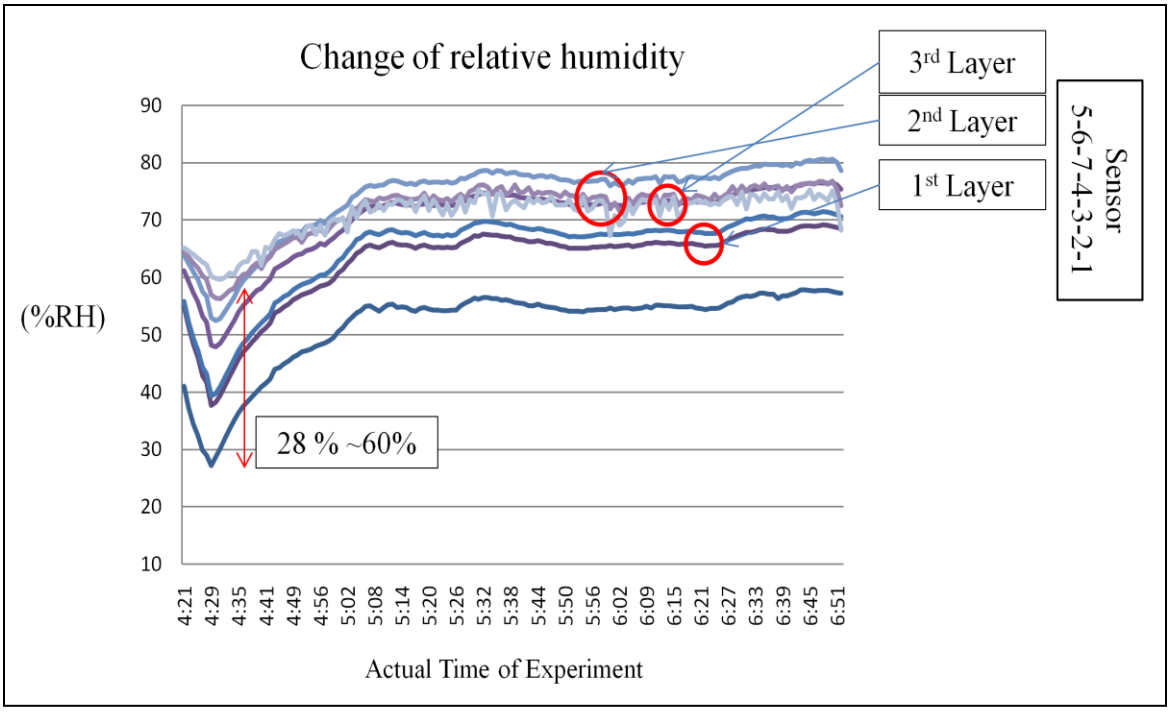

Figure 68. Change of relative humidity of multilayered system consisting of spun polyester woven fabric at each sensor under standard conditions in the environmental chamber

Figure 68 shows change of relative humidity of multilayered system consisting of spun polyester woven fabrics at each sensor under standard condition in the environmental chamber. The range of % relative humidity for the spun polyester woven multilayered fabric system range is approximately from 28 % to 60 % before the humidifier was activated. Following activation of the humidifier, the %RH increases during the following 47 minutes and shows that the fabric in the second layer records the highest %RH. Figure 68 shows the %RH of the spun polyester outer fabrics maintains an average of 71.1 %RH in the 65 % RH of the standard conditions

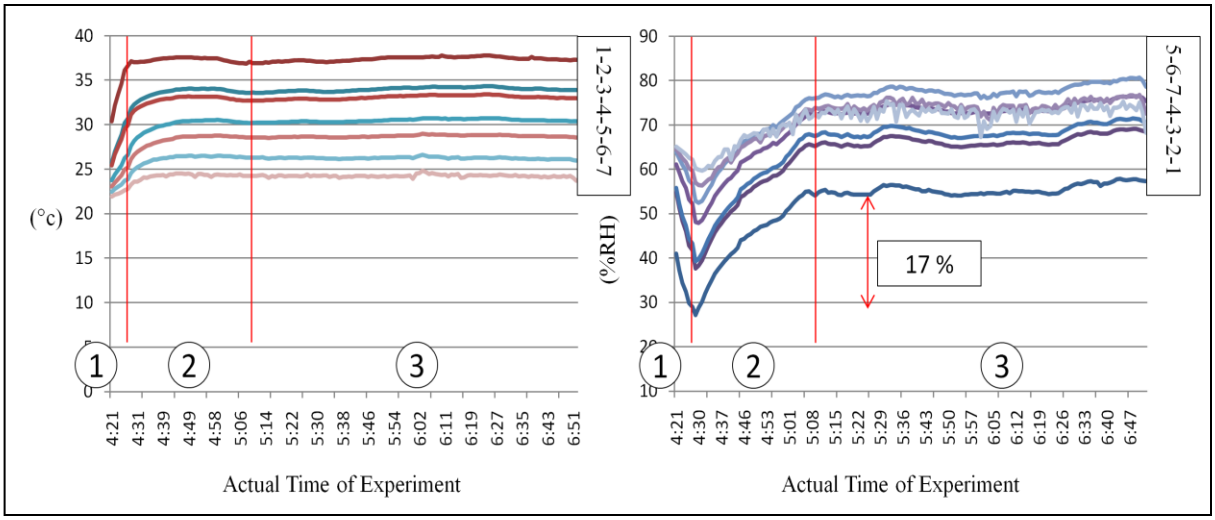

(A) (B)

Figure 69. Response time of temperature (A) and relative humidity (B) of multilayered system consisting of polyester woven against internal and external environments

In addition, Figure 69 divides change of the % relative humidity into three sections according to experiment time. Stage one indicates the area where heat energy increases. As temperature also increases in this section, the response time of the spun polyester fabric multilayered system is faster than that of the textured polyester knit multilayered system. For example, it takes only about four minutes to reach at 37 ℃ at sensor 1 in Figure 69, temperature change (A).

This response time is shorter than that of the textured polyester knit fabric multilayered system in Figure 64. Specifically, it takes approximately 40 minutes to achieve 17 % increase of relative humidity at sensor 7. This time is slightly shorter than was found with the textured polyester knit.

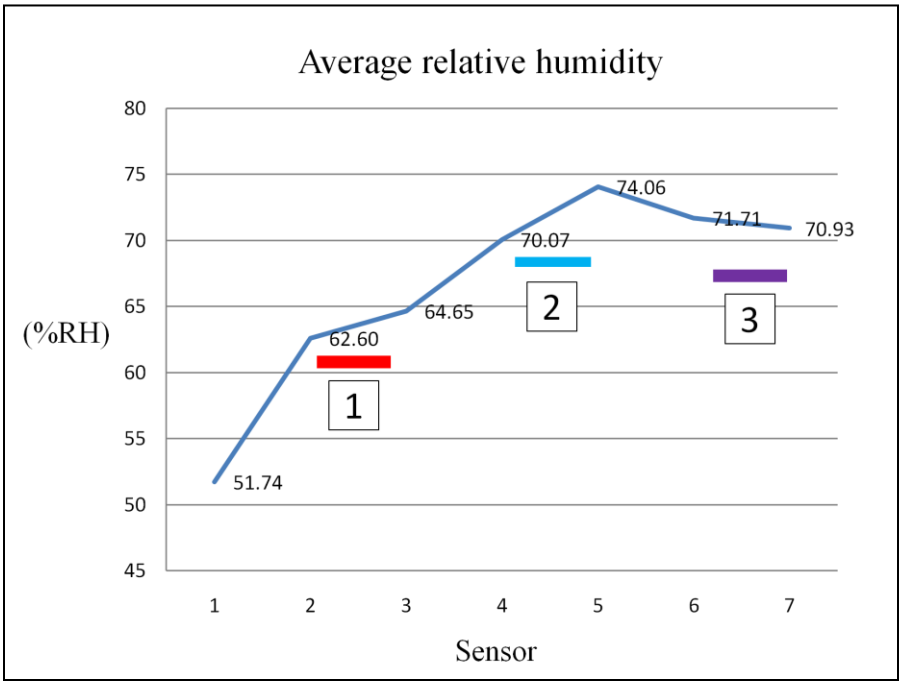

Figure 70. Average relative humidity at each sensor under standard conditions in the environmental chamber

The influence of %RH for spun polyester fabric can also be observed from Figure 70 that shows the average %RH for all seven sensors. The average % relative humidity of the middle layer is higher than that of the other two spun polyester fabrics in the multilayered system. Figure 70 shows average relative humidity change at each sensor under standard conditions. The rate of increases of average % relative humidity in the first microclimate and the second spun polyester woven fabric layer is the highest. In particular, as the first microclimate shows about 11 % difference of the relative humidity between the first and second sensors, it is similar to that of the textured polyester knit multilayered system. The second spun polyester woven fabric between the fourth and fifth sensor shows the highest average % relative humidity for the spun polyester multilayered system. The fifth sensor, in

particular, indicates the highest relative humidity, which means that water molecules in the vapor flow accumulated in this area of the spun polyester fabric system, i.e. the third microclimate. From the fourth sensor to the seventh sensor, the average % relative humidity was maintained at about 70 % RH or higher.

Table 25 shows the amount of radiation, convection, conduction, and enthalpy of vaporization in the fabrics and microclimates. In particular, this spun polyester woven fabric, which has low air permeability, shows higher energy flow via conduction. The enthalpy of vaporization is responsible for energy flow but it will be noticed that the energy flow rate through the microclimates is almost constant for this fabric multilayered system. Compared to the other multilayered fabrics discussed above, energy flow attributed to radiation and energy flow attributable to convection are all similar.

Table 25. The amount of radiation, convection, conduction, and enthalpy change for the spun polyester woven fabric multilayered system

	D1(Air)	1st Layer	D2 (Air)	2nd Layer	D3 (Air)	3rd Layer	Standard condition
Radiation (W)	0.51	N/A	0.30	N/A	0.25	N/A	0.32
Convection (W)	2.42	N/A	1.81	N/A	1.57	N/A	2.16
Conduction (W)	N/A	23.70	N/A	37.50	N/A	44.05	N/A
Enthalpy Change (ΔH) (Watt-Hour)	12.31	N/A	11.94	N/A	12.00	N/A	12.54

4.5. Comprehensive analysis of standard multilayered systems

Figure 71 shows comparison of average temperature change for the four multilayered systems consisting of standard fabric layers. In general, as the average temperature ranges from energy source to the chamber environment from 23 ℃ to 37 ℃, approximately. It can also be observed that the average temperature of the multilayered systems made with cotton fabric is normally lower than that of multilayered systems composited of polyester.

In Figure 71, it can also be observed that the rate of temperature decrease in the first fabric layer is generally lower than that of the second or third layer because heat flow, which is generated from a Flew Watt heat tape, quickly passes the first layer due to high energy flow from conduction or enthalpy change of vaporization. Therefore, the first fabric layer of a multilayered system has an important role to play in energy flow management.

The reason the temperature of the multilayered systems composed by polyester layers is higher than that of cotton layers is attributable to free water molecules that can be quickly moved in a multilayered fabric system. Therefore, heat can be quickly transferred by water molecules, which have high heat conductivity (0.6 W/m*K) from the first fabric layer to the third layer. In addition, average temperature for the knit fabric types, which have higher air permeability, are higher than that of the woven fabric made with the same fiber type. Figure 71 also shows that temperature decrease in microclimates is higher than that of layers because of the low heat conductivity of air. Therefore, the research demonstrates that the microclimates play an important role in the transfer of heat energy in a multilayered system.

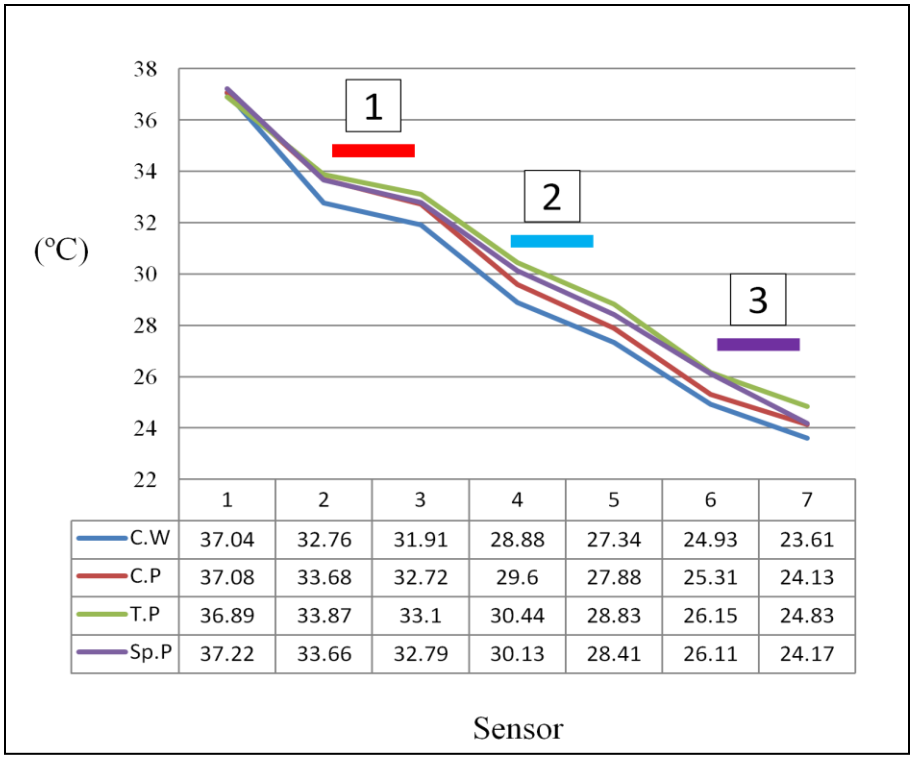

	1	2	3	4	5	6	7
C.W	37.04	32.76	31.91	28.88	27.34	24.93	23.61
C.P	37.08	33.68	32.72	29.6	27.88	25.31	24.13
T.P	36.89	33.87	33.1	30.44	28.83	26.15	24.83
Sp.P	37.22	33.66	32.79	30.13	28.41	26.11	24.17

C.W = Bleached mercerized cotton woven, C.K = Cotton knit,

T.P = Textured double knit polyester, Sp.P = Spun polyester

Figure 71. Average temperature change of the four multilayered system

Figure 72 illustrates a comparison of the average relative humidity for the four fabric forming the multilayered systems. It can be seen that the %RH of the two polyester fabrics is higher than that of the cotton fabrics. The reason for the different level of relative humidity between the polyester and cotton fabric multilayered systems can be explained since cotton is hygroscopic and water molecules are absorbed by the first cotton fabric layer and the %RH decreases. Since polyester fibers do not absorb water molecules, the number of water molecules in the polyester fabric layers would be higher than that found in cotton fabric layers.

In addition, % relative humidity in knitted fabrics was observed to have more variation than that of the woven fabrics forming the multilayered systems. It is hypothesized that the %RH variation is due to increased air permeability since higher permeability of a fabric will result in lower temperature. It will be noted that the enthalpy change due to vaporization for bleached mercerized cotton poplin woven is higher than the cotton knit which may be ascribed to the higher regain of mercerized cotton.

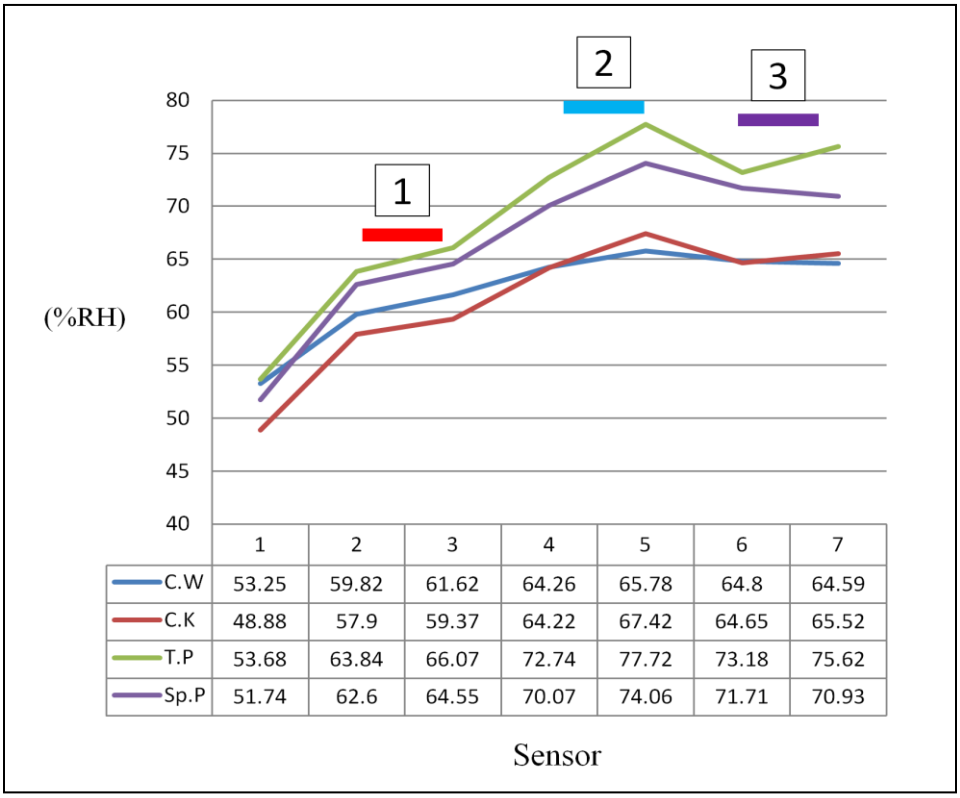

	1	2	3	4	5	6	7
C.W	53.25	59.82	61.62	64.26	65.78	64.8	64.59
C.K	48.88	57.9	59.37	64.22	67.42	64.65	65.52
T.P	53.68	63.84	66.07	72.74	77.72	73.18	75.62
Sp.P	51.74	62.6	64.55	70.07	74.06	71.71	70.93

C.W = Bleached mercerized cotton woven, C.K = Cotton knit,

T.P = Textured double knit polyester, Sp.P = Spun polyester

Figure 72. Average relative humidity of the four fabric types in the multilayered system

Table 26 summarizes of the calculated energy flow for four fabric types used in three fabric layers when the environmental chamber was operated under standard conditions. From Table 26, it can be seen that calculated radiation does not account for much of the energy flow in terms of watts in three layer fabric systems. This implies that radiation energy moves quickly through the microclimate. Convection energy plays a more important role for energy flow but it has a slower flow rate than radiation energy. Conduction is, overall, the largest contributor to energy flow in these test fabrics. The type of fabric and composition appear to have an importance influence on this type of energy flow. Enthalpy change of vaporization shows the rate of energy flow and is weight for first fabric layer of the cotton fabrics, thereafter this energy flow appears to be reasonably constant and independent of fabric layer or fabric type.

Table 26. Comparison of the amounts of radiation, convection, conduction, and enthalpy change for all of the standard multilayered system

	1st layer				2nd layer				3rd layer			
Multilayer-ed system	C.W	C.K	T.P	Sp.P	C.W	C.K	T.P	Sp.P	C.W	C.K	T.P	Sp.P
Radiation (W)	0.60	0.48	0.43	0.51	0.32	0.33	0.30	0.30	0.25	0.26	0.29	0.25
Convection (W)	2.91	2.31	2.06	2.42	2.06	2.12	1.81	1.81	1.64	1.75	1.82	1.57
Conduction (W)	14.25	7.31	10.62	23.70	27.22	12.93	22.21	37.50	22.14	8.97	18.54	44.05
Enthalpy Change (ΔH)(Watt-Hour)	26.54	16.61	11.54	12.31	11.93	11.54	11.17	11.94	12.42	11.54	12.31	12.54

C.W = Bleached mercerized cotton woven, C.K = Cotton knit,

T.P = Textured double knit polyester, Sp.P = Spun polyester

4.6. Data analysis of activewear multilayered systems

The experimental set up was used to evaluate four types of activewear clothing system which consisted of activewear fabrics purchased from retail. Table 27 shows that these multilayered systems have a range of fiber contents, such as cotton, nylon, polyester and Spandex, and construction, such as woven and knit. In addition, the experimental conditions were altered to add two environmental conditions (12 ℃ & 75 % and 30 ℃ & 90 %) as well as standard conditions (21 ℃ & 65%). Hence, the research is able to analyze response or change of the multilayered systems under all three environments in the environmental chamber. Table 27

shows the activewear fabric information regarding weight, thickness, and air permeability of the activewear layers compositing the four types of the actual multilayered systems.

Table 27. Activewear fabric properties and the position of fabrics in the multilayered system

Weight (21C +/- 1C & 65% +/- 2%: 5.25 inch * 5.25 inch)/yd^2				
Layer	A.Multi (1)	A.Multi (2)	A.Multi (3)	A.Multi (4)
1st	4.6	6.1	6.6	5.6
2nd	5.3	6.4	8.3	5.4
3rd	7.6	8.9	7.3	6.3
Thickness (21C +/- 1C & 65% +/- 2%, gf/cm^2)				
1st	0.75	0.88	0.76	0.78
2nd	0.41	0.61	1.1	0.96
3rd	2.16	2.57	2.05	1.27
Air permeability (21C +/- 1C & 65% +/- 2%, kPa*s/m)				
1st	0.08	0.44	1.41	0.54
2nd	0.37	0.69	1.87	0.19
3rd	0.38	0.64	0.48	0.19
Material contents (%): Chapter 3				
1st	Polyester (100)	Cotton (50) / Polyester (50)	Polyester (92) / Spandex (8)	Cotton (100)
2nd	Polyester (77) / Spandex (23)	Nylon (76) / Spandex (24)	Nylon (95) / Spandex (5)	Polyester (100)
3rd	Cotton (80) / Polyester (20)	Cotton (80) / Polyester (20)	Polyester (100)	Polyester (100)

Figure 73 shows temperature profiles for the activewear multilayered systems under

standard conditions in the environmental chamber room. It will be noted that the overall temperature changes for the activewear system systems are similar to each other. However, their temperature range and the temperature at each layer are slightly different. Normally, their temperature ranges are maintained from 24 ℃ to 38 ℃. The first layers in each activewear systems are 32.5 ℃, 33.5 ℃, 34 ℃, and 32 ℃, approximately. The temperature of the second layers is approximately 27 ℃, 28 ℃, 28 ℃, and 27 ℃, respectively. Finally, the temperature of all of the third layers is 25 ℃, approximately.

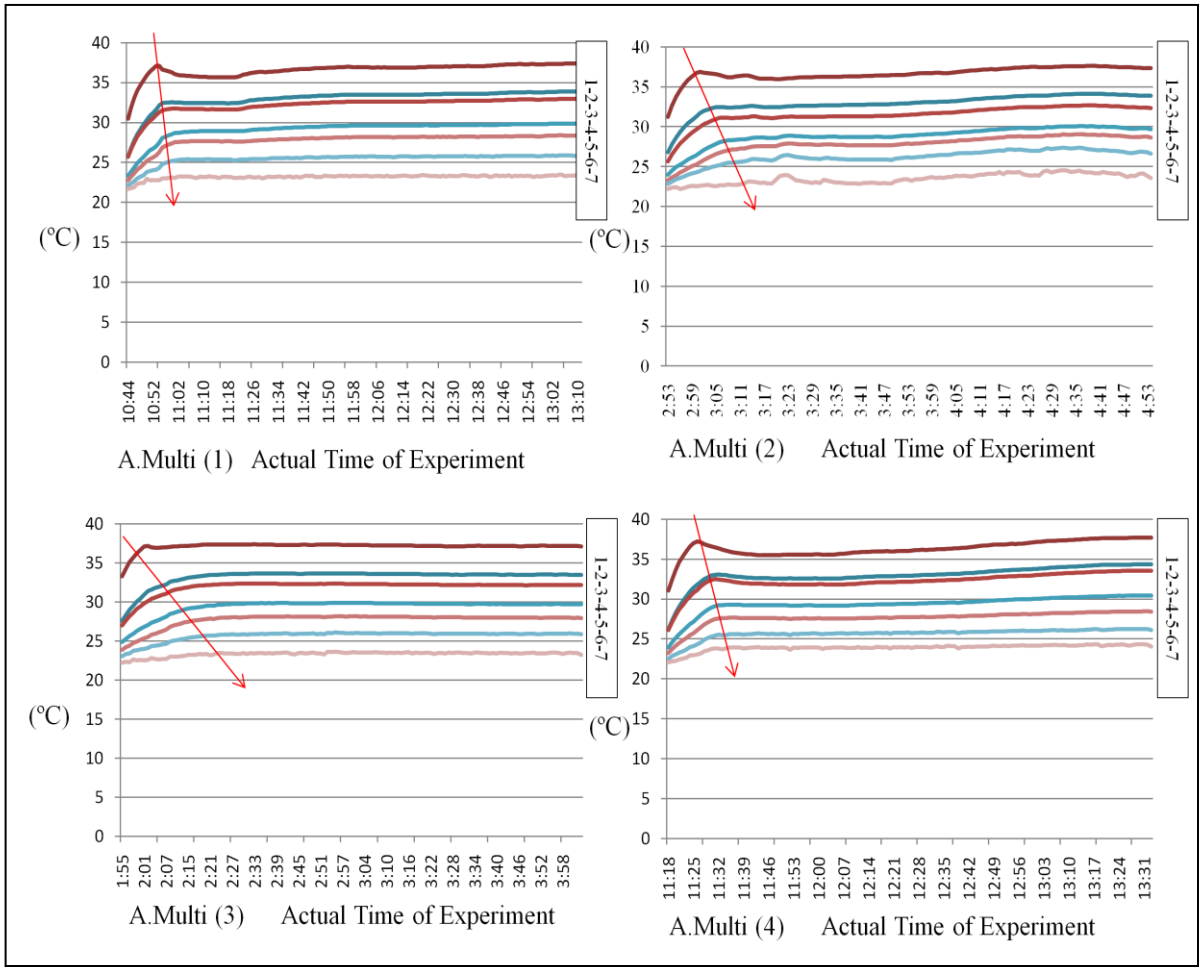

Figure 73. Temperature change and temperature response time (red arrow) of the four activewear systems under standard conditions in the environmental chamber

Among the four activewear systems, the third activewear system evaluated shows stability of temperature, hence a constant energy flow. For the third activewear system, the first layer consists of 92 % polyester and 8 % spandex, the second layer is 95 % nylon and 5 % spandex, and finally the last layer is composited with 70 % cotton and 30 % polyester. The graph shape of the third activewear system is similar to the first standard multilayered system which consists of cotton poplin woven layers. In particular, the temperature response time of each layer occurred in sequence and slower than other activewear systems after activating the humidifier. On the other hand, the temperature profiles for the other activewear systems show differences in time and rates of response and more variation in temperature as the experiment continues.

Figure 74 shows a comparison of the average temperatures for the activewear systems with those of the TestFabrics multilayered systems discussed earlier. Even though the entire temperature range is similar to each other, it can be seen that the average temperature at each layer differs. The average temperature of the TestFabrics multilayered systems is slightly higher than that of the activewear multilayered systems. In addition, the first layer of the second activewear multilayered system shows a lower temperature in comparison with the other systems. This data shows that thermal resistance of the activewear systems overall is higher than that of the standard TestFabrics multilayered systems.

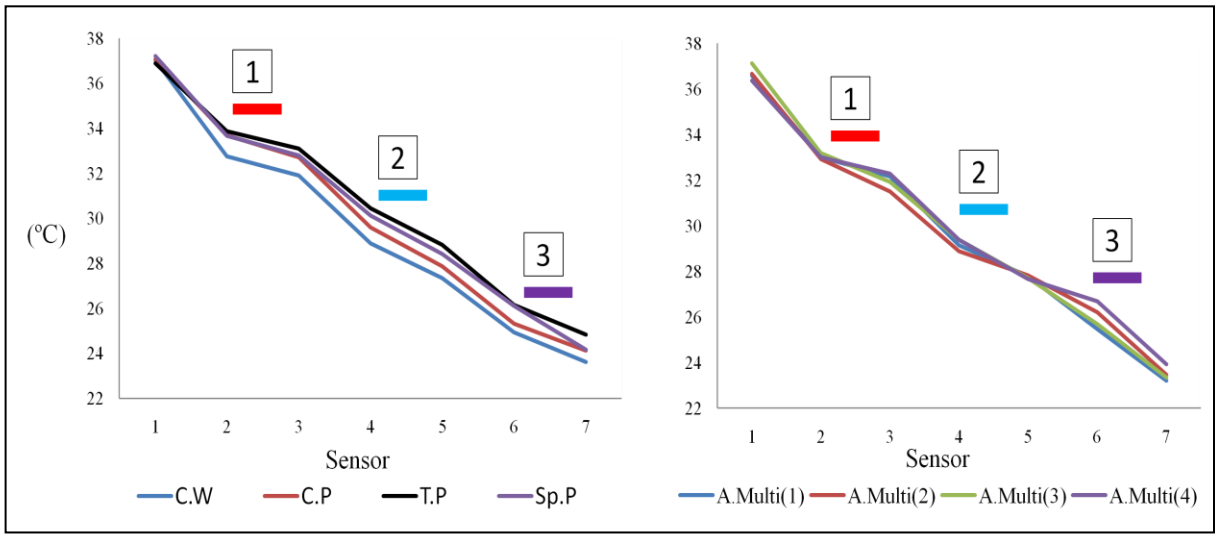

(A) (B)

Figure 74. Comparison of average temperature change of standard multilayered systems (A) with that of activewear systems (B)

Figure 75 shows the change in % relative humidity for the four activewear systems. It is clear that each activewear system has a different %RH profile over the time of the experiment. As their range of the % relative humidity is between 30 % and 75 %, it is generally wider than a level of relative humidity of the standard TestFabrics multilayered systems discussed earlier. Fluctuation of %RH in each activewear system can be observed, for example, the third activewear system shows a slow increase in %RH, while the fourth activewear system shows a fairly rapid increase followed by a slow decrease.

The %RH of the third activewear system illustrates that there is almost no difference in relative humidity between the first two fabric layers and the % relative humidity is concentrated at approximately 67 %. It should be noted that this phenomenon occurs when the fabrics are nylon/Spandex having low air permeability and the hygroscopicity of nylon

and cotton. On the other hand, the % RH of the second activewear system stabilizes after achieving a balance between actual vapor density and saturated vapor density at 60 % to 70 %. Its shape is similar to the fourth standard TestFabrics multilayered system because response time of the multilayered system is short for vapor flow, and variation in data recorded quickly stabilizes. However, the difference in % relative humidity between layers is not maintained consistently.

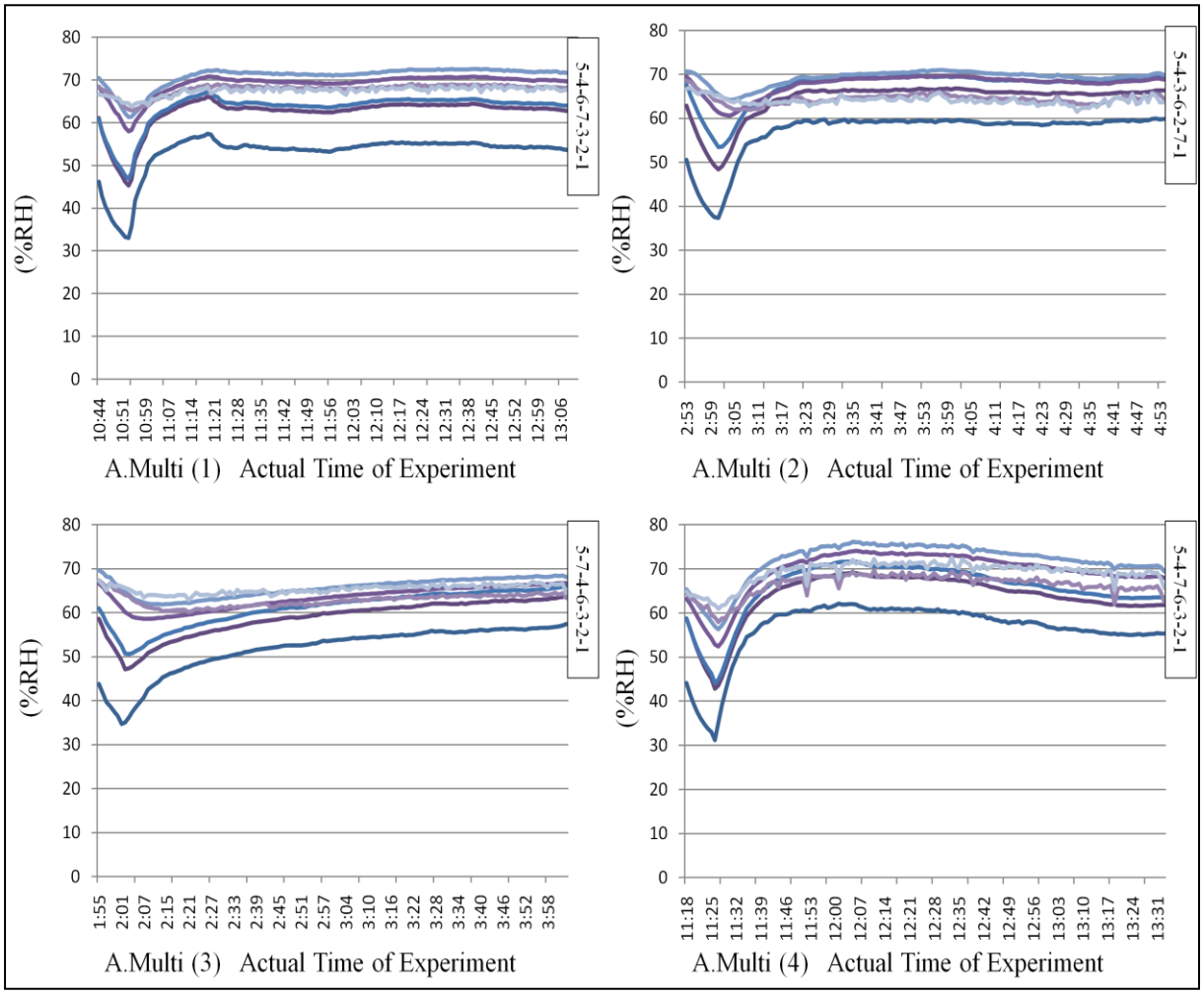

Figure 75. Change of relative humidity of the four types of multilayered systems under standard conditions in the environmental chamber

Figure 76 compares the average % relative humidity of standard TestFabrics multilayered systems with that of activewear systems at each sensor under standard conditions in the environmental chamber. While the % relative humidity profiles the standard TestFabrics multilayered systems shows differences between the systems, the activewear systems show the %RH to have a narrower range of %RH.

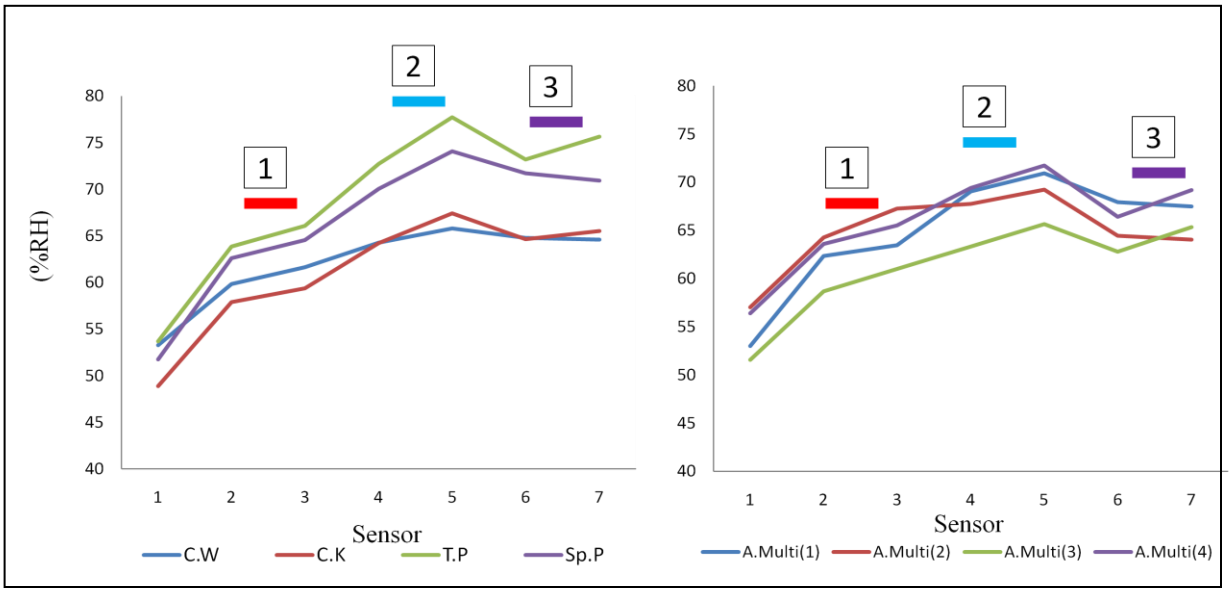

(A) (B)

Figure 76. Comparison of change of average relative humidity of standard multilayered systems (A) with that of actual multilayered ones (B) under standard conditions in the environmental chamber

The range of % relative humidity of activewear system is from 51 % to 72. This can be attributed to the higher temperatures measured for activewear systems compared to the standard TestFabrics system. Based on numerical information of average temperature and

relative humidity on Figure 75 and 77, Table 28 shows the calculated heat flow in terms of amount of radiation, convection, conduction, and enthalpy change of vaporization in each layer and microclimate of the activewear system under standard conditions in the environmental chamber.

Table 28. Amount of radiation, convection, conduction, and enthalpy change for activewear systems under standard conditions in the environmental chamber

1st Actual Multilayered system	D1(Air)	1st Layer	D2 (Air)	2nd Layer	D3 (Air)	3rd Layer	Standard condition
Radiation (Watt)	0.51	N/A	0.33	N/A	0.26	N/A	0.22
Convection(Watt)	2.44	N/A	2.06	N/A	1.58	N/A	1.50
Conduction (Watt)	N/A	12.06	N/A	51.12	N/A	7.79	N/A
Enthalpy change (ΔH) (Watt -hour)	11.55	N/A	11.27	N/A	11.61	N/A	11.87
2nd Actual Multilayered system							
Radiation (Watt)	0.53	N/A	0.29	N/A	0.19	N/A	0.25
Convection(Watt)	2.55	N/A	1.79	N/A	1.11	N/A	1.68
Conduction (Watt)	N/A	14.07	N/A	86.60	N/A	7.87	N/A
Enthalpy change (ΔH) (Watt -hour)	12.28	N/A	12.01	N/A	11.47	N/A	12.21
3rd Actual Multilayered system							
Radiation (Watt)	0.56	N/A	0.23	N/A	0.23	N/A	0.23
Convection(Watt)	2.67	N/A	1.72	N/A	1.38	N/A	1.59
Conduction (Watt)	N/A	14.39	N/A	43.68	N/A	8.96	N/A
Enthalpy change (ΔH) (Watt -hour)	11.71	N/A	12.75	N/A	11.23	N/A	11.93
4th Actual Multilayered system							
Radiation (Watt)	0.47	N/A	0.31	N/A	0.21	N/A	0.30
Convection(Watt)	2.29	N/A	1.97	N/A	1.35	N/A	1.99
Conduction (Watt)	N/A	6.12	N/A	19.53	N/A	15.01	N/A
Enthalpy change (ΔH) (Watt -hour)	11.63	N/A	11.76	N/A	11.51	N/A	12.37

Figure 77 shows temperature of the activewear systems under a warm and humid environmental condition (30 ℃ and 90 %) in the environmental chamber. The data illustrates how activewear systems react to change of an external environment; i.e. the temperature level is increased about 7-8 ℃ due to increase of external temperature and humidity. Therefore, a thermal equilibrium point is relatively increased in between heat energy created by the Flew Watt heat tape and the other heat energy of environmental chamber (Zeroth thermodynamics law). In addition, the research presumes that water molecules, which have high heat conductivity, increase the temperature of activewear systems.

The fourth activewear system shows the highest temperature level, and each fabric in the multilayered system is at a higher temperature compared to the other three activewear systems. The second and third layers of the fourth activewear system consist mainly of polyester fabrics which have relatively high heat conductivity.

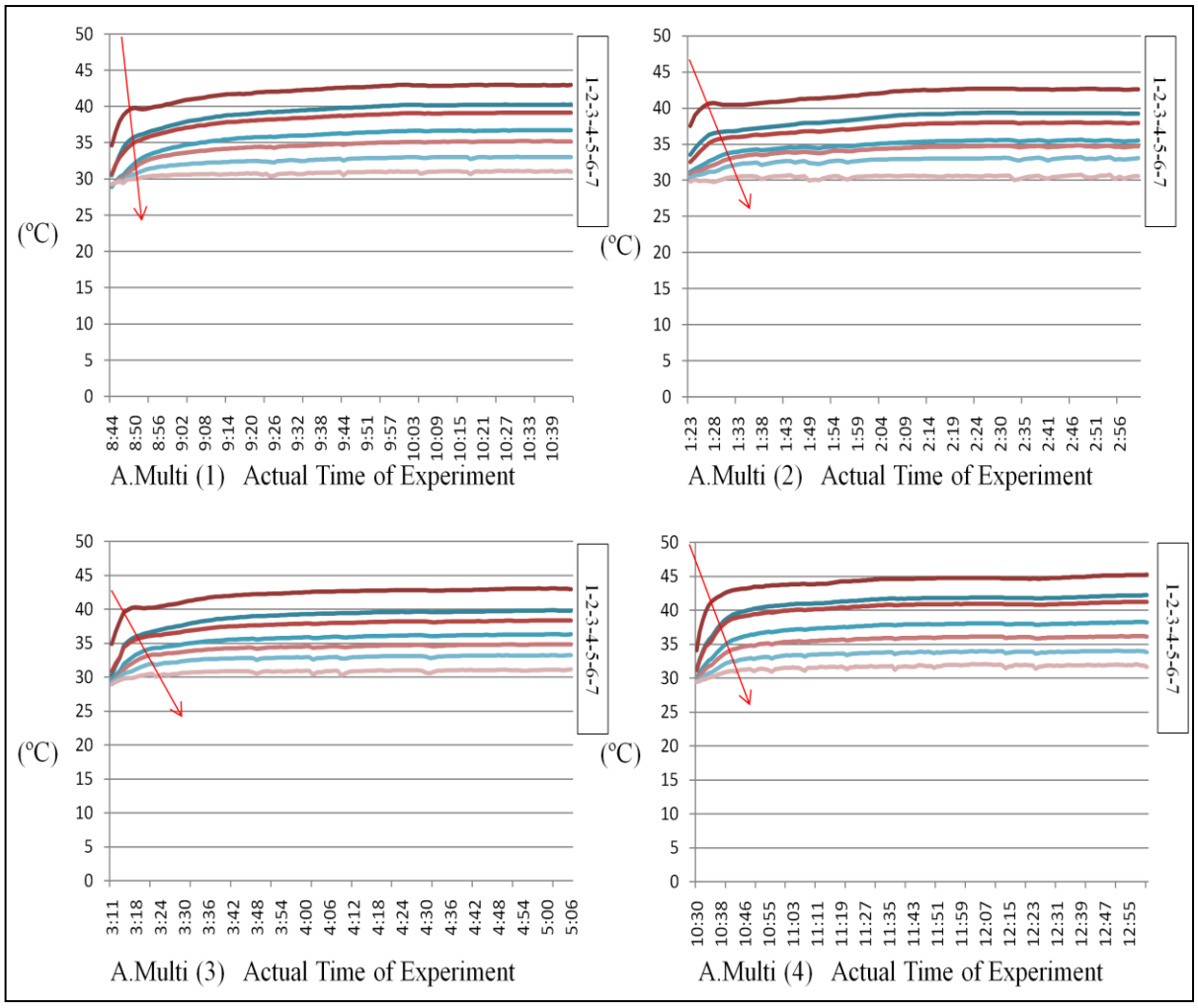

Figure 77. Temperature profiles and temperature response time (red arrow) for the four activewear systems under warm conditions in the environmental chamber

Figure 78 shows change in % relative humidity of the activewear systems when the environmental chamber is set at 30 degree C and 90 %RH. With 90 % relative humidity in the environmental chamber, the range of % relative humidity of the activewear system is from 40 % to 89 %, approximately. In all activewear cases, the last fabric layer's %RH is similar to the chamber environment which shows the importance of external environment in

determining the energy flow in activewear systems.

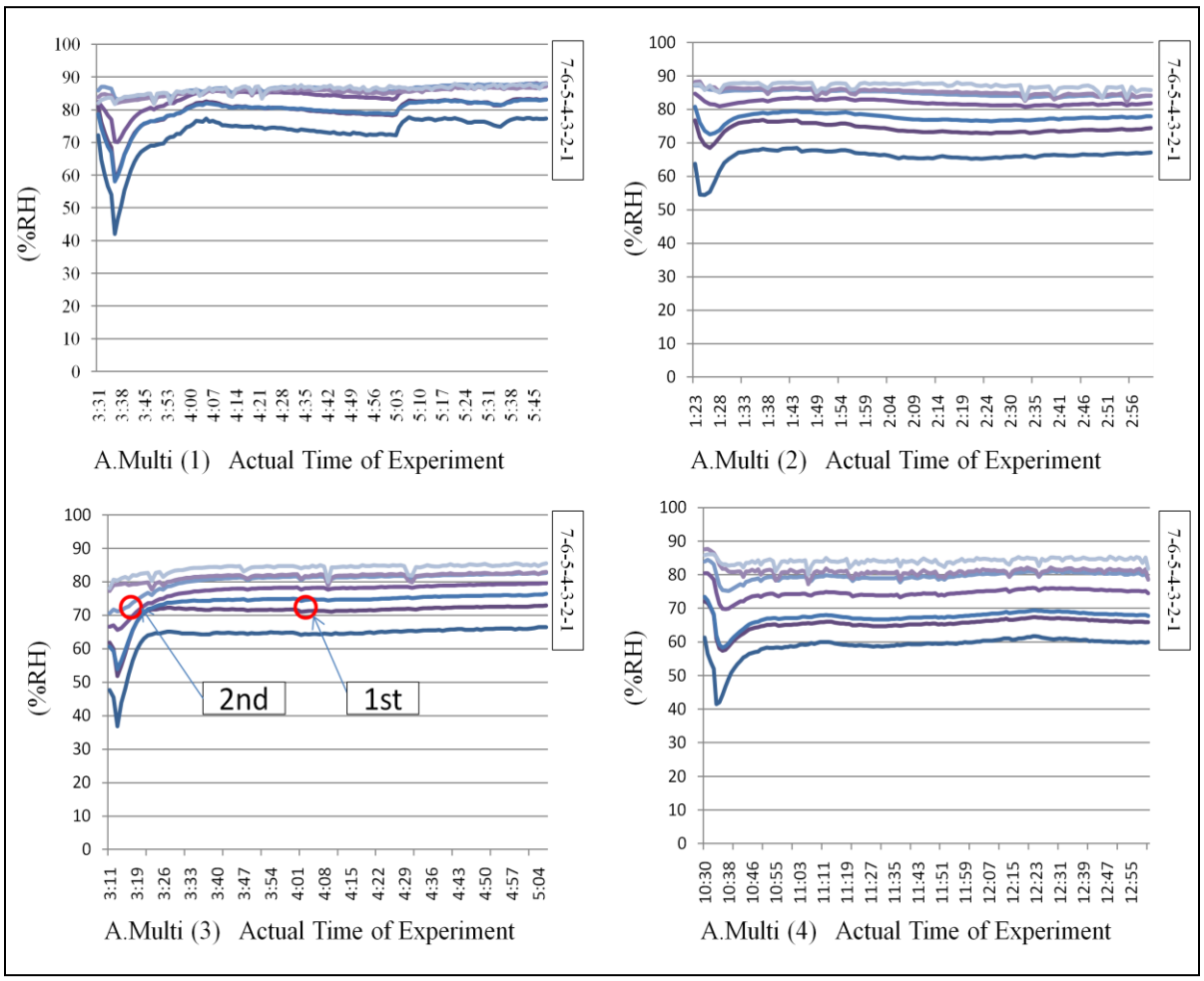

Figure 78. % relative humidity of the four activewear systems under warm conditions in the environmental chamber

Based on numerical information of average temperature and relative humidity on Figure 77 and 78, Table 29 shows the calculated heat flow in terms of amount of radiation, convection, conduction, and enthalpy change of vaporization in each layer and microclimate of the activewear system under warm conditions in the environmental chamber.

Table 29. Amount of radiation, convection, conduction, and enthalpy change for activewear systems under warm conditions in the environmental chamber

1st Actual Multilayered system	D1(Air)	1st Layer	D2 (Air)	2nd Layer	D3 (Air)	3rd Layer	Standard condition
Radiation (Watt)	0.43	N/A	0.29	N/A	0.22	N/A	0.10
Convection (Watt)	1.99	N/A	0.97	N/A	1.27	N/A	0.66
Conduction (Watt)	N/A	14.67	N/A	85.98	N/A	5.14	N/A
Enthalpy change (ΔH) (Watt -hour)	11.65	N/A	11.86	N/A	11.57	N/A	13.15
2nd Actual Multilayered system							
Radiation (Watt)	0.52	N/A	0.27	N/A	0.18	N/A	0.05
Convection (Watt)	2.34	N/A	1.65	N/A	0.99	N/A	0.30
Conduction (Watt)	N/A	12.18	N/A	59.13	N/A	6.40	N/A
Enthalpy change (ΔH) (Watt -hour)	11.84	N/A	12.23	N/A	11.97	N/A	14.21
3rd Actual Multilayered system							
Radiation (Watt)	0.50	N/A	0.23	N/A	0.18	N/A	0.08
Convection (Watt)	2.29	N/A	1.37	N/A	1.01	N/A	0.53
Conduction (Watt)	N/A	17.07	N/A	63.48	N/A	7.43	N/A
Enthalpy change (ΔH) (Watt -hour)	12.15	N/A	10.95	N/A	11.62	N/A	13.63
4th Actual Multilayered system							
Radiation (Watt)	0.47	N/A	0.33	N/A	0.24	N/A	0.18
Convection (Watt)	2.09	N/A	1.97	N/A	1.38	N/A	1.09
Conduction (Watt)	N/A	7.21	N/A	20.66	N/A	16.05	N/A
Enthalpy change (ΔH) (Watt -hour)	11.23	N/A	11.60	N/A	11.81	N/A	12.00

It can be readily observed in Table 29 that the calculated energy flow for conduction differs from one multilayered system to the other.

Figure 79 shows temperature change of activewear systems under cold and humid conditions (12 ℃ and 75 %). In this case, the humidifier does not run because the first sensor does not exceed 37 ℃. Hence, heat transfer, passing through the activewear system, is only driven by its reaction between heat energy and the external environmental condition. The range of temperature is from 16 ℃ to 34.5 ℃ approximately which is a considerably wider range of temperature than that of the activewear systems under warm conditions in the environmental chamber. In addition, as temperature of the last layer at each multilayered system is about 16 ℃, which is considerably higher than temperature (12 ℃) of a chamber room demonstrates that heat energy generated from the Flew Watt heat tape has an impact on the external fabric layer even under cold conditions.

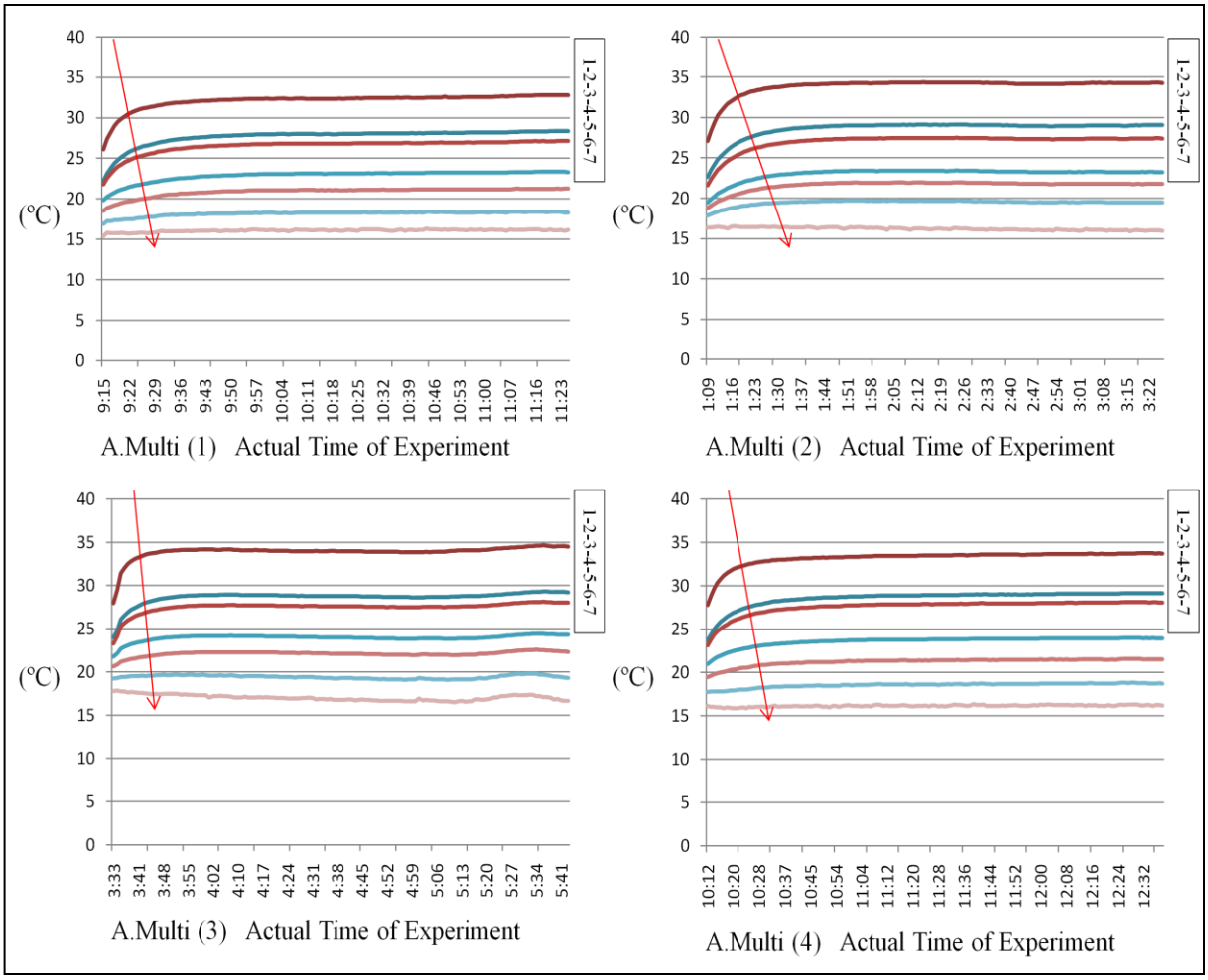

Figure 79. Temperature change and temperature response time (red arrow) of the four activewear systems under cold condition in the environmental chamber

From Figure 79, the temperature change in each layer is considerably increased in comparison with those under standard or warm conditions. According to Equation 32, the thermal resistance (R) of each layer is increased due to the decreased heat energy flow. Based on Fourier's law, this thermal resistance is proportional to thickness of a fabric. For example, temperature difference of the second activewear system is higher than that of the other three

activewear systems because the fabrics of the second activewear system are thicker than the other three activewear systems. In this experiment, the humidifier was not activated. Therefore, heat transfer effect of the additional water vapor, which has high heat conductivity, is absent. Figure 79 shows that reaction of the thermal resistance of each layer is changed according to an environmental condition, such as temperature and humidity.

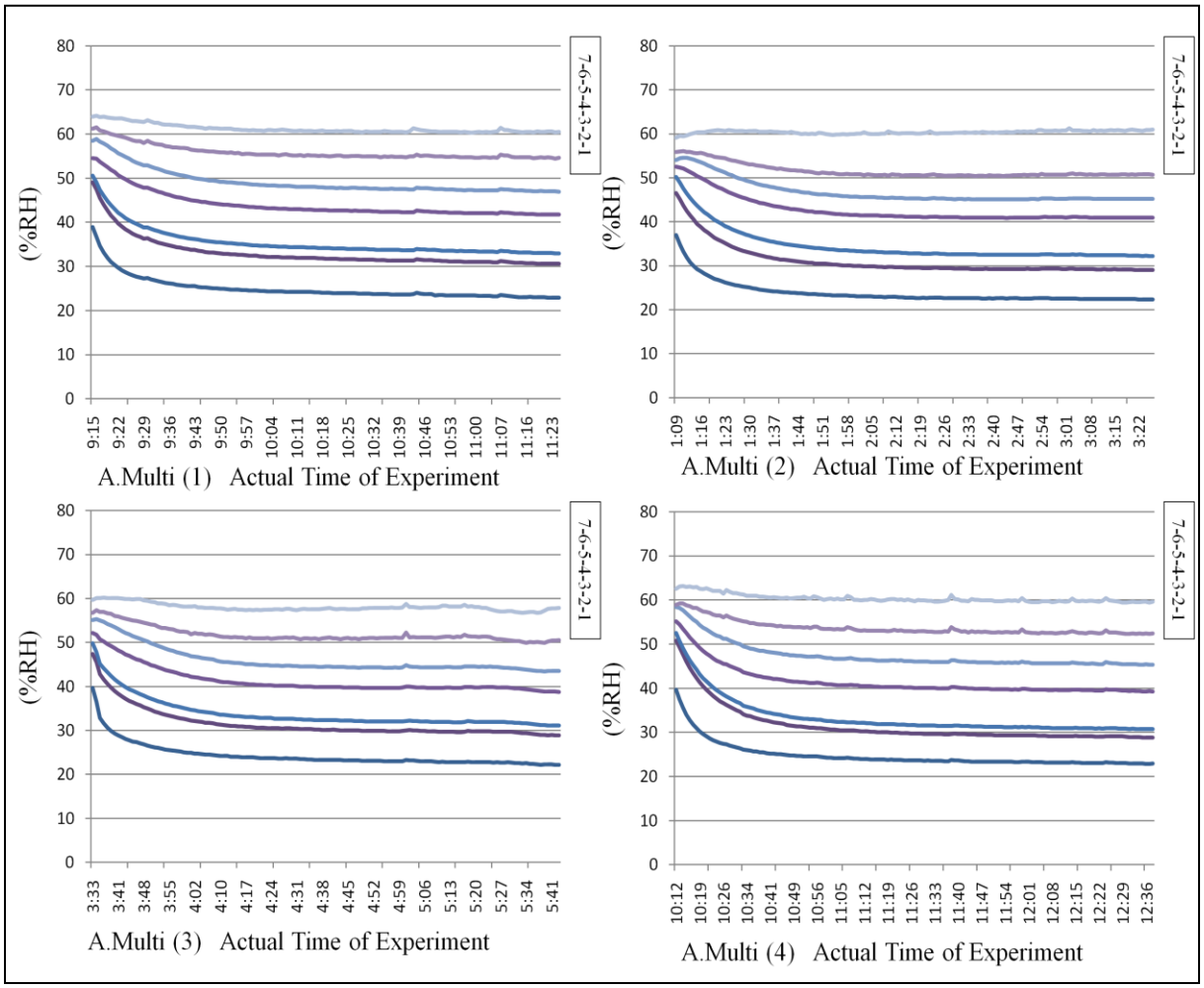

Figure 80. % relative humidity of the four activewear systems under cold conditions in the environmental chamber

Figure 80 illustrates that, the range of relative humidity is 22 % to 60 %, which is lower than 75 % in the environmental chamber room. As heat energy increases the capacity of saturated vapor density in a given space, it decreases a level of % relative humidity. The data confirms that the sensors indicating % relative humidity record an opposite response to temperature in each graph (1-2-3-4-5-6-7 (T) vs. 7-6-5-4-3-2-1 (R.H.)). For example, if temperature increases, relative humidity is decreased under these experimental conditions.

Based on numerical information of average temperature and relative humidity on Figure 79 and 80, Table 30 shows the calculated heat flow in terms of amount of radiation, convection, conduction, and enthalpy change of vaporization in each layer and microclimate of the activewear system under cold conditions in the environmental chamber.

Table 30. Amount of radiation, convection, conduction, and enthalpy change for activewear systems under cold conditions in the environmental chamber

1st Actual Multilayered system	D1(Air)	1st Layer	D2 (Air)	2nd Layer	D3 (Air)	3rd Layer	Standard condition
Radiation (Watt)	0.60	N/A	0.38	N/A	0.27	N/A	0.37
Convection (Watt)	3.01	N/A	2.48	N/A	1.90	N/A	2.78
Conduction (Watt)	N/A	16.85	N/A	73.06	N/A	7.21	N/A
Enthalpy change (ΔH) (Watt -hour)	11.48	N/A	11.76	N/A	11.72	N/A	11.63
2nd Actual Multilayered system							
Radiation (Watt)	0.73	N/A	0.41	N/A	0.22	N/A	0.39
Convection (Watt)	3.59	N/A	2.70	N/A	1.46	N/A	2.78
Conduction (Watt)	N/A	15.85	N/A	113.47	N/A	9.04	N/A
Enthalpy change (ΔH) (Watt -hour)	12.39	N/A	11.92	N/A	12.04	N/A	13.42
3rd Actual Multilayered system							
Radiation (Watt)	0.72	N/A	0.37	N/A	0.29	N/A	0.46
Convection (Watt)	3.58	N/A	2.42	N/A	1.84	N/A	3.42
Conduction (Watt)	N/A	18.97	N/A	89.64	N/A	9.14	N/A
Enthalpy change (ΔH) (Watt -hour)	11.78	N/A	12.17	N/A	11.77	N/A	11.78
4th Actual Multilayered system							
Radiation (Watt)	0.63	N/A	0.40	N/A	0.27	N/A	0.39
Convection (Watt)	3.15	N/A	2.71	N/A	1.84	N/A	2.83
Conduction (Watt)	N/A	8.47	N/A	26.79	N/A	20.51	N/A
Enthalpy change (ΔH) (Watt -hour)	11.52	N/A	11.88	N/A	11.64	N/A	11.90

It is important to note that the energy flow in the microclimates in similar to that observed in standard or warm conditions in the environmental chamber. Figure 81 shows temperature profiles of the four activewear systems using two layers under standard conditions in the environmental chamber. To conduct this experiment regarding behavior of a two layer activewear system, the third layer is removed as well as the two sensors. The experiment is conducted in standard conditions (21 ℃ and 65 %) in the environmental chamber and the humidifier is operated once the temperature reaches 37 ℃.

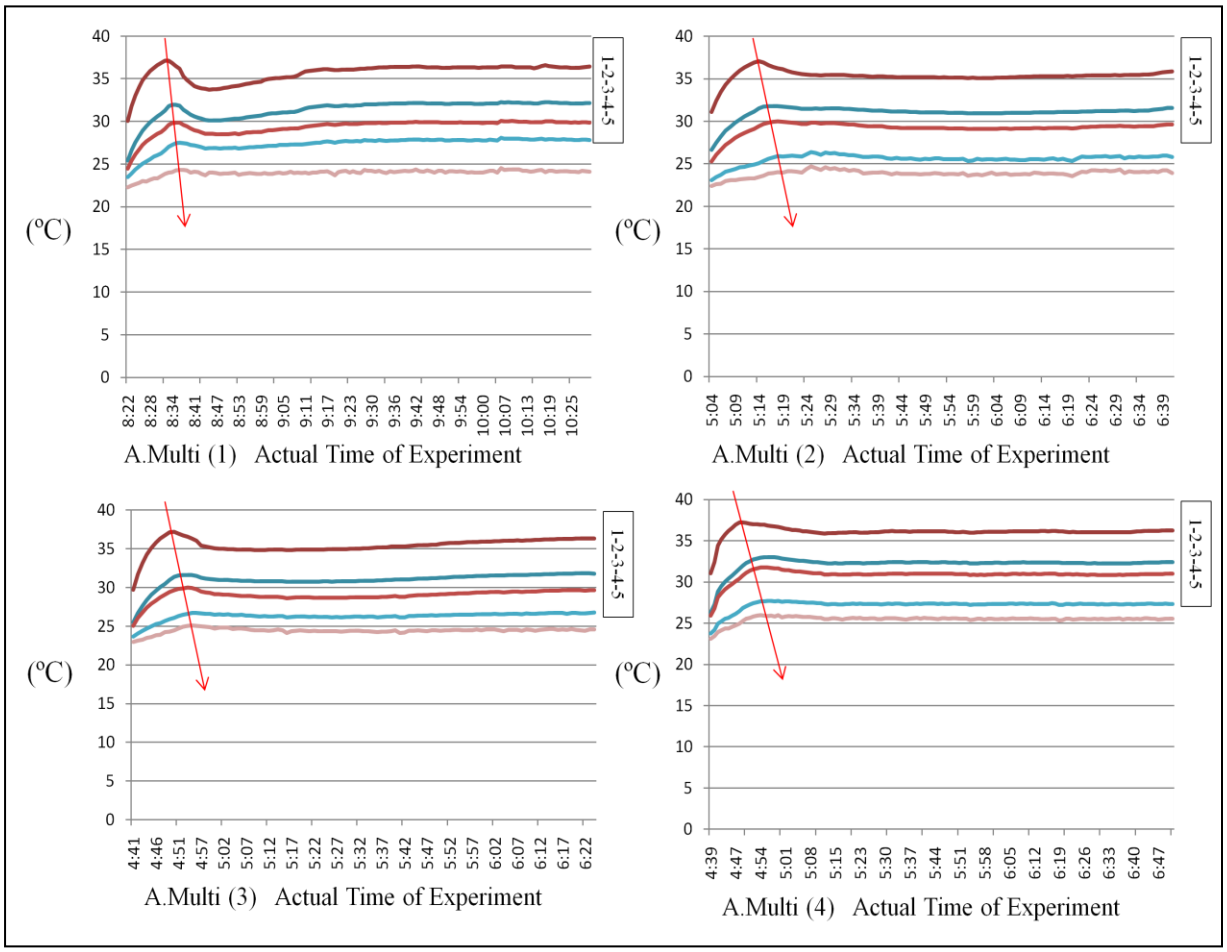

Figure 81. Temperature change and temperature response time (red arrow) of the four activewear systems using two layers under standard conditions in the environmental chamber

The range of temperature is from 24.5 ℃ to 35.5 ℃ approximately and this temperature is lower than that of the multilayered system using three layers in general. In particular, the temperature at the first sensor is about 35.5 ℃ which is lower than that of the multilayered system consisting of three layers. This demonstrates that this system cannot maintain heat energy 37 ℃ and heat energy quickly flows from a region of higher temperature to a region of lower temperature by eliminating the external fabric layer. In addition, temperature positions of the first and second layer are also placed at a lower temperature than those in the activewear systems consisting of three layers.

It can be observed that 10 minutes are needed to stabilize temperature for the second activewear system using two layers, while that of the system using three layers needs approximately 6 minutes. This demonstrates the difference in thermal resistance between the activewear systems consisting of two and three layers. Additionally, temperature difference between the first and second layer is increased compared to that of activewear systems using three layers. For instance, the temperature difference is 1.42 (32.93 ℃ – 31.51 ℃) on the first layer (sensor no.2 and 3) in the second activwear system using three layers, while it is 1.83 (31.05 ℃ – 29.22 ℃) on the first layer in the second activewear system using two layers.

Figure 82 shows % relative humidity of the four activewear systems using two layers under standard conditions in the environmental chamber. As a range of relative humidity of the multilayered systems using two layers is about 30 % to 76 %, their variation is relatively stable in comparison with that of the multilayered system consisting of three layers.

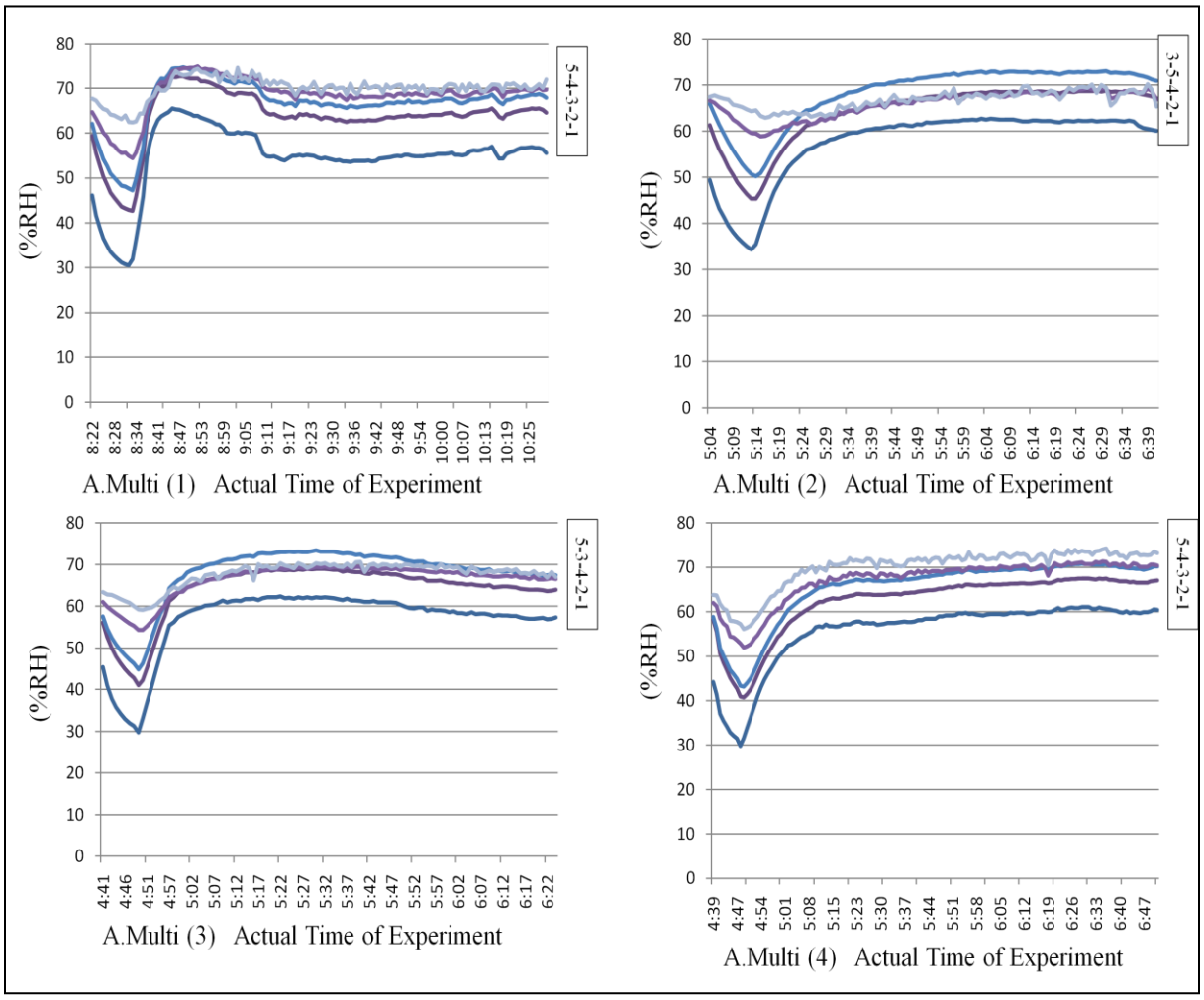

Figure 82. Relative humidity change of the four activewear systems using two layers under standard conditions in the environmental chamber

Based on numerical information of average temperature and relative humidity in Figure 81 and 82, the research measures the amount of radiation, convection, conduction, and enthalpy change of vaporization in each layer and microclimate of the actual multilayered system consisting of two layers. Table 31 shows the amount of each energy flow, radiation, convection, conduction, and enthalpy change of vaporization for activewear systems under standard conditions with using two layers in the environmental chamber

Table 31. Amount of radiation, convection, conduction, and enthalpy change for activewear systems under standard conditions with using two layers in the environmental chamber

1st Actual Multilayered system	D1(Air)	1st Layer	D2 (Air)	2nd Layer	Standard condition
Radiation (Watt)	0.60	N/A	0.21	N/A	0.31
Convection (Watt)	2.91	N/A	1.36	N/A	2.04
Conduction (Watt)	N/A	29.94	N/A	126.30	N/A
Enthalpy change (ΔH) (Watt -hour)	11.83	N/A	12.22	N/A	11.69
2nd Actual Multilayered system					
Radiation (Watt)	0.59	N/A	0.39	N/A	0.32
Convection (Watt)	2.92	N/A	2.48	N/A	1.96
Conduction (Watt)	N/A	12.39	N/A	135.84	N/A
Enthalpy change (ΔH) (Watt -hour)	12.04	N/A	12.15	N/A	11.89
3rd Actual Multilayered system					
Radiation (Watt)	0.74	N/A	0.30	N/A	0.36
Convection (Watt)	3.64	N/A	1.85	N/A	2.34
Conduction (Watt)	N/A	17.72	N/A	89.64	N/A
Enthalpy change (ΔH) (Watt -hour)	11.74	N/A	12.31	N/A	12.33
4th Actual Multilayered system					
Radiation (Watt)	0.55	N/A	0.49	N/A	0.66
Convection (Watt)	2.66	N/A	2.48	N/A	3.48
Conduction (Watt)	N/A	11.24	N/A	11.35	N/A
Enthalpy change (ΔH) (Watt -hour)	6.98	N/A	11.56	N/A	12.14

Figure 83 shows temperature profiles for the four activewear systems using one layer under standard conditions in the environmental chamber. This one layer is formed by removing the second and third layers from the activewear system which consists of three layers. As the range of temperature is from 27 ℃ to 37 ℃, the research is able to directly compare thermal resistance of each layer through temperature difference between the second and third sensor. From Figure 83, temperature difference of a single fabric can be observed and each fabric shows differences in temperature change from one side to the other. According to Fourier's law, the thermal conduction is proportionally related by thickness (Δx) and the fabric in the second single layer activewear system is thicker than the other three fabrics thus partially explains the higher temperature change.

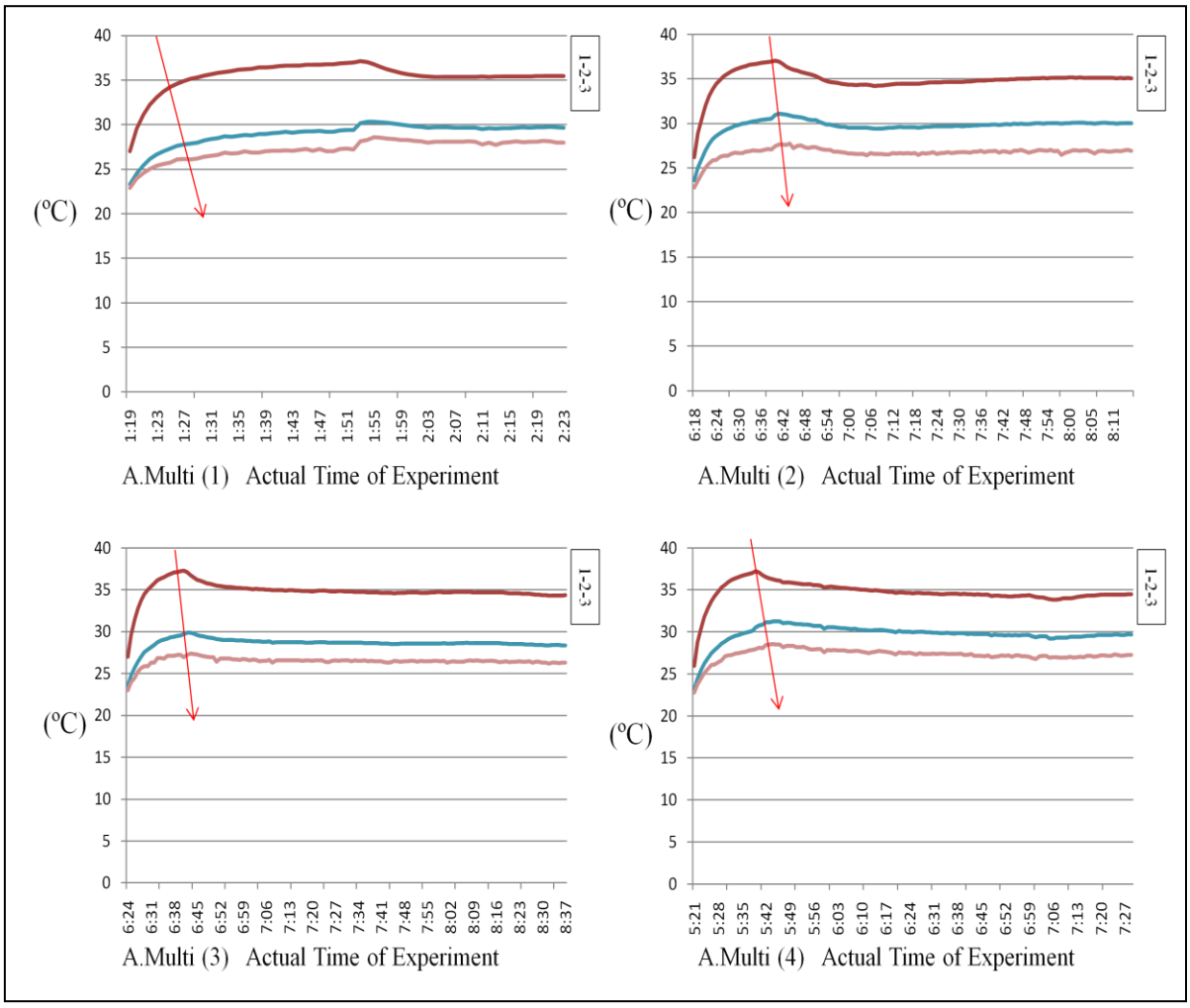

Figure 83. Temperature change and temperature response time (red arrow) of the four activewear systems under standard conditions in the environmental chamber

Table 32 shows the thickness and temperature difference of the first layer between the second and third sensor. While thickness is an important factor, other factors contribute to the temperature gradient as can be seen by comparing the thickness of the 1st, 3rd, and 4th systems where the temperature gradient varies.

Table 32. Thickness and temperature difference of the single layer activewear systems

	1st System	2nd System	3rd System	4th System
Thickness of 1st layer (mm)	0.75	0.88	0.76	0.78
Temperature Difference between T_3 and T_2 (℃)	1.23	3.00	2.13	2.45

Figure 84 shows % relative humidity for one layer activewear systems under standard conditions in the environmental chamber. The %RH profiles vary considerably in comparison with the activewear system consisting of two or three layers. The data demonstrates why test methods relying on data from a single fabric layer yield highly variable results.

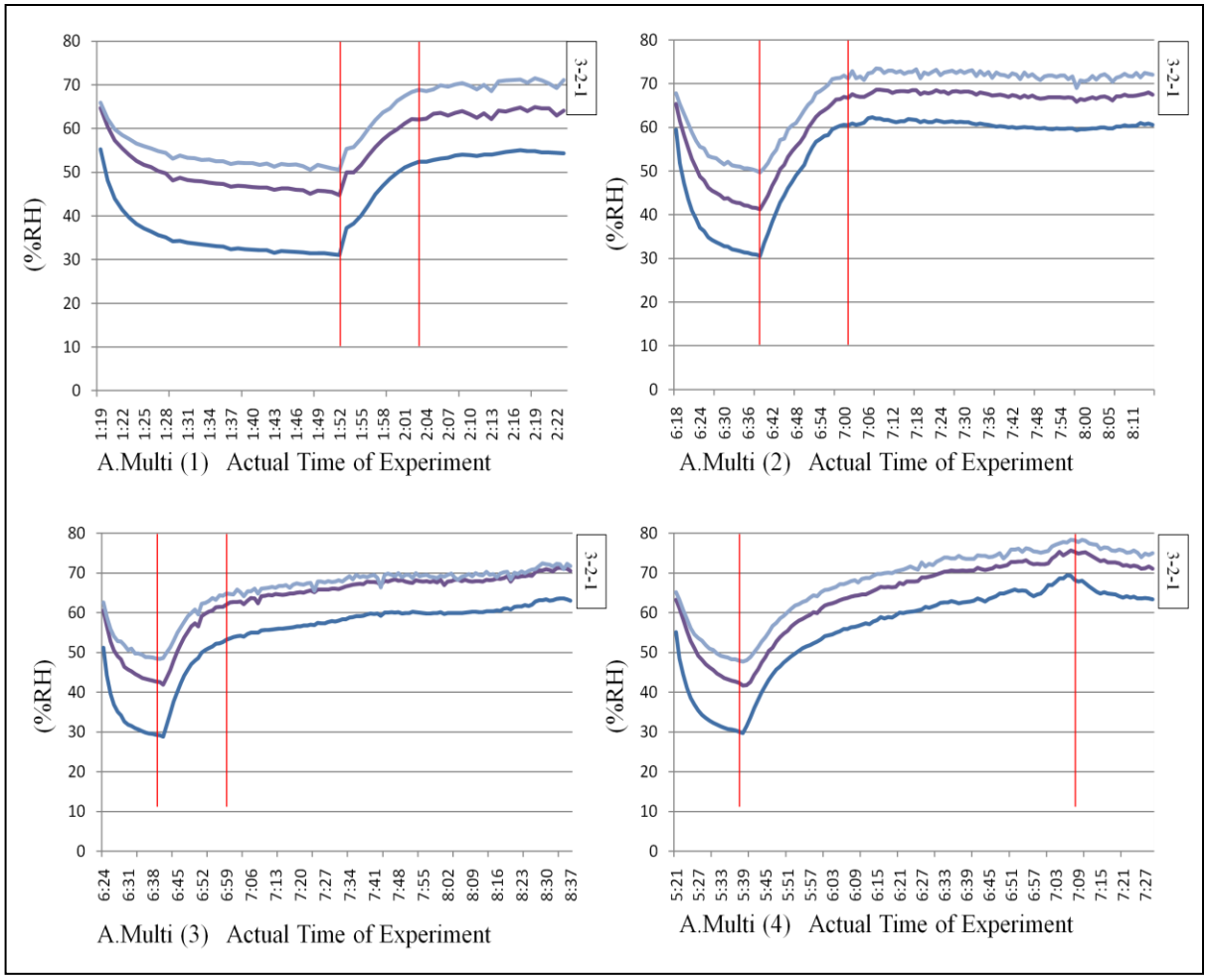

Figure 84. % relative humidity of one layer system under standard conditions in the environmental chamber

Variation of % relative humidity is inversely proportional to change of temperature at the initial section, i.e. the % relative humidity is decreased during temperature increases. In addition, the data shows that it requires different times for humidity to be stabilized for one fabric layer systems. The stabilization time is shown in Figure 84 as the distance between two red vertical lines. Table 33 shows comparison of stabilization time and material content of each layer. The data suggests that as the amount of polyester increases, the stabilization

time is relatively short.

Table 33. Comparison of stabilization time and material content of one layer activewear systems under standard conditions in the environmental chamber

Actual System No.	1st	2nd	3rd	4th
Stabilization Time (Minute)	14	25	15	90
Material content (%)	Polyester (100)	Cotton (50) / Polyester (50)	Polyester (92) / Spandex (8)	Cotton (100)

Based on numerical information of average temperature and relative humidity on Figures 83 and 84, the research measures the amount of radiation, convection, conduction, and enthalpy change of vaporization in each layer and microclimate of the actual system consisting of one layer. Table 34 shows the amount of radiation, convection, conduction, and enthalpy change for activewear systems with using one layer under standard conditions in the environmental chamber.

Table 34. Amount of radiation, convection, conduction, and enthalpy change for activewear systems with using one layer under standard conditions in the environmental chamber

1st Actual Multilayered system	D1(Air)	1st Layer	Standard condition
Radiation (Watt)	0.61	N/A	0.64
Convection (Watt)	3.1	N/A	4.25
Conduction (Watt)	N/A	25.00	N/A
Enthalpy change (ΔH) (Watt -hour)	11.79	N/A	12.01
2nd Actual Multilayered system			
Radiation (Watt)	0.71	N/A	0.58
Convection (Watt)	3.51	N/A	3.90
Conduction (Watt)	N/A	32.29	N/A
Enthalpy change (ΔH) (Watt -hour)	11.77	N/A	12.05
3rd Actual Multilayered system			
Radiation (Watt)	0.85	N/A	0.57
Convection (Watt)	4.25	N/A	3.9
Conduction (Watt)	N/A	34.45	N/A
Enthalpy change (ΔH) (Watt -hour)	11.69	N/A	11.92
4th Actual Multilayered system			
Radiation (Watt)	0.69	N/A	0.63
Convection (Watt)	3.40	N/A	4.32
Conduction (Watt)	N/A	20.12	N/A
Enthalpy change (ΔH) (Watt -hour)	11.99	N/A	11.84

5. Conclusion and Future Works

The research confirms that the energy source can be used to compare energy flow for multilayered clothing systems. Recently developed sensors permit accurate measure of temperature and % relative humidity and allow the computation of heat energy flow. Through experimental data, the research validates that there is an inverse relationship between temperature and relative humidity in a multilayered system. In addition, it is possible to calculate the amount of energy in terms of radiation, convection, conduction, and enthalpy change of vaporization based on Stefan Boltzmann equation, Newton's law of cooling, Fourier's law, and Clausius-Clapeyron relation, respectively. This means that the energy source is able to measure and analyze features of a multilayered garment system and its individual layers by calculating heat energy flow.

The external environment in the environmental chamber is also a core factor affecting flow of the heat energy and relative humidity because rate of heat energy flow can be significantly influenced by temperature difference between internal and external environment. Based on resultant data of the experiment, the research recognizes several features of a multilayered garment system as follows:

1. Temperature and relative humidity in a multilayered system can be changed in accordance with a material property of each layer.
2. External conditions, such as temperature and relative humidity, significantly influence on heat energy and vapor flow passing through a multilayered system.

3. Temperature and relative humidity in microclimates largely varied. Therefore, it is important to know how to build the microclimates in a multilayered system.
4. According to alteration of the number of layer in a multilayered garment system, the level of temperature and relative humidity are changed.
5. Temperature and relative humidity have an inverse relationship.
6. Heat energy is mainly transferred by conduction and enthalpy change of vaporization.

Among the features above, the research, in particular, recognizes that the material contents and fabrication of the layers influence on change of temperature and relative humidity in a multilayered garment system. Normally, the multilayered garment system, which consists of polyester layers, maintains higher temperature and relative humidity than another multilayered garment system which is composited by cotton layers. The research notices that the polyester multilayered garment system reacts relatively sensitively to heat energy and vapor flow, while the cotton multilayered garment system slowly responds to them.

In addition, a knit type needs more time to balance between actual vapor density and saturated vapor density relative humidity than a woven type in Equation 33. This means that, since vapor flow can be more freely moved in a multilayered system, it is not easy for a level of actual and saturated vapor density to be balanced. This fabrication also influences on movement of water molecules, which results in promotion of heat transfer between layers because the water molecule has high heat conductivity. As another core factor influencing heat energy and vapor flow among physical properties of material, thickness (Δx) is significantly related to the flows. Thickness of a layer is related to thermal resistance (R) and

temperature gradient ($T_1 - T_2$) based on Equation 32. Therefore, the research verified a relationship between thickness of a layer and change of heat energy flow. Further conclusions drawn based on the experimental results have been listed as follows:

1. Response time of temperature and relative humidity is different from material contents in a multilayered garment system. While polyester layers sensitively reacts to heat energy and vapor flow, cotton layers slowly responds to them.
2. Reaction of temperature and relative humidity is different from fabrication of a layer in a multilayered garment system. A knit type needs more time to balance between actual vapor density and saturated vapor density than a woven type.
3. Thickness of layer is significantly related to change of heat energy and vapor flow because of thermal resistance.

References

[1] Adler, M. M. (1984). Mechanisms of Transient Moisture Transport Between Fabrics, *Textile Research Journal, 54*, 334-343.

[2] Albert, R. E., and E. D. Palmes. (1951) Evaporation rate patterns from small skin areas as measured by an infrared gas analyzer, *Journal of Applied Physiology*, 4, 208-214.

[3] Albert-Wallerstrom, B. and Holmer, I. (1985). Efficiency of sweat evaporation in unacclimatized man working in a hot humid environment, *European Journal of Applied Physiology*. 480-487.

[4] Ansari, N. (2000). The Wicking of Water in yarn as measured by an electrical resistance technique. *Journal of Textile Inst. 91*(3), 401-419.

[5] ASHRAE Handbook, (2009). Two-Phase Flow, American Society of Heating, Refrigerating and Air-Conditioning Engineers, Inc. Atlanta, GA.

[6] ASHRAE Handbook, (2006). Two-Phase Flow, American Society of Heating, Refrigerating and Air-Conditioning Engineers, Inc. Atlanta, GA.

[7] ASTM D 1776-04 (2004). Conditioning and Testing Textiles, *Annual book of ASTM standards,* West Conshohocken, PA

[8] ASTM E96, (2000). Standard Test Methods for Water Vapor Transmission of Materials, *Annual book of ASTM standards,* Philadelphia, PA, 907–914.

[9] Ayling, J. H. (1986). Reginal rates of sweat evaporation during leg and arm cycling, *British Journal of Sports Med*. 35-37.

[10] Barker, R. L., Guerth-Schacher, C., Grimes, R. V., and Hamouda, H. (2006). Effects

Of Moisture on the Thermal Protective Performance of Firefighter Protective Clothing in Low-Level Radient Heat Exposure, *Textile Research Journal*, 27-31 (2006).

[11] Bass, D. E., and A. Henschel. (1956). Responses of body fluid compartments in heat and cold. *Physiol. Rev*, 36, 128-144.

[12] Baxter, S. (1946). The Thermal Conductivity of Textiles, *Proc Phys Soc*. 58, 105-118.

[13] Beaumond, V. W. and Bullard, R. W. (1963). Sweating: its rapid response to muscular work, Science. 643-646.

[14] Belding, H. S. (1946). Analysis of Factors Concerned In Maintaining Energy Balance for Dressed Men In Extreme Cold; Effects of Activity on The Protective Value and Comfort of An Arctic Uniform. 223-239.

[15] Bendkowska, W. (2005). Determining temperature regulating factor for apparel fabrics containing phase change material. *International Journal of Clothing Science and Technology, 17*(3/4), 209-214.

[16] Benedict, M. (1937). Pressure, Volume, Temperature properties of nitrogen at high density at high density, 1 and 2. Journal of American Chemists Society. 59, 2224-2233.

[17] Bhat, N. V. (1990). Effect of Perspiration on the Fine Structure of Cotton Fabrics. *Textile Journal Research*, 60, 240-244.

[18] Bunsell, A. R. and Hearle, J.W.S. (1971). A mechanism of Fatigue Failure in Nylon Fiber. *Journal of Material Science*, 6, 1303-1311.

[19] Branson, D. H., Abusamra, L., and Hoener, C. (1988). Effect of Glove Liners on

Sweat Rate, Comfort, and Psychomotor Task Performance, *Textile Research Journal*. 58, 166-173.

[20] Braton, F. B. (2004). Classification of Farnworth Munsell 100-hue Test Results in the early treatment diabetic retinopathy study. *American Journal of Ophthalmology,* 119-124.

[21] BS7209, (1990). *Specification for Water Vapour Permeable Apparel Fabrics*, British Standards Institute, London.

[22] Burdett, R. G., and Skrinar, G. S. (1983). Comparison of Mechanical Work and Metabolic Energy Consumption during Normal Gait. *Journal of Orthopedic Research*, 63-72.

[23] Candas, V., Libert, JP, and Vogt, JJ. (1979). Human skin wetness and evaporative efficiency of sweating, Journal of Applied Physiol Respirat Environ Exercise Physiol. 522-528.

[24] Chaudhari, S. S., Chitnis, R. S., Ramkrishan, R. (2001). Waterproof Breathable Active Sports Wear Fabrics. 1-14.

[25] Chen, J. J. and Yu, W. D. (2008). Theoretical and experimental analysis on thermal properties of flexible thermal insulation composite fabric.

[26] Cho, G.S., Cho, J.Y. (2005). Physiological and Subjective Evaluation of the Rustling Sounds of Polyester Warp Knitted Fabrics. *Textile Research Journal*, *75*(4), 312-318.

[27] Civoni, B. and Coldman, R. F. (1971). Predicting Metabolic Energy Cost. *Journal of Applied Physiology,* 30(3), 429-433.

[28] Colin, J., and Y. Houdas. (1965). Initiation in sweating in man after abrupt rise in

environmental temperature. *Journal of Applied Physiology*, 20, 984-990.

[29] Consolazio, C. F. and Matoush, L. R. O. (1962). Environmental temperature and energy expenditures. 65-68.

[30] Das, B., Kothari, V. K., Fangueiro, R., Araujo, M. de. (2007). Moisture Transmission through Textiles: Part2, Evaluation Methods and Mathematical Modeling. *AUTEX Research Journal*, 7(3), 194-216.

[31] Dasgupta, S. and Hammond, W. B. (1996) Crystal Structures and Properties of Nylon Polymers from Theory. *Journal of American Chemical Society*, 118, 12291-12301.

[32] de Dear, R. J., Arens, E., and Hui, Z. (1997). Convective and radiative heat transfer coefficients for individual human body segments, *Inter Journal Biometeorol*. 141-156.

[33] Dionne, J. P., Semeniuk, K., Makris, A. (2003). Thermal Manikin Evaluation of Liquid Cooling Garments Intended for Use in Hazardous Waste Management. 23-27.

[34] Durnin, JVGA and Wemersley, J. (1974). Body fat assessed from total body density and its estimation from skinfold thickness: measurements on 481men and women aged from 16 to 72y. *Br. J. Nutr*, 32, 77-97.

[35] Egan, M. D. (1975). Concepts in Thermal Comfort, Prentice-Hall, Inc, Englewood Cliffs, New Jersey.

[36] Elizabeth, P. (2006). Evaluation of the care and performance of comfort-stretch knit fabrics, *AATCC review, 6(11)*, 1-6

[37] Eunae, K. (2006). Performance of Selected Clothing System under Subzero Conditions: Determination of performance by a Human-Clothing-Environment Simulator.

Textile Research Journal, 7(301), 301-308.

[38] Eunae, K and Shinjung, Y. (2010). Human-clothing-environmental simulator, United Patent, 7680638.

[39] Fahmy, S. M. A., and Slater, K. (1976). A new apparatus to measure the resistance of textiles to water-vapor diffusion, *Journal of Textile Institutes*, 67, 273-276.

[40] Fanger, P. O. (1970). Thermal Comfort: Analysis and Applications in Environmental Engineering, Danish Technical Press, Copenhagen.

[41] Farnworth, B. (1990). Variation of Water Vapor Resistance of Micro-porous and Hydrophilic Film with Relative Humidity. *Textile Research Journal, 60(1),* 50-53.

[42] Fohr, J. P. (2002). Dynamic Heat and Water Transfer Through Layered Fabrics. *Textile Research Journal, 72*(1), 1-12.

[43] Fowler, M. (2005). Heat Transfer: Conduction, Convection, Radiation. Retrieved from http://galileo.phys.virginia.edu/classes/152.mf1i.spring02/HeatTransport.htm.

[44] Frydrych, I., Dziworska, G., and Bilska, J. (2002). Comparative Analysis of the Thermal Insulation Properties of Fabric Made of Natural and Man-made Cellulose Fibres, *Fibres & Texiles in Eastern Europe*. 40-44.

[45] Galimidi, U. C. and Stewart, J. M. (1979). The effect of body motion on convective heat transfer from a nude man, *Journal of South African Institute of Mining and Metallurgy.* 485-488.

[46] Gibson, P. (2008). Water-repellent treatment on military uniform fabrics: Physical and comfort implications. *Journal of Industrial Textile, 38*(1), 43-53

[47] Gibson, P. (1997). The use of volume-averaging techniques to predict temperature

transients due to water vapor sorption in hygroscopic porous polymer materials. *Journal of Apply Polymer Science*, 64, 493-505.

[48] Givoni, B. (1976). Man, climate and architecture, Applied Science Publishers, London, 27-29.

[49] Gollnick, P. D. and Hermansen, L. (1973). Biochemical adaptations to exercise: anaerobic metabolism. *In Exercise and Sport Sciences Reviews,* 1, 1-43.

[50] Gordon, K. E. (2009). Metabolic and Mechanical Energy Costs of Reducing Vertical Center of Mass Movement During Gait. Arch Phys Med Rehabil, 90, 136-144.

[51] Gretton, J. C. (1998). Moisture Vapor Transport Through Waterproof Breathable Fabrics and Clothing Systems Under Temperature Gradient. *Textile Research Journal, 68(12),* 936-941.

[52] Grucza, R. (1983). Body Heat Balance in Man Subjected to Endogenous and Exogenous Heat Load, *European Journal of Applied Physiology*. 51, 419-433.

[53] Guyton, A. C. (2000). Textbook of medical physiology. Philadelphia, Saunders.

[54] Gupta, B. S. and Hong, C. J. (1994). Changes in web dimensions during fluid uptake and the impact on absorbency, *Tappi Journal*. 77, 181-188.

[55] Hardy, J., and Du Bois, E. F. (1937). Basal metabolism, radiation, convection and vaporization at temperature. The Journal of Nutrition, 15(5), 477-497.

[56] Havenith, G. (2005). Temperature Regulation, Heat Balance and Climatic Stress. 69 -80.

[57] Havenith, G. (2002). Moisture Accumulation in Sleeping Bags at Subzero Temperatures-Effect of Semipermeable and Impermeable Covers.

Textile Research Journal, 72(4), 281-284.

[58] Hearle, J. W. S. (2001). High-Performance Fibers. Woodhead Publishing Limited, NW.

[59] Hernett, P. R., and Mehta, P. N. (1984). A survey and comparison of Laboratory Test Methods for Measuring Wicking. *Textile Research Journal*, 54, 471-478.

[60] Hes, L. and Araujo, M. D. (1996). Effect of Mutual Bonding of Textile Layers on Thermal Insulation and Thermal Contact properties of Fabric Assemblies. *Textile Research Journal, 66(245),* 245-250.

[61] Holcombe, B. V. and Hoschke, B. N. (1983). Dry heat transfer characteristics of underwear fabrics, *Textile Research Journal*, 368-374.

[62] Hollies, N. R. S., and Kaessinger, M. M. (1957). Water transport mechanisms in Textile Materials: Part II: Capillary-Type Penetration in yarn and fabrics. *Textile Research Journal*, 27, 8-13.

[63] Hong, K. (1988). Dynamic moisture vapor transfer through textiles, Part 1: Clothing hygrometry and influence of fiber type, *Textile Research Journal, 58(12),* 697-706.

[64] Hope, P. R. (1993). Heat balancing model. *Experientia*, 49, 741-746.

[65] Howell, J. R. and Buckius, R. O. (1992). Funcdamentals of Engineering Thermodynamics, 2nd ed. McGraw-Hill, New York.

[66] Hu, J., Li, Y., Yeung, K. W., Wong, A. S. W., Xu, W. (2005). Moisture Management Tester: A Method to Characterize Fabric Liquid Moisture Management Properties. *Textile Research Journal, 75*(1), 57-62.

[67] Huang, J. (2007). A new test method for determining water vapor transport properties

of polymer membranes. *Polymer Testing, 26, 685-691*.

[68] Isamil, M. I., Ammar, A. S. A., and El-Okeily, M. (1985). On Thermal Conductivity of Some Fabric, *Journal of Applied Polymer Science*. 30, 2343-2350.

[69] Ishigaki, H., Horikoshi, T., and Uematsu, T. (1993). Experimental study on convective heat transfer coefficient of the human body, *Journal of Thermal Biology*. 18, 455-458.

[70] ISO 11092, (1993). *Textiles-Physiological Effects-Measurement of Thermal and Water Vapour Resistance under Steady-State Conditions (Sweating Guarded-Hotplate Test),*International. Organization for Standardization, Geneva.

[71] Janna, W. S. (2000). Engineering Heat Transfer, CRC Press, Washing D.C.

[72] Jassal, M., Khungar, A., Bajaj, P. (2004). Waterproof Breathable Polymeric Coating Based on Polyurethanes. *Journal of Industrial Textile, 33*(4), 269-280.

[73] J. Q, and Ruckman. (2006). A new calculation method of water vapor permeability at unsteady state. *Journal of Textile Institute, 97*, 449-453.

[74] Kakitsuba, N.(2004). Dynamic changes in sweat rates and evaporation rates through clothing during hot exposure, Journal of Thermal Biology. 739-742.

[75] Kaminski, D. A. and Jensen, M. K. (2005). Introduction to Thermal and Fluid Engineering, John Wiley & Sons, Inc, Hoboken, NJ.

[76] Kandjov, I. M. (1999). Heat and mass exchange processes between the surface of the human body and ambient air at various altitudes, *Int. Journal Biometeorol*. 43, 38-44.

[77] Kannekens, A. (1994). Breathable Coatings and Laminates. *Journal of Industrial Textiles, 24*, 51-59.

[78] Kerslake, D. M. (1972). The stress hot environments, Cambridge University Press,

Cambridge.

[79] Kissa, E. (1996). Wetting and Wicking. *Textile Research Journal*, 66, 660-668.

[80] Kondepudi, D. (2008). Introduction to Modern Thermodynamics, John Wiley & Sons, Inc, Hoboken, NJ.

[81] Koronthalyova, O. (2003). Thermal Conductivity of Fibre Reinforced Porous Calcium Silicate Hydrate-Based Composites. *Journal of Thermal Envelope and Building Science, 27*, 71-89.

[82] Kraning, K. (1978). A gas stream heater to control local skin temperature under evaporative sweat capsules. *American Physiological Society*, 981-985.

[83] Kurazumi, Y., Tsuchikawa, T, Matsubara, N., and Horikoshi, T. (2004). Convective heat transfer area of the human body, *European Journal of Physiology*. 273-285.

[84] Laing, R. M. (2007). Response of Wool Knit Apparel Fabrics Water Vapor and Water. *Textile Research Journal, 77(3)*, 165-171.

[85] Li, Y., Aihua, M., Ruomei. (2006). P-smart- a virtual system for clothing thermal functional design. Computer-Aided Design, 38, 726-739.

[86] Li, Y. (2002). Influence of Thickness and Porosity on Coupled Heat and Liquid Moisture Transfer in Porous Textile. *Textile Research Journal, 72(5),* 435-446.

[87] Li, Y. (1998). Mathematical Simulation of Heat and Moisture Transfer in a Human-Clothing-Environment System. *Textile Research Journal, 68(6), 389-397.*

[88] Logan, E. (1999). Thermodynamics: Processes and Applications, Marcel Dekker, Inc, New York.

[89] Lomax, R (1990). Hydrophilic Polyurethane Coatings. *Journal of Industrial Textile*

, 20, 1-21

[90] Mao, N. and Russell, S. J. (2007). The Thermal Insulation Properties of Spacer Fabrics with a Mechanically Integrated Wool Fiber Surface, *Textile Research Journal*. 77, 914-922.

[91] Marcus, S. M. and Blaine, R. L. (1998). Thermal Conductivity of Polymers, Glasses & Ceramics By Modulated DSC, TA Instruments. 1-9.

[92] Martin, J. J. and Hou, Y. (1955). Development of an equation of state for gases, *AIChE Journal*, 1-142.

[93] McCullough. E. A. (2004). An Explanation and Discussion of sweating hot plate standards. *Journal of ASTM Int*, 1. 1.

[94] McCullough, E. (2003). Comparison of standard methods for measuring water vapour permeability of fabrics. *Measurement Science and Technology*, 14, 1402-1408.

[95] McPherson, M. J. (1993). Subsurface Ventilation and Environmental Engineering: Introduction to Fluid Machanics, Springer.

[96] Mikolajczyk, T., Wolowska-Czapnik, D. (2005). Multifunctional Alginate Fibres with Anti-bacterial Properties. *Fibres & Textile in Eastern Europe, 13*(3), 35-40.

[97] Mitchell, D., and Senay, L. C. (1976). Acclimatization in a hot, humid environment: energy exchange, body temperature, and sweating. *Journal of Applied Physiology*, 40(5), 768-778.

[98] Milenkovic, L., Skundric, P. (1999). Comfort properties of Defense Protective Clothings, *The scientific journal FACTA UNIVERSITATIS,* 4, 101-106

[99] Miller, A. T. (1968). Energy metabolism. Philadelphia, F.A. Davis Co.

[100] Modakef, S. (1986). Simultaneous heat and mass transfer with phase change in a porous slab, *International Journal of Heat Mass Transfer, 29*(10), 1503-1512.

[101] Moran, M. J. and Shaprio, H. N. (2008). Fundamentals of Engineering Thermodynamics, John Wiley & Sons, Inc, Hoboken, NJ.

[102] Nelbace, J. H. and Herrington, L. P. (1942). A note on the hygroscopic properties of clothing in relation to human heat loss, *Science*. 387–388.

[103] Ng. T. W. (2005). Inexpensive color evaluation of dyed-based pressure-sensitive films for plantar studies. *Journal of Biomechanics, 38*, 1-4.

[104] Nilsson, A. L. (1987). Blood Flow, Temperature, and Heat Loss of Skin Exposed to Local Radiative and Convective Cooling. *The Journal of Investigative Dermatology , 88*(5), 586-593.

[105] Niwa, M., Inoue, M. (1999). The objective evaluation of blanket hand and durability. *International Journal of Sports Science and Engineering,11*(2/3), 90-104.

[106] Nyoni, A. B. (2006). Wicking Mechanisms in yarns-the key to fabric wicking performance. *Textile Research Journal, 97*(2). 119-128.

[107] Ostwald, W. (1891). Solutions, Longmans, Green, And Co. New York.

[108] Parsons, K. The estimation of metabolic heat for use in the assessment of thermal comfort, 1-8.

[109] Partsch, H. (2006). Interface pressure and stiffness of ready made compression stockings: Comparison of in Vivo and in Vitro measurement. Journal of Vascular surgery, 44(4), 809-814.

[110] Powers, S. K. and Howley, E. T. (2007). Exercise physiology: theory and applications

to fitness and performance, Boston: McGraw-Hill Publishers.

[111] Prahsarn, C., Barker, R. L., and Gupta, B. S. (2005). Moisture Vapor Transport Behavior of Polyester Knit Fabrics, *Textile Research Journal*. 75, 346-351.

[112] Ramachandran, T., Kesavaraja, N. (2004). A Study on Influencing Factors for Wetting and Wicking Behaviour. *84*, 37-41.

[113] Ribeiro, A. C. (2002). Diffusion Coefficients in Aqueous Solutions Cobalt Chloride at 298. 15 K. *Journal of Chemical & Engineering DATA, 47(3),* 539-541.

[114] Rintamaki, H., Rissanen, S. (2006). Heat Strain in Cold. *Industrial Health, 44*, 427-432.

[115] Roberts, B. C., Waller, T. M., Caine, M. P. (2007). Thermoregulatory Response to Base-layer Garments During Treadmill Exercise. *International Journal of Sports Science and Engineering, 1*(1), 29-38.

[116] Ruckman, J.E., Hayes, S.G., Cho, J.H. (2002). Development of a perfusion suit incorporating auxiliary heating and cooling system. *International Journal of Clothing Science and Technology, 14*(1), 11-24.

[117] Ruckman, J.E., Murray, R. (1999). Engineering of clothing systems for improved thermophysiological comfort: The effect of openings. *International Journal of Clothing*

Science and Technology, 11(1), 37-52.

[118] Sadikoglu, T. G. (2005). Effect on Comfort Properties of Using Superabsorbent Fibres in Nonwoven Interlinings. *Fibers & Textiles in Eastern Europe, 13*(3), 54-57.

[119] Scheurell, D. M., Spivak, S. M. (1985). Dynamic Surface Wetness of Fabrics in relation to Clothing Comfort. *Textile Research Journal, 55*, 394-399.

[120] Schilling, C. H., Letscher, D., and Palsson, B. (2000). Theory for the systemic definition of metabolic pathways and their use in interpreting metabolic function from a pathway-oriented perspective, Journal of Theory Biology. 229-248.

[121] Schuhmeister, M., Ber. K. Akad. Wien (Math-Naturw. Klasse). (1877). 76, 283.

[122] Snellen, J. W. (1960). External Work in level and grade walking on a motor-driven treadmill. *Journal of Applied Physiol*, 15, 759-763.

[123] Stoecker, W. F. and Jones, J. W. (1982). Refrigeration and air conditioning, 2nd. McGraw-Hill, New York.

[124] Tagaya, H. (1987). Measurement of capillary rise in fabrics by electric capacitance method. *Sen-I Gakkaishi, 63*(7), 414-420.

[125] Tazelaar, D. J. (1999). Long Cotton Wool Rolls as Compression Enhancers in Macrosclerotherapy for VaricoseVeins. *Dermatol Surg, 25*, 38-40.

[126] Verry, J., Michaud, V., and Manson, J. A. (2006), Dynamic capillary effects in liquid composite moulding with non-crimp fabric, *Journal of Composites*. 37, 92-102.

[127] Vigneswaran, C. and Chandrasekrara, K. (2009). Effect of Thermal Conductivity Behavior of Jute/Cotton Blended Knitted Fabrics, Journal of Industrial Textiles. 38, 289-306.

[128] Wallace, M. (2002). 100% Cotton Moisture Management. *Journal of Textile and Apparel. Technology and Management, 2*(3), 1-11.

[129] Whang, H. S. and Gupta, B. S. (2000), Surface Wetting Characteristics of Cellulosic Fibers, *Textile Research Journal*. 70, 351-358.

[130] Wang, S. X., Li, Y., Tokura, H., Hu, J. Y. (2007). Effect of Moisture Management on Functional Performance of Cold Protective Clothing. *Textile Research Journal, 77*(12), 968-980.

[131] Wehner, J. A. (1988). Dynamics of water vapor transmission through fabric barriers. *Textile Research Journal, 58*(10), 581-592.

[132] Wilmore, J. H. and Costill, D. L. (1999). Physiology of sport and exercise, Human Kinetics, Champion, IL.

[133] Wong, A.S.W., Li, Y. (2004). Influence of the Fabric Mechanical Property on Clothing Dynamic Pressure Distribution and Pressure Comfort on Tight-Fit Sportwear. *Sen'I Gakkahishi, 60*(10), 293-299.

[134] Wong, A.S.W., Li, Y. (2004). Relationship between thermophysiological responses and Psychological thermal perception during exercise wearing aerobic wear. *Journal of Thermal Biology, 29*, 791-796.

[135] Woodcock, A. H. (1962). Moisture Transfer in Textile Systems: Part I: *Textile Research Journal*, 32, 628-633.

[136] Wren, R. E., and Blume, H. (1997). Body composition, resting metabolic rate, and energy requirements of short and normal stature, low income Guatermalan children. American Journal of Clinical Nutrician, 66, 406-412.

[137] Yoo, S., and Barker, R. (2005). Comfort Properties of Heat-Resistant Protective Workwear in Varying Conditions of Physical Activity and Environment. Part I: Thermophysical and Sensorial Properties of Fabrics, *Textile Journal Research*, 523-530.

[138] Yoon, H. N., and Buckley, A. (1984). Improved comfort polyester: Part I: Transport properties and Thermal Comfort of Polyester/Cotton Blend Fabrics. *Textile Research Journal,* 54, 289-298.

[139] Zhuang, Q. (2002). Transfer Wicking Mechanisms of Knitted Fabrics Used as Undergarments for Outdoor Activities, *Textile Research Journal, 72(8),* 724-734

Appendices

A. How to calculate the amount of Radiation, Convection, Conduction, and Enthalpy change of Vaporization

The research shows how to calculate radiation power, the amount of convection and conduction, and enthalpy change of vaporization with using temperature gradient and relative humidity which are formed by the first layer and microclimate in the first standard multilayered system. This Table is a part of Table 19.

	D1(Air)	1st Layer
Material thickness(Δx) ($2gf/cm^2$)	21 mm	0.39 mm
Material thickness (Δx) ($100gf/cm^2$)		0.34 mm
Material emissivity (ε, 20℃)	N/A	0.77
Convective heat transfer coefficient (h)	3.122 (W/m^2K): Natural convection, (ASHARE, 2006)	
Material thermal Conductivity (W/m*k)	0.024	0.03
Temperature gradient ($T_1 - T_2$) (℃)	37.04 ~ 32.76	32.76 ~ 31.91
Relative Humidity (R.H.) (%)	53.25	59.82
Weight (g) (5.25 inch*5.25 inch)	N/A	3.2
Air permeability (kPa*s/m)	N/A	1.57

- Stefan-Boltzmannn (Radiation Power): $P = A \varepsilon \sigma (T_1^4 - T_2^4)$

$0.98\ (\varepsilon) * 5.6703 * 10^{-8}\ (\sigma) * 2.18 * 10^{-2}\ (A) * ((273 + 37.04)^4 : T_1^4 - (273+32.76)^4 : T_2^4)$

- Newton's law of Cooling (Convection): $Q = -h\,A\,(T_1 - T_2)$

$$3.122(h) * 2.18 * 10^{-2}\ (A) * ((273 + 37.04): T_1 - (273+32.76): T_2)$$

- Fourier's Law (Conduction): $Q = \frac{kA}{\Delta x}(T_1 - T_2)$

$$\frac{0.03 * 2.18 * 10^{-2}\ (A) * ((273 + 32.76): T_1 - (273 + 31.91): T_2)}{0.00039}$$

- Clausius-Clapeyron Relation(Enthalpy Change of Vaporization):

$$\ln\left(\frac{P_1}{P_2}\right) = \frac{\Delta H_{vap}}{R}\left(\frac{1}{T_2} - \frac{1}{T_1}\right)$$

$$P_1 = \exp\left(20.386 - \frac{5132}{(273+37.04)}\right) = \exp(3.84) = 46.525$$

$$P_2 = \exp\left(20.386 - \frac{5132}{(273+32.76)}\right) = \exp(3.61) = 36.96$$

$$\text{Ln}\left(\frac{36.96}{46.525}\right) = \frac{H_{vap}}{8.31}\left(\frac{1}{(273+32.76): T_1} - \frac{1}{(273+31.91): T_2}\right)$$

B. Functional Fabric Trends in an Activewear Market

2.1. Introduction

This section has analyzed functional fabric trends for four brands of activewear; adidas, Nike, Asics, and Mizuno to study how activewear companies manage the heat and moisture flow for the winter seasons of 2008' and 2009'. This survey is basically based on information about activewear products on their websites and 'Datamonitor.' These brands are chosen based on their market share, a detailed description of the products' materials on their websites, and their functional purpose. In particular, this survey has focused on the fiber material and composition considering heat and moisture transfer.

Table 35 and Figure 85 show the total number of target products on the market from the 4 brands of interest. A total of 452 products (196 men and 256 women) have been investigated from the major companies: adidas (92), Nike (184), Asics (103), and Mizuno (73). This shows that, there are normally more types and numbers of products for women than there are for men. In particular, the amount and type of the Nike products for women represents a wide and specialized assortment.

Table 35. The number of total products

	adidas	Asics	Mizuno	Nike	Total
Men	51	44	30	71	196
Women	41	59	43	113	256
Total	92	103	73	184	452

Through this analysis, the researcher is able to analyze how manufacturers want to pursue

comfort of the human body by taking advantage of the materials used.

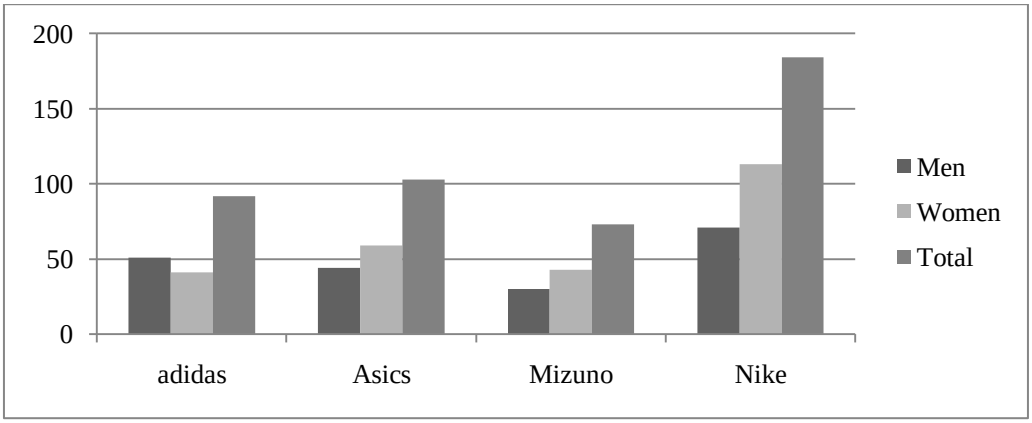

Figure 85. The number of total products offered online by adidas, Asics, Mizuno, and Nike (%) '2008 (2009)

2.2. Material analysis of functional products of four brands

2.2.1. adidas

The data in the adidas section results from fabric materials of 51 products for men and 41 products for women in adidas' website (http://www.adidas.com/us/homepage.asp). Table 36 and Figure 86 show the fiber content per product and types of fiber in all products used for adidas. While M1 means fiber content per product for men, F1 explains fiber content per product for women. For instance, M1 and F1 indicate how much one product includes nylon or polyester fiber. In addition, M2 and F2 mean type of fibers in all products for respectively men and women. For instance, that M2 and F2 imply how much all products include nylon fiber. According to the data, this brand uses polypropylene, wool, Spandex, polyester, and nylon to make functional activewear products. Furthermore, polyester usage is higher than

that of all other fibers but Spandex is used to give better fit for the human body. In addition, 100% nylon and 100% polyester are used to make products. As for natural fibers, a tiny amount of wool is used in the 'Supernova Sports wool Half Zip' product.

Table 36. Fiber content product and type of fibers in all products of adidas (%)

	Material	Nylon	Polyester	Spandex (Elastane)	Wool	Polyprop-ylene
Sub Total	Fiber content per product (M1)	83.2	91.24	11.35	23	24
	Type of fibers in all products (M2)	9.43	94.34	37.04	1.89	2.38
Sub Total	Fiber content per product (F1)	82.56	94.06	10.07	0.00	1.71
	Type of fibers in all products (F2)	21.4	83.3	33.3	0	2.38
Total	(M1+F1)/2	82.88	92.65	10.71	11.50	12.86
Use Ratio	(M2+F2)/2	15.43	88.84	35.19	0.943	4.02

Table 36 shows fiber content per product. As mentioned above, the ratios of polyester or nylon are approximately 92.65% or 82.88% per product in total average of the fiber content per product. The fiber content ratio is adjusted to optimize properties of the final fabric by compositing another assistant fiber material. For instance, Spandex can't be used for a product independently but as a blend to assist the function of the activewear products.

Hence, the composition of nylon-Spandex, polyester-Spandex, or polyester-nylon-

Spandex is used to make functional activewear for specific functions. The use of blended fabric materials means that adidas products are actively dealing with a space related to microclimate and fitting between fabric and skin. This means that adidas tries to influence physical and physiological comfort sensation of the human body through control of this space by using the material composition.

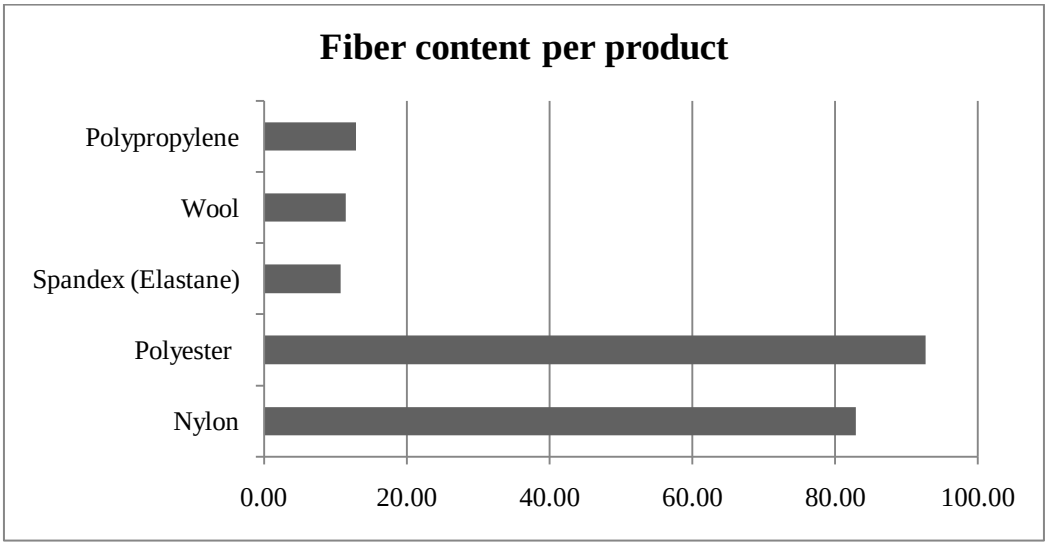

Figure 86. Fiber Content per product of adidas (%)

Reviewing the fiber content per product and the types of fiber in all products, the usage ratio of polyester is significant, and it is recognized as a core material making functional activewear products of adidas in Figure 86. adidas chiefly uses 'Coolmax fabric' which is also classified into ClimaCool®, ClimaLite®, Formotion™, ClimaProof®, and ClimaWarm™, each in accordance with a specific purpose. For example, ventilated ClimaCool® lets a body be dry and comfortable; ClimaLite® quickly sweeps perspiration

away from your skin; Formotion™ actively supports athlete's muscles for improved comfort; ClimaProof® provides lightweight and breathable protection from wind and rain; and finally, ClimaWarm™ keeps your temperature regulated in cold and windy condition. This means that the Coolmax fabric has various properties: some of them are easily dryable; and others are able to control moisture absorption and desorption at the same time, meaning that one of main roles of the fabric is to quickly absorb and disperse perspiration and expose it to the outside through heat loss by evaporation.

adidas does not use any natural materials except a small amount of wool, even though natural materials have various advantages with regard to moisture management and thermal regulation. In the case of adidas, wool is used in 1.89 % for men's clothing and 0% for women's or about 0.94% for total adidas products. Cotton and rayon were never used during the winter season of 2008 and 2009.

Figure 87 shows the types of fiber in all products. adidas used polyester almost 88.84 %, and used nylon 15.43 % in total. In addition, even though the content ratio of Spandex or elastane is not used much for individual products, its ratio is considerably high for the material distribution of total products. This means that Spandex or elastane used for controlling fit and compression should be considered along with the movement of the human body.

Tazelaar (1999) mentions that fabrics composed with Spandex material can be normally applied to sports clothes, leisure clothes, hosiery, underwear and swimwear for maintaining a stable shape of the body under changeable load. The pressure caused by Spandex also reduces the microclimate between skin and fabric surface. Therefore, a role of

Spandex is to let four types of heat energy transfer be changed. In the process of heat energy transfer, conduction increases, while vaporization, convection and radiation are relatively reduced. Thus, due to the pressure, the heat energy flow originating from metabolic energy is directly transferred into functional materials of the clothing, perspiration is not divided into sensible and insensible one, and all of the perspiration is directly absorbed into the clothing.

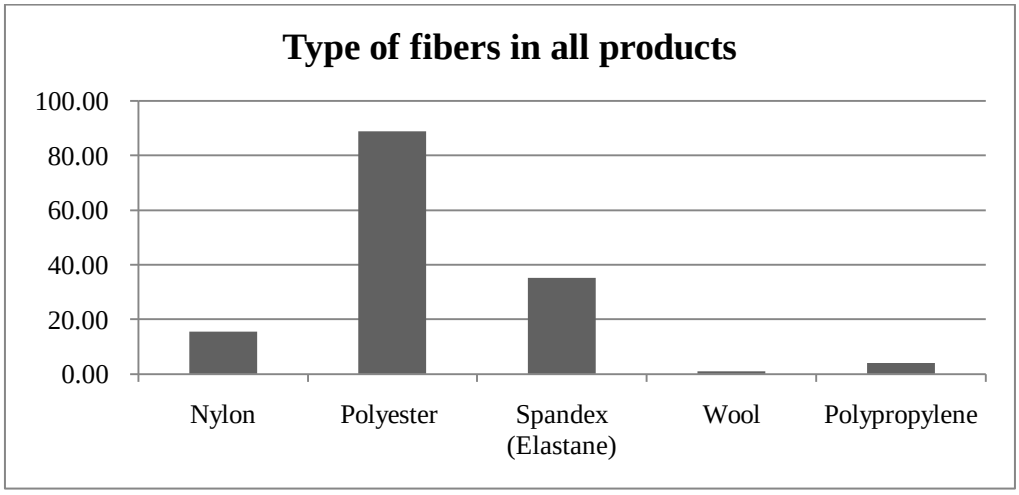

Figure 87. Types of fiber in all products of adidas (%)

In the adidas line, Nylon is unique because its existence in all products is low, while its fiber content per product is high. Even though nylon is used less for the entire product, it is used to make a product without mixing it with other materials. As manufactured nylon is normally formed by a long chain synthetic polyamide, it has a linkage attached to two aromatic rings. Dasgupta and Hammond (1996) explain that nylon-n and nylon-m have the following polymer structures:

Nylon-n: -[-(NH-CO)-(-CH2)*n*-1-]- (Eq. 34)

Nylon-m, n: -[-(NH-CO)-(CH2)*n*-2-(CO-NH)-(CH2)*m*-]- (Eq. 35)

Dasgupta explains that the peptide units (NH-CO) have a hydrophilic property because of a hydrogen bond.

Nylon has diverse properties, such as stiffness, toughness, lubricity, abrasion resistance and fatigue. Dasgupta (1996) explains that nylon fiber, with a diameter of normally 10 to 500μm, is produced by traditional methods, such as melt, dry, and wet spinning. Currently, nylon manufacturing technology is chiefly concentrated on producing ultra fibers which have great mechanical properties (diameter range from 50 to 500 nm) as well as smooth fibers similar to skin. Figure 88 shows representative products made by a composition of nylon and Spandex.

(A) (B)

Figure 88. (A) Supernova seamless long sleeve half zip and (B) Response astro pants

Bunsell and Hearle (1971) mention that nylon having a medium tenacity is generally about 48cN/Tex. Its breaking strain is 20%, and its initial modulus is 3cN/Tex. In addition, its standard moisture regain is about 4.0 to 4.5 (%) at 70℉ and 65% relative humidity. As for other representative fiber materials, there are polyester and Spandex. Many products are mainly made from the composition of polyester (77-97%) and Spandex (3-23%). Generally,

tensile strength, elastic recovery, and stiffness of the polyester are very different from those of Spandex based on information of 'Textile World (http://www.textileworld.com).' While polyester has great ability regarding tensile strength, Spandex is superior in elastic recovery and has a low degree of stiffness. Therefore, it is presumed that polyester and Spandex have a complementary relationship with each other. This means that Spandex deals with a beginning load by movement of athletes' strong muscle, and polyester mainly treats strong tensile strength along with having a hydrophobic property to settle moisture and evaporation at the same time.

Finally, adidas officially used about 5 materials to manufacture 92 activewear products for winter season of 2008' and 2009'. adidas uses no natural fibers with the exception of a tiny amount of wool, even though natural fibers have diverse advantages, such as water absorbency and non-pollution. In addition, there is almost no difference in the usage ratio of Spandex between men's and women's products, which implies that adidas does not consider any differences in the muscle movement between men and women.

2.2.2. Asics

This research investigated 44 products for men and 59 products for women manufactured and marketed by Asics. For the most part, Asics uses five materials, nylon, polyester, polyester microfiber, Spandex and 100% meryl nylon nano durable water repellent (DWR) to make its functional activewear products. The unique finding of this investigation is that Asics does not use any natural fibers, such as cotton or wool, for manufacturing its products. In addition, Asics makes use of a remarkable polyester microfiber to make about 10%

of its products improve quick moisture reduction, dryness and breathability. Figure 89 shows men and women's products which are made of 100% polyester microfiber.

(A) (B) (C) (D)

Figure 89. (A) Storm shelter jacket (M), (B) Core pocket shorter (M), (C) Storm shelter jacket (F), (D) Performance 2-N-1 short (F)

According to information from microfiber.com, this polyester microfiber is extremely fine less than one denier, strong, precise and absorbent. In particular, it has a great water absorption facility. Since the polyester microfiber is a hydrophobic material, its material property and structure do not hold water molecules which are quite fairly distributed. This prevents clothing from becoming wet and allow it to dry quickly through vaporization. For example, the fabric is specifically used for a cyclist because it strongly absorbs perspiration through a capillary power. This is helpful for the skin to dry quickly and feel cool. Figure 90 shows the capillary phenomenon in polyester microfiber.

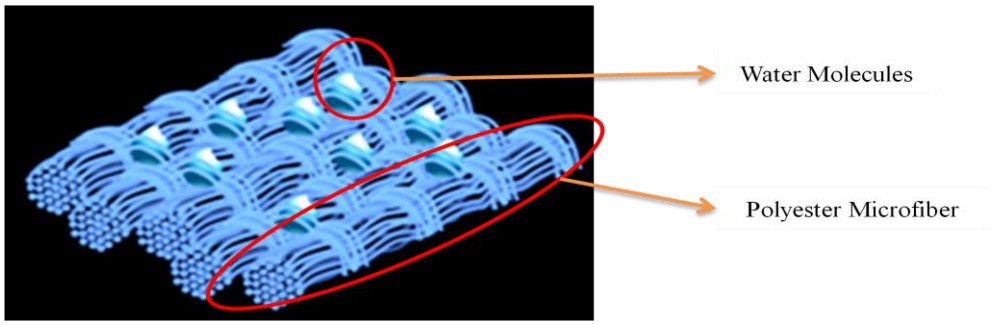

Figure 90. Capillary phenomenon of water molecules in polyester microfiber

Reproduced from http://www.microfiber.com/microfiber.html

Another unique point is that Asics shows a higher usage ratio of nylon for women's products than other brands, such as adidas and Nike. In the Asics section, this nylon (82-95%) is normally composited with Spandex (5-18%). The moisture regains are about 3.5-5.0% for nylon and 1.3% for Spandex. In addition, this composition enhances breathability as it specifically increases moisture wicking in the sports bra product category. According to 'Man-Made Fiber Chart' of Textile World, Nylon has different physical properties than polyester as a main material. Its breaking tenacity and elastic recovery are generally higher than that of polyester. However, the tensile strength and stiffness of nylon are similar of those of polyester.

Figure 91 and 93 show two interesting fibers, polyester microfiber and 100% meryl nylon nano DWR. Only Asics uses them to manufacture functional products. However, the amount of products which use these materials is just about 12.5% of the total amount. In particular, Asics uses a specific fabric called 100% meryl nylon nano DWR to make a Rapido™ jacket, which emphasizes a lightweight or shelter function for men and women.

Table 37 shows fiber content per product and material distribution of Asics.

Table 37. Fiber content per product and types of fiber in all products of Asics (%)

Material		Nylon	Polyester	Polyester Microfiber	Spandex (Dow XLA)	100% Meryl Nylon Nano DWR
Sub-Total	Fiber content per product (M1)	95.00	95.42	100.00	8.84	100.00
	Type of fibers in all products (M2)	5.36	80.36	12.50	44.64	1.79
Sub-Total	Fiber content per product (F1)	91.24	93.81	100.00	10.41	100.00
	Type of fibers in all products (F2)	33.33	56.00	9.33	61.33	1.33
Total	(M1+F1)/2	93.12	94.62	100.00	9.63	100.00
Using Ratio	(M2+F2)/2	19.35	68.18	10.92	52.99	1.56

To give a stretch force, about 5-20% Spandex is used for each product mixed with polyester or nylon. Hence, in the case of Inner Muscle™ Sprinter or ARD™ Warm-Up Jacket or Inner Muscle™ Long Sleeve in the women products, 20% Dow XLA material is used, which is an olefin-based stretch fiber. It is used to improve muscle and bone activity levels. An olefin is a man-made fiber, or "a long chain synthetic polymer composed of a minimum of 85% of ethylene, propylene and other olefin units except amorphous poly-olefins" according to Hearle (2001)

Generally, these stretchable fibers are mainly used for women's clothing. Their

material distribution trends for a stretch force are similar to Spandex of Nike because the usage amount ratio of women's Spandex is relatively higher than that of men. Figure 92 shows women's products, which use 20% Dow XLA to improve stabilization of scapula movement, straightening the spine and improving posture.

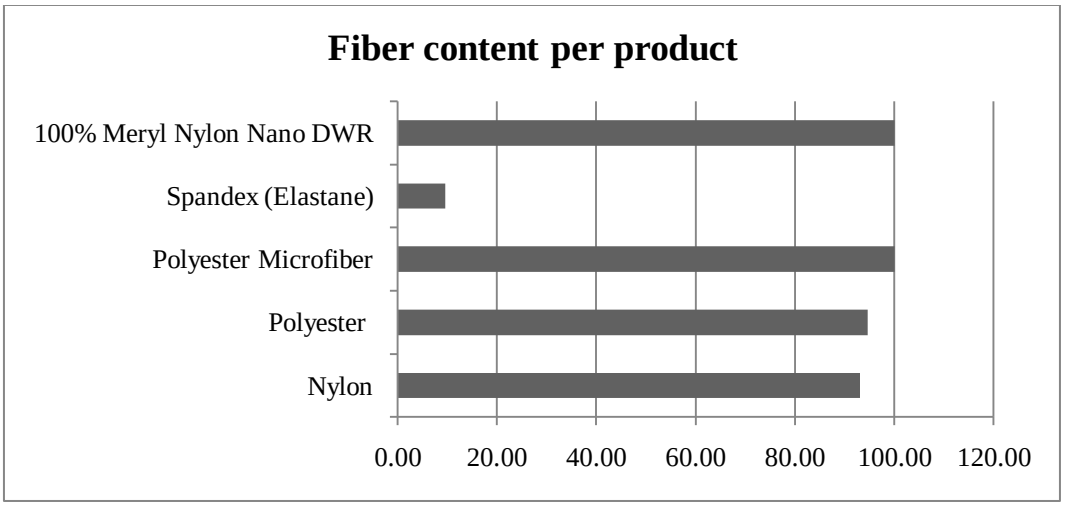

Figure 91. Fiber content per product of Asics (%)

In addition, the usage ratio of nylon (19.35%) is clearly higher than that of adidas (15.43%) or Nike (7.04%). On the other hand, the usage ratio of polyester (68.18%) is relatively lower than that of adidas (88.84%) or Nike (92.68%). Asics uses mostly three types of polyesters, Hydrology™, Thermopolis, and Storm Shelter™. Hydrology™ emphasizes breathability and moisture transfer. Thermopolis focuses on lightweight and warm comfort, and finally Storm Shelter™ is used for water proofing and wind resistance. These polyesters are basically blended with other materials, such as Spandex and the Dow XLA. The usage amount ratio of stretchable fibers, Spandex and the Dow XLA (52.99%), is higher than that

of adidas or Nike.

(A) (B)

Figure 92. (A) Inner Muscle™ Long Sleeve and (B) Inner Muscle™ Sprinter

In conclusion, Asics has tried to use unique materials, such as polyester microfiber, 100% meryl nano DWR, and Dow XLA to improve comfort of the human body. Although the polyester microfiber, as mentioned above, has various advantages, only 14 of 103 products using it seem to greatly improve vaporization of perspiration.

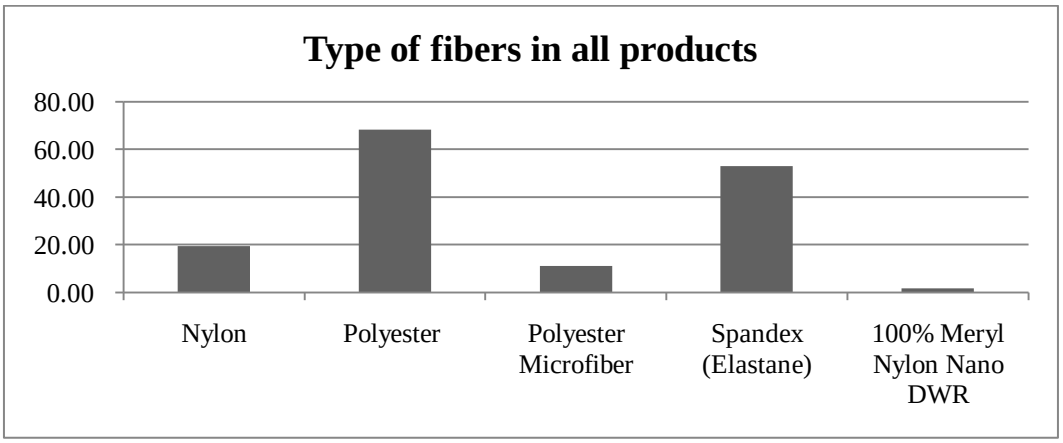

Figure 93. Type of fibers in all products of Asics (%)

2.2.3. Mizuno

Mizuno is a Japanese activewear brand. This research investigates its 30 products for men and 43 products for women. Mizuno uses four materials: polyester, polyester- microfiber, polyacrylate, and Spandex. They make all products using only these four materials. Nor does Mizuno use any natural fibers, such as cotton or wool, to produce the products. Remarkably, it does not use nylon as a main material, either. Table 38 shows the fiber content per product and types of fibers in all products in Mizuno

Table 38. Fiber content per product and type of fibers in all products of Mizuno (%)

	Material	Polyester	Polyester Microfiber	Polyacryla -te	Spandex (Elastane)
Sub-Total	Fiber content per product (M1)	94.65	100.00	8.40	9.17
	Type of fibers in all products (M2)	78.79	21.21	30.30	18.18
Sub-Total	Fiber content per product (F1)	93.07	100.00	9.17	8.29
	Type of fibers in all products (F2)	89.13	10.87	26.09	45.65
Total	(M1+F1)/2	93.86	100.00	8.78	8.73
Use Ratio	(M2+F2)/2	83.96	16.04	28.19	31.92

Mizuno uses two kinds of polyester microfibers, Windlite™ and MzW, which are developed for setting up a breathable shell fabric including a function for water and wind resistance. The microfibers are also lightweight and ultra soft-tough. Their usage amount

ratio (16.04%) is relatively higher than that (10.92%) of Asics. The polyester microfiber is solely used to make the products without mixing with other materials, such as Spandex.

Mizuno uniquely uses about 7% to 14% polyacrylate, which provides a function of superior moisture absorption, to improve overall body warmth. Mizuno produces several products using polyacrylate. They include Breath Thermo Stretch Crew and Breath Thermo Stretch 1/2 Crew. As these functional garments are tight, they are capable of directly absorbing perspiration and seem to take advantage of conduction as a means of heat energy transfer. Through polyacrylate fabric and distinguished design, Mizuno considers heat and energy flow to improve the comfort of the human body. Figure 94 shows products using polyacrylate fabric.

In addition, Figure 95 and 96 show fiber content per product and type of fibers in all products for Mizuno, respectively. The main materials are also polyester and Spandex. Mizuno develops specific polyesters called 'DRYSCIENCE,' which emphasize facilitation of rapid vaporization. Drylite™ fabric consisting of 92% polyester and 8% Spandex is also used to handle moisture management by transporting perspiration vapor. Mizuno, for the most part, takes advantage of the two polyesters. It manufactures 21 products which use 100% polyester material among their total of 73 products.

(A) (B)

Figure 94. Breath Thermo Stretch Crew(A) and Breath Thermo Stretch 1/2 Crew (B)

A composition of the polyester with polyester microfiber, Spandex and polyacrylate is considerably simpler for Mizuno than other brands such as adidas, Nike, and Asics. In particular, a composition of polyester (87-93%) and polyacrylate (7-13%) or polyester (79%), polyacrylate (14%), and Spandex (7%) are distinguished because Mizuno mentions that the compositions create a uniquely stretchable insulation fabric which absorbs moisture and hold heat through their thermal insulation effect in cold temperature.

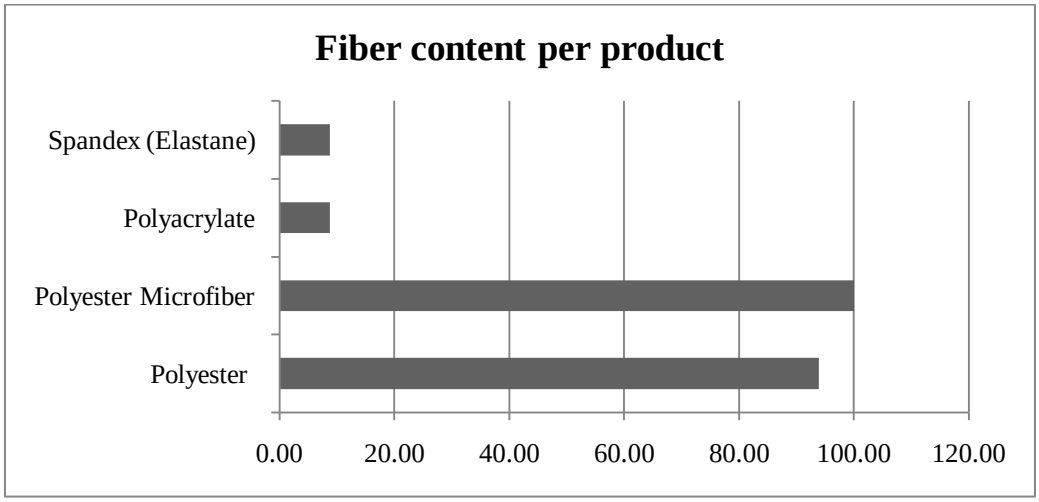

Figure 95. Fiber content per product of Mizuno (%)

In addition, a big difference between the fiber content per product and types of fiber in all products of Mizuno is the polyester microfiber. Also, the usage amount of Spandex is clearly classified into 18.18% for men and 45.65% for women similar to Nike. This suggests Mizuno also takes account of the difference of the muscle movement between men and women.

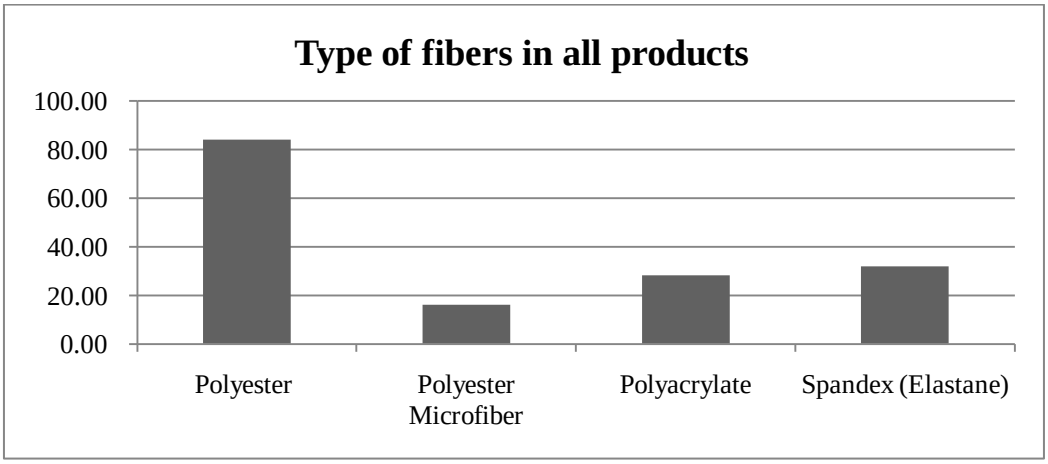

Figure 96. Type of fibers in all products of Mizuno (%)

However, the Spandex usage ratio of Mizuno is relatively different from that of Nike in each product. Mizuno uses Spandex approximately 7% to 12%, while Nike makes use of it from about 5% to 20% with varying ratios. Although Nike's Spandex usage ratio is considerably complex in comparison with that of Mizuno, the usage ratio of anyone product does not often exceed 20%. Mizuno efficiently treats moisture management, clothing weight, and heat energy flow through their various compositions with using only four types of fibers.

2.2.4. Nike

In the Nike section, the research investigates fabric materials of 71 products for men and 113 products for women from its website. For the most part, Nike uses six kinds of fibers (nylon, polyester, Spandex, polyurethane, cotton, and rayon). The ratio of the polyester is relatively higher than that of any other fibers. As the polyester is a core fiber to make functional fabric like adidas, its ratio is up to about 87.43%. Table 39 shows the fiber content of several products. Nike has used mainly 87.43% polyester, 72.96% nylon, 12.57% Spandex and 13.75% polyurethane.

Table 39. Fiber content per product and type of fibers in all products of Nike (%)

	Material	Nylon	Polyester	Spandex (Elastane)	Polyure-thane	Cotton (organic)	Rayon
Sub-Total	Fiber content per product (M1)	69.14	89.13	12.11	11.5	47.5	12
	Type of fibers in all products (M2)	7.95	94.32	42.05	2.27	9.09	3.41
Sub-Total	Fiber content per product (F1)	76.77	85.73	13.03	16.00	73.04	12.00
	Type of fibers in all products (F2)	6.13	91.04	73.11	0.94	10.85	0.472
Total	(M1+F1)/2	72.96	87.43	12.57	13.75	60.27	12
Use Ratio	(M2+F2)/2	7.04	92.68	57.58	1.61	9.97	1.94

While polyester, nylon and cotton are used to make each product independently, rayon, polyurethane, and Spandex have been used as assistant ingredients to efficiently improve

product functions. Based on the "Manufactured Fiber Fact Book and High Performance Fibers," the tensile properties of polyester are as follows: medium tenacity of 47cN/Tex, breaking strain is 15%, and initial modulus is 11N/Tex. In addition, its standard moisture regain is 0.4 to 0.8 % in the same condition as above.

Since the moisture regain percentage of polyester is considerably lower than any other materials, such as rayon or nylon, it does not retain water for a long time. It quickly emits perspiration to the outside as soon as possible. Therefore, the most important facility of polyester, as a functional material, is not only to absorb perspiration and emit it, but also to block water from external environments. However, appropriate vaporization speed should also be considered to avoid after-chilling and provide a warm feeling to the human body.

In addition, polyester is diversely classified into Clima-Fit, Dri-Fit, Therma-Fit, and Storm-Fit in accordance with various purposes, such as moisture management and thermal insulation. The polyesters have a variety of composition ratios with Spandex, cotton, polyurethane, and nylon: Clima-Fit is breathable as well as wind and water resistant; Dri-Fit is mainly used for wicking perspiration, helping keep athletes dry and comfortable; and Therma-Fit is to help athletes stay warm and insulated; Storm-Fit is used for repelling wind, rain and snow to encourage dryness and comfort.

There is a unique composition that results from mixing rayon with polyester. Polyester is a representative example of a hydrophobic material; it is mixed with rayon to establish a hydrophilic property. According to the "Man-Made Fiber Chart of Textile World," moisture regain of polyester is 04-0.8%, while rayon is 10.7-16.0%. Normally, the rayon material is made from regenerated cellulose which includes less than 15 % of the hydrogen of the

hydroxyl groups. All of the mixed ratios are rayon 12% and polyester 88%. This mixed fabric is mainly used for a back panel on the human body. Nike mentions that this composition is helpful to keep a body cool and dry during competition.

Normally, the tensile properties of common rayon are a tenacity of 22cN/Tex, a breaking strain of 18%, an initial modulus of 6 N/Tex respectively, and the moisture regain is about 11% to 13 % under 20℃ and 65% relative humidity. Rayon's moisture regain is higher than other synthetic fibers, such as polyester or polyurethane, and is similar to that of silk. Therefore, its water-absorbing ability is easily capable of retaining about 80% of its own weight within the fibers due to its cross sectional surface.

Figure 97 shows the fiber content per product and material distribution of the total products of Nike for men and women. In particular, there is a big difference between men and women in regard to Spandex distribution for the products. The data in Table 39 shows that Nike considers fitting more for physical movement in women's clothing than for men in many products. According to the data, it is supposed that a woman's body needs more elastic materials, such as Spandex or polyurethane than do men's bodies. The pressure of these materials indirectly affects blood flow and metabolic energy, which means that velocity of the blood flow pressed by Spandex, is faster and increases energy delivery inside of the body through the blood cells.

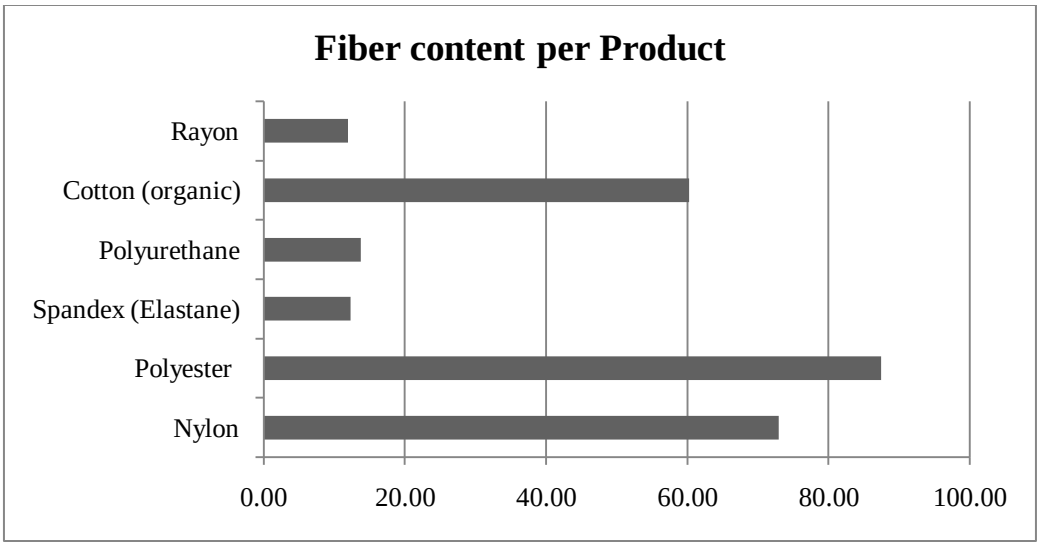

Figure 97. Fiber content per product of Nike (%)

Normally, the properties of general Spandex are as follows: breaking tenacity is 0.7, and standard moisture regain is 0.75 to 1.3 % at 70°F and 65 % relative humidity (Bunsell and Hearle, 1971). Figure 98 shows a product consisting of 78% polyester and 22% Spandex, which maximizes a usage of Spandex among Nike products

Figure 98. Nike Baggy Microfiber 4" Men's Running Shorts

Partsch (2006) explain that, because Spandex is a polymer, it has two main structures,

a long amorphous segment and a short rigid segment. This means that the elastic feature of Spandex originates from the material's chemical composition. The principle of elasticity is the following; when stretch force is applied, the bonds between the rigid segments are broken, and its amorphous segment straightens out. When the stretch comes at a maximum point, the rigid segments are connected with each other again. Hence, Spandex is stronger and stiffer at that time. After removing the stretch force, the amorphous segment recoil and the fiber return. Figure 99 shows a chemical structure of Spandex consisting of soft and rigid segments.

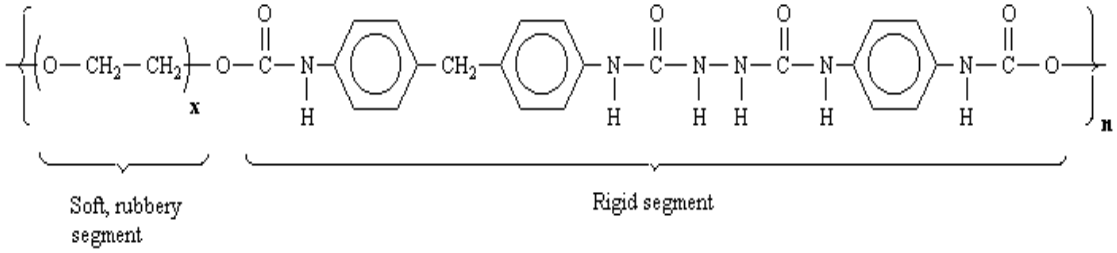

Figure 99. A structure of the Spandex consisting of soft and rigid segment

Through change of this structure or fiber amount, its stretch force can be applied for human body. The Federal Trade Commission (FTC) defines a variety of characteristics of the Spandex;

- Generally, can be stretched more than 500% without breaking
- More durable and higher retroactive force than rubber
- Lightweight, soft, smooth
- Provide a combination of comfort and fit
- Dyeable
- Abrasion resistant

The big difference between the type of fibers in all products and fiber content per product is the usage level of the nylon and extreme usage of the polyester in overall Nike products. This means that the polyester is a core content and accounts for up to 92.68 %. Thus, almost all of the products seem to be made from polyester material. In addition, Nike seems to clearly classify the products into men (42%) and women (73%) in accordance with usage level of Spandex in the material distribution of the total product. Figure 100 shows Nike's type of fibers in all products.

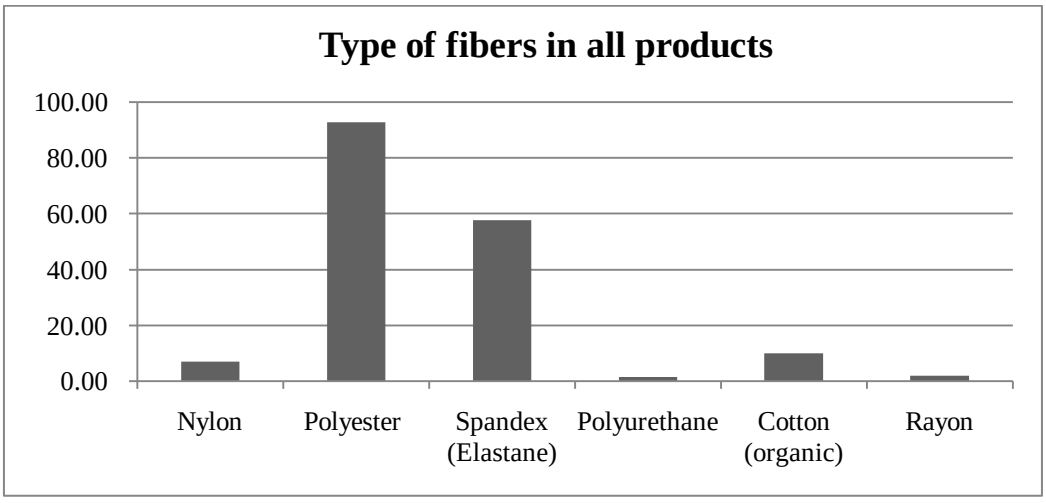

Figure 100. Type of fibers in all products of Nike (%)

2.2.5. Conclusion

Based on the material data of adidas, Asics, Mizuno and Nike, they seem to take advantage of diverse man-made fibers as well as natural ones to achieve comfort sensation of the human body or competitiveness. adidas uses 5 to 6 materials to make 92 products, Nike only takes advantage of 6 or 7 materials to manufacture 184 products, Asics makes use of 5

to 6 materials to provide 103 products, and Mizuno also uses 4 to 5 materials to make 83 products. This means that they try to create various functional fabrics through only four to six fabric materials or their composition.

In addition, this research has found four unique things from the above data:

- Various transformation of polyester
- Disappearance of natural fiber
- A difference of usage ratio of Spandex or urethane between men's and women's clothing
- Importance of the material composition

In particular, as polyester is a main material for almost all of the products, it is used to produce various types of functional fabrics for managing moisture, heat, and wind. Its usage range is from about 68% to 92% of almost all products. Generally, it is used with several materials, such as nylon, cotton, and Spandex, to actively deal with perspiration and vapor under internal and external environments.

The second noticeable aspect is that the companies, Asics and Mizuno, no longer use natural plant and animal fibers, such as cotton and wool. adidas only uses 0.94% wool and Nike makes use of only 9.97% cotton, even though natural fiber has various advantages in the manufacture of functional activewear. Table 40 clearly shows the advantages and disadvantages of natural fiber.

Table 40. Advantages and disadvantages of natural fibers

Advantages	Disadvantages
1. Non-pollution 2. Low likelihood of skin trouble 3. Good absorption	1. Expensive 2. Not easy to maintain consistent quality of a product 3. Hard to expect accurate production amount due to weather 4. Generally, difficult to control its thickness

Therefore, this research assumes that the reason why the natural fibers are not used that the disadvantages make then unsuitable for efficiently driving mass production systems and saving production costs.

The next thing to consider is the usage of Spandex. Normally, about 2% to 5% of Spandex is used for the fit function of clothing, and 10% to 20% for muscle stabilization. In here, a difference of usage ratio of the Spandex or urethane between women and men's products is remarkable in the total product because muscle movement across genders is not the same. In particular, Nike and Mizuno make use of the Spandex to increase the stretch force of many products for women compared with men. Since a stretchable product affects microclimate between skin and fabric, the amount and speed of heat energy flow including perspiration a human body emits are significantly changed. Therefore, comfort sensation

level of the human body is changed in accordance with the usage ratios of the Spandex or urethane. This indicates that the usage of Spandex is related to not only physical movement of the human body but also to its heat energy flow.

Finally, the composition of materials and their categories are different in accordance with the sports brands, even though the use of polyester and Spandex is general and representative in all of the brands. This suggests that they consider physical movement of athletes and moisture management simultaneously. Also, the composition of nylon and Spandex is frequently used to make many functional activewear products. In addition, variously mixed ratios of these compositions largely are related to gender and specific purposes regarding moisture or thermo-management, and external environments.

C. Sensiron’s Data Sheet (SHT-71)

SHT71 digital humidity and temperature sensor is the all-round version of the pin-type humidity sensor series that combines decent accuracy at a competitive price. The internal calibration allows for simple and easy replacement in demanding environments. As every other sensor type of the SHTxx family, the capacitive humidity sensor SHT71 is fully calibrated and provides a digital output.

-Features

Energy consumption:	80uW (at 12bit, 3V, 1 measurement / s)
(RH) operating range:	0 – 100% RH
(T) operating range:	-40 – +125℃ (-40 – +257℉)
(RH) response time:	8 sec (tau63%)
Output:	digital (2-wire interface)

Maximal accuracy limits for relative humidity and temperature: